Elucidating the molecular mechanisms of Alzheimer's disease and the use of artificial intelligence in clinical treatment

A thesis

Submitted in fulfillment of the requirement for the degree of

Ph.D.

at

The University of Brighton

by

Dorothy Keine

University of Brighton

2019

I declare that the research contained in this thesis, unless otherwise formally indicated within the text, is the original work of the author. The thesis has not been previously submitted to this or any other university for a degree, and does not incorporate any material already submitted for a degree.

10/27/2019

Signed Date

Table of Contents

Abstract

Alzheimer's disease (AD) is the most prevalent form of dementia. It is often characterized by amyloid-β (Aβ) accumulation and aggregation, and neurofibrillary tau tangles. Many different mechanisms are hypothesized to contribute to the disease process, from a reduction in Aβ clearance, electrical imbalances leading to excitotoxicity, widespread inflammation, genetic factors, to poor nutrition and exercise. The research presented in this thesis led to a new method of *in vivo* apolipoprotein E measurement using microdialysis to assess dynamic changes in response to therapeutic methods in real-time. The work presented here also establishes new methods for Aβ clearance, neuronal protection, and restoration of cognitive function in both animal and human models. Receptor-mediated endocytosis by the low-density lipoprotein receptor-related protein 1 is important in neuronal clearance of Aβ. When disrupted in conditional knock-out cell culture and murine models, Aβ plaque deposition and insoluble Aβ levels increase. Aβ can also be taken up and degraded by astrocytes. Increasing the activation of transcription factor EB stimulates the biogenesis of lysosomes and increases cellular uptake pathways that promote the uptake and degradation of Aβ by astrocytes. Our research also showed that neurons can be protected from aberrant electrical activity that is often found with AD. By constructing antisense oligonucleotides specific to endogenous murine tau, we were able to protect against hyperexcitability in chemically-induced seizures. Further, by reducing transcription of the amyloid precursor protein, which is thought to be overexpressed in AD, abnormal EEG activity was reduced without changing Aβ plaque load. A similar transgenic reduction in APP also restored cognitive function in mice by decreasing soluble Aβ while leaving plaque loads unchanged. These and other findings show that AD has multiple underlying mechanisms that contribute to AD disease state and progression. Taking the multifactorial nature of the disease into account, further research led to the creation of a combination therapy approach informed by precision medicine software that enabled the creation of a personalized therapeutic approach to AD. This software was then further expanded to track and enable improved prescription methods to prevent interactions and cognitive burden related to polypharmacy. This expansion also allowed for the exploration into preventing other drug-induced cognitive issues that may contribute to cognitive decline, such as depression.

Introduction

The first recorded case of Alzheimer's disease (AD) was in 1901, Auguste Deter. She began to suffer from delusions, memory impairment, and became very restless, often aimlessly wandering her house. She was 51 when her family started to notice the changes and troubles. With time, she lost all sense of money, and could no longer find objects that she had put away. As the months progressed, so did her illness. Five years later, in 1906, she died. Dr. Alois Alzheimer was convinced that Auguste's presentation was different from the other neurological diseases he studied (Lage 2006).

Using a silver staining technique, he was able to identify microscopic lesions that later became known as neurofibrillary tangles. Alzheimer published his findings in 1907, describing the neurological degeneration he observed. His paper ended with the statement "As a whole, it is clear that this disorder which, over the course of five years, caused profound dementia in a young adult, represents an entirely new clinicopathological entity" (Lage 2006).

This new disease went relatively unnoticed for decades after Alzheimer's initial publication. More modern ideas about AD began in the 1960s when interest in the quickly growing aging population started to gain momentum. It was not until 1977 that the first National Institute of Health (NIH) organized meeting about AD took place. This meeting had a profound impact on the AD world, as it was the trigger for more extensive research into the disorder, as well as increased funding (Lage 2006).

Today, AD is a growing concern around the world, and is the most common form of dementia, accounting for 65% of all dementia cases. It is estimated that by 2050, 1.34% of people worldwide will be living with AD (J. Cummings et al. 2016). Prevalence of AD almost doubles every five years in individuals 65 to 85 years (Atri 2019).

There are two recognized forms of Alzheimer's, familial (or genetic) and the sporadic late-onset. The familial form of the disease also referred to as early onset (EOAD) is thought to be caused by three main genes which are all autosomally dominant. The amyloid precursor protein gene on chromosome 21, the presenilin 1 gene on

chromosome 14, and the presenilin 2 gene on chromosome 1 (Chu 2012; Loy et al. 2014; Cummings et al. 2019). Mutations in these genes lead to an overproduction of amyloid-beta (Aβ) peptides, Aβ40 and Aβ42. This, in turn, results in a misfolding of these proteins and overproduction of Aβ, leading to eventual synaptic dysfunction, neurotoxicity, and Aβ plaques (Chu 2012; Mayeux 2003).

Late-onset Alzheimer's disease (LOAD) also has genetic components and risk factors. The most well-known of which is apolipoprotein E (APOE) ε4. Heterozygous ε4 increases the risk of developing AD by approximately three-fold, whereas homozygous individuals have a 15-fold increased risk (Chu 2012; Mayeux 2003). A multitude of other genes have also been found to increase risk or have a protective role against developing AD (Corder et al. 1994; Sassi et al. 2016; Cuyvers & Sleegers 2016). The Alzheimer's Disease Neuroimaging Initiative (ADNI) keeps an updated dataset of genome-wide associated studies (GWAS) and their corresponding single nucleotide polymorphisms (SNPs) that have been associated with AD (Alzheimer's Disease Neuroimaging Initiative n.d.).

There are many other known risk factors for AD, many of which are modifiable (see Table 1). Age and gender are both risk factors, with the risk of AD doubling every five years after 65 (Lista et al. 2015). Women are also at a higher risk than men for developing dementia. The mechanisms behind this are not fully understood, but it is thought that the higher availability of testosterone has a protective effect for men (Chu 2012). Lack of education also increases risk, with increasing years of education increasing what is referred to as "cognitive reserve." A family history of the disease also plays a role in risk, with 15% of AD patients presenting with a close relative who also had the disease. It is estimated that family history increases risk by about four-fold (Chu 2012). Alcohol consumption may have both a positive and negative impact on risk, depending on the amount that is consumed. Moderate levels of drinking are associated with being protective, while heavy drinking and complete abstinence both increase risk (Chu 2012). There is conflicting research on alcohol consumption and AD though. Physical activity is known to reduce neurodegeneration, while smoking, depression, and cardiovascular disease are all associated with an increased risk of AD (Chu 2012).

Table 1 Risk factors for AD

Nonmodifiable	Age
	APOE ε4
	Cerebral amyloidosis
	Down syndrome
	Family history
	Gender
	Race
Modifiable	
Vascular risks	Diabetes
	Hypertension
	Dyslipidemia
	Metabolic syndrome and obesity
	Cerebral hypoperfusion, stroke or cerebrovascular injury
Lifestyle-related	Smoking tobacco
	Depression
	Low cognitive reserve
	Excessive alcohol intake
	Low education level
	Social inactivity
Other	Severe head trauma or traumatic brain injury
	Hearing loss

(Atri 2019; Ngandu et al. 2015; Cummings et al. 2019; Lista et al. 2015; Xu et al. 2015)

Pathogenesis

The exact cause of AD is not entirely understood and is still under study and debate. The dominant theory for the development of AD is the amyloid cascade hypothesis. This is characterized by increased levels of Aβ and reduced clearance of the protein, leading to neuritic plaques that are found both intracellularly and extracellularly. Neurofibrillary tangles are also a hallmark of the disease. These are formed by hyperphosphorylated tau protein and are mainly located in the cortex. The plaques and tangles eventually lead to neuronal cell death, leading to a loss of cognitive function (Chu 2012; Jellinger & Bancher 1998; Hyman et al. 2012).

LOAD is associated with reduced clearance of plaques (Hardy & Selkoe 2002; Wavrant-DeVrièze et al. 1999; Zlokovic & Frangione 2013). Aβ is known to come in three basic forms: monomers, soluble oligomers, and insoluble fibrillar plaques (Goure et al. 2014; Lesné et al. 2013). The monomeric form of the protein has no known direct toxic effect.

The insoluble fibrillar plaques exhibit low levels of toxicity, the exact level of which is still debated (Mroczko et al. 2018). These insoluble plaques have long been the hallmark of AD and its original proposed cause (Lage 2006; Selkoe & Hardy 2016; Hardy & Selkoe 2002). More research has shown that the soluble form of Aβ is the more toxic configuration though (Goure et al. 2014; Mroczko et al. 2018; Dodart et al. 2002; Shankar et al. 2008; Lesné et al. 2006). Soluble Aβ aggregates form dimers, trimers, and oligomers which all account for neuronal dysfunction (Goure et al. 2014).

It has been proposed in a number of studies that monomeric Aβ combine to form soluble Aβ oligomers, which then further aggregate to form fibrillar plaques (Broersen et al. 2010; Morgado & Fändrich 2011). It is not yet determined if plaques and oligomers exist in equilibrium or apart (Benilova et al. 2012).

The oligomers are the most toxic form of the plaques. It has been proposed that the oligomers and not the fibrillar Aβ may be the early-acting toxic factors in the beginning stages of the disease (Mroczko et al. 2018). Supporting this theory is the finding that Aβ plaque levels do not correlate with AD severity in patients (McLean et al. 1999; Lue et al. 1999; Terry et al. 1991; Perrin et al. 2009). Fibrillar Aβ has even been found in the brains of non-demented patients. These patients had a lower oligomer-to-plaque ratio than mildly demented patients who also had fibrillar plaques (Selkoe & Hardy 2016). Furthermore, concentrations of Aβ oligomers in the cerebrospinal fluid (CSF) of AD patients do correlate with worsening cognitive test scores (Mroczko et al. 2018).

This does not mean that insoluble plaques are not toxic or play no pathogenic role in AD. Neurons in proximity to insoluble Aβ plaques show synaptic loss and elevated calcium levels. Plaques are also very hydrophobic, and their intracellular presence may invoke an inflammatory response that ultimately leads to neuronal damage (Benilova et al. 2012).

Their inevitable presence and accumulation suggest that these plaques may serve as a type of reservoir for soluble forms of Aβ (Haass & Selkoe 2007; Koffie et al. 2009). These reservoirs may act in two ways: disassembling when in the presence of lipids and leading to a higher concentration of soluble Aβ (Martins et al. 2008), and potentially also

acting as a removal mechanism for the same toxic soluble Aβ (Cheng et al. 2007; Baglioni et al. 2006; Treusch et al. 2009). This two-way mechanism is hypothesized to be based on certain physical limits of the plaques themselves. Once the plaques grow to a certain size, they start releasing soluble Aβ instead of sequestering it (Hong et al. 2014). The precise mechanism of fibril formation has not yet been fully established though (Goure et al. 2014).

The toxic soluble form of Aβ has been shown to reduce long-term potentiation (LTP) through synaptic binding (Cleary et al. 2005; Reed et al. 2011; Poling et al. 2008), enhance long-term depression (LTD), and reduce dendritic spine density in rodents (Shankar et al. 2008). They have also been shown to bind with high affinity to synapses of the hippocampus and the cerebrum (Moreth et al. 2013; Barghorn et al. 2005; Shughrue et al. 2010).

Soluble Aβ toxicity may be due to its hydrophobic surface binding and altering cell membranes (Campioni et al. 2010). They may also predispose neurons to the formation of tau aggregates, and cause neuronal signaling to dysfunction (Benilova et al. 2012; Mroczko et al. 2018).

Furthermore, soluble Aβ oligomers may cause excessive activation of N-methyl-D-aspartate (NMDA) receptors causing an influx of calcium into the cell and leading to excitotoxicity and eventual loss of synapses (Zhao et al. 2004). It has also been suggested that toxicity of soluble Aβ may be linked with impaired insulin receptors, and nerve growth factor (NGF) (De Felice et al. 2014; Yamamoto et al. 2007).

The buildup of Aβ plaque and tau tangles leads to the activation of the brain's immune system and neuroinflammatory responses. Oxidative stress, mitochondrial dysfunction, and disturbed homeostasis are all presumed to add to neuronal decline, neurotransmitter deficits, and cell death (Cummings 2004; García-Escudero et al. 2013; Hirai et al. 2001; Perez Ortiz & Swerdlow 2019; Bezprozvanny & Mattson 2008).

Neurofibrillary tau accumulation impairs intracellular transport as tau proteins are important to microtubules. In AD, tau aggregates and forms tangles inside the neurons, concentrating in the hippocampus, amygdala, and neocortical areas. The formation of

neurofibrillary tangles, oxidation and lipid peroxidation, and glutaminergic excitotoxicity are thought to the secondary to the Aβ plaques (Chu 2012).

One of the earliest pathological events in AD is the degeneration of acetylcholine-synthesizing neurons. Acetylcholine was the first identified neurotransmitter, and it is used by all cholinergic neurons (Ferreira-Vieira et al. 2016). These neurons are widely distributed throughout the brain, including the spinal cord, hindbrain, and striatum. Almost all regions of the brain are innervated by cholinergic neurons (Woolf & Butcher 2011).

Acetylcholine is a major neurotransmitter in the brain and plays a fundamental role in memory, learning, stress response, sleep, and attention (Mega 2000; Ferreira-Vieira et al. 2016). Human studies have shown that this cholinergic loss is presynaptic, the cholinergic neuron and its axon are degraded (Hampel et al. 2018). This neuronal loss, in turn, leads to a loss of nicotinic receptors and dysfunction in muscarinic receptors of the cerebral cortex (Hampel et al. 2018; Jiang et al. 2014). Nicotinic receptors are ligand-gated ion channels. Their primary role is to regulate the release of neurotransmitters (Ferreira-Vieira et al. 2016). Muscarinic receptors are G protein-coupled receptors that most often produce cell excitation, but they can also lead to inhibition depending on the cell type they are expressed in (Ferreira-Vieira et al. 2016). The loss of cholinergic neurons is likely caused by neurofibrillary tangles (Mesulam 2013). The resulting deficit in cholinergic transmission due to cholinergic neuronal loss has been postulated to lead to changes in cognition, behavior, and psychiatric symptoms (Ferreira-Vieira et al. 2016; Rosenberg et al. 2015).

Inflammation is also a pathological hallmark of AD. There are studies showing that the central nervous system (CNS) immune response results from systemic inflammation (Holmes & Butchart 2011; Rebeck 2017; Leonard 2007). Peripheral inflammation is signaled through the vagus nerve to the brain (Walker et al. 2019). This signaling results in modification of inflammation through acetylcholine secretion. Circulating cytokines and inflammatory mediators in the blood also activate perivascular macrophages, initiating the transcription of pro-inflammatory cytokines in the brain (Ek et al. 2001; Kaczmarczyk et al. 2017; Walker et al. 2019). And finally, these mediators interact with

lipid mediators that can communicate across the blood-brain barrier (BBB) (Ek et al. 2001). There is also evidence of a breakdown in the BBB in AD patients, increasing permeability and making the brain more susceptible to changes in peripheral inflammation (Holmes & Butchart 2011).

Systemic infection is the major cause of delirium in the elderly, which in turn has been associated with an increased risk of developing dementia (Dunn et al. 2005; Walker et al. 2019). Looking at retrospective data, the presence of one or more infections over a five year period increased the odds of developing AD by two-fold (Holmes & Butchart 2011; Tilvis et al. 2004). Other chronic and inflammatory conditions, such as depression, obesity, and atherosclerosis, have also been associated with increased risk of AD. Each taken on their own, these risk factors likely contribute a small effect, but the combined risks overtime might be substantial (Holmes & Butchart 2011; Tilvis et al. 2004).

In a healthy brain, microglia are down-regulated, and there is little to no detection of cell surface antigens such as major histocompatibility complex (MHC) class I and II (Perry & Gordon 1988). Following an injury or infection, these microglia activate to produce pro-inflammatory cytokines and increase their cell surface receptors. (Holmes & Butchart 2011) Studies have shown that MHC class II is found at higher levels on microglial cells in AD patients than controls (McGeer et al. 1989).

It is postulated that these immune responses are initiated to help prevent the accumulation of Aβ plaques. It has been shown that microglial cells concentrate around Aβ plaques more than around diffuse Aβ and phagocytose exogenous fibrillar Aβ (Ard et al. 1996).

There are also peripheral blood tests that can be used to detect systemic inflammation. Inflammatory proteins such as C-reactive protein (CRP) and Interleukin 6 (IL6) have been found in elevated levels five years before clinical diagnosis of AD (Engelhart et al. 2004; Tilvis et al. 2004).

Clinical Presentation

AD patients present with well-characterized cognitive dysfunction. The disease trajectory includes loss of memory, deteriorating cognitive function, deterioration of activities of daily living, deteriorating social functioning, and overall loss of quality of life. Common memory complaints include repeating questions and misplacing items (Chu 2012). Age of onset can be anywhere from 40 to 90, with EOAD resulting in earlier disease onset (Chu 2012).

Progressive decline eventually leads to a loss of abstract thinking, judgment, aphasia, personality changes, and aggression. With continued progression, the patient will lose the ability to make daily decisions and judgments, manage financial matters, and speech and comprehension will also disappear. Complete aphasia may be present at the severe stages of the disease, as well as the failure to recognize family members, frequently getting lost, inability to recognize common objects (agnosia), and an inability or unwillingness to perform familiar tasks (apraxia) such as putting on clothes (Chu 2012).

The clinical presentation and rate of decline vary from patient to patient. The disease may last anywhere from two to 20 years, with three to four years being the median (Chu 2012). As was the case with Auguste D., patients will often present with emotional, behavioral, or psychological changes. These can range from agitation, depressive mood, euphoria, anxiety, irritability, social withdrawal, apathy, sundowning, sleep disorders, suspiciousness, disinhibition, delusion, hallucinations, and repetitive behavior. These symptoms often become worse as the disease progresses.(Chu 2012; Palasí et al. 2015; Blenkinsop et al. 2020; Förstl & Kurz 1999)

Progressive weight loss is also a hallmark of the disease (Chu 2012).

Diagnosis

There is no definitive diagnostic test to diagnose Alzheimer’s in living patients. Instead, it is based on clinical judgment, ruling out, an extensive patient history, and a series of

tests including cognitive and blood work. With cognitive testing, there is commonly a deficit in two or more areas of cognition. It is essential to rule out other causes of cognitive decline as many disorders can present similarly to AD, especially other types of dementia. Vascular dementia, frontal lobe dementia, and Lewy body dementia should all be considered as differential diagnoses (Chu 2012).

Other conditions may also account for a patient's presentation of cognitive loss. B12, folate, thyroid issues, and red blood cell count should all be performed to help exclude these deficiencies (Chu 2012; Atri 2019). Other causes also include drug interactions and side effects from inappropriate prescribing of medications including anticholinergics and benzodiazepines (Szeto & Lewis 2016; Pfistermeister et al. 2017; Richardson et al. 2018). Further guidance for inappropriate prescriptions for elderly populations can be found in Beer's Criteria (American Geriatrics Society 2015 Beers Criteria Update Expert Panel 2015).

In 2011, the National Institute on Aging updated the diagnostic guidelines for diagnosing AD (McKhann et al. 2011). The work group's core clinical criteria include cognitive or behavioral symptoms that: 1) interfere with activities of daily living or function at work, 2) represent a decline from previous levels, 3) are not explained by delirium or other psychiatric disorder, 4) detectable cognitive impairment diagnosed through patient history and neuropsychological testing, and 5) impairment involves a minimum of two of the following domains, impaired ability to acquire new information, impaired reasoning and/or poor judgment, impaired visuospatial abilities, impaired language, and changes in personality, behavior or comportment (McKhann et al. 2011).

With new technology and testing, it is becoming possible to diagnose AD earlier in the clinical presentation. Research now shows that AD actually starts up to 20 years before clinical diagnosis (Chu 2012; Fjell et al. 2009; Hampel et al. 2008; Tondelli et al. 2012). Many patients have neuropathology that can be observed on MRI and PET scans 10 to 20 years before symptoms even appear (Chu 2012). Many patients have cortico-subcortical microhemorrhages that can be detected (Atri 2019; Attems et al. 2011).

MRIs and PET scans are increasingly being used to diagnose and confirm diagnosis of AD. Physicians use these imaging techniques to look for “biomarkers of neuronal injury” (Albert et al. 2011). For MRIs, these biomarkers include hippocampal or medial temporal lobe atrophy. PET scans look for temporoparietal/precuneus hypometabolism or hypoperfusion. (Albert et al. 2011) The clinical diagnostic accuracy of AD is very high, with studies reporting sensitivity levels of 81% and specificity at 70% (Knopman et al. 2001). Due to this high level of accuracy and the high cost associated with imaging tests, MRIs and PET scans offer only modest incremental benefits over clinical diagnosis for AD (Albert et al. 2019).

Even with the prohibitive costs, imaging tests are still routinely ordered when there is a suspected diagnosis of AD. Historically MRIs were used to rule out other neurological conditions that could potentially be treated surgically. With recent advances in imaging techniques, these types of tests are now also used to provide support for clinical diagnoses (Johnson et al. 2012).

Imaging is still recommended for clinical trials though, as many drugs in the testing phase aim to reduce Aβ and tau burden (Albert et al. 2019). MRIs and PET scans can serve as a valid marker to track disease progression and may have a higher level of precision than using cognitive scales alone (Frisoni et al. 2010).

There is also an early clinical phase of decline, or predementia phase referred to as mild cognitive impairment (MCI) (Albert et al. 2011). Of Americans older than 60, 16% have MCI, equaling about 11.6 million people (Atri 2019). These patients present with gradually progressive cognitive decline and are often still able to function in daily life. It can be difficult to distinguish between when a patient progresses from the predementia stage to inevitable dementia (Albert et al. 2011).

The National Institute on Aging workgroup also updated the diagnostic guidelines for the diagnosis of MCI due to AD in 2011 (Albert et al. 2011). The core clinical criteria for a diagnosis of amnestic MCI include concern regarding a change in cognition, impairment in one or more cognitive domains, preservation of independence, and cognitive changes

that are sufficiently mild so that there is no evidence of significant impairment in social or occupational functioning (Albert et al. 2011).

As with AD, it is important to rule out other disorders or diseases that could account for the decline in cognition (Albert et al. 2011; McKhann et al. 2011).

Current Pharmacological Treatments

While there is no cure for AD, there are pharmacological treatment options available that may improve symptoms and delay disease progression in the early to middle stages of dementia (Knowles 2006; Cummings 2004; Schneider & Sano 2009). The currently approved medications only address symptomatic (Cummings et al. 2017) issues, though, they are not disease-modifying treatments. As such, the current medications do not prevent, delay, slow progression, or target the underlying mechanisms of the disease.

Currently, there are five prescription medications approved in the United States for the treatment of AD. Four cholinesterase inhibitors, and one NMDA receptor agonist. Responses to these medications vary per individual, but studies suggest that cognition, activities of daily living, behavioral symptoms, and global clinical impression of change may improve in a minority of patients (10-30%) in the first six to twelve months (Atri 2019). There have also been studies showing that vitamin E may be an effective treatment to delay clinical worsening, but studies of vitamin E alone or in combination with other pharmacological treatments provide conflicting evidence (Farina et al. 2017; Morris et al. 2002; Engelhart et al. 2002; Gray et al. 2008; Luchsinger et al. 2003; Masaki et al. 2000). Vitamin E is included in some treatment guidelines to delay time to clinical worsening though (Atri 2019; Petersen et al. 2005; Knowles 2006; Doody et al. 2001).

Cholinesterase inhibitors were the first pharmacological options on the market. Tacrine was approved in 1993, donepezil (Aricept) in 1996, rivastigmine (Exelon) in 2000, and galantamine (Razadyne/Reminyl) was approved in 2001 (Knowles 2006). Memantine (Namenda), an NMDA receptor agonist, was the most recent in 2002 and remains the

sole medication in its class (Knowles 2006; Atri 2019). The standard care for patients in the mild to moderate stages of dementia are cholinesterase inhibitors (ChEIs), and patients in the moderate to severe stages are treated with memantine and donepezil (Szeto & Lewis 2016; National Institute for Health and Care Excellence 2011). There are no approved pharmacological treatments for MCI patients, and there is little evidence to suggest currently approved medications would slow progression or can prevent the development of dementia (Loy & Schneider 2006; Russ & Morling 2012).

ChEIs

Significant cholinergic deficits have been observed in neuropathological and imaging studies of Alzheimer's. These deficits are primarily seen in the hippocampus (Mega 2000; Perry et al. 1993).

Tacrine was the first approved medication for AD, but it has since fallen out of favor due to adverse events, including hepatotoxicity (Knowles 2006; Rabins 1997). Of the remaining three medications, all have demonstrated small to medium treatment effect (Atri 2019; Farlow & Cummings 2007).

Rivastigmine inhibits cortical acetylcholinesterase in the CNS and inhibits butyrylcholinesterase, which is the predominant cholinesterase in many of the regions affected by AD (Anand & Singh 2013). Galantamine has two major mechanisms, inhibiting cholinesterase as well as binding to nicotinic acetylcholine receptors to modulate ligand action (Anand & Singh 2013; Harvey 1995). These two medications have shown improvements on cognitive testing and global scales when compared to placebo, but the gains have been described as "small" (Knowles 2006).

Donepezil is a specific, and reversible selective cholinesterase inhibitor that delays the breakdown of acetylcholine released into synaptic clefts. By doing so, it enhances cholinergic transmission (Anand & Singh 2013). Improvements on this medication are often modest, but there is strong evidence that the medication does provide improvements in global outcomes and cognition in the first 12-24 weeks (Birks & Harvey

2018). There is little evidence to show that the effect on global outcomes is maintained beyond 24 weeks (Knowles 2006).

Improvements that result from taking donepezil are typically modest, although there is evidence of stabilization of cognitive and functional symptoms for a brief time which is a clinically significant outcome. Despite these effects, studies have not provided consistent results concerning the effects on patients' quality of life (Knowles 2006; Andersen et al. 2004).

Overall, ChEIs provide a stabilizing effect, but the clinical significance of this requires further investigation (Giacobini 2000). The optimal treatment duration is still under debate (Cummings 2004).

Memantine

Memantine is a non-competitive NMDA receptor antagonist with low to moderate affinity. It helps to modulate the flow of glutamatergic neuronal transmission and block the excitotoxic effects of overactive glutamatergic activity that may lead to neuronal dysfunction (Szeto & Lewis 2016; Cummings 2004). It was approved in 2003 for the treatment of moderate to severe AD and remains the only drug in its class for AD (Szeto & Lewis 2016; Knowles 2006; Danysz & Parsons 2003; Matsunaga et al. 2015). Memantine has a small, but detectable, effect on cognition in patients with moderate to severe AD (Szeto & Lewis 2016).

Studies show that memantine improved cognition, behavior, activities of daily living, and global function over six months or less. The effect size was small though and suggested limited clinical benefit. Only one non-industry sponsored trial showed that memantine was better than placebo at improving cognitive function (Matsunaga et al. 2015; Atri 2019; Howard et al. 2012).

There is no evidence that any current pharmacological monotherapy alters the course of AD. Even though some marginal aspects of improvement are seen, these benefits are not sustained (Atri 2019; Szeto & Lewis 2016; Sugino et al. 2015; Bond et al. 2012).

The development costs for CNS drugs are among the highest for any therapeutic area (Sugino et al. 2015). One reason for the low efficacy associated with the existing pharmaceutical options for AD may be that the trials conducted so far may not have been long enough (Arrowsmith & Miller 2013). A recent example of this can be found in the 2018 trial of BAN2401 (ClinicalTrials.gov 2014). This phase II trial was designed to run 18 months but was almost stopped after 12 when it failed to reach specified primary cognitive endpoints. After the full 18 months though, the drug did show a slowing of cognitive decline and increased Aβ clearance, but it has not been approved as of March 2019 (Sullivan n.d.). The Food and Drug Administration (FDA) recognized the need for improved trial efficiency and cost reduction (Sugino et al. 2015), but the question of who pays for extended trials remains.

The Cost of Care

Dementia is one of the most expensive conditions to society (Alzheimer's Association 2018). In the US, total payments for AD and other dementias is estimated at $277 billion for 2018 (Alzheimer's Association 2018). Medicare and Medicaid, US government run programs to provide healthcare coverage to individuals over 65 and those with a disability or low income, are expected to cover $186 billion of that cost, or 67% of the total healthcare and long-term care costs (Alzheimer's Association 2018). This still leaves patients and their families with a high out-of-pocket spending of $60 billion. An estimated $10,598 per person annually (Alzheimer's Association 2018).

The expected lifetime cost of care, including out-of-pocket, unpaid care, and US government spending, is $341,840 per person in 2017 (Alzheimer's Association 2018). In the last five years of life, a dementia patient is estimated to spend $350,725 compared to only $223,605 for people without dementia (Alzheimer's Association 2018). The cost of long-term care services are also more expensive for dementia patients, $48,028 annually compared to just $13,705 for those without dementia (Alzheimer's Association 2018). The cost of long-term care is expected to increase to over $1.1 trillion by 2050 (in 2018 dollars) if the trend continues (Alzheimer's Association 2018).

The cost of dementia care in the United Kingdom (UK) is also a burden that largely falls to patients. In 2014, the UK Alzheimer's Society published an updated report on the current costs and prevalence of dementia (Prince et al. 2014). They found that two-thirds of the cost of care is currently being paid by patients and their families (Prince et al. 2014). This is in stark contrast to other conditions where National Health System (NHS) covers the cost of care in total (Alzheimer's Society n.d.).

The UK Alzheimer's Society found that AD and dementia are costing the UK an estimated £26.3 billion a year (Prince et al. 2014), which breaks down to £32,250 per person. They found that the average cost for an individual with dementia is £100,000 over the course of the disease (Prince et al. 2014).

The total cost of unpaid care adds up to £11.6 billion, accounting for three-quarters of the total cost for people living with dementia in the community (Prince et al. 2014).

Drug costs are also a concern for patients in the US, averaging from $177 to over $400 per month (Consumer Reports 2012). In the UK, the NHS covers the cost of medications (see Table 2).

Table 2: Cost of AD Medications Per Year

	Donepezil	Galantamine	Memantine	Rivastigmine
US	$2436-$3,708	$2,124-$2,352	$3,192-$3,552	$2628-$3984
UK	£9.62-£109.98	£794.69-£1037.40	£19.36-£897.04	£75.40-£946.04

(Regional Drugs and Therapeutics Centre 2018; Consumer Reports 2012)

Several research groups have estimated the possible savings of delaying the onset of dementia (Galvin 2017; Jutkowitz et al. 2017; Zissimopoulos et al. 2014). One group found that if a treatment to delay onset by five years could be introduced by 2025 it would reduce total payments by 33% and out-of-pocket costs by 44% in the US (Jutkowitz et al. 2017). A three-year delay would reduce payments by 27%, and even a one-year delay would result in significant savings of around 14% (Zissimopoulos et al. 2014).

Why Current Treatments Are Not Enough

The process of developing and bringing a new AD drug to market is time-consuming, expensive, and fraught with failure. Drug development for AD has a 99.6% failure rate (Cummings et al. 2014; Sugino et al. 2015). These efforts are hindered by our incomplete understanding of the disease, the complex physiology, and multifactorial etiology, as well as the high level of comorbidity in an elderly population (Cummings 2004; Sugino et al. 2015). The high failure rate may also be partially attributed to starting pharmacological interventions too late in the disease, leading to the clinical failure of disease-modifying drugs going through the approval pipeline (Khoury et al. 2017).

Disease-modifying therapies have focused on Aβ plaques and neurofibrillary tau tangles. Aside from starting too late in the disease process, these drugs may also be failing because they are so narrowly focused on the amyloid cascade, ignoring the many other contributors to this complex, multifactorial disease. Even EOAD, which is heavily driven by genes related to Aβ and tau, the accumulation of these proteins and subsequent plaque and tangle formation does not occur without other pathophysiological system changes, such as oxidative stress, inflammation, and metabolic alterations (Lista et al. 2016; Hampel et al. 2012; Hampel et al. 2017).

The amyloid cascade theory has been challenged again and again with the repeating failure of clinical trials to modulate Aβ production or increase clearance (Doody et al. 2013; Salloway et al. 2014; Doody et al. 2014). It is increasingly clear that AD is influenced and caused by factors independent of Aβ and tau (Galvin 2017). Adopting a more integrative treatment approach targeting multiple physiological pathways is likely the key to achieving better outcomes.

It has recently been recognized that AD is a complex disease, and it not homogenous at all (J. Cummings et al. 2016; Lista et al. 2015; Reitz 2016). Instead, it is better thought of as a spectrum of neurodegenerative disease processes that manifest across an individual's lifetime and is influenced by a multitude of factors (Stephenson et al. 2015; McKhann et al. 2011). The mechanisms involved in AD are dynamic and involve a

complex interactive network of biological systems (Cummings et al. 2019; Mizuno et al. 2012). In fact, AD differs by patient in terms of risk factors, age of onset, presentation, progression, and pathology burden (Galvin 2017).

After over 100 years of research, there is still no monotherapy solution for AD. Many researchers now postulate that our myopic view of the disease, the traditional "reductionist approach" which aims to characterize single pathophysiological pathways affecting specific components is far over-simplified (Hampel et al. 2017; Stephenson et al. 2015). Traditional drug development focused on one "magic bullet" drug has proven ineffective.

It is time to shift our treatment approach to incorporate the heterogeneous nature of AD. As Galvin puts it in "Prevention of Alzheimer's disease: lessons learned and applied" (Galvin 2017), "Perhaps it is time to abandon generalized approaches to AD and consider neurodegenerative disorders as diseases of a lifetime and that there may be individualized ways to build a better brain as we age."

Multimodal Therapies: A Better Approach

Combination, or multimodal, therapies have been in use since the 1960s when a regimen of four chemotherapy drugs were first combined to improve remission rates of childhood leukemia (DeVita & Chu 2008). Since then, combination treatments have become the standard of care for many other diseases, including HIV, oncology, tuberculosis, and autoimmune disorders (Stephenson et al. 2015). Many of these conditions were once considered fatal, but are now treatable if not completely curable, with combination treatments (Stephenson et al. 2015).

It has become increasingly recognized in recent years that this type of multimodal approach could also benefit AD patients. Research is now shifting from treating patients in the dementia stage of the disease to ones in the early and presymptomatic stages (Isaacson 2017; Galvin 2017; J. Cummings et al. 2016). Drugs and other therapeutic approaches that were not effective on their own may provide additive benefits by nature

of addressing the multiple pathways and systems affected by and that lead to AD (Stephenson et al. 2015).

Because of the heterogeneous nature of AD, drugs that have only one target are not likely to produce measurable improvement. Instead, many biological systems must be addressed simultaneously for the successful treatment of AD (Cummings et al. 2019; Schmitt et al. 2004; Fessel 2017; Hampel et al. 2017).

This systematic approach is also referred to in the literature as “systems biology” (SB). SB aims to understand genotype-phenotype relationships and the mechanisms at the level of the genome and epigenome, transcriptome, microRNome, proteome, metabolome, microbiome, lifestyle, and environmental factors participating in the complex cellular networks (Lista et al. 2016; Hampel et al. 2012).

There are many risk factors for AD, many of which are modifiable (see Table 1). With the various risk factors and inherent differences in lifestyle and environment for individuals, each patient’s risk profile must be considered in an n-of-1 fashion instead of with a one-size-fits-all approach (Galvin 2017; Isaacson 2017). Commonly, medical treatments are designed for the average patient based on the best available evidence from carefully crafted trials. This does not match up with real life though. Grouping patients with individual risk profiles and AD variations into a single entity hides the small groups that may be responding to treatments (Reitz 2016; Galvin 2017).

Research and clinical studies have shown that AD is non-linear and dynamic; it is the result of many systems failures, signaling pathways, and pathophysiological processes (Lista et al. 2016). Treatments must be individualized to fit the symptoms, functional status, comorbidities, behaviors, and situation of every patient, as each will respond uniquely to different interventions (Cummings et al. 2015).

To address these individual needs, the best path forward for AD treatment is precision medicine (PM). PM utilizes an extensive clinical history, lifestyle, diet, environmental exposures, genomics, physical examinations, biomarkers, and cognitive performance to help craft the best approach for each patient on an individual basis (Schelke et al. 2016; Seifan & Isaacson 2015).

Precision Medicine

PM is an approach to disease treatment and prevention that takes into account individual variability in genes, environment, and lifestyle for each person (National Institutes of Health n.d.). According to the NIH, the focus of PM is on identifying which approaches will be effective for which patients, based on the individual (National Institutes of Health n.d.). At its heart, PM aims to tailor treatments for each patient based on their pathophysiological and clinical characteristics (US National Research Council 2011). The ultimate goal of PM is to improve the quality of patient care as well as clinical outcomes (Lyman & Moses 2016).

Along with the NIH, other government and research consortiums have started to recognize the importance of this growing area of research and disease treatment. In 2015, President Obama outlined the opportunities PM presents in his State of the Union Address. In this same speech, he also announced a national PM Initiative (The White House n.d.). The Alzheimer's Precision Medicine Initiative was also formed as an international collaboration of leading interdisciplinary clinicians and researchers to bring PM to the fields of neurology, psychiatry, and neuroscience (Hampel et al. 2017).

This is in sharp contrast to the traditional "one-drug-fits-all" approach. PM, however, does not mean that the drugs themselves are tailored to fit the person. This approach would not be sustainable or scalable. Instead, it is taking existing treatments and combining them in such a way as to systemically address an individual's needs. Patients all respond differently to therapeutics, and while this difference in response may not always be dramatic, it can now be taken into account with PM with the use of genetic screening, biomarkers, and phenotypic characteristics (Reitz 2016).

With the new technological developments and high-throughput screening methods, PM for complex diseases is becoming a reality. Physicians and researchers now have access to large-scale biological databases that track information, such as human genetic variation. Coupled with the advances in proteomics, metabolomics, transcriptomes, and genetic sequencing and the computational tools needed to

complete analyses of large data sets, we can address the multifactorial nature of complex diseases (Reitz 2016).

PM is made up of three key elements: stratification by risk, detection of pathophysiological processes early on, and alignment of the mechanism of action of intervention with an individual's molecular drivers of disease (Montine & Montine 2015). Thorough risk analysis requires that each individual's environment, lifestyle, and inherent risk be evaluated (Cholerton et al. 2016).

Given the complexities of AD that have been presented, it is highly unlikely that a single drug will be found to treat or cure the disease (Lista et al. 2016). Therefore, it becomes increasingly important to focus on prevention strategies and individualized treatment approaches. PM is beginning to be applied to AD in clinics across the US.

In 2012, the Alzheimer's Prevention Clinic (APC) at Weill Cornell Medicine was founded by Dr. Richard Isaacson (Seifan & Isaacson 2015). In 2014, the Alzheimer's Risk Assessment and Intervention Clinic at the University of Alabama in Birmingham was begun, quickly followed by the Alzheimer's Prevention Program at Cedars Sinai Medical Center in Los Angeles in 2015. In 2016, the APC and Research Center in San Juan, Puerto Rico opened (Isaacson 2017). Each of these programs applies the best available science to treat patients (Isaacson 2017), but none of them utilize software to enable their programs.

As Isaacson points out in "Is Alzheimer's prevention possible today" (2017), the most efficient way forward may be termed as "clinical precision medicine." An expanded medical history including neurodevelopment, academic trajectory, past, and current lifestyle patterns, and environmental exposures are combined with past medical history, physical and neurological examination, and then interpreted in combination with blood biomarkers, genetics, and cognitive performance. A comprehensive multidomain plan can then be made by cross-referencing each data point, and the patient followed longitudinally to evaluate the efficacy of the treatment (Isaacson 2017).

The long-term benefits from PM include: more extensive ability of doctors to use patient's genetic and molecular information as part of routine care, improved ability to

predict which treatments will work best for each patient, better understanding of the mechanisms driving diseases, and improved approaches to preventing, diagnosing, and treating a wide range of complex diseases (National Institutes of Health n.d.).

Modifiable Risk Factors

PM targets the underlying molecular and heterogeneous causes of disease by identifying a person's specific risk, their unique underlying pathophysiological processes, and then creating a preventative treatment plan, or a therapeutic intervention that is personalized to their identified molecular pattern of risk and disease process (Reitz 2016). Thus, PM allows a clinician to accurately identify the most effective intervention for each patient.

In 2014 AD experts estimated that about half of AD cases worldwide could be attributed to modifiable risk factors (Smith & Yaffe 2014). In 2017, it was estimated that up to one-third of cases could be prevented (Livingston et al. 2017). Many risk factors now fall into this preventable category (see Table 1), including cardiovascular risk, cerebrovascular, metabolic, psychiatric factors, diet, lifestyle, and education (Norton et al. 2014).

Even some risk factors that are considered unmodifiable, such as age, might be less powerful once other risks and comorbidities are addressed (Livingston et al. 2017). These addressable risk factors fall into every stage of life.

Early life

Autopsies have shown that not everyone with the neuropathological markers of AD shows clinical signs of the disease (Sonnen et al. 2011), indicating that some people may have resilience (Livingston et al. 2017). This has led researchers to conclude that individuals can build up cognitive reserve, allowing them to tolerate more neuropathy without experiencing cognitive decline. It is theorized that these individuals would eventually develop dementia if they lived long enough (Stern 2012).

This resilience in later life is likely due to the building of such a reserve in earlier life through education and other forms of cognitive and intellectual stimulation (Larson

2010). This theory of cognitive reserve also matches the findings that people who attain higher education levels have a lower occurrence of AD (Livingston et al. 2017). Advanced education is assumed to be associated with higher levels of cognitive reserve, therefore decreasing the impact of AD on cognitive function. This is even the case when individuals have genetic risk factors for AD (Lista et al. 2015; Ferrari et al. 2014). The opposite is presumed true for those who only attain lower levels of education, with a presumed vulnerability resulting from their lower educational attainment (Valenzuela & Sachdev 2006; Valenzuela 2008).

Midlife

Regular exercise in midlife has been linked to a lower risk of developing AD (Andel et al. 2008; Reiner et al. 2013; Cummings et al. 2015; Lista et al. 2015). It is postulated that exercise exerts a neuroprotective effect, possibly through the release of Brain-Derived Neurotrophic Factor (Vaughan et al. 2014; Leckie et al. 2014), which results in reduced cortisol levels and a lowered vascular risk (Livingston et al. 2017), More physical exercise is also associated with prolonged life after a diagnosis of AD (Scarmeas et al. 2011).

Cardiovascular risk factors are also important considerations in midlife. Elevated levels of cholesterol have been correlated with higher amounts of neurological amyloid deposits (Solomon et al. 2007). Hyperlipidemia is known to induce atherosclerosis, leading to an elevated risk of cardiovascular and cerebrovascular disorders (Kivipelto et al. 2001; Lista et al. 2015).

Hypertension has also been associated with a decline in cognition (Wysocki et al. 2012; Kivipelto et al. 2001; Lista et al. 2015). This risk factor appears to act in an age-dependent manner (Shah et al. 2012), and also increases the risk of other cardiovascular factors.

Hearing loss is also thought to add to the long-term risk of developing AD (Livingston et al. 2017). Even mild levels of hearing loss can increase an individual’s long-term risk. The exact mechanisms underlying this association are not fully understood. It has not

been established if correction with hearing aids could prevent or help delay AD onset (Livingston et al. 2017). It may be that hearing loss overtaxes an already vulnerable brain, leading to further degradation (McCoy et al. 2005). Alternatively, the risk may come from resulting social isolation after hearing loss (Huang et al. 2010; Gopinath et al. 2009).

Hearing loss may be separated into two categories: central and peripheral. Peripheral loss can be aided by the implantation of cochlear implants or hearing aids, while central hearing loss involves problems processing speech in the brain (Gates 2012). Central hearing loss may actually be a prodromal sign of AD, and would not be a modifiable risk factor (Gates et al. 2002).

Obesity, pre-diabetes, and metabolic syndrome are also risk factors for AD. These are characterized by insulin resistance and high levels of peripheral insulin, which is thought to decrease brain insulin production, impairing amyloid clearance (Luchsinger & Gustafson 2009). Increased inflammation and high blood glucose are also possible mechanisms through which diabetes may impair cognitive function (Yaffe 2007).

Late life

Cognitive training in later life, possibly even with a lack of early education, may improve cognitive function (Williams et al. 2010; Sitzer et al. 2006; Cummings et al. 2015). Physical activity also remains essential. Older adults who maintain a healthy exercise level are also more likely to maintain their cognitive levels. A meta-analysis found that physical activity has a significant protective effect against cognitive decline (Livingston et al. 2017).

Diabetes and metabolic syndrome also remain important considerations in late life (Tolppanen et al. 2013; Livingston et al. 2017). Both are associated with atherosclerosis and brain infarcts. Glucose-mediated toxicity can lead to microvascular abnormalities and neurodegeneration (Qiu et al. 2014; Livingston et al. 2017). Impaired insulin receptor activation has been found in AD (Frölich et al. 1998), which has led to the hypothesis that AD may represent an insulin-resistant brain state (Biessels et al. 2006).

Increasing inflammation and high blood glucose concentrations are also possible mechanisms by which diabetes impairs cognition (Yaffe 2007). Diabetes may also interact with other AD risk factors, resulting in an additive effect (Vagelatos & Eslick 2013).

Smoking has many known cardiovascular risks associated with it. These risks are likely what links smoking to an increased risk of developing AD (Livingston et al. 2017). Cigarettes also contain other neurotoxins that likely increase the risk as well (Swan & Lessov-Schlaggar 2007).

Depression has long been associated with AD. It is not yet known whether this is prodromal or an independent risk factor (Livingston et al. 2017; Byers & Yaffe 2011; Saczynski et al. 2010). If depression is a risk factor, the mechanisms behind it are likely to be multifactorial. Linking cardiovascular risk, stress, neuronal growth factor, and hippocampal volume (Alexopoulos 2003).

Many of these risk factors result in oxidative stress and inflammation. Both of which are associated with an increase in Aβ deposition (Casserly & Topol 2004). Vascular damage also results from many of the above risk factors. This is known to increase microvascular and macrovascular lesions, and lead to an increase in atrophy and neurodegeneration (Livingston et al. 2017).

Diet also plays a crucial role in late life. The Mediterranean diet, which is low in meat and dairy consumption, and high in fruit, vegetables, and fish, is known to reduce cardiovascular risk factors, plasma glucose levels, serum insulin, oxidative stress, and inflammation (Scarmeas et al. 2009). Multiple longitudinal studies show that those who have higher adherence to the Mediterranean diet also have reduced cognitive decline, lowered risk of progression from MCI to AD, and a reduction in all-cause mortality (V Solfrizzi et al. 2011; Vincenzo Solfrizzi et al. 2011; Singh et al. 2014). The Mediterranean diet may not only reduce the risk of AD but also have a positive impact on predementia syndromes and their advancement to AD (Lista et al. 2015).

There is also growing evidence that social isolation is also a late-life risk factor for AD. Social isolation results in a lack of cognitive activity, which has also been linked to

increased cognitive decline (Kuiper et al. 2015). Social isolation is also associated with an increased risk of hypertension (Yang et al. 2016), coronary heart disease (Hemingway & Marmot 1999), and depression (Santini et al. 2015).

As with central hearing loss, social isolation may also be a prodromal symptom (Livingston et al. 2017). The NIH and the National Institute for Health and Care Excellence (NICE) both now list social isolation as a risk factor for AD (Livingston et al. 2017).

In 2017, the Lancet formed an International Commission on Dementia Prevention and Care (Livingston et al. 2017). This commission looked at the current state of AD research, and their results suggest that 35% of dementia can be attributed to a combination of the risk factors listed above. In comparison, eliminating the risk from the APOE ε4 gene would only result in a 7% reduction (Livingston et al. 2017). It is clear from their findings that the modifiable risk factors need to be addressed at each stage of life, as early and completely as possible. The interconnectedness of these risk factors is also crucial. Just addressing one will not likely result in a measurable difference in disease progression or cognition. Each of these risk factors, both the modifiable ones and the nonmodifiable, are all interdependent and must be addressed systemically (Lista et al. 2015). PM can help achieve this goal, both by increasing preventative measures and helping clinicians address the disease systemically.

Multidomain Clinical Trials

Many clinical trials have been formed based on the study of modifiable risk factors. As previously stated, the most efficacious way to treat AD is to address multiple underlying factors simultaneously. The trials listed in Table 3 all addressed at least two modifiable risk factors for AD with at least 100 participants. Some were preventative trials in early dementia or even the presymptomatic stage, others recruited patients already diagnosed with dementia. Trials were identified on ClinicalTrials.gov and NCBI using the search terms “Alzheimer's,” “Dementia,” “multimodal,” or “multidomain.”

Of these trials, FINGER is the largest trial to-date that showed a multidomain intervention could improve or maintain cognitive status, and reduce the risk of cognitive decline over time (Ngandu et al. 2015). Overall, FINGER found that a multidomain treatment was feasible and safe for patients. Significant effects on overall cognition were noted, as well as secondary cognitive outcomes on executive functioning (83% higher) and processing speed (150% higher). The authors of the study acknowledged that the overall cognitive improvement level was small, and suggest that the results be interpreted in a public health context “in which small long-term effects on common disorders could have high relevance” (Ngandu et al. 2015).

Table 3 Multimodal clinical trials for AD

Trial name	Patient base	Target recruitment	Modifiable targets	Primary endpoint	Date range
Finnish Geriatric Intervention Study to Prevent Cognitive Impairment and Disability (FINGER)	60-77 yr old at-risk individuals	60-77 yr old at-risk individuals	Diet Exercise Cognitive training Vascular risk monitoring	Comprehensive neuropsychological testing	2009-2011
INnovative, Midlife INtervention for Dementia Deterrence (In-MINDD)	40-60 yr old at-risk individuals	40-60 yr old at-risk individuals	Modifiable dementia risk factors, individualized per patient	Change in dementia risk modification score	6 months
Multimodal Preventive Trial for Alzheimer's Disease (MIND-ADmini)	60-85 yr old prodromal AD	60-85 yr old prodromal AD	Nutritional guidance Exercise Cognitive training Monitoring and management of vascular Monitoring and management of metabolic risk factors	Feasibility of multimodal intervention	2019; 6 months
Mediterranean Diet, Exercise and Dementia Risk in UK Adults (MedEx-UK)	55-74 yr old subjective cognitive impairment	55-74 yr old subjective cognitive impairment	Physical activity Mediterranean diet	Increase in following Mediterranean diet using 14-point MEDAS scale; increase in physical activity	2020, 24 weeks

Trial name	Patient base	Target recruitment	Modifiable targets	Primary endpoint	Date range
Systematic Multi-domain Alzheimer's Risk Reduction Trial (SMARRT)	70-89 yr old with a score between 26-29 on Cognitive Abilities Screening Instruments	200	Physical activity Mental and social activity Cardiovascular risk factors Smoking Depressive symptoms Sleep Neuroprotective diet Decreasing harmful medications	Cognitive change as measured by Neuropsychological testing	2021
The Comparative Effectiveness Dementia & Alzheimer's Registry (CEDAR)	18+ yr old with family history of AD and no cognitive complaints, OR subjective cognitive	1000	Education Pharmacologic Non-pharmacologic	Change from baseline in Alzheimer's Prevention Initiative Cognitive Composite (APCC)	2016-2026
EMuNI Project: Multiple Nonpharmacological Interventions (EMuNI)	60-80 yr old with subjective cognitive decline	12	Nutritional supplements Diet Exercise Cognitive training	Neuropsychological test performance	2016-2017
Prevention of Dementia by Intensive Vascular Care (preDIVA)	70-78 yr old	3700	Hypertension Hypercholesterolemia Diabetes Weight reduction Smoking Exercise	Decreased incidence of dementia and reduced disability	2006-2009

Trial name	Patient base	Target recruitment	Modifiable targets	Primary endpoint	Date range
Multidomain Alzheimer Preventive Trial (MAPT)	70+ yr old at-risk individuals	1680	• Nutritional supplementation • Exercise • Cognitive stimulation • Nutritional counseling	Overall adherence and retention rate	2008-2011, 3 years
Healthy Ageing Through Internet Counselling in the Elderly (HATICE)	65+ yr old with two or more cardiovascular disease risk factors or history of cardiovascular disease	2600	• Self-management of vascular risk factors	Composite score of systolic blood pressure, low-density lipoprotein, and body mass index	2015-2018

Clinical Decision Support Software

Multidomain clinical trials are a step in the right direction to help prevent AD. With the multitude of possible risk factors and disease contributors though, each person will have a unique set of issues putting them on the path to AD. While many past and planned trials help to address some of these issues simultaneously, they do not take each patient's individuality into account, and they do not address everything that is driving the patient towards AD.

As Isaacson stated, "It may be most practical to provide patients with an individualized, detailed plan (fortified with qualifiers) for reducing the risk of dementia after an extensive evaluation of their medical history, lifestyle factors, body composition, laboratory, and cognitive assessments" (Isaacson 2017). As previously mentioned, the APC at Weill Cornell Medical College, which is run by Dr. Isaacson, offers patients a PM approach to delaying AD.

The clinic focuses on presymptomatic patients as well as those with prodromal AD. This target range was chosen because of the research that interventions at midlife can potentially slow or delay cognitive decline (Smith & Yaffe 2014). The APC utilizes multiple biomarkers to determine patients' pharmacogenomics, nutrigenomics, current cognitive state, inflammation levels, and lipid profile to tailor their individualized therapy. Health behaviors are also assessed to help identify any potentially modifiable risk factors for targeted intervention (Seifan & Isaacson 2015).

The physician then analyzes all these results to create the final treatment plan. Patients are also provided with educational tools to help modify behaviors (Seifan & Isaacson 2015).

This type of personalized approach to AD is important to maximize preventative strategies. However, it is not scalable. Many clinics do not have the time, or the expertise needed to create a personalized treatment plan that considers the multitude of factors that need to be addressed for each patient.

To help address these deficiencies in expertise and time, clinical decision support software (CDSS) can be used to provide patient-specific assessments and recommendations to aid in clinical decision making and help realize PM in clinics (Kawamoto et al. 2005). CDSS enables individual patients to be matched to a computerized knowledge base so that software algorithms can generate patient-specific information in the form of recommendations (Haynes et al. 2010).

CDSS are systems that “provide clinicians or patients with computer-generated clinical knowledge and patient-related information, intelligently filtered or presented at appropriate times, to enhance patient care” (Osheroff et al. 2005). These systems are designed to improve clinical care and decrease errors (Muro et al. 2017). Because it is software-based, CDSS can process large amounts of data in a quick, predictable, and repeatable manner.

The algorithms that make up the CDSS are based on formalized clinical practice guidelines (Muro et al. 2017). The guidelines are developed through a systematic review of evidence by experts in each field and are intended to optimize patient care (Institute of Medicine (US) Committee on Standards for Developing Trustworthy Clinical Practice Guidelines 2011). These guidelines are the same standard that any physician would use in their routine practice to help reduce variation, improve quality of care, and decrease costs (Hébert-Croteau et al. 2004).

With these guidelines as their decision-making base, CDSS’s recommendations are based on available best-evidence for each patient (Jaspers et al. 2011). Through computer reasoning, the software platforms can evaluate the data provided on each patient and execute the same decision-tree process that a trained physician would, but in a much faster and more predictable manner. Thus CDSS offers a way to improve medical standards, clinical efficiency, and patient safety (Jaspers et al. 2011; Kushniruk et al. 2013).

CDSS has been a topic of research for over 50 years (Kulikowski & Weiss 1982), and simple CDSSs are common in clinical use today. These systems can check input provided by clinicians, set alerts for out of range biomarkers in real-time, provide dosing

calculators, check for allergies, check drug-drug interactions, and even provide oxygen levels (O'Sullivan et al. 2014; Lyman et al. 2010; Saverno et al. 2011).

CDSS platforms are also increasingly integrated into electronic health records and computerized physician order entry systems (Jaspers et al. 2011). Combining these two technologies allows CDSS platforms to have quick access to patient information, reducing the amount of input needed from clinicians and therefore the time needed to create personalized treatment plans.

CDSS is particularly helpful when it comes to treating patients with complex disease states, such as AD. Utilizing this type of automated platform can allow even an inexperienced clinician to formulate a diagnosis based on the available data, and a subsequent treatment plan based on current guidelines (Jaspers et al. 2011). There is significant evidence that CDSS positively impacts patient care and healthcare providers' performance (Jaspers et al. 2011).

CDSS has even been tested against a clinician-only approach (Walker et al. 2017). In this comparative study, five subjects from the APC clinic were chosen to receive treatment plans from both the APC and from a CDSS platform. The APC compared an average of 334 data points per patient to create the treatment plans. The CDSS platform used over 1,000 (Walker et al. 2017). Given the complexity of PM and AD prevention, it is not surprising that algorithmic-based approaches can offer a more comprehensive set of therapeutic recommendations than a physician-based approach.

Complex CDSS platforms such as this are sometimes referred to as task-networks models (TNM) (Peleg 2013). TNM are artificial intelligence (AI) computer platforms that utilize computer-interpretable guidelines (CIGs) to execute knowledge against patient data, allowing the CDSS to provide patient-specific recommendations (Peleg 2013). These sophisticated algorithms use decision-making logic and if-then-else rules to decompose clinical guidelines into networks of component tasks that unfold over time (Peleg 2013).

This complexity inherent in the system enables these platforms to manage the many exceptions that arise with real patient data. The CDSS can identify the exception, and if

it has been programmed with the appropriate clinical guidelines, it will respond accordingly (Peleg 2013).

These exceptions are often categorized as obstacles or hazards. Obstacles prevent guidelines from being followed or achieving their intended effect. While hazards are likely harmful states that may be a threat to patient safety (Peleg 2013). The platform should notify the clinician of either case in the eventual output. Ideally, the system would be able to provide actionable steps to overcome obstacles and avoid hazards.

Complex CDSS platforms often use AI techniques such as rule-based systems, machine learning, and natural language generation to produce their output (Peleg 2013). These complex platforms can also use data mining techniques or statistical methods to reason about the classification or prediction of a disease or patient state. Patients' issues are often categorized by ontology, which "describes the concepts of medical terminologies and the relationship between them" (Aldosari et al. 2017). The sources of this ontological information include clinical practice guidelines and scientific papers related to the specific set of diseases and syndromes of interest (Peleg 2013). Each ontology is in turn related to a specified set of interventions that represent the corresponding treatment.

Patients' plans are then personalized by identifying their unique ontology or condition based on the inputted data and then personalizing their intervention plan based on their ontology. Comorbid conditions can also be considered; these would be integrated into a unified intervention plan (Peleg 2013).

Through these steps, CDSS can automatically identify key features important in the clinical classification of the patient and use mathematics to determine the optimal way in which treatment strategies should be combined (Greenes 2006; O'Sullivan et al. 2014). These complex CDSS platforms have been applied in a wide range of clinical decision-making problems, including prostate cancer diagnosis, screening for obstructive sleep apnea, and identification of psychiatric problems (Lee et al. 2010; Laporta et al. 2012; Suhasini et al. 2011). Their importance in clinical practice will only continue to grow as

high-volume data sets, genomic information, and PM continue to become common practice (Kawamoto et al. 2009).

Challenges in CDSS implementation

Despite its inherent ability for accuracy and documented impact on healthcare providers' performance, CDSS faces many challenges in the clinic. Particularly the platforms with more complex algorithms.

The first of these challenges is implementation. To realize PM, a large amount of data must be collected, translated to a machine-readable state, and input into the system. This can require more time and effort on the part of healthcare providers, and often interrupts their daily workflow (O'Sullivan et al. 2014).

Commonly used techniques in these more complex CDSS platforms include logistic regression, artificial neural networks, and support vector machines (O'Sullivan et al. 2014). Because of these advanced mathematical and non-linear transformations, it can often be difficult for clinicians to understand how the platform reaches a treatment conclusion. Some CDSS platforms that utilize neural networks and AI are referred to as using a "black-box" method due to their decision-making opacity (O'Sullivan et al. 2014). Further complicating this issue is that software engineers code these platforms. These software engineers are specialists in neural networks and AI, they are not experts in medicine like the clinicians. Many times, these engineers are developing software for complex clinical concepts that they may not fully understand in a global-patient context. Unlike the clinicians who have a deep understanding of the disease states but who do not understand the technologies and methods that construct the CDSS platforms (O'Sullivan et al. 2014).

In a more simplified, or mid-level CDSS system, such as those that check for drug-drug interactions, the decision-tree the platform goes through can be easily explained and comprehended. The mathematics and technology that contribute to CDSS's decision-making-logic and if-then-else rules for the complex systems though, the so-called "black-box" systems, are not so easily understood. However, the more complex systems

better mirror a clinician's actual decision-making process by integrating reasoning over multiple facets of patient data and computing likely outcomes for a specific patient state (O'Sullivan et al. 2014).

CDSS-enabled PM also requires more buy-in from patients as well. The complex analysis requires more time up front from the patient to gather data through clinical evaluations, biomarkers, and questionnaires. Also, the resulting multidomain treatment plan requires a bigger commitment from patients than taking a pill.

There is also a patient knowledge barrier. While clinicians concern of not understanding how the CDSS reaches treatment decisions, patients face an even more significant educational barrier as they do not have the medical training to understand the disease state or the potential benefits from the different treatment recommendations. It is therefore essential that patients are educated about multidomain interventions, and the requirements and time commitments needed to succeed with these treatment plans.

Regulation has also long complicated the CDSS field. For many years the FDA did not provide guidance on where CDSS fell; was it considered software or a medical device? In 2016, the 21st Century Cures Act was passed by Congress, removing CDSS from FDA regulation (114th Congress 2016). In 2017, the FDA further clarified CDSS's regulatory position by providing guidance that if a software platform meets four requirements, it is not classified as a device: 1) not intended to acquire, process, or analyze a medical image or a signal from an *in vitro* diagnostic device or a pattern or signal from a signal acquisition system, 2) intended for the purpose of displaying, analyzing, or printing medical information about a patient or other medical information (such as peer-reviewed clinical studies and clinical practice guidelines), 3) intended for the purpose of supporting or providing recommendations to a health care professional about prevention, diagnosis, or treatment of a disease or condition, and 4) intended for the purpose of enabling such health care professional to independently review the basis for such recommendations that such software presents so that it is not the intent that such health care professionals rely primarily on any of such recommendations to make a clinical diagnosis or treatment decision regarding an individual patient (114th Congress 2016).

CDSS is not intended to replace clinicians and their knowledge. Instead, it is meant to be a tool to help enable better patient care.

Expanding the Use Of CDSS

The potential use cases for CDSS expand beyond personalizing treatment plans. CDSS also has the capability to improve patient safety by reducing medical errors and improving the process of prescribing (Jia et al. 2016).

Medication errors are recognized as the single most preventable cause of patient harm (Lainer et al. 2013), making their reduction of singular importance. The British Medical Journal published a report on medical errors and found that they are the third-leading cause of death in the U.S.(Makary & Daniel 2016) Medication errors and adverse drug events (ADE) are both common and costly for patients (Kaushal et al. 2003).

CDSS can help ameliorate medication errors and promote patient safety because they follow current evidence-based clinical guidelines every time. They are not capable of making human error or mistakes. Because of this, these software platforms can be more widely employed to reduce harmful medication errors and improve healthcare system efficiency (Hemens et al. 2011; Berner 2009).

CDSS platforms can help clinicians tailor medication doses to individuals, discontinue inappropriate medications, better ensure long-term monitoring of medication use, as well as reduce the incidence of drug interactions (Alldred et al. 2013; Walton et al. 1999). CDSS can be especially useful when treating patients who have their own set of prescription guidelines, such as elderly populations.

Beers criteria are clinical medical guidelines for older adults that is kept up-to-date by the American Geriatrics Society. These criteria list out all potentially inappropriate medications for older populations. These are medications that have been found to cause poor health outcomes, including falls, confusion, and death (American Geriatrics Society 2015 Beers Criteria Update Expert Panel 2015). Knowledge-based CDSS can assist physicians in making sure that all medications they order are safe and follow Beers criteria guidelines (Bates & Gawande 2003).

The National Academies of Sciences, Engineering and Medicine observed that "A number of studies have shown that clinical decision support systems can improve the rates of certain desirable clinician behaviors such as appropriate test ordering, disease management, and patient care" (Committee on Diagnostic Error in Health Care et al. 2015). A meta-analysis of CDSS platforms in clinical use also indicated that CDSS can help improve patient outcomes (Hemens et al. 2011; Sahota et al. 2011; Nieuwlaat et al. 2011; Gillaizeau et al. 2013; Bayoumi et al. 2014; Pearson et al. 2009; Walton et al. 1999; Jia et al. 2016).

Inappropriate medication use is also a problem when it comes to AD patients specifically. Many prodromal and demented AD patients are placed on a large number of medications, which can be challenging to manage (Lau et al. 2010). This often results in errors, redundancies, and interactions. Because of these issues, many researchers and geriatric experts recommend additional pharmacological management when it comes to treating AD patients (American Geriatrics Society 2015 Beers Criteria Update Expert Panel 2015).

The initial step in this management is to eliminate redundancies and potentially dangerous medications (American Geriatrics Society 2015 Beers Criteria Update Expert Panel 2015). When patients are on five or more medications, referred to as polypharmacy, it can be difficult for their physicians to know all the medications their patients are taking. This is primarily due to the fact that patients are prescribed medications by different doctors, and the doctors do not have the full list of medications that others have prescribed (Bikowski et al. 2001; Garcia 2006). This can easily lead to duplicate prescriptions (Garcia 2006). Potentially dangerous medications for AD patients include those listed under the Beers criteria, and also anticholinergics which can cause cognitive impairment (Pfistermeister et al. 2017; Atri 2019).

Polypharmacy also significantly increases the risk of experiencing drug interactions (Lau et al. 2010). Dementia patients generally are on a higher number of medications than those without dementia, and as a patient's medication number increases, so does their likelihood of experiencing problems due to those medications (Lau et al. 2010).

Interactions are not the only concern these patients face though. A drug's side effects can also have serious health consequences. One of the more concerning side effects for AD patients is drug-induced depression. Depression has been shown to double a person's risk of developing dementia (Saczynski et al. 2010). Depression has long been associated with AD, but it is not yet known if it is a risk factor or a symptom of decline (Butters et al. 2008).

Drug-induced depression has been implicated as a side effect of numerous medications and medication classes (Rogers & Pies 2008). These include drugs that are commonly prescribed in older populations such as statins and beta-blockers (Chandragiri 2016).

CDSS has applications in all these medication issues. It can help improve safety and reduce medication-related interactions and side effects. Studies have shown that prevention of medication errors is most effective when targeting systems rather than individuals (Leape et al. 1995).

By combining medication management guidelines with PM treatment plans, CDSS has the potential to not only prevent or delay disease but also to significantly improve patient safety and clinicians' effectiveness.

Aims of the Research

The research presented here begins by exploring the molecular mechanisms of AD to gain a better understanding the disease. The experiments looked at the interplay between neurons, tau, amyloid precursor protein (APP), and Aβ in cognition and Aβ clearance. It also examines how these molecular mechanisms connect and manifest as phenotypic symptoms of AD.

As discussed in this introduction, Aβ is not the only or the primary target for AD treatment. Patients have multiple underlying risk factors that lead them to AD, from environmental, dietary, genetic, and even social factors (Atri 2019; Ngandu et al. 2015; Cummings et al. 2019; Lista et al. 2015; Xu et al. 2015).

My research began with trying to uncover the biological mechanisms and drivers of AD. The experiments presented here examine and provide insight to the neuronal and glial

clearance mechanisms of Aβ and potential targets to increase the elimination and degradation of Aβ and new techniques for in vivo, real-time analysis of APOE.

The findings also shed light on the complex mechanisms behind the documented neuronal hyperexcitability and excitotoxicity in AD, adding to knowledge of tau, APP, and Aβ's roles in hypersynchronicity and cognitive loss.

This research, along with the larger base of AD research worldwide, demonstrates that the mechanisms behind AD are complex and interconnected. AD is not a homogenous disease, but instead is a heterogenous disorder with multiple factors that converge to a common endpoint (Hampel et al. 2017; Galvin 2017; Reitz 2016; Livingston et al. 2017).

Based on these findings, my work then moved into the clinical realm, exploring how AI platforms could be used to address this complexity in a clinical setting. The clinical work combined previous mechanistic knowledge from my own research and the research that has been completed by others with PM to create personalized treatment plans for AD patients. By utilizing AI technology, we were able to help identify patients' underlying drivers of the disease to recommend treatments to address those drivers systematically, instead of the typical one-size-fits all approach.

With this base of information, I was then able to expand the use of the AI platform to explore polypharmacy and depression in an AD population with the aim of better equipping physicians to manage these patients' complex medication regimes.

Chapter 1: Neuronal Clearance of Amyloid-β by Endocytic Receptor LRP1

As discussed, Aβ is a hallmark of AD. It's accumulation, aggregation, and deposition is considered to be key factors in the neuronal degeneration associated with the disease (Goure et al. 2014; Lesné et al. 2013; Mroczko et al. 2018; Rodrigue et al. 2013; Hardy & Selkoe 2002; Selkoe & Hardy 2016). Aβ is associated with both EOAD as well as LOAD (Hardy & Selkoe 2002; Wavrant-DeVrièze et al. 1999; Zlokovic & Frangione 2013). Evidence suggests that a decrease in Aβ clearance is partially responsible for LOAD and that its production is greatly increased in EOAD (Bateman et al. 2006; Hardy & Selkoe 2002; Goedert & Spillantini 2006; Koffie et al. 2011).

Aβ is produced in neurons, which are also the cells most affected by its oligomerization and plaque formation (Zhang et al. 2011; Koffie et al. 2009; Hardy & Selkoe 2002; Gong et al. 2003; Jellinger & Bancher 1998). Aβ is found both internally in neurons as well as free in the cerebrospinal fluid (CSF) and the interstitial fluid (ISF) in gray and white matter (Hardy & Selkoe 2002; Selkoe & Hardy 2016; Cirrito et al. 2003). It is not clear how involved neurons are in the clearance of Aβ though.

To further understand the role of neurons in Aβ clearance, we performed *in vivo* and *in vitro* testing to see if the low-density lipoprotein receptor-related protein 1 (LRP1) plays a role in receptor-mediated endocytosis. We hypothesized that decreasing LRP1, which is a known endocytic receptor for Aβ, levels in neurons would lead to a significant reduction in the neuronal uptake of Aβ and subsequent Aβ clearance.

To test this, we first established the role of LRP1 in human neuroblastoma cells. Then amyloid model mice were bred with a conditional knock-out of LRP1 in their forebrains. Levels of Aβ and Aβ clearance were measured in real-time *in vivo* using microdialysis and brain slices were stained and analyzed.

My role in this research was to perform the *in vivo* microdialysis surgeries on the mice. After probes were inserted and the mice recovered, I was also responsible for collecting the ISF samples, and dosing the mice with Compound E at appropriate times. Once the

collection was through, I perfused the mice and dissected their brains for preservation and further testing.

This publication has been cited in 122 other publications, including publications in high-influence journals such as the Journal of Clinical Investigation (impact factor 13.251), Trends in Neurosciences (impact factor 17.755), and the Journal of Experimental Medicine (impact factor 10.790).

Neurobiology of Disease

Neuronal Clearance of Amyloid-β by Endocytic Receptor LRP1

Takahisa Kanekiyo,[1] John R. Cirrito,[2,3,4] Chia-Chen Liu,[1,5] Mitsuru Shinohara,[1] Jie Li,[1] Dorothy R. Schuler,[2] Motoko Shinohara,[1] David M. Holtzman,[2,3,4] and Guojun Bu[1,5]

[1]Department of Neuroscience, Mayo Clinic, Jacksonville, Florida 32224, [2]Department of Neurology, [3]Knight Alzheimer's Disease Research Center, and [4]Hope Center for Neurological Disorders, Washington University, St. Louis, Missouri 63110, and [5]Fujian Provincial Key Laboratory of Neurodegenerative Disease and Aging Research, Institute of Neuroscience, College of Medicine, Xiamen University, Xiamen 361005, China

Alzheimer's disease (AD) is the most prevalent form of dementia in the elderly population. Accumulation, aggregation, and deposition of amyloid-β (Aβ) peptides generated through proteolytic cleavage of amyloid precursor protein (APP) are likely initiating events in the pathogenesis of AD. While Aβ production is accelerated in familial AD, increasing evidence indicates that impaired clearance of Aβ is responsible for late-onset AD. Because Aβ is mainly generated in neurons, these cells are predicted to have the highest risk of encountering Aβ among all cell types in the brain. However, it is still unclear whether they are also involved in Aβ clearance. Here we show that receptor-mediated endocytosis in neurons by the low-density lipoprotein receptor-related protein 1 (LRP1) plays a critical role in brain Aβ clearance. LRP1 is known to be an endocytic receptor for multiple ligands including Aβ. Conditional knock-out of *Lrp1* in mouse forebrain neurons leads to increased brain Aβ levels and exacerbated amyloid plaque deposition selectively in the cortex of amyloid model APP/PS1 mice without affecting Aβ production. *In vivo* microdialysis studies demonstrated that Aβ clearance in brain interstitial fluid is impaired in neuronal *Lrp1* knock-out mice. Because the neuronal LRP1-deletion did not affect the mRNA levels of major Aβ degrading enzymes, neprilysin and insulin-degrading enzyme, the disturbed Aβ clearance is likely due to the suppression of LRP1-mediated neuronal Aβ uptake and degradation. Together, our results demonstrate that LRP1 plays an important role in receptor-mediated clearance of Aβ and indicate that neurons not only produce but also clear Aβ.

Introduction

Alzheimer's disease (AD) has emerged as the most prevalent form of late-life dementia in humans. Accumulation, aggregation, and deposition of amyloid-β (Aβ) peptides generated through proteolytic cleavage of amyloid precursor protein (APP) are major features of AD pathogenesis (Hardy and Selkoe, 2002, Blennow et al., 2006, Zheng and Koo, 2011). The toxic forms of Aβ aggregates, oligomers, and fibrils, injure synapses and neurons, which leads to synaptic dysfunction, neurodegeneration, and cognitive impairments (Hardy and Selkoe, 2002, Blennow et al., 2006, Koffie et al., 2011). The majority of AD cases are sporadic and late onset, and the disease is thought to be initiated by Aβ accumulation in the brain through an overall impairment in Aβ clearance (Mawuenyega et al., 2010). A major pathway through which Aβ is cleared from the brain is cellular uptake and subsequent degradation (Bu, 2009). Several studies have shown that endocytosed Aβ can be delivered to lysosomes for degradation (Mandrekar et al., 2009, Li et al., 2012). Recently, we have demonstrated that the low-density lipoprotein receptor-related protein 1 (LRP1) mediates Aβ cellular uptake by regulating its endocytosis in neuronal cells in culture (Kanekiyo et al., 2011). LRP1 is abundantly expressed in various brain cell types including neurons and glial cells in brain parenchyma, and smooth muscle cells and pericytes in cerebral vasculature to mediate cellular uptake of an array of ligands including APP, apolipoprotein E, α2-macroglobulin, and receptor-associated protein (RAP), all of which function in either Aβ production or clearance (Herz and Strickland, 2001, Bu, 2009). Furthermore, LRP1 can couple with other cell-surface signaling receptors to regulate signal transduction (Herz and Strickland, 2001).

Previous studies have shown that externally injected radioisotope-labeled Aβ is eliminated from the brain in mice in an LRP1-dependent manner (Shibata et al., 2000). Our recent study has also shown that conditional knock-out of the *Lrp1* gene in vascular smooth muscle cells exacerbated Aβ deposition in an amyloid mouse model (Kanekiyo et al., 2012). Despite increasing evidence to support important roles of LRP1 in Aβ metabolism, whether LRP1-mediated Aβ clearance plays a role in neurons *in vivo* is not clear. Here, using *Lrp1* conditional forebrain neuronal knock-out mice, we show definitively that LRP1 plays an impor-

Received Aug. 13, 2013; revised Oct. 3, 2013; accepted Nov. 1, 2013.

Author contributions: T.K. and G.B. designed research; T.K., J.R.C., C.-C.L., Mitsuru Shinohara, J.L., D.R.S., and Motoko Shinohara performed research; T.K., J.R.C., C.-C.L., Mitsuru Shinohara, J.L., D.R.S., Motoko Shinohara, D.M.H., and G.B. analyzed data; T.K., J.R.C., D.M.H., and G.B. wrote the paper.

This work was supported by National Institutes of Health (NIH) grants P01NS074969, R01AG027924, R01AG035355, and P01AG030128 (to G.B.); P01NS074969 and R01AG042513 (to J.R.C.); P01NS074969 and R37AG13956 (to D.M.H.); NIH Mayo Clinic ADRC pilot grant P50AG16574; and Mayo Clinic CRM Career Developmental Award (to T.K.). We thank Monica Castanedes Casey, Linda Rousseau, Virginia Phillips, and Dr. Dennis Dickson for histology and immunohistochemistry. We also thank Aurelie N'songo, Victoria Fasolino, Melissa C. Wren, and Caroline S. Casey for technical assistance and careful readings of this manuscript.

Correspondence should be addressed to either Guojun Bu or Takahisa Kanekiyo, Department of Neuroscience, Mayo Clinic, 4500 San Pablo Road, Jacksonville, Florida 32224, E-mail: bu.guojun@mayo.edu or kanekiyo.takahisa@mayo.edu.

DOI:10.1523/JNEUROSCI.3487-13.2013

 0270-6474/13/3319276-08$15.00/0

tant role in neuronal Aβ clearance in the brain. More importantly, we demonstrate that neurons are involved in both Aβ production and clearance.

Materials and Methods

Aβ peptides. Aβ42 and 5(6)-carboxyfluorescein (FAM)-Aβ42 were purchased from AnaSpec. Dry peptide was pretreated with neat trifluoroacetic acid, distilled under nitrogen, washed with 1,1,1,3,3,3-hexafluoro-2-propanol, distilled under nitrogen, and stored at −20°C. Aβ peptides were freshly dissolved in dimethylsulfoxide at 200 μM for each experiment.

Cell culture and LRP1-knockdown by siRNA. Human neuroblastoma NT2 cells were cultured in DMEM with 10% fetal bovine serum under standard culture conditions. Knockdown of LRP1 was performed as described previously (Li et al., 2003). Single-stranded, LRP1-specific, sense and antisense RNA oligonucleotides were synthesized by Ambion. Cells were transfected with siRNA (100 nM) using Lipofectamine 2000 (Invitrogen) according to the manufacturer's specifications and used for analysis 48 h after transfection.

Confocal microscopy. Cells were cultured on eight-well slides (Lab-Tek II Chamber Slide System; Nalge Nunc International) at 37°C for at least 24 h before experiments. After incubation with FAM-Aβ42 (1 μM) at 37°C for 24 h, fluorescence associated with Aβ was observed by confocal laser-scanning fluorescence microscopy (model LSM 510 invert; Carl Zeiss). LysoTracker (50 nM; Molecular Probe) was added 30 min before confocal imaging.

Animals and tissue preparation. Forebrain neuron-specific *Lrp1*-KO mice (*Lrp1* $^{-/-}$) were generated by breeding the *Lrp1* floxed mice with α-calcium-calmodulin-dependent kinase II (αCaMKII)-driven Cre recombinase mice (Liu et al., 2007). Littermates of male *Lrp1* $^{-/-}$ mice (*LRP1* $^{flox/flox}$, αCaMKII-*Cre* $^{+/-}$) or controls (*LRP1* $^{flox/flox}$, αCaMKII-*Cre* $^{-/-}$) with B6/C3H mixed background were used. Furthermore, amyloid model APP/PS1 (APPswe/PSEN1ΔE9) mice (Borchelt et al., 1997) were crossed with *Lrp1* $^{-/-}$ mice. Littermates of male APP/PS1 mice (APP/PS1, *Lrp1* $^{flox/flox}$, αCaMKII-Cre $^{-/-}$) and APP/PS1 mice lacking LRP1 in forebrain neurons, APP/PS1; *Lrp1* $^{-/-}$ (APP/PS1, *Lrp1* $^{flox/flox}$, αCaMKII-Cre $^{+/-}$) were used for analysis. After perfusion with PBS, brain tissues were dissected and kept frozen at −80°C until further analysis. Some brain tissues were fixed in 10% neutralized formalin for histological analysis. All animal procedures were approved by the Animal Study Committee at Mayo Clinic and in accordance with the regulations of the American Association for the Accreditation of Laboratory Animal Care.

Western blotting. Samples were lysed in PBS containing 1% Triton X-100 and protease inhibitor cocktail from Roche. Protein concentration was determined in each sample using a Protein Assay kit (Bio-Rad). An equal amount of protein for each sample was used for SDS-PAGE. Immunoreactive bands were detected and quantified using Odyssey Infrared Imaging System (LI-COR Biosciences). Rabbit polyclonal anti-LRP1 antibody was produced in our laboratory. Anti-APP C-terminal, sAPPα, and sAPPβ antibodies were purchased from IBL.

Aβ ELISA. For measurements of Aβ in APP/PS1 mouse brain, samples were sequentially homogenized in Tris-buffered saline (TBS), TBS buffer containing 1% Triton X-100 (TBS-TX), and then 5 M guanidine in 50 mM Tris-HCl, pH 8.0 (Youmans et al., 2011). Cell-associated Aβ levels were analyzed after being dissolved in guanidine in 50 mM Tris-HCl, pH 8.0. The levels of human Aβ40 and human Aβ42 were determined by ELISA as previously described (Shinohara et al., 2013) using an end-specific monoclonal antibody (13.1.1 for Aβ x-40 and 2.1.3 for Aβ x-42) and a horseradish peroxidase-conjugated detector antibody (Ab5, human Aβ 1–16 specific, all antibodies were produced in-house by the Mayo Clinic).

CTFβ ELISA. The levels of APP-CTFβ were determined by ELISA on TBS with 1% Triton X-100 fraction of the mouse bran lysates using a rabbit anti-C terminus of APP capture antibody (a gift from Dr. Pritam Das, Mayo Clinic) and biotin-conjugated 82E1 detector antibody (IBL-America). Synthetic peptides, consisted of 15 aa of N terminus of Aβ and 20 aa of C terminus of APP, were used as standards (Shinohara et al., 2013).

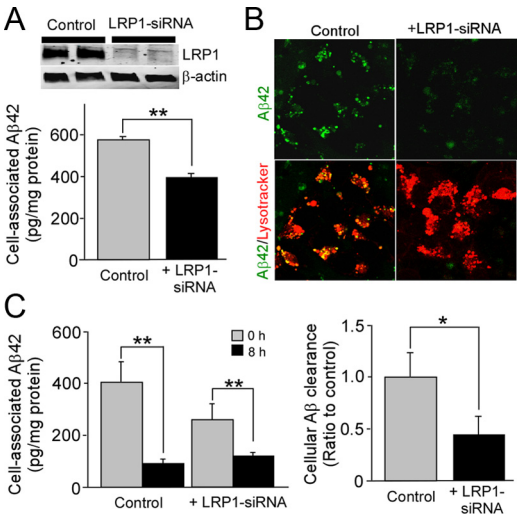

Figure 1. LRP1 mediates Aβ uptake and degradation in neuronal cells. ***A***, NT2 cells were transfected with LRP1-siRNA and used for analysis 48 h after transfection. Western blotting showed that LRP1 expression was suppressed by LRP1-siRNA. Cellular uptake of Aβ42 (1 μM) was analyzed by ELISA in control and LRP1-suppressed NT2 cells after incubation for 24 h. ***B***, Subcellular localization of internalized FAM-Aβ42 (1 μM) and its colocalization with lysosomal marker were observed by confocal microscopy in control and LRP1-suppressed NT2 cells after incubation for 24 h. ***C***, Control and LRP1-suppressed NT2 cells were allowed to internalize Aβ42 (1 μM) for 2 h at 37°C (gray bars); parallel cultures were washed and incubated for an additional 8 h in medium lacking Aβ42 (black bars) and analyzed by ELISA. The decrease of internalized Aβ after 8 h of incubation is estimated as cellular clearance. Data were plotted as mean ± SD ($n = 3$). *$p < 0.05$; **$p < 0.01$.

Immunohistochemical imaging and image processing. Paraffin embedded sections were immunostained using pan-Aβ antibody 33.1.1 (human Aβ1–16 specific), and visualized through the Dako Envision Plus visualization system (Chakrabarty et al., 2010). Immunohistochemically stained sections for pan-Aβ were captured using the ScanScope XT image scanner (Aperio Technologies) and analyzed using the ImageScope program (Chakrabarty et al., 2010). The final images and layouts were created using Photoshop CS2 (Adobe). Immunostained total Aβ plaque burdens in the cortex were calculated using the Positive Pixel Count program available with the ImageScope software (Aperio Technologies). All of the above analyses were performed in a blinded manner. For double immunostaining, deparaffinized sections were preincubated with citrate buffer (10 mM sodium citrate buffer with 0.05% Tween 20, pH 6.0) at 95°C for 20 min. They were incubated at 4°C overnight with a rabbit polyclonal anti-LRP1 antibody and a mouse monoclonal anti-NeuN antibody (Millipore) or a mouse monoclonal anti-GFAP antibody (Millipore), followed by Alexa488-conjugated anti-rabbit IgG (Invitrogen) and Alexa568-conjugated anti-mouse IgG (Invitrogen) for 2 h at room temperature. Rabbit polyclonal anti-LRP1 antibody was produced in our laboratory.

Reverse transcription and PCR. Total RNA was isolated from tissues or cells using RNeasy Mini Kit (Qiagen) and subjected to DNase I digestion to remove contaminating genomic DNA. Total RNA was dissolved in nuclease-free water and stored at −80°C. Reverse transcription was performed using a SuperScript II RNase H-reverse transcriptase (Invitrogen), and the reaction mix was subjected to quantitative real-time (qRT)-PCR to detect levels of the corresponding mouse actin, neprilysin (NEP) and insulin-degrading enzyme (IDE). The set of actin primers (Qiagen) was used as an internal control for each specific gene amplification. The relative levels of expression were quantified and analyzed by using Bio-Rad iCycler iQ software. The real-time value for each sample was averaged and compared using the CT method, where the amount of target RNA ($2^{-\Delta\Delta CT}$) was normalized to the endogenous actin reference (ΔCT) and related to the amount of target gene in tissue cells, which was set as the calibrator at 1.0. The primers used to amplify target genes by reverse transcription (RT)-PCR and qPCR were as follows: mouse

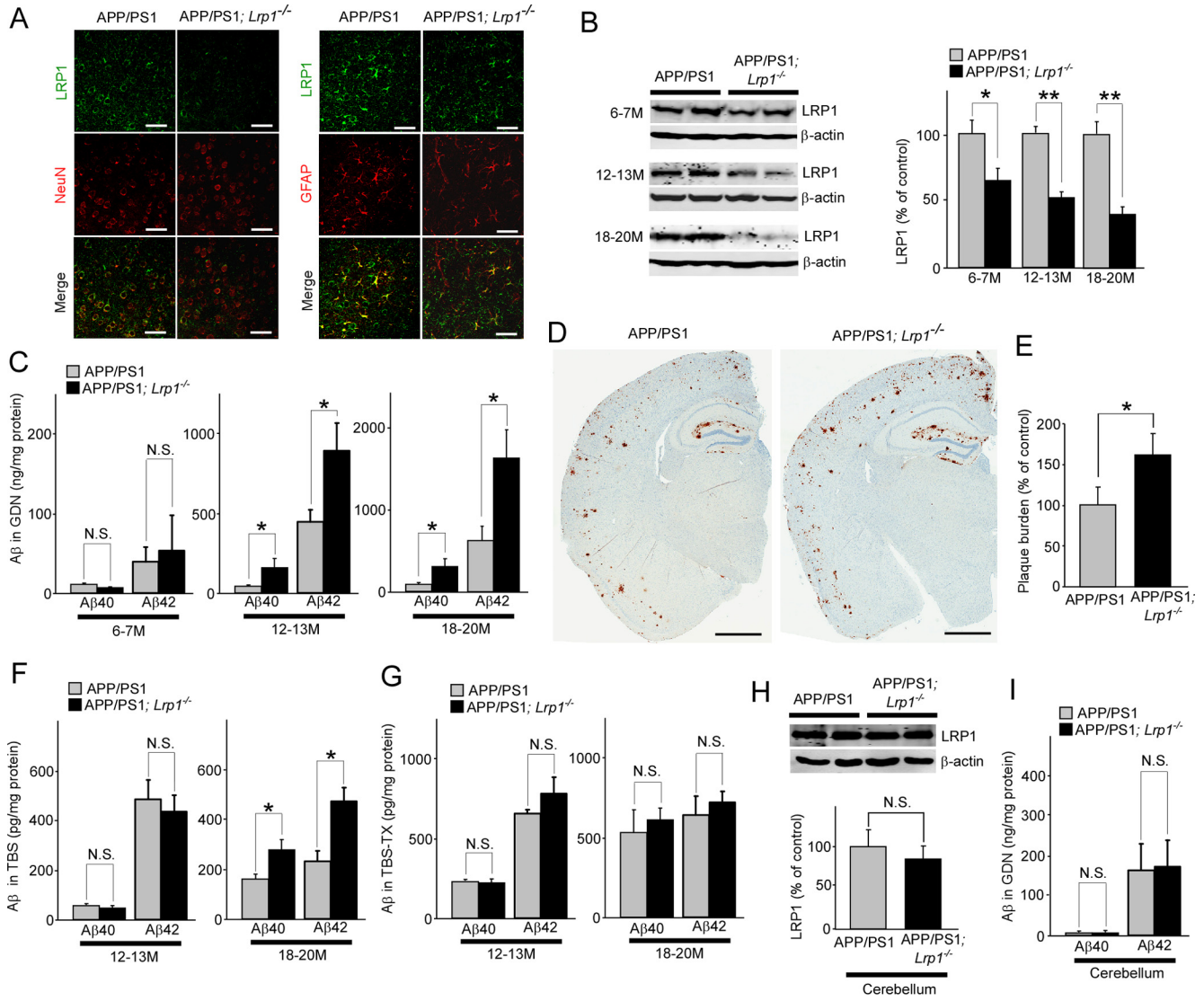

Figure 2. LRP1 deletion in neurons exacerbates Aβ deposition in the cortex of APP/PS1 mice. ***A***, Cortex from control APP/PS1 and APP/PS1; *Lrp1*$^{-/-}$ mice were costained with an LRP1 antibody and a neuronal marker NeuN or an astrocyte marker GFAP at 12 months of age. Scale bar, 50 μm. ***B***, LRP1 expression in cortex from APP/PS1 and APP/PS1; *Lrp1*$^{-/-}$ mice was detected by Western blot at 6–7 ($n = 4$–5), 12–13 ($n = 6$–7), and 18–20 months ($n = 5$–6) of age. ***C***, The concentrations of insoluble Aβ40 and Aβ42 levels in the cortex extracted in guanidine (GDN) from control APP/PS1 and APP/PS1; *Lrp1*$^{-/-}$ mice were analyzed by ELISA at 6–7 ($n = 4$–5), 12–13 ($n = 6$–7), and 18–20 months ($n = 5$–6) of age. ***D***, Aβ plaques in brain sections from control APP/PS1 and APP/PS1; *Lrp1*$^{-/-}$ mice (12–13 months of age) were immunostained with a pan-Aβ antibody. Scale bar, 1 mm. ***E***, Amyloid plaque burdens in the cortex from control APP/PS1 and APP/PS1; *Lrp1*$^{-/-}$ mice were quantified after scanning Aβ immunostaining by the Positive Pixel Count program (Aperio Technologies) at 12–13 months of age ($n = 6$–7). ***F***, ***G***, The concentrations of soluble Aβ40 and Aβ42 levels in the cortex extracted in TBS (***F***) and TBS-TX (***G***) from control APP/PS1 and APP/PS1; *Lrp1*$^{-/-}$ mice were analyzed by ELISA at 12–13 ($n = 6$–7) and 18–20 months ($n = 5$–6) of age. ***H***, ***I***, LRP1 expression in cerebellum from APP/PS1 and APP/PS1; *Lrp1*$^{-/-}$ mice was detected by Western blot at 12–13 months ($n = 4$), and the concentrations of insoluble Aβ40 and Aβ42 levels in the cortex extracted in GDN were analyzed (***I***). Data were plotted as mean ± SEM *$p < 0.05$; **$p < 0.01$. N.S., Not significant.

NEP-F (5′-GCA GCC TCA GCC GAA ACT AC-3′), mouse NEP-R (5′-CAC CGT CTC CAT GTT GCA GT-3′); and mouse IDE-F (5′-ACT AAC CTG GTG GTG AAG-3′), mouse IDE-R (5′-GGT CTG GTA TGG GAA ATG-3′).

In vivo microdialysis. *In vivo* microdialysis in APP/PS1 and APP/PS1; *Lrp1*$^{-/-}$ littermates was performed essentially as described previously (Cirrito et al., 2003, 2011). After microdialysis probes were inserted into the cortex, mice recovered for at least 6 h before experiments were performed. Microdialysis perfusion buffer consisted of 0.15% bovine serum albumin (Sigma) in artificial CSF. Basal level of interstitial fluid (ISF) Aβ40 was defined as the mean concentration of Aβ over 7.5 h before drug administration using a constant flow rate of 1.0 μl/min. Compound E (200 nM), a potent γ-secretase inhibitor (by AsisChem) was administered directly to the cortex through the microdialysis probe (reverse microdialysis) into each mouse to rapidly block Aβ production. After treatment with compound E, microdialysis samples were collected every 60 min for 5 h and assayed for Aβ40 by sandwich ELISA similar to (Cirrito et al., 2011), where mHJ2 (mouse-anti-Aβ35–40) was used as the capture antibody and biotinylated mHJ5.1 (mouse-anti-Aβ13–28) as the detection antibody. The half-life of ISF Aβ40 was calculated from the slope of the semilog plot of percentage change in Aβ versus time (Cirrito et al., 2003).

Statistical analysis. All quantified data represents an average of samples. Statistical significance was determined by two-tailed paired Student's *t* test, and $p < 0.05$ was considered significant.

Results

LRP1 mediates Aβ metabolism in neuronal cells

To determine the roles of LRP1 in Aβ metabolism in human neuroblastoma NT2 cells, we first examined if LRP1 knockdown

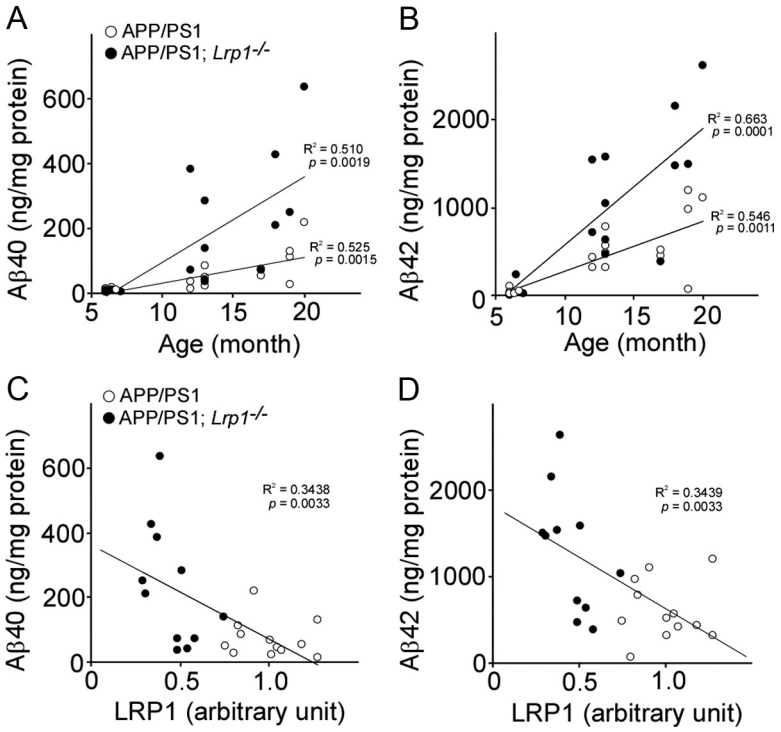

Figure 3. Association of Aβ levels with age and LRP1 in the cortex of APP/PS1 and APP/PS1; $Lrp1^{-/-}$ mice. ***A***, ***B***, The correlations of insoluble Aβ40 (***A***) and Aβ42 (***B***) levels in cortex with age are plotted. APP/PS1 ($n = 16$) and APP/PS1; $Lrp1^{-/-}$ mice ($n = 16$) were analyzed at 6–20 months of age. ***C***, ***D***, The correlations of insoluble Aβ40 (***C***) and Aβ42 (***D***) levels with LRP1 levels in the cortex are plotted. APP/PS1 ($n = 12$) and APP/PS1; $Lrp1^{-/-}$ mice ($n = 11$) were analyzed at 12–20 months of age. LRP1 levels were quantified by Western blot and normalized to β-actin. Data were plotted as the ratios to mean value of control APP/PS1 mice. The correlation coefficient (R^2) and p values are shown in the graph.

by siRNA affects cellular Aβ uptake (Fig. 1*A*). We incubated control and LRP1-suppressed NT2 cells with Aβ42 for 8 h. ELISA revealed that cell-associated Aβ42 levels were significantly decreased in LRP1-suppressed cells (Fig. 1*A*). Consistent with our ELISA results, we observed less internalized Aβ in LRP1-suppressed NT2 cells in the lysosomal compartments by confocal microscopy when cells were incubated with FAM)-Aβ42 for 24 h (Fig. 1*B*). To determine whether internalized Aβ is degraded, NT2 cells were incubated with Aβ42 for 2 h at 37°C. The Aβ-containing media were then replaced with medium without Aβ, and the cells were incubated for an additional 8 h before analysis of cell-associated Aβ42 by ELISA. The internalized Aβ was cleared following 8 h of incubation in both control and LRP1-suppressed NT2 cells (Fig. 1*C*). When Aβ clearance was calculated under each condition, we found that it was decreased in LRP1-suppressed NT2 cells compared with control cells (Fig. 1*C*). These results demonstrate that LRP1 mediates Aβ uptake and subsequent degradation in neuronal cells.

Conditional knock-out of *Lrp1* in forebrain neurons exacerbates Aβ deposition in the cortex of amyloid model mice

We have previously generated forebrain neuron-specific LRP1-knock-out ($Lrp1^{-/-}$) mice by breeding the *Lrp1* floxed mice with αCaMKII-driven Cre recombinase mice (Liu et al., 2007). To examine the effect of LRP1 deletion in neurons on Aβ metabolism *in vivo*, the $Lrp1^{-/-}$ mice were further crossed with amyloid model APP/PS1 mice (Borchelt et al., 1997). We compared amyloid plaque deposition and Aβ levels between littermates of control APP/PS1 and APP/PS1 mice lacking LRP1 in forebrain neurons. First, the brain sections of those mice were stained with an LRP1-specific antibody at 12 months of age. In cortex, LRP1 was abundantly expressed in neurons and to a lesser extent in glial cells in APP/PS1 mice (Fig. 2*A*). LRP1 appears to be deleted specifically in neurons in APP/PS1; $Lrp1^{-/-}$ mice (Fig. 2*A*). Western blotting also confirmed that the LRP1 level in cortex from APP/PS1; $Lrp1^{-/-}$ mice was significantly reduced compared with APP/PS1 mice in an age-dependent manner (Fig. 2*B*). The remaining LRP1 expression in APP/PS1; $Lrp1^{-/-}$ mice likely represents those in glial cells and in cells making up vasculature. ELISA demonstrated that the concentrations of insoluble Aβ40 and Aβ42 in the guanidine fractions were significantly higher in APP/PS1; $Lrp1^{-/-}$ mice than APP/PS1 mice, when they were analyzed at 12–13 and 18–20 months of age, although there was no significant difference at 6–7 months of age (Fig. 2*C*). Consistent with increased insoluble Aβ levels, Aβ deposition in the cortex of APP/PS1; $Lrp1^{-/-}$ mice was significantly higher than that of control APP/PS1 mice at 12–13 months of age (Fig. 2*D*,*E*). While the soluble Aβ40 and Aβ42 levels in the TBS fractions were increased in the cortex from APP/PS1; $Lrp1^{-/-}$ mice compared with APP/PS1 mice at 18–20 months of age, we did not detect any significant difference at 12–13 months of age (Fig. 2*F*). In addition, there was no significant difference in the detergent-soluble Aβ40 and Aβ42 levels in the TBS-TX fractions between APP/PS1 and APP/PS1; $Lrp1^{-/-}$ mice both at 12–13 and 18–20 months of age (Fig. 2*G*).

Insoluble Aβ levels were increased in an age-dependent manner in those mice. When the correlations of insoluble Aβ40 (Fig. 3*A*) and Aβ42 (Fig. 3*B*) levels in cortex with age (6–20 months) were analyzed, significant positive correlations were detected for both Aβ40 ($R^2 = 0.525$, $p = 0.0015$) and Aβ42 ($R^2 = 0.510$, $p = 0.0019$) in APP/PS1 mice ($n = 16$). Similarly, APP/PS1; $Lrp1^{-/-}$ mice ($n = 16$) also showed positive correlations of Aβ40 ($R^2 = 0.546$, $p = 0.0011$) and Aβ42 ($R^2 = 0.663$, $p = 0.0001$) with age. The age-dependent increases of Aβ levels are higher in APP/PS1; $Lrp1^{-/-}$ mice compared with controls in these scatter plots, suggesting a protective role of LRP1 against age-dependent increases of insoluble Aβ (Fig. 3). We next assessed whether LRP1 levels in the cortex correlate with Aβ levels in aged APP/PS1 mice (12–20 months of age, $n = 12$) and APP/PS1; $Lrp1^{-/-}$ mice ($n = 11$). LRP1 levels were quantified by Western blotting. When correlations of insoluble Aβ40 (Fig. 3*C*) and Aβ42 (Fig. 3*D*) levels in the cortex from both APP/PS1 mice and APP/PS1; $Lrp1^{-/-}$ mice with LRP1 levels were plotted, significant inverse correlations were detected for both Aβ40 ($R^2 = 0.344$, $p = 0.0033$) and Aβ42 ($R^2 = 0.344$, $p = 0.0033$). Since LRP1 was specifically deleted in forebrain neurons in $Lrp1^{-/-}$ mice (Liu et al., 2010), the expression level of LRP1 in the cerebellum of APP/PS1; $Lrp1^{-/-}$ mice was not changed (Fig. 2*H*). Accordingly, we did not detect any differences in insoluble Aβ40 and Aβ42 levels in this brain region at 12–13 months of age (Fig. 2*I*). To examine whether LRP1

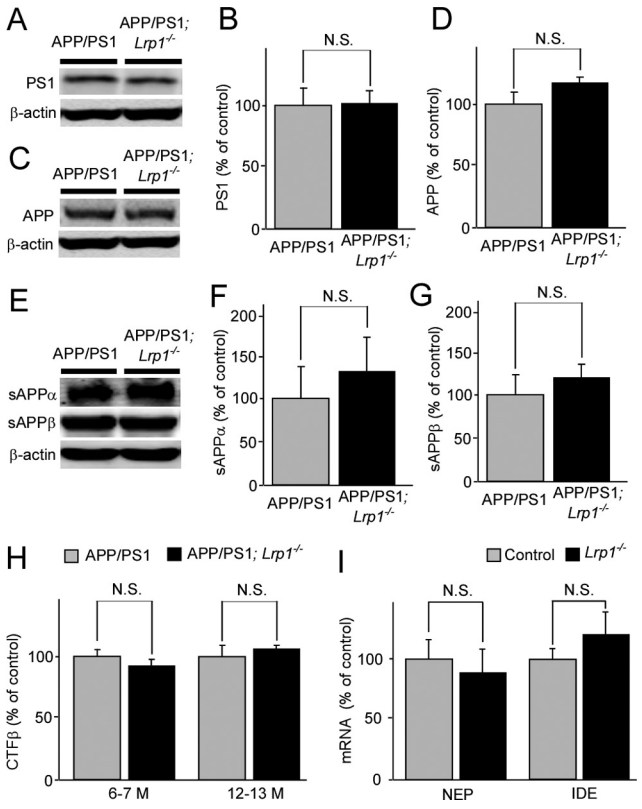

Figure 4. LRP1 deletion in neuron does not affect APP processing and mRNA levels of NEP and IDE. ***A–G***, Levels of PS1 (***A***, ***B***), full-length APP (***C***, ***D***), sAPPα (***E***, ***F***), and sAPPβ (***E***, ***G***) were analyzed by Western blot in both APP/PS1 and APP/PS1; *Lrp1*$^{-/-}$ mice at the age of 12–13 months ($n = 5$). ***H***, CTFβ levels were analyzed by ELISA at the age of 6–7 ($n = 5$) and 12–13 months ($n = 5$). ***I***, The mRNA levels of two major Aβ degrading enzymes, NEP and IDE, in the cortex from control and *Lrp1*$^{-/-}$ mice were quantified by RT-PCR at the age of 12 months. Data are plotted as mean ± SEM ($n = 6$). N.S., Not significant.

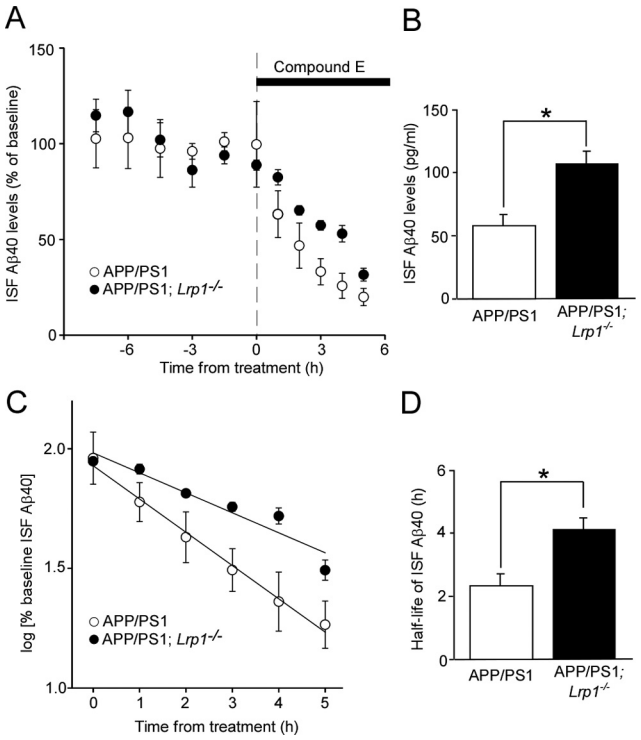

Figure 5. LRP1 deletion in neurons suppresses cortical ISF Aβ clearance in APP/PS1 mice. ***A***, ***B***, APP/PS1 and APP/PS1; *Lrp1*$^{-/-}$ mice were analyzed at the age of 8–10 months. The mice were treated with a γ-secretase inhibitor compound E, and the cortical ISF levels of Aβ40 were monitored for 5 h (***A***) after a baseline of cortical ISF Aβ40 levels was achieved through 7.5 h monitoring (***B***). ***C***, ***D***, The common logarithm of percentage baseline ISF Aβ40 concentrations versus time were plotted (***C***). The slope from the individual linear regressions from log [% ISFAβ40] versus time for each mouse was used to calculate the mean half-life ($t_{1/2}$) of elimination for Aβ from the ISF (***D***). Data were plotted as mean ± SEM ($n = 4–5$) *$p < 0.05$.

deletion in neurons affects APP processing, PS1 levels and APP processing products in both APP/PS1 and APP/PS1; *Lrp1*$^{-/-}$ mice were analyzed. There were no significant differences in the levels of PS1 (Fig. 4*A*,*B*), full-length APP (Fig. 4*C*,*D*), and soluble forms of APP (sAPPα and sAPPβ; Fig. 4*E–G*) between APP/PS1 and APP/PS1; *Lrp1*$^{-/-}$ mice when analyzed by Western blotting at 12–13 months of age. Specific ELISA also did not detect any significant differences in APP C-terminal fragments β (CTFβ) levels between these mice both at 6–7 and 12–13 months of age (Fig. 4*H*), indicating that LRP1 expression in these aged mice does not significantly affecting APP processing.

LRP1 deletion in neurons suppresses Aβ clearance in the cortex of amyloid model mice

Having demonstrated that LRP1 deletion in neurons leads to increased insoluble Aβ and amyloid plaque deposition without affecting APP processing, we analyzed the mRNA levels of NEP and IDE, which are major Aβ degrading enzymes in the brain, in the cortex of control and *Lrp1*$^{-/-}$ mice (Fig. 4*I*). The qRT-PCR showed no significant differences in the mRNA levels of these enzymes in our experimental mice. Next, we directly assessed the roles of neuronal LRP1 in Aβ clearance. To measure the half-lives of Aβ clearance, we used *in vivo* microdialysis in the cortex of APP/PS1; *Lrp1*$^{-/-}$ mice and APP/PS1 littermates at 8–10 months of age. Soluble Aβ in ISF, which is exchangeable across a 38 kDa dialysis membrane, has been shown to be significantly correlated with the levels of total soluble Aβ present in extracellular pools of the brain (Cirrito et al., 2003, 2011). We infused a potent γ-secretase inhibitor directly into the cortex of APP/PS1 and APP/PS1; *Lrp1*$^{-/-}$ mice to rapidly block Aβ production, thus allowing sensitive measurement of the elimination rate of Aβ from the ISF (Fig. 5*A*). ISF Aβ level gradually decreased in a time-dependent manner after treatment of γ-secretase inhibitor, where APP/PS1; *Lrp1*$^{-/-}$ mice showed a slower decline compared with control APP/PS1 mice (Fig. 5*C*,*D*). The half-life of elimination from the ISF for Aβ40 was calculated as 2.4 and 4.2 h in APP/PS1 mice and APP/PS1; *Lrp1*$^{-/-}$ mice, respectively (Fig. 5*C*). These results indicate that deletion of LRP1 in neurons significantly suppresses the elimination of soluble Aβ from the ISF. In addition, the higher baseline concentration of ISF Aβ40 was detected in APP/PS1; *Lrp1*$^{-/-}$ mice, which is likely due to disturbed Aβ clearance in the cortical extracellular space (Fig. 5*B*). Together, these results indicate that LRP1 deletion in forebrain neurons exacerbates Aβ deposition through a disturbance of cellular Aβ clearance rather than affecting the levels of Aβ degrading enzymes.

LRP1 deletion in neurons does not affect insoluble Aβ levels in the hippocampus of amyloid model mice

We further assessed the effects of neuronal LRP1 deletion on insoluble Aβ levels in the hippocampus of APP/PS1 mice. As expected, LRP1 is highly expressed in CA1 neurons and to a lesser extent in glial cells in the hippocampus (Fig. 6*A*). Neuronal LRP1 was specifically suppressed in APP/PS1; *Lrp1*$^{-/-}$ mice at 12 months of age (Fig. 6*A*). Western blotting confirmed that LRP1

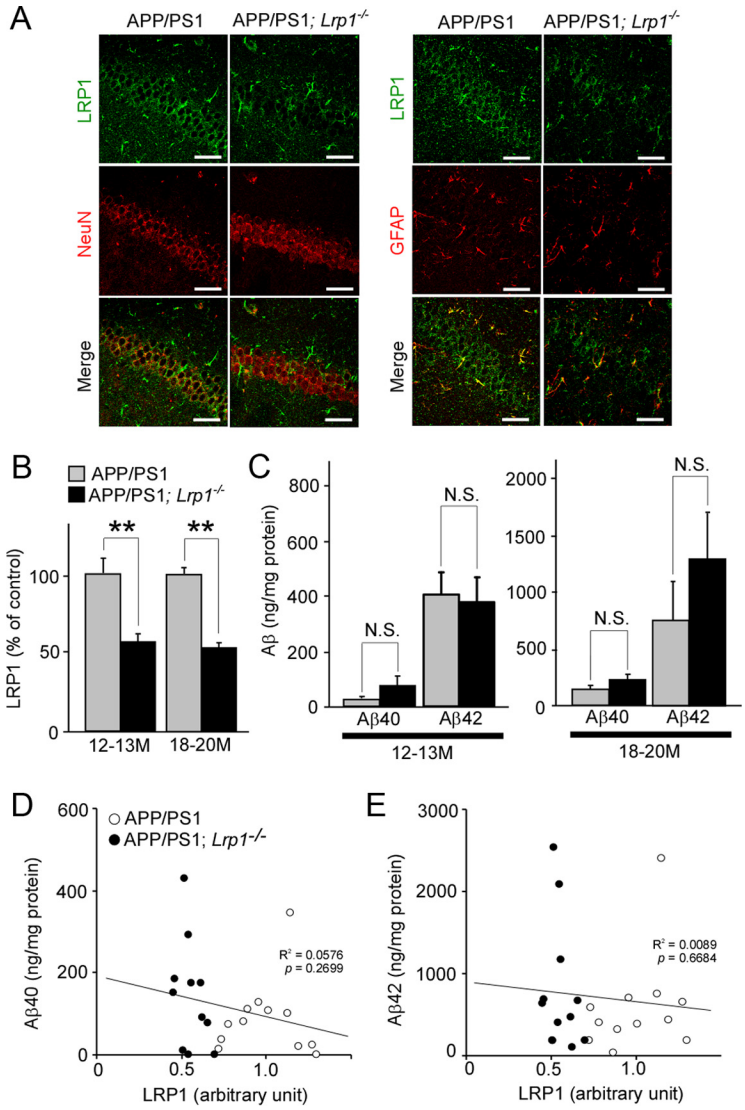

Figure 6. LRP1 deletion in neurons in APP/PS1 mice does not affect Aβ levels in the hippocampus. ***A***, Hippocampus from control APP/PS1 and APP/PS1; *Lrp1*$^{-/-}$ mice were costained with an LRP1 antibody and a neuronal marker NeuN or an astrocyte marker GFAP at 12 months of age. Scale bar, 50 μm. ***B***, LRP1 expression in the cortex from APP/PS1 and APP/PS1; *Lrp1*$^{-/-}$ mice was detected by Western blot at 12–13 ($n = 6–7$) and 18–20 months ($n = 5–6$) of age. ***C***, The concentrations of insoluble Aβ40 and Aβ42 levels in the hippocampus from control APP/PS1 and APP/PS1; *Lrp1*$^{-/-}$ mice analyzed by ELISA at 12–13 ($n = 6–7$) and 18–20 months ($n = 5–6$) of age. Data were plotted as mean ± SEM; $^{**}p < 0.01$. N.S., Not significant. ***D***, ***E***, The correlations of insoluble Aβ40 (***D***) and Aβ42 (***E***) levels with LRP1 levels in the hippocampus are plotted. APP/PS1 ($n = 12$) and APP/PS1; *Lrp1*$^{-/-}$ mice ($n = 11$) were analyzed at 12–20 months of age. LRP1 levels were quantified by Western blot and normalized to β-actin. Data were plotted as the ratios to mean value of control APP/PS1 mice. The correlation coefficient (R^2) and *p* values are shown in the graph.

expression in the hippocampus of APP/PS1; *Lrp1*$^{-/-}$ mice was significantly reduced (Fig. 6*B*). However, different from the results of cortex, we found that the concentrations of insoluble Aβ40 and Aβ42 in the guanidine fractions were not altered in the APP/PS1; *Lrp1*$^{-/-}$ mice compared with APP/PS1 mice (Fig. 6*C*). In addition, no significant inverse correlations were detected in both Aβ40 ($R^2 = 0.0576$, $p = 0.2699$) and Aβ42 ($R^2 = 0.0089$, $p = 0.6684$) and LRP1 levels (Fig. 6*D*,*E*). These results indicate that LRP1-mediated neuronal Aβ clearance is regional specific in the brain.

Discussion

In this study, we have demonstrated critical roles of neuronal LRP1 in mediating brain Aβ clearance using *in vitro* cellular and *in vivo* animal models. Previous studies have shown that astrocytes (Wyss-Coray et al., 2003, Koistinaho et al., 2004), microglia cells (Wyss-Coray et al., 2001), and vascular smooth muscle cells (Kanekiyo et al., 2012) can degrade Aβ to eliminate it from the brain. However, Aβ clearance through neurons has received little attention compared with other brain cell types despite the fact that neurons produce Aβ. Neurons are predicted to have the highest risk for encountering Aβ among all cell types in the brain, as Aβ is mainly generated locally in these cells. As Aβ is highly toxic to neurons, it is likely that neurons possess efficient mechanisms to eliminate Aβ. APP is known to be cleaved in the endosomes upon its endocytosis in both presynapses and postsynapses with Aβ secreting into extracellular space (Cirrito et al., 2005, 2008). Our findings showed that neuronal LRP1, which is predominantly expressed in the postsynaptic region (May et al., 2004) and the cell body (Bu et al., 1994), mediates Aβ uptake and subsequent degradation. Impairment of this pathway leads to acceleration of Aβ accumulation and deposition (Fig. 7). A variety of lysosomal acid hydrolases including cathepsin B and cathepsin D can efficiently degrade Aβ (Nixon et al., 2001). When the lysosomal system is modulated via Z-Phe-Ala-diazomethylketone treatment, there was a reduction in Aβ deposition by increasing neuronal cathepsin B levels in amyloid model mice (Butler et al., 2011). These findings indicate that neuronal lysosome-dependent Aβ clearance is a major pathway to eliminating Aβ and that disturbance of this pathway might be involved in AD pathogenesis.

In previous studies, a potential role of neuronal LRP1 in brain Aβ clearance was suggested but not proven. It has been shown that clearance of exogenous Aβ from the brain is suppressed by LRP1 antagonist, RAP, or antibodies against LRP1 (Shibata et al., 2000). Furthermore, partial reductions in RAP disturbed the maturation of LRP1 and enhanced Aβ deposition in APP/PS1 mice (Xu et al., 2008). Because RAP is ubiquitously expressed in all cell types and also inhibits other members of the LDL receptor family (Bu and Schwartz, 1998), a specific role of LRP1 in neurons was not defined. In the current study, we have used *Lrp1*-conditional knock-out mice to demonstrate directly that deletion of LRP1 in forebrain neurons exacerbates amyloid pathology in aged APP/PS1 mice. Importantly, using *in vivo* microdialysis techniques, we demonstrated directly that the elimination rate of ISF Aβ was significantly slower in the cortex of APP/PS1; *Lrp1*$^{-/-}$ mice than that of control APP/PS1 mice. Because the neuronal LRP1 deletion did not affect the mRNA levels of major Aβ degrading enzymes, the disturbed Aβ clearance is likely caused by the

suppression of LRP1-mediated neuronal Aβ uptake and lysosomal degradation. It is important to note that our studies are possible because *Lrp1* gene deletion using the αCaMKII-Cre mice occurs only in adult mice (Liu et al., 2010), allowing us to address age-dependent effects in amyloid model mice.

While our findings showed the importance roles of neuronal LRP1 in Aβ clearance in the cortex, there was no significant difference in insoluble Aβ levels in the hippocampus between APP/PS1 mice and APP/PS1; *Lrp1*$^{-/-}$ mice. These results suggest that Aβ is differently eliminated depending on brain regions and that LRP1-mediated neuronal Aβ clearance pathway may not be a major pathway in the hippocampus. Cell populations of hippocampus are different from cortex; therefore, Aβ clearance through astrocytes or Aβ degrading enzymes may be more prominent in the hippocampus. Indeed, GFAP-positive activated astrocytes are more abundant in the hippocampus than in the cortex (Lein et al., 2007, Hewett, 2009). Further, Aβ degrading enzyme NEP is more abundant in the hippocampus compared with cortex in mouse brain (Fukami et al., 2002). Thus, Aβ clearance through proteolytic enzymes, glial cells, and/or cerebrovascular system (Fig. 7) might compensate the impaired neuronal Aβ clearance pathway upon deletion of LRP1 in hippocampus. Consistent with our results, another recent study reported that there was no significant effect of LRP1 reduction on the severity of amyloid deposition, Aβ accumulation, or the architecture of amyloid plaques in the hippocampus of APP/PS1 mice when LRP1 was deleted in neurons (Xu et al., 2012). In addition, we did not detect significant differences in insoluble Aβ levels at 6–7 months of age in our mouse models. In *Lrp1*$^{-/-}$ mice, LRP1 deletion in the cortex starts between 3 and 6 months of age and gradually reaches maximum at 12 months of age (Liu et al., 2010). Thus, the insufficient deletion of LRP1 in neurons may not induce significant effects on Aβ clearance in young APP/PS1; *Lrp1*$^{-/-}$ mice. Another possible contributing factor is that the neuronal LRP1-mediated Aβ clearance pathway might be critical after Aβ concentration reaches sufficiently high levels in aged APP/PS1 mice. Further experiments are needed to clarify these possibilities.

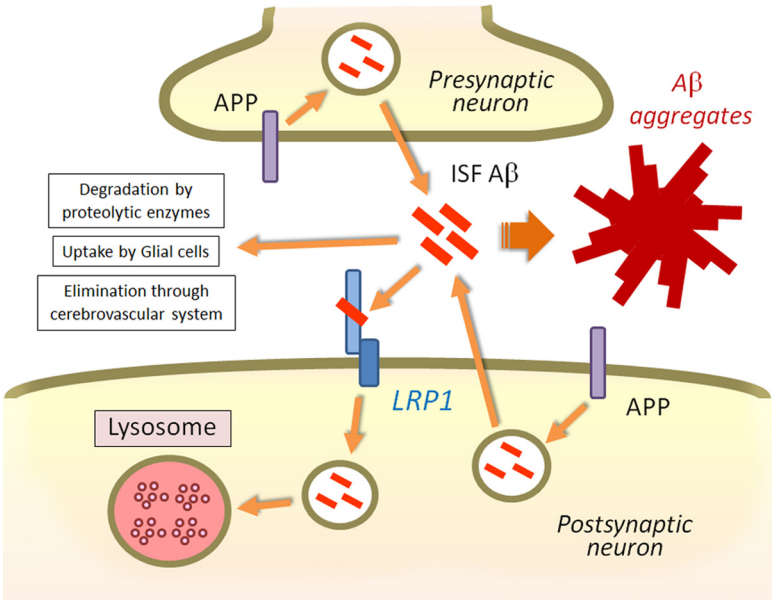

Figure 7. Model of neuronal Aβ clearance by LRP1. APP is cleaved and processed to Aβ in the endosomes upon endocytosis, and Aβ is secreted from the neuron into the brain ISF. LRP1 is abundantly expressed in neurons, predominantly in the postsynaptic region and cell body. As an efficient endocytic receptor, LRP1 mediates Aβ uptake and subsequent lysosomal degradation. Although Aβ is also eliminated through proteolytic enzymes, glial cell, and cerebrovascular system, disturbance of the LRP1 pathway is sufficient to induce Aβ accumulation and deposition in the cortex as shown in this work.

Previous studies have shown that LRP1 levels were significantly decreased during aging and AD (Kang et al., 2000). When LRP1 expression levels in the mid-frontal cortex of AD and normal control age-matched subjects were analyzed by Western blotting, LRP1 levels were ~2-fold lower in AD brains compared with those of control subjects (Kang et al., 2000). Therefore, restoring LRP1 expression in neurons might be an attractive approach to prevent or treat AD by improving Aβ clearance. Enhancing LRP1 expression in neurons should also be beneficial in promoting synapse plasticity by facilitating lipid transport (Liu et al., 2010), neurite outgrowth (Holtzman et al., 1995), and neuronal survival (Fuentealba et al., 2009).

In summary, we have directly demonstrated that neuronal LRP1 critically mediates Aβ clearance in the cortex of APP/PS1 mice. We also report for the first time, to our knowledge, that neurons are capable of mediating local clearance of Aβ through receptor-mediated endocytosis *in vivo*. Our findings provide novel insights in to the molecular mechanisms of AD pathogenesis and further support LRP1 as a potential target for AD therapy.

References

Blennow K, de Leon MJ, Zetterberg H (2006) Alzheimer's disease. Lancet 368:387–403. CrossRef Medline

Borchelt DR, Ratovitski T, van Lare J, Lee MK, Gonzales V, Jenkins NA, Copeland NG, Price DL, Sisodia SS (1997) Accelerated amyloid deposition in the brains of transgenic mice coexpressing mutant presenilin 1 and amyloid precursor proteins. Neuron 19:939–945. CrossRef Medline

Bu G (2009) Apolipoprotein E and its receptors in Alzheimer's disease: pathways, pathogenesis and therapy. Nat Rev Neurosci 10:333–344. CrossRef Medline

Bu G, Schwartz AL (1998) RAP, a novel type of ER chaperone. Trends Cell Biol 8:272–276. CrossRef Medline

Bu G, Maksymovitch EA, Nerbonne JM, Schwartz AL (1994) Expression and function of the low density lipoprotein receptor-related protein (LRP) in mammalian central neurons. J Biol Chem 269:18521–18528. Medline

Butler D, Hwang J, Estick C, Nishiyama A, Kumar SS, Baveghems C, Young-Oxendine HB, Wisniewski ML, Charalambides A, Bahr BA (2011) Protective effects of positive lysosomal modulation in Alzheimer's disease transgenic mouse models. PLoS One 6:e20501. CrossRef Medline

Chakrabarty P, Ceballos-Diaz C, Beccard A, Janus C, Dickson D, Golde TE, Das P (2010) IFN-gamma promotes complement expression and attenuates amyloid plaque deposition in amyloid beta precursor protein transgenic mice. J Immunol 184:5333–5343. CrossRef Medline

Cirrito JR, May PC, O'Dell MA, Taylor JW, Parsadanian M, Cramer JW, Audia JE, Nissen JS, Bales KR, Paul SM, DeMattos RB, Holtzman DM (2003) In vivo assessment of brain interstitial fluid with microdialysis reveals plaque-associated changes in amyloid-beta metabolism and half-life. J Neurosci 23:8844–8853. Medline

Cirrito JR, Yamada KA, Finn MB, Sloviter RS, Bales KR, May PC, Schoepp DD, Paul SM, Mennerick S, Holtzman DM (2005) Synaptic activity regulates interstitial fluid amyloid-beta levels in vivo. Neuron 48:913–922. CrossRef Medline

Cirrito JR, Kang JE, Lee J, Stewart FR, Verges DK, Silverio LM, Bu G, Mennerick S, Holtzman DM (2008) Endocytosis is required for synaptic

activity-dependent release of amyloid-beta in vivo. Neuron 58:42–51. CrossRef Medline

Cirrito JR, Disabato BM, Restivo JL, Verges DK, Goebel WD, Sathyan A, Hayreh D, D'Angelo G, Benzinger T, Yoon H, Kim J, Morris JC, Mintun MA, Sheline YI (2011) Serotonin signaling is associated with lower amyloid-beta levels and plaques in transgenic mice and humans. Proc Natl Acad Sci U S A 108:14968–14973. CrossRef Medline

Fuentealba RA, Liu Q, Kanekiyo T, Zhang J, Bu G (2009) Low density lipoprotein receptor-related protein 1 promotes anti-apoptotic signaling in neurons by activating Akt survival pathway. J Biol Chem 284:34045–34053. CrossRef Medline

Fukami S, Watanabe K, Iwata N, Haraoka J, Lu B, Gerard NP, Gerard C, Fraser P, Westaway D, St George-Hyslop P, Saido TC (2002) Abeta-degrading endopeptidase, neprilysin, in mouse brain: synaptic and axonal localization inversely correlating with Abeta pathology. Neurosci Res 43:39–56. CrossRef Medline

Hardy J, Selkoe DJ (2002) The amyloid hypothesis of Alzheimer's disease: progress and problems on the road to therapeutics. Science 297:353–356. CrossRef Medline

Herz J, Strickland DK (2001) LRP: a multifunctional scavenger and signaling receptor. J Clin Invest 108:779–784. CrossRef Medline

Hewett JA (2009) Determinants of regional and local diversity within the astroglial lineage of the normal central nervous system. J Neurochem 110:1717–1736. CrossRef Medline

Holtzman DM, Pitas RE, Kilbridge J, Nathan B, Mahley RW, Bu G, Schwartz AL (1995) Low density lipoprotein receptor-related protein mediates apolipoprotein E-dependent neurite outgrowth in a central nervous system-derived neuronal cell line. Proc Natl Acad Sci U S A 92:9480–9484. CrossRef Medline

Kanekiyo T, Zhang J, Liu Q, Liu CC, Zhang L, Bu G (2011) Heparan sulphate proteoglycan and the low-density lipoprotein receptor-related protein 1 constitute major pathways for neuronal amyloid-{beta} uptake. J Neurosci 31:1644–1651. CrossRef Medline

Kanekiyo T, Liu CC, Shinohara M, Li J, Bu G (2012) LRP1 in brain vascular smooth muscle cells mediates local clearance of Alzheimer's amyloid-beta. J Neurosci 32:16458–16465. CrossRef Medline

Kang DE, Pietrzik CU, Baum L, Chevallier N, Merriam DE, Kounnas MZ, Wagner SL, Troncoso JC, Kawas CH, Katzman R, Koo EH (2000) Modulation of amyloid beta-protein clearance and Alzheimer's disease susceptibility by the LDL receptor-related protein pathway. J Clin Invest 106:1159–1166. CrossRef Medline

Koffie RM, Hyman BT, Spires-Jones TL (2011) Alzheimer's disease: synapses gone cold. Mol Neurodegener 6:63. CrossRef Medline

Koistinaho M, Lin S, Wu X, Esterman M, Koger D, Hanson J, Higgs R, Liu F, Malkani S, Bales KR, Paul SM (2004) Apolipoprotein E promotes astrocyte colocalization and degradation of deposited amyloid-beta peptides. Nat Med 10:719–726. CrossRef Medline

Lein ES, Hawrylycz MJ, Ao N, Ayres M, Bensinger A, Bernard A, Boe AF, Boguski MS, Brockway KS, Byrnes EJ, Chen L, Chen TM, Chin MC, Chong J, Crook BE, Czaplinska A, Dang CN, Datta S, Dee NR, Desaki AL, et al. (2007) Genome-wide atlas of gene expression in the adult mouse brain. Nature 445:168–176. CrossRef Medline

Li J, Kanekiyo T, Shinohara M, Zhang Y, LaDu MJ, Xu H, Bu G (2012) Differential regulation of amyloid-beta endocytic trafficking and lysosomal degradation by apolipoprotein E isoforms. J Biol Chem 287:44593–44601. CrossRef Medline

Li Y, Lu W, Bu G (2003) Essential role of the low density lipoprotein receptor-related protein in vascular smooth muscle cell migration. FEBS Lett 555:346–350. CrossRef Medline

Liu Q, Zerbinatti CV, Zhang J, Hoe HS, Wang B, Cole SL, Herz J, Muglia L, Bu G (2007) Amyloid precursor protein regulates brain apolipoprotein E and cholesterol metabolism through lipoprotein receptor LRP1. Neuron 56:66–78. CrossRef Medline

Liu Q, Trotter J, Zhang J, Peters MM, Cheng H, Bao J, Han X, Weeber EJ, Bu G (2010) Neuronal LRP1 knockout in adult mice leads to impaired brain lipid metabolism and progressive, age-dependent synapse loss and neurodegeneration. J Neurosci 30:17068–17078. CrossRef Medline

Mandrekar S, Jiang Q, Lee CY, Koenigsknecht-Talboo J, Holtzman DM, Landreth GE (2009) Microglia mediate the clearance of soluble Abeta through fluid phase macropinocytosis. J Neurosci 29:4252–4262. CrossRef Medline

Mawuenyega KG, Sigurdson W, Ovod V, Munsell L, Kasten T, Morris JC, Yarasheski KE, Bateman RJ (2010) Decreased clearance of CNS beta-amyloid in Alzheimer's disease. Science 330:1774. CrossRef Medline

May P, Rohlmann A, Bock HH, Zurhove K, Marth JD, Schomburg ED, Noebels JL, Beffert U, Sweatt JD, Weeber EJ, Herz J (2004) Neuronal LRP1 functionally associates with postsynaptic proteins and is required for normal motor function in mice. Mol Cell Biol 24:8872–8883. CrossRef Medline

Nixon RA, Mathews PM, Cataldo AM (2001) The neuronal endosomal-lysosomal system in Alzheimer's disease. J Alzheimers Dis 3:97–107. Medline

Shibata M, Yamada S, Kumar SR, Calero M, Bading J, Frangione B, Holtzman DM, Miller CA, Strickland DK, Ghiso J, Zlokovic BV (2000) Clearance of Alzheimer's amyloid-ss(1–40) peptide from brain by LDL receptor-related protein-1 at the blood-brain barrier. J Clin Invest 106:1489–1499. CrossRef Medline

Shinohara M, Petersen RC, Dickson DW, Bu G (2013) Brain regional correlation of amyloid-beta with synapses and apolipoprotein E in nondemented individuals: potential mechanisms underlying regional vulnerability to amyloid-beta accumulation. Acta Neuropathol 125:535–547. CrossRef Medline

Wyss-Coray T, Lin C, Yan F, Yu GQ, Rohde M, McConlogue L, Masliah E, Mucke L (2001) TGF-beta1 promotes microglial amyloid-beta clearance and reduces plaque burden in transgenic mice. Nat Med 7:612–618. CrossRef Medline

Wyss-Coray T, Loike JD, Brionne TC, Lu E, Anankov R, Yan F, Silverstein SC, Husemann J (2003) Adult mouse astrocytes degrade amyloid-beta in vitro and in situ. Nat Med 9:453–457. CrossRef Medline

Xu G, Karch C, Li N, Lin N, Fromholt D, Gonzales V, Borchelt DR (2008) Receptor-associated protein (RAP) plays a central role in modulating Abeta deposition in APP/PS1 transgenic mice. PLoS One 3:e3159. CrossRef Medline

Xu G, Green CC, Fromholt SE, Borchelt DR (2012) Reduction of low-density lipoprotein receptor-related protein (LRP1) in hippocampal neurons does not proportionately reduce, or otherwise alter, amyloid deposition in APPswe/PS1dE9 transgenic mice. Alzheimers Res Ther 4:12. CrossRef Medline

Youmans KL, Leung S, Zhang J, Maus E, Baysac K, Bu G, Vassar R, Yu C, LaDu MJ (2011) Amyloid-beta42 alters apolipoprotein E solubility in brains of mice with five familial AD mutations. J Neurosci Methods 196:51–59. CrossRef Medline

Zheng H, Koo EH (2011) Biology and pathophysiology of the amyloid precursor protein. Mol Neurodegener 6:27. CrossRef Medline

Conclusions

Previous studies have suggested that LRP1 is important in neuronal degradation of Aβ. Using these techniques, we were able to demonstrate directly that LRP1 does indeed play an important role in neuronal Aβ uptake and clearance. These findings are important because neurons have the highest risk of encountering Aβ, but their role in clearance was not clearly defined.

Our work shows that LRP1 in the postsynaptic region, as well as the cell body, does mediate Aβ uptake and degradation by lysosomal bodies. Lysosome-dependent clearance of Aβ is likely a major pathway for eliminating endocytosed Aβ. Impairment of which leads to an acceleration of Aβ deposition, and may be a risk factor for or a mechanism in AD.

It is likely that there are other pathways for Aβ degradation and elimination by neurons, many of which may be an important therapeutic target for future drug development. Our results showed that clearance of insoluble Aβ levels is impacted by LRP1 in the cortex, but there was not a significant difference in Aβ plaque burden in the hippocampus. Degradation pathways in the hippocampus are likely different as cellular makeup varies between the cortex and the hippocampus. Suggesting that Aβ is degraded by different pathways and that one approach may not be sufficient to address the disease.

This conclusion is supported by past research that also found no significant effect on Aβ accumulation or plaques in the hippocampus if APP/PS1 mice after the deletion of LRP1 in neurons (Xu et al. 2012). Other studies have also found changes in levels Aβ degradation enzymes (Zhao et al. 2007; Yasojima et al. 2001), and have demonstrated many different clearance systems present in the brain, as discussed in “Clearance systems in the brain—implications for Alzheimer disease” (Tarasoff-Conway et al. 2015).

Previous human studies have shown that there is a measurable decrease in LRP1 levels with age and in AD patients (Kang et al. 2000). This increase is even greater in

AD patients than with normal aging though (Kang et al. 2000), further indicating that LRP1 may be a good therapeutic target for future investigations.

The important findings in this research have had a major impact on the understanding of Aβ clearance pathways and has also led to many different avenues of research. The findings presented in this paper helped to show that removal of Aβ from the brain occurs via various, overlapping clearance systems. Neuronal clearance, along with glial, endothelial, and lymphatic all play an important role (Tarasoff-Conway et al. 2015). A better, and more precise understanding of these pathways and mechanisms is required to further treatment strategies to prevent and potentially halt the progression of AD.

One study identified a novel way to target and increase LRP-1 mediated clearance through supplements (Ishida et al. 2020). Others have highlighted the importance of LRP-1 in regulating insulin signaling/glucose metabolism (Liu et al. 2015; Gali et al. 2019). This work has also been furthered through research on APOE's impact on LRP-1 mediated clearance (Tachibana et al. 2019), which has produced some surprising results. Tachibana et al. found that APOE ε4 exacerbates Aβ pathology through a mechanism that is dependent on LRP-1. When LRP-1 KO mice were crossed with APP/PS1/APOE ε4 mice Aβ levels actually decreased, suggesting a more complicated clearance mechanism.

LRP-1 has also been a therapeutic target for drug development. Pharmacological interventions targeting LRP-1 for AD treatment include intravenous immunoglobulin (Gu et al. 2014), statins, and α-secretase inhibitors (Shinohara et al. 2017).

Chapter 2: *In vivo* measurement of apolipoprotein E from the brain interstitial fluid using microdialysis

APOE ***ε***4 is a strong, and well-known genetic risk factor for AD. The ***ε***4 allele is known to impact the metabolism of A**β** in the brain. The APOE gene provides instructions for a protein also called apolipoprotein e (apoE). Once made, this protein combines with lipids to form lipoproteins which are important in the transportation of cholesterol in the bloodstream, as well as the removal of lipid debris and degenerating cellular membranes in the CNS (Rebeck 2017). The APOE gene has three different allele types, as discussed previously. Each of these alleles differs in its ability to promote cholesterol efflux, with ***ε***2 having the highest efficiency, and ***ε***4 the lowest. The ***ε***4 allele is also associated with lower clearance of A**β** from the brain. As such, both the protein and the ***ε***4 gene are strong therapeutic targets for the treatment of AD.

Little is known about the *in vivo* regulation of apoE and lipidation though. Research has so far been limited to *in vitro* cell culture analysis and homogenized brain extracts, which present only a partial understanding of apoE's role and regulation.

To better understand apoE in the brain, it is important to have live models to research. In this work, we undertook to see if apoE could be collected in real-time using microdialysis on mouse models of AD. Microdialysis is a tested technique for small molecule and peptide collection in the brain. The high molecular weight of apoE has impeded the use of this technique in collecting apoE thus far. Here, we were able to use a high molecular weight collection probe to quantify apoE levels in awake and freely moving mice.

My role in this research was to prepare the microdialysis probes, perform the microdialysis surgeries on the mice, properly dose the mice with the retinoid-X-receptor agonist bexarotene via oral gavage, and collect and store the ISF samples for further testing.

This paper has been cited in 66 subsequent publications, including publications in high-influence journals such as Nature Medicine (impact factor 32.621), the Journal of Experimental Medicine (impact factor 10.790), Neuron (impact factor 14.318), and Nature Genetics (impact factor 27.125), Molecular Psychiatry (impact factor 13.204).

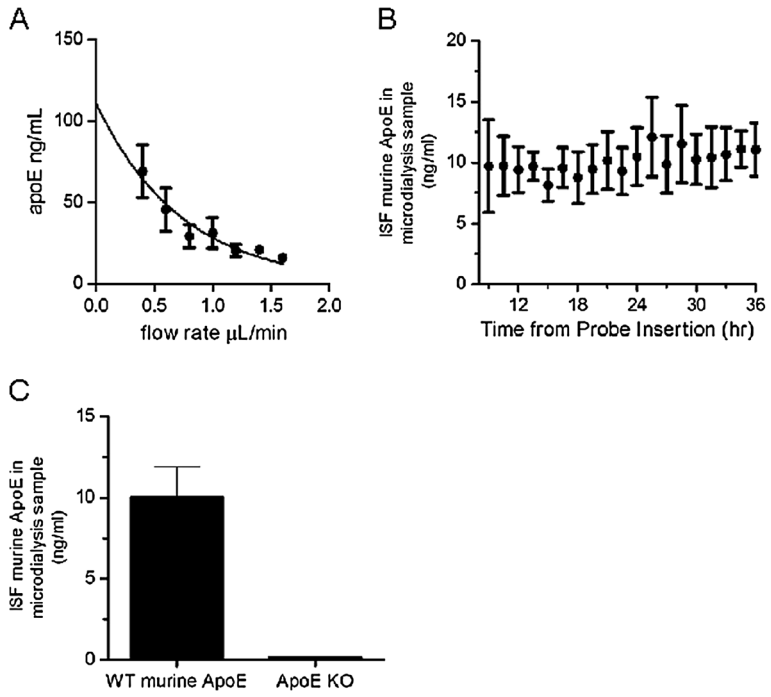

Figure 1 Analysis of apoE levels by microdialysis *in vitro* and *in vivo*. A. Microdialysis samples were collected hourly from human CSF *in vitro* at flow rates ranging from 0.4 µL/min to 1.6 µL/min. The concentration of apoE within microdialysis samples and CSF was determined by ELISA. Data points represent mean ± SEM (n=3). A single-phase exponential decay curve (r^2=0.93) was used to calculate the estimated mean concentration of apoE at zero flow. **B.** Microdialysis probes were implanted into the hippocampus of 3-4 month old mice and ISF collected bi-hourly for 36 hours. The concentration of apoE within microdialysis samples was determined by ELISA. Data points represent mean ± SEM (n=5). **C.** The mean concentration of murine apoE in ISF microdialysis samples from WT (n=5) and apoE KO mice (n=2) was determined by ELISA. ISF samples were collected at a constant flow rate of 1.0 µL/min. Data are presented as mean ± SEM.

receptor agonists may be an effective therapeutic target for AD [8,17]. We tested whether we could detect changes in ISF apoE and Aβ levels following administration of the retinoid-X-receptor (RXR) agonist bexarotene using microdialysis. We monitored hippocampal ISF apoE and Aβ levels in 2-month old APP/PS1 mice. Following establishment of a 6-hour baseline apoE and Aβ level, bexarotene (100 mg/kg) or vehicle (water) were administered to the mice via oral gavage. Bexarotene treatment led to a steady increase in ISF apoE levels beginning ~12 hours post-administration (Figure 2A). ISF apoE levels were increased 2.5-fold 30-36 hours post-

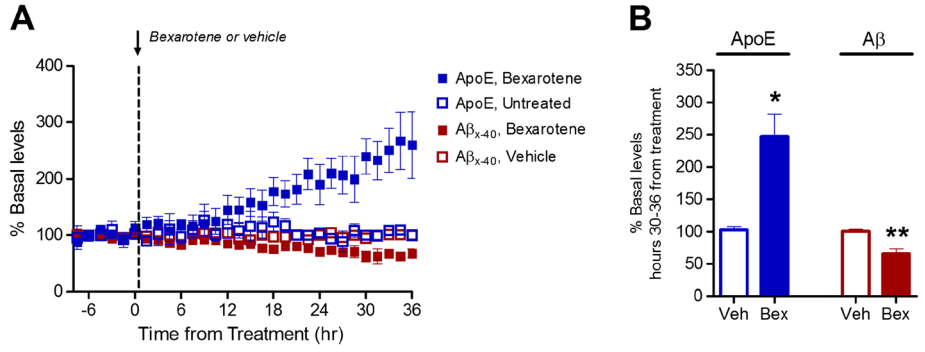

Figure 2 Bexarotene increases ISF apoE levels and decreases ISF Aβ levels. A. ISF $Aβ_{x-40}$ and apoE levels in the hippocampus of 2-month old APP/PS1 mice were monitored using *in vivo* microdialysis. Following establishment of a 6 hour baseline ISF level for $Aβ_{x-40}$ and apoE, mice were administered bexarotene (100 mg/kg p.o.) or vehicle (water) and ISF $Aβ_{x-40}$ and apoE levels assessed for an additional 36 hours. **B.** The mean percent change from baseline of ISF apoE and $Aβ_{x-40}$ levels 30-36 post-administration was compared between vehicle and bexarotene treated mice. Bexarotene significantly increased ISF apoE levels (247 ± 34.3%, n=2) compared to vehicle (103 ± 5.2%, n=3) (*p<0.05, unpaired t-test). Bexarotene decreased ISF Aβ levels (65.1 ± 8.1%, n=3) compared to vehicle (100 ± 3.7%, n=6). (**p<0.005, unpaired t-test).

treatment (Figure 2A and B). ISF Aβ levels were decreased by ~35%, similar to previous observations (Figure 2A and B) [8]. These data demonstrate the utility of microdialysis to detect biologically relevant, pharmacologically-induced changes in ISF apoE levels.

To further validate our technique we tested whether we could determine an absolute concentration of recoverable apoE within the hippocampal ISF by the extrapolated zero-flow method. We implanted microdialysis probes into the hippocampus of 3-4 month old apoE3 KI mice and collected ISF dialysate at flow rates ranging from 0.4 μL/min to 1.6 μL/min. We then fit a single-exponential decay curve to the concentration of apoE as a function of flow rate (Figure 3A). Our analysis determined the concentration of recoverable apoE3 in the ISF under steady-state conditions was 38.1 ± 4.0 ng/mL (n=4).

ApoE particles in the CSF or secreted by cultured astrocytes are a heterogeneous mixture that vary in size depending upon the degree of lipidation [5,18-20]. We compared the lipidation of apoE3 particles collected from brain parenchymal ISF to apoE3 particles in CSF by non-denaturing gel electrophoresis, which separates proteins based upon their hydrated diameter. As previously reported, apoE3 particles in CSF were heterogeneous in size, ranging from 8.1 nm to 17.0 nm (Figure 2B) [21]. ApoE3 particles collected from ISF were lipidated and were similar in size to particles found in CSF (Figure 3B). We further verified that the lipidated apoE3 particles in ISF samples were not due to contamination from the artificial cerebral spinal fluid (aCSF) used for microdialysis (Figure 3B).

Previous studies found an isoform-dependent effect on apoE levels in the hippocampus, cortex, and CSF in apoE KI mice with apoE2-expressing mice having the highest levels of apoE and apoE4 expressing mice the lowest [22,23]. Therefore, we tested whether we could detect isoform-dependent differences in apoE levels in the hippocampal ISF by microdialysis. We implanted microdialysis probes into the hippocampus of 3-4 month old apoE2, apoE3 or apoE4 KI mice and assessed the absolute concentration of human apoE in the ISF dialysate by ELISA. The concentration of apoE2 within the ISF (46.7 ± 15.6 ng/mL, n=3) was significantly greater than that of apoE4 (12.6 ± 1.8 ng/mL, n=4) and the concentration of apoE3 (18.7 ± 5.3, n=6) was at a level between that of apoE2 and apoE4 (Figure 4A). To confirm that the observed differences were not due to differential detection of apoE isoforms by the antibodies used in the ELISA, we measured equal amounts of recombinant apoE2, apoE3, and apoE4 by ELISA and found no significant difference in detection among the apoE isoforms (Figure 4B). Therefore, these results support the utility of our assay for observing differences in apoE levels in the ISF that are similar to those seen in CSF and in the brain.

Conclusions

We have developed a sensitive microdialysis assay for assessing the levels and lipidation of apoE within the

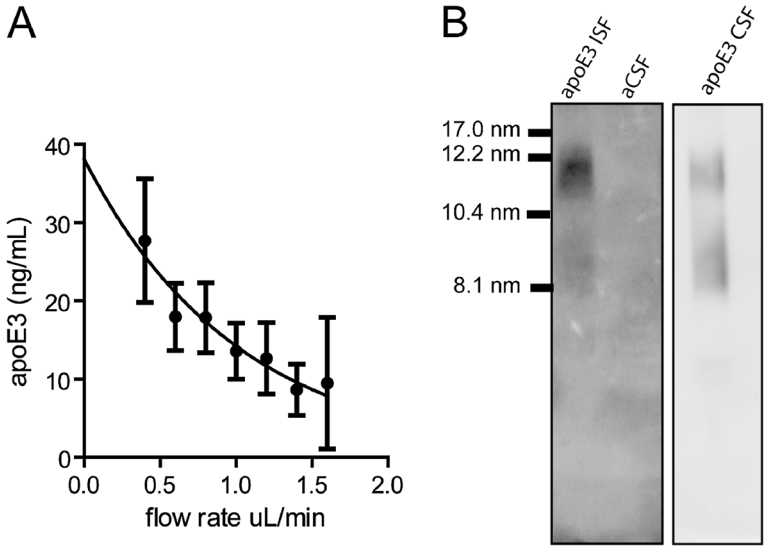

Figure 3 Analysis of hippocampal ISF apoE3 levels and lipidation. A. The apoE concentration in microdialysis samples collected at flow rates ranging from 0.4 μL/min to 1.6 μL/min was determined by ELISA. Data are presented as mean ± SEM (n=4). A single-phase exponential decay curve (r^2=0.93) was used to calculate the estimated mean concentration of apoE3 at zero flow. **B.** The lipidation of apoE in ISF and CSF samples was analyzed by non-denaturing gel electrophoresis using 4-20% Tris-glycine gradient gels. No apoE was detected in the aCSF used for microdialysis. The samples were run on the same gel; however the CSF panel is from a shorter exposure than the ISF panel for clarity.

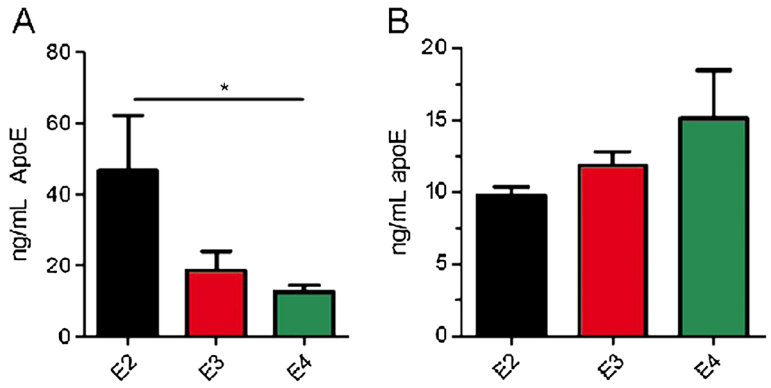

Figure 4 Isoform-dependent differences in apoE levels in the hippocampal ISF. A. ISF samples from the hippocampus of apoE2 KI, apoE3 KI, and apoE4 KI mice were obtained by microdialysis using a constant flow-rate of 1.0 μL/min. ApoE levels were assessed by ELISA and compared by ANOVA followed by Tukey's post hoc test. * $p<0.05$, n=3-6 mice per genotype. Data are presented as mean ± SEM. **B.** 12.5 ng/mL of recombinant apoE2, apoE3, or apoE4 was measured by ELISA and compared by ANOVA (p=0.22).

brain parenchymal ISF in awake and freely moving animals. Despite being the strongest genetic risk factor for developing late-onset AD, the precise molecular mechanism by which *APOE* genotype influences the risk of developing AD remains unknown. Previous studies indicate that apoE affects the metabolism and oligomerization of Aβ within the brain [3,4,24] as well as influences a variety of other biological processes [2]. Recent studies have therapeutically targeted the levels and lipidation of apoE to enhance clearance of Aβ from the brain [8]. The method described here will be useful in sampling ISF apoE levels over time in order to assess the relationship between apoE levels and lipidation and Aβ metabolism in the brain. Furthermore, assessment of apoE by microdialysis could prove useful in investigating the regulation of extracellular lipid homeostasis within the brain. This may be important in synaptic plasticity and repair after brain injury, as well as potentially play a role in neurodegenerative diseases such as Niemann-Pick disease [25].

Methods

Materials

Mouse apoE monoclonal antibodies (mHJ 6.1, mHJ 6.2, and mHJ 6.3) were generated in-house and have been described previously [9]. Polyclonal apoE antibody (50A-G1b) was purchased from Academy Bio-medical Co. (Houston, TX, USA). Recombinant apoE3 was purchased from Leinco Technologies (St. Louis, MO, USA). Bexarotene (Targretin™) was provided by Dr. Gary Landreth (Case Western Reserve University).

Animals

ApoE2, apoE3, and apoE4 knock-in (KI) mice were generously provided by Dr. Patrick M. Sullivan (Duke University) and have been previously described [26]. To assess murine apoE, wild type mice on a mixed C57BL6/C3H background were utilized (Jackson Labs). APPswe/PS1δE9 mice (APP/PS1) and ApoE knock-out (KO) mice were obtained from Jackson Labs. Mice were housed under constant light/dark conditions and had access to food and water *ad libitum*. All experimental protocols were approved by the Animal Studies Committee at Washington University in St. Louis.

In vitro microdialysis

Human CSF was collected by lumbar puncture from cognitively normal research volunteers from the Washington University Memory and Aging Project [27]. 1,000 kDa MWCO membrane microdialysis probes (AtmosLM Microdialysis probe, PEP-X-0Y, Eicom, San Diego, CA, USA) were connected to a two-channel peristaltic push-pull pump (MAB20, SciPro, Sanborn, NY, USA). The inlet-port of the microdialysis probe was connected to the push channel of the pump using Joint Teflon Tubing (inner diameter 0.1 mm) (JT-10-100, Eicom, San Diego, CA, USA) and the outlet-port was connected to the pull channel of the pump using Teflon (FEP) tubing (inner diameter 0.12 mm). The flow rates of the push and pull channels were calibrated to within 5% tolerance. The probes were then flushed with microdialysis perfusion solution (4% human albumin (Gemini Bioproducts, West Sacramento, CA, USA)-containing artificial CSF (aCSF) (in mM: 1.3 $CaCl_2$, 1.2 $MgSO_4$, 3 KCl, 0.4 KH_2PO_4, 25 $NaHCO_3$, 122 NaCl, pH 7.35) that had been prepared on the day of use and filtered through a 0.1 μm PES membrane. Microdialysis was performed at flow rates of 0.4 μL/min to 1.6 μL/min and samples were collected hourly using a refrigerated fraction collector (Univentor 820 Microsampler, SciPro). Extrapolation from zero-flow analysis was performed by fitting single-phase exponential decay curve to the mean apoE concentrations at varying flow rates with the constraint that the plateau

was set to 0. Percent recovery for each flow rate was calculated using $C_x/E * 100$, where C_x was the apoE concentration at a given flow rate and E was the estimated apoE concentration at steady-state.

In vivo microdialysis

Mice were anesthetized using 1.5%-2.5% isoflurane, the head shaved, and an anterior to posterior incision made along the midline of the head to expose the skull from several mm anterior of bregma to several mm posterior of lambda. The mouse was then mounted onto a manipulator arm-equipped small animal stereotaxic apparatus (David Kopf Instruments, Tujunga, CA, USA). The skull was then leveled to within 0.1 mm at lambda, bregma, and two points 2.2 mm lateral of midline. A bore hole (1.0 mm diameter) was then created above the left hippocampus (bregma -3.1 mm, 2.5 mm lateral, dura mater -0.6 mm). A second bore hole (0.75 mm) was placed in the right, anterior quadrant of the skull in which to place an anchoring bone screw. An AtmosLM Guide Cannula (PEG-X, Eicom, San Diego, CA, USA) was then stereotactically inserted into the left hippocampal formation (12° angle, dura mater -1.2 mm). The cannula was then secured into place using a binary dental cement. An AtmosLM Dummy Cannula (PED-X, Eicom, San Diego, CA, USA) was then inserted into the guide cannula and secured with a plastic cap nut. The wound was then closed using surgical adhesive and the animal placed into a clean cage and provided with access to food and water *ad libitum*.

1,000 kDa microdialysis probes (AtmosLM Microdialysis probe, PEP-X-0Y, Eicom, San Diego, CA, USA) were prepared as described above. Mice were then briefly anesthetized with isoflurane and probes were inserted into the hippocampus through the guide cannula and the mouse fitted with a plastic collar. Mice were then placed into a cage designed to allow for free movement without placing stress on the Teflon tubing or probe apparatus (Raturn Stand-Alone System, BASi, West Lafayette, IN, USA). The mice were kept under constant light conditions for the remainder of the experiment. Peristaltic pumps were operated at maximum speed for two hours to prevent clogging of the microdialysis membrane. Flow rates were then reduced to 1.0 μL/min to measure apoE. Samples were collected bi-hourly using a refrigerated fraction collector (Univentor 820 Microsampler, SciPro).

ApoE and Aβ ELISAs

The apoE concentration in microdialysis samples were analyzed by an apoE sandwich ELISA. For human apoE, a 96-well plate (Nunc) was coated with 500 ng/well HJ 6.2 overnight at 4°C. For murine apoE, 1% milk served as the capture ligand. The plate was then blocked with 1% milk for 60 min. at 37°C. Microdialysis samples were diluted with our standard ELISA buffer (0.5% BSA, 0.025% Tween-20 in PBS, pH 7.4). For human apoE isoforms recombinant apoE3 standards were diluted with ELISA buffer and microdialysis perfusion buffer to match the buffer composition of microdialysis samples. For quantification of murine apoE, pooled C57BL/6J plasma was used as a standard. Samples and standards were loaded and incubated overnight at 4°C. Biotinylated mHJ 6.3 or mHJ 6.1 was used as a detection antibody for mouse or human apoE, respectively. Following a 90 min. incubation at 37°C with detection antibody, poly-streptavidin-horseradish peroxidase (HRP) (Thermo Scientific) was applied to the plate and incubated for 90 min. at room temperature. ELISAs were then developed using Super Slow ELISA TMB (Sigma) and read using a Bio-Tek FL-600 plate reader at 650 nm. $A\beta_{x\text{-}40}$ was analyzed by sandwich ELISA as described previously, using HJ 2 as the capture antibody and biotinylated HJ 5.1 as the detection antibody [8].

Nondenaturing gradient gel electrophoresis and western blotting

Microdialysis, CSF, or microdialysis buffer samples were diluted with Native PAGE sample buffer (Life Technologies, Carlsbad, CA, USA) and electrophoresed on a 4-20% Tris-Glycine gel (Life Technologies, Carlsbad, CA, USA) at 100V for 24 hours at 4°C. A mixture of proteins with defined hydrated diameters was used for size standards (Amersham™ HMW Calibration Kit for Native Electrophoresis, Cat. # 17-0445-01, GE Healthcare). Proteins were transferred to a nitrocellulose membrane and probed with antibodies recognizing goat anti-human apoE (50A-G1b, 1:200, Academy Biomedical). Membranes were then washed extensively and probed with a donkey anti-goat IgG conjugated to HRP (1:5000, sc-2056, Santa Cruz Biotechnology). Blots were then developed using enhanced chemiluminescence (Lumigen-TMA6, Lumigen Inc.) and imaged with a Syngene G-Box (Syngene, Cambridge, UK).

Statistical analysis

Statistical analysis was performed using PRISM version 5.0 (GraphPad). Data are presented as mean ± SEM. Comparisons between two groups were made using a two-tailed unpaired t-test. Multiple groups were compared using ANOVA followed by Tukey's *post hoc* test. Statistical significance was assigned to p-values less than 0.05.

Competing interests

DMH co-founded and is on the scientific advisory board of C2N Diagnostics and currently serves as a consultant for Astra Zeneca, Bristol Myers Squibb, and Genentech. GEL co-founded ReXceptor, Inc.

Authors' contributions

JDU, GEL, JRC, JMC and DMH conceived and designed the experiments. JDU, JMC, TEM and DRS performed microdialysis experiments. JDU, JMC and JMB analyzed microdialysis samples. JLR, JMB, and JRC performed bexarotene

experiments. HJ prepared CSF samples. JDU and PBV performed native gel electrophoresis analysis. JDU wrote the paper and JRC and DMH revised the paper. All authors gave final approval of the version to be published. All authors read and approved the final manuscript.

Acknowledgments

This work was supported by R37 AG13956 (DMH), Ellison Medical Foundation Senior Scholar Award (DMH), the Cure Alzheimer's Fund (DMH), R01 AG042513 (JRC), P01 NS07496901 (JRC), K01 AG029254 (JRC). We thank Floy Stewart, Kaoru Yamada, and Mary Beth Finn for expert technical advice and assistance. ApoE2 KI, apoE3 KI, and apoE4 KI mice were generously provided by Dr. Patrick M. Sullivan (Duke University).

Author details

[1]Department of Neurology, Saint Louis, MO, USA. [2]Hope Center for Neurological Disorders, Saint Louis, MO, USA. [3]Developmental Biology, Saint Louis, MO, USA. [4]Knight Alzheimer's Disease Research Center, Washington University School of Medicine, Saint Louis, MO 63110, USA. [5]Department of Neurosciences, Case Western Reserve University, School of Medicine, Cleveland, OH, 44106 USA.

Received: 29 January 2013 Accepted: 16 April 2013
Published: 19 April 2013

References

1. Vance JE, Hayashi H: **Formation and function of apolipoprotein E-containing lipoproteins in the nervous system.** *Biochimica Biophysica Acta (BBA) Molecular Cell Biol Lipids* 2010, **1801:**806–818.
2. Holtzman DM, Herz J, Bu G: **Apolipoprotein e and apolipoprotein e receptors: normal biology and roles in Alzheimer disease.** *Cold Spring Harb Perspect Med* 2012, **2:**a006312.
3. Castellano JM, Kim J, Stewart FR, Jiang H, DeMattos RB, Patterson BW, Fagan AM, Morris JC, Mawuenyega KG, Cruchaga C, *et al*: **Human apoE Isoforms Differentially Regulate Brain Amyloid-β Peptide Clearance.** *Sci Transl Med* 2011, **3:**89ra57.
4. Hashimoto T, Serrano-Pozo A, Hori Y, Adams KW, Takeda S, Banerji AO, Mitani A, Joyner D, Thyssen DH, Bacskai BJ, *et al*: **Apolipoprotein E, Especially Apolipoprotein E4, Increases the Oligomerization of Amyloid β Peptide.** *J Neurosci* 2012, **32:**15181–15192.
5. Wahrle SE, Jiang H, Parsadanian M, Kim J, Li A, Knoten A, Jain S, Hirsch-Reinshagen V, Wellington CL, Bales KR, *et al*: **Overexpression of ABCA1 reduces amyloid deposition in the PDAPP mouse model of Alzheimer disease.** *J Clin Invest* 2008, **118:**671–682.
6. Hirsch-Reinshagen V, Zhou S, Burgess BL, Bernier L, McIsaac SA, Chan JY, Tansley GH, Cohn JS, Hayden MR, Wellington CL: **Deficiency of ABCA1 Impairs Apolipoprotein E Metabolism in Brain.** *J Biol Chem* 2004, **279:**41197–41207.
7. Kim J, Jiang H, Park S, Eltorai AEM, Stewart FR, Yoon H, Basak JM, Finn MB, Holtzman DM: **Haploinsufficiency of Human APOE Reduces Amyloid Deposition in a Mouse Model of Amyloid-β Amyloidosis.** *J Neurosci* 2011, **31:**18007–18012.
8. Cramer PE, Cirrito JR, Wesson DW, Lee CYD, Karlo JC, Zinn AE, Casali BT, Restivo JL, Goebel WD, James MJ, *et al*: **ApoE-Directed Therapeutics Rapidly Clear β-Amyloid and Reverse Deficits in AD Mouse Models.** *Science* 2012, **335:**1503–1506.
9. Kim J, Eltorai AEM, Jiang H, Liao F, Verghese PB, Kim J, Stewart FR, Basak JM, Holtzman DM: **Anti-apoE immunotherapy inhibits amyloid accumulation in a transgenic mouse model of Aβ amyloidosis.** *J Exp Med* 2012, **209:**2149–2156.
10. Chefer VI, Thompson AC, Zapata A, Shippenberg TS: **Overview of Brain Microdialysis.** *Curr Protoc Neurosci* 2009, **47:**7.1.1–7.1.28.
11. Cirrito JR, Yamada KA, Finn MB, Sloviter RS, Bales KR, May PC, Schoepp DD, Paul SM, Mennerick S, Holtzman DM: **Synaptic Activity Regulates Interstitial Fluid Amyloid-β Levels In Vivo.** *Neuron* 2005, **48:**913–922.
12. Bero AW, Yan P, Roh JH, Cirrito JR, Stewart FR, Raichle ME, Lee J-M, Holtzman DM: **Neuronal activity regulates the regional vulnerability to amyloid-[beta] deposition.** *Nat Neurosci* 2011, **14:**750–756.
13. Roh JH, Huang Y, Bero AW, Kasten T, Stewart FR, Bateman RJ, Holtzman DM: **Disruption of the Sleep-Wake Cycle and Diurnal Fluctuation of β-Amyloid in Mice with Alzheimer's Disease Pathology.** *Sci Transl Med* 2012, **4:**150ra122.
14. Cirrito JR, May PC, O'Dell MA, Taylor JW, Parsadanian M, Cramer JW, Audia JE, Nissen JS, Bales KR, Paul SM, *et al*: **In Vivo Assessment of Brain Interstitial Fluid with Microdialysis Reveals Plaque-Associated Changes in Amyloid-β Metabolism and Half-Life.** *J Neurosci* 2003, **23:**8844–8853.
15. Takeda S, Sato N, Ikimura K, Nishino H, Rakugi H, Morishita R: **Novel microdialysis method to assess neuropeptides and large molecules in free-moving mouse.** *Neuroscience* 2011, **186:**110–119.
16. Verges DK, Restivo JL, Goebel WD, Holtzman DM, Cirrito JR: **Opposing Synaptic Regulation of Amyloid-β Metabolism by NMDA Receptors In Vivo.** *J Neurosci* 2011, **31:**11328–11337.
17. Mandrekar-Colucci S, Karlo JC, Landreth GE: **Mechanisms Underlying the Rapid Peroxisome Proliferator-Activated Receptor-γ-Mediated Amyloid Clearance and Reversal of Cognitive Deficits in a Murine Model of Alzheimer's Disease.** *J Neurosci* 2012, **32:**10117–10128.
18. Fan J, Stukas S, Wong C, Chan J, May S, DeValle N, Hirsch-Reinshagen V, Wilkinson A, Oda MN, Wellington CL: **An ABCA1-independent pathway for recycling a poorly lipidated 8.1 nm apolipoprotein E particle from glia.** *J Lipid Res* 2011, **52:**1605–1616.
19. DeMattos RB, Brendza RP, Heuser JE, Kierson M, Cirrito JR, Fryer J, Sullivan PM, Fagan AM, Han X, Holtzman DM: **Purification and characterization of astrocyte-secreted apolipoprotein E and J-containing lipoproteins from wild-type and human apoE transgenic mice.** *Neurochem Int* 2001, **39:**415–425.
20. Wahrle SE, Jiang H, Parsadanian M, Hartman RE, Bales KR, Paul SM, Holtzman DM: **Deletion of Abca1 Increases Aβ Deposition in the PDAPP Transgenic Mouse Model of Alzheimer Disease.** *J Biol Chem* 2005, **280:**43236–43242.
21. Fagan AM, Holtzman DM, Munson G, Mathur T, Schneider D, Chang LK, Getz GS, Reardon CA, Lukens J, Shah JA, LaDu MJ: **Unique Lipoproteins Secreted by Primary Astrocytes From Wild Type, apoE (–/–), and Human apoE Transgenic Mice.** *J Biol Chem* 1999, **274:**30001–30007.
22. Bales KR, Liu F, Wu S, Lin S, Koger D, DeLong C, Hansen JC, Sullivan PM, Paul SM: **Human APOE Isoform-Dependent Effects on Brain β-Amyloid Levels in PDAPP Transgenic Mice.** *J Neurosci* 2009, **29:**6771–6779.
23. Riddell DR, Zhou H, Atchison K, Warwick HK, Atkinson PJ, Jefferson J, Xu L, Aschmies S, Kirksey Y, Hu Y, *et al*: **Impact of Apolipoprotein E (ApoE) Polymorphism on Brain ApoE Levels.** *J Neurosci* 2008, **28:**11445–11453.
24. Liu CC, Kanekiyo T, Xu H, Bu G: **Apolipoprotein E and Alzheimer disease: risk, mechanisms and therapy.** *Nat Rev Neurol* 2013, **9:**106–118.
25. Rosenbaum AI, Maxfield FR: **Niemann-Pick type C disease: molecular mechanisms and potential therapeutic approaches.** *J Neurochem* 2011, **116:**789–795.
26. Sullivan PM, Mace BE, Maeda N, Schmechel DE: **Marked regional differences of brain human apolipoprotein e expression in targeted replacement mice.** *Neuroscience* 2004, **124:**725–733.
27. Fagan AM, Younkin LH, Morris JC, Fryer JD, Cole TG, Younkin SG, Holtzman DM: **Differences in the Abeta40/Abeta42 ratio associated with cerebrospinal fluid lipoproteins as a function of apolipoprotein E genotype.** *Ann Neurol* 2000, **48:**201–210.

doi:10.1186/1750-1326-8-13
Cite this article as: Ulrich *et al.*: In vivo measurement of apolipoprotein E from the brain interstitial fluid using microdialysis. *Molecular Neurodegeneration* 2013 **8**:13.

Conclusions

Through this research, we were able to prove that apoE can be collected in real-time *in vivo* for awake and freely moving mice. This was the first time that apoE has been measured for an extended period of time in a freely moving mouse model. Previously, the only way to obtain *in vivo* apoE measurements was to test CSF levels from human volunteers, which is a painful procedure that has many inherent risks. Because of this, little is known about the physiological regulation of this important protein.

The methods described here will be useful in further elucidating apoE's regulation in the brain, as well as the molecular mechanisms by which the APOE genotype influences the risk of AD. The surgical technique described here can be adapted for many different pharmacological and genetic testing studies to help further our understanding.

Other studies have shown that therapeutically targeting apoE lipidation can enhance Aβ clearance in the brain. The method used in our research can be used to help advance these types of studies by providing a way to test apoE levels in ISF over time in the same animal.To date, no further research has been completed utilizing microdialysis to measure apoE levels *in vivo*. A clinical trial testing bexarotene in AD patients was completed, but resulted in no measurable cognitive improvements or improvements in any other clinical measure (J. L. Cummings et al. 2016).

Further research around apoE has been completed, including research showing that apoE complexes in the CSF vary in size by genotype, with apoE ε2 > apoE ε3 > apoE ε4 in size (Heinsinger et al. 2016). The authors suggest that the smaller ε4 complexes may be deficient in clearing lipid debris (Heinsinger et al. 2016).

Chapter 3: Antisense Reduction of Tau in Adult Mice Protects Against Seizures

Recent human and animal studies have shown there is a link between AD and an increased risk for seizures (Born 2015; Palop et al. 2007). In AD, these seizures are typically nonconvulsive, and therefore often go unnoticed, but it is postulated that these seizures and other electroencephalographic abnormalities occur far more often than previously thought (Born 2015). Seizures can result in a destabilization of neuronal network activity, which may contribute to the cognitive impairment often seen in AD patients (Born 2015; Palop et al. 2007).

It has been documented that tau knock-out mice have substantially reduced seizure activity in models of chemically-induced seizure compared to nontransgenic mice (Roberson et al. 2007; Roberson et al. 2011). This suggests that tau may protect against excitotoxicity and neuronal hyperexcitability. When $tau^{-/-}$ mice are crossed with an AD mouse model line, the offspring show not only a reduction in seizures but also improved learning and memory (Roberson et al. 2007; Roberson et al. 2011).

Since these experiments were performed on knock-out mice though, it could not be determined if this protective effect was due to the reduction in tau levels or was due to a developmental compensation. In this experiment, we sought to test if antisense oligonucleotide (ASO) reduction in tau would have the same protective effect against seizures.

My role in this research was to perform the *in vivo* microdialysis surgery and sample collections on the mice. I was also responsible for creating the modified microdialysis cannulas with attached electrodes to record EEG activity in the awake and freely moving mice and dosing the mice with picrotoxin through reverse microdialysis. After EEG data was collected, I went through the experimental time points to identify seizure activity. Once these mice had finished their ISF collection

for tau quantification, I perfused the mice and preserved their brains for further testing.

This paper has been cited in 126 subsequent publications, including publications in high-influence journals such as the Journal of Clinical Investigation (impact factor 13.251), Neuron (impact factor 14.318), Lancet Neurology (impact factor 27.144), the Lancet (impact factor 53.254), and the Journal of Cellular Biology (impact factor 8.784).

Neurobiology of Disease

Antisense Reduction of Tau in Adult Mice Protects against Seizures

Sarah L. DeVos,[1] Dustin K. Goncharoff,[1] Guo Chen,[1] Carey S. Kebodeaux,[1] Kaoru Yamada,[1] Floy R. Stewart,[1] Dorothy R. Schuler,[1] Susan E. Maloney,[2] David F. Wozniak,[2] Frank Rigo,[5] C. Frank Bennett,[5] John R. Cirrito,[1] David M. Holtzman,[1,3,4] and Timothy M. Miller[1,4]

[1]Department of Neurology, Hope Center for Neurological Disorders, [2]Department of Psychiatry, [3]Department of Developmental Biology, and [4]Knight Alzheimer's Disease Research Center, Washington University, St. Louis, Missouri 63110, and [5]Isis Pharmaceuticals, Carlsbad, California 90201

Tau, a microtubule-associated protein, is implicated in the pathogenesis of Alzheimer's Disease (AD) in regard to both neurofibrillary tangle formation and neuronal network hyperexcitability. The genetic ablation of tau substantially reduces hyperexcitability in AD mouse lines, induced seizure models, and genetic *in vivo* models of epilepsy. These data demonstrate that tau is an important regulator of network excitability. However, developmental compensation in the genetic tau knock-out line may account for the protective effect against seizures. To test the efficacy of a tau reducing therapy for disorders with a detrimental hyperexcitability profile in *adult* animals, we identified antisense oligonucleotides that selectively decrease endogenous tau expression throughout the entire mouse CNS—brain and spinal cord tissue, interstitial fluid, and CSF—while having no effect on baseline motor or cognitive behavior. In two chemically induced seizure models, mice with reduced tau protein had less severe seizures than control mice. Total tau protein levels and seizure severity were highly correlated, such that those mice with the most severe seizures also had the highest levels of tau. Our results demonstrate that endogenous tau is integral for regulating neuronal hyperexcitability in adult animals and suggest that an antisense oligonucleotide reduction of tau could benefit those with epilepsy and perhaps other disorders associated with tau-mediated neuronal hyperexcitability.

Introduction

As a member of the microtubule-associated protein family (Weingarten et al., 1975), the protein tau is enriched in axons of mature and growing neurons (Kempf et al., 1996). However, under certain conditions, tau can become hyperphosphorylated and accumulate into oligomeric species and neurofibrillary tangles, resulting in a group of disorders known collectively as tauopathies (Billingsley and Kincaid, 1997; Lovestone and Reynolds, 1997; Buée and Delacourte, 1999) with the most common being Alzheimer's disease (AD).

Received May 16, 2013; revised June 26, 2013; accepted July 2, 2013.

Author contributions: S.L.D., C.F.B., J.R.C., D.M.H., and T.M.M. designed research; S.L.D., D.K.G., G.C., C.A.K., K.Y., F.R.S., D.R.S., S.E.M., F.R., J.R.C., and T.M.M. performed research; F.R. and C.F.B. contributed unpublished reagents/analytic tools; S.L.D., D.K.G., G.C., C.A.K., K.Y., S.E.M., D.F.W., F.R., J.R.C., D.M.H., and T.M.M. analyzed data; S.L.D. and T.M.M. wrote the paper.

This work was supported by the Tau Consortium (D.M.H. and T.M.M.), The National Institutes of Health (Grant #P50 AG05681 to T.M.M., J.C. Morris, PI; National Institute of Neurological Disorders and Stroke Grant #R01NS078398 to T.M.M.; and National Institute on Aging Grants #R21AG044719-01 to T.M.M. and #R01AG042513 to J.R.C.), Cure PSP (T.M.M.), and a Paul B. Beeson Career Development Award (Grant #NINDS K08NS074194 to T.M.M.) The microscopy work was supported by the Hope Center Alafi Neuroimaging Laboratory and P30 Neuroscience Blueprint Interdisciplinary Center Core award to Washington University (Grant #P30 NS057105). We thank Chengjie Xiong and Mateusz Jasielec (Knight Alzheimer's Disease Center, Washington University) for assistance with statistical analysis and Michael Wong for assistance with induced seizure models.

Isis Pharmaceuticals supplies the authors with the ASOs in the described work. Both Isis Pharmaceuticals and Washington University have filed for patents based on using Tau ASOs to treat CNS disorders. The authors declare no other competing financial interests.

Correspondence should be addressed to Timothy M. Miller, Washington University in St. Louis, 115 Biotech Bldg, Box 8111, 660 S. Euclid St., St. Louis, MO 63110. E-mail: millert@neuro.wustl.edu.

DOI:10.1523/JNEUROSCI.2107-13.2013

 0270-6474/13/3312887-11$15.00/0

Although the role of tau in proteinaceous aggregates has long been studied (Iqbal et al., 1975; Brion et al., 1985), a new role has emerged that implicates tau as a regulator of neuronal hyperexcitability. Tau knock-out (tau $^{-/-}$) mice demonstrate substantially reduced seizure severity in models of chemically induced seizures (Roberson et al., 2007, 2011; Ittner et al., 2010) and genetic models of severe epilepsy (Holth et al., 2013). These data suggest that tau plays a role in neuronal hyperexcitability and provide evidence that a tau-reducing therapy may be beneficial for those with seizure disorders. In addition, amyloid precursor protein overexpression/amyloid-β-depositing mouse lines show increased baseline neuronal hyperexcitability and spontaneous seizures. When placed onto a tau $^{-/-}$ background, these AD mouse models show both decreased seizure frequency and improved learning and memory (Roberson et al., 2007, 2011; Ittner et al., 2010), suggesting that tau-linked neuronal hyperexcitability may be an important component of AD pathophysiology.

However, whether reducing tau levels in an adult animal will modulate neuronal hyperexcitability similar to genetic deletion remains unknown. For example, developmental compensation could contribute to the protective effect of tau $^{-/-}$, such as the reported increase in microtubule-associated protein 1A (Harada et al., 1994). Here, we tested directly the effect of reducing tau in adult nontransgenic mice by reducing endogenous tau levels and subsequently analyzing the effects on baseline behavior and induced seizure severity. We reduced murine endogenous tau levels using antisense oligonucleotides (ASOs) delivered directly to the CSF (DeVos and Miller, 2013a). Recent data

demonstrating safety of CSF-delivered ASOs in humans (Miller et al., 2013) suggests that the strategy used here may be translated into therapy for seizures and possibly other neurodegenerative disorders.

Materials and Methods

Animals. All ASO-treated mice were C57BL/6J nontransgenic mice ordered directly from The Jackson Laboratory. Tau $^{-/-}$ mice containing a GFP-encoding cDNA integrated into exon 1 of MAPT gene (Tucker et al., 2001) were obtained from The Jackson Laboratory and maintained on a C57BL/6J background. Characterization and behavioral experiments were performed using gender-balanced groups age 2–4 months (Figs. 1,2,3,4,5). Seizure experiments were performed using males age 3–5 months (Figs. 6,7,8). Mice had access to food and water *ad libitum* and were housed on a 12 h light/dark cycle. All animal protocols were approved by the institutional animal care and use committee at Washington University.

ASOs. The ASOs had the following modifications: 5 nucleotides on the 5′- and 3′-termini containing 2′-O-methoxyethyl modifications and 10 unmodified central oligodeoxynucleotides (DeVos and Miller, 2013b) to support RNaseH activity and a phosphorothioate backbone to improve nuclease resistance and promote cellular uptake (Bennett and Swayze, 2010). ASOs were synthesized as described previously (McKay et al., 1999; Cheruvallath et al., 2003) and solubilized in 0.9% sterile saline immediately before use. ASO sequences were as follows: Tau $^{ASO\text{-}1}$: 5′-GCAGGAGTTCTTAGATGTCT-3′; Tau $^{ASO\text{-}2}$: 5′-AAGCAGGTTAGGTGACAAGC-3′; Tau $^{ASO\text{-}3}$: 5′-ATCACTGATTTTGAAGTCCC-3′; Scrambled ASO: 5′-CCTTCCCTGAAGGTTCCTCC-3′.

Surgical placement of intracerebroventricular pumps and tissue collection. As described previously (Smith et al., 2006; DeVos and Miller, 2013a), mice were anesthetized with isoflurane and 28 d osmotic intracerebroventricular (ICV) pumps (ALZET) with ASO were implanted in a subcutaneous pocket that was formed on the back of the mouse. The catheter was placed in the right lateral ventricle using the following coordinates based on bregma: −0.5 mm posterior, −1.1 mm Lateral (right), −2.5 mm ventral. For CSF collection, mice were placed on a heating pad and anesthetized with isoflurane. CSF was drawn through the cisterna magna as described previously and immediately frozen on dry ice (Barten et al., 2011). For tissue collection, mice were anesthetized with isoflurane and perfused using chilled PBS-heparin. Brain and spinal cords were rapidly removed and either snap-frozen in liquid nitrogen and stored at −80°C or postfixed in 4% paraformaldehyde at 4°C and transferred to 30% sucrose 24 h later.

Quantitative real-time PCR. RNA analyses were performed using qRT-PCR. Total RNA was extracted from brain tissue using a QIAGEN RNeasy Kit. For total tau analyses, RNA was reverse transcribed and amplified using the EXPRESS One-Step Superscript qRT-PCR Universal Kit (Invitrogen). For Nsmaf mRNA levels, RNA was reverse transcribed and amplified with the *Power* SYBR Green RT-to-Ct 1-Step Kit (Invitrogen). The qRT-PCRs were run and analyzed on the ABI PRISM 7500 Fast Real-Time PCR System (Applied Biosystems). Total tau and Nsmaf mRNA expression levels were normalized to GAPDH mRNA levels and analyzed using the ΔΔCt method for relative expression analysis. The primer/probe sequences were as follows: total tau: forward 5′-GAA CCA CCA AAA TCC GGA GA-3′; reverse 5′-CTC TTA CTA GCT GAT GGT GAC-3′; Probe 5′-/56-FAM/CC AAG AAG GTG GCA GTG GTC C/3IABkFQ/-3′, Nsmaf: forward 5′-CTTACTGCTTCTCAACTTGGA-3′; reverse 5′-GAACATATCTTTAAGGAGCCTC-3′, GAPDH: forward 5′-TGC CCC CAT GT TGT GAT G-3′; reverse 3′-TGT GGT CAT GAG CCC TTC C-3′; and Probe 5′/56-FAM/AAT GCA TCC TGC ACC ACC AAC TGC TT/3AHBkFQ/3′ (IDT).

Tau protein analysis. Tissues were weighed and homogenized in 10× volume RAB buffer containing the following (in mM): 100 MES, 1 EDTA, 0.5 $MgSO_4$, 750 NaCl, 20 NaF, and 1 Na_3VO_4, supplemented with protease inhibitor (Complete Protease Inhibitor; Roche) and phosphatase inhibitor (Sigma). Homogenate was spun at 21,000 × *g* on a tabletop centrifuge for 10 min at 4°C. Supernatant was collected and protein concentration measured using a Pierce BCA Protein Assay Kit (Thermo Scientific). For tau protein quantification in brain, interstitial fluid (ISF), and CSF, tau concentrations were analyzed using the published Tau5-BT2 sandwich ELISA (Yamada et al., 2011). Briefly, 96-half-well plates (Nunc) were coated with the Tau-5 antibody (Millipore) overnight at 4°C. Plates were blocked with 4% BSA for 60 min at 37°C, brain homogenate, ISF, or CSF diluted in standard buffer (0.25% BSA, 300 mM Tris, 0.05% azide, and 1× protease inhibitor in PBS) was added and incubated overnight at 4°C. For the standard curve, the longest mouse tau isoform recombinant protein was used (mTau40). The detection antibody biotinylated BT-2 (Pierce) was added the next day, followed by streptavidin poly-horseradish peroxidase-40 (Fitzgerald). Plates were developed using Super Slow ELISA TMB (Sigma) and read on an Epoch Microplate Spectrophotometer (BioTek).

Immunofluorescence. Brains postfixed in 4% paraformaldehyde were sliced at 50 μm on a freezing microtome. Brain slices were treated with Citra Plus antigen retrieval (BioGenex) before antibody application. Brains were incubated with the primary antibodies Tau46 (1:300; Cell Signaling Technology) and Pan-ASO (1:1000; Isis) in 3% horse serum overnight at 4°C, followed by a 1 h incubation at room temperature with fluorescent-conjugated secondary antibodies (1:3000, DyLight; Thermo Scientific). Fluorescent images were captured using the Olympus Nanozoomer 2.0-HT (Hamamatsu) and processed using the NDP viewer software (Hamamatsu).

In vivo microdialysis for ISF collection. In vivo microdialysis experiments to assess brain ISF tau levels from awake and freely moving mice were developed with modifications of our previously described method (Yamada et al., 2011). A guide cannula (Eicom Microdialysis) was stereotaxically implanted in the left hippocampus under isoflurane anesthesia and cemented. After implantation of the cannula and dummy probes (Eicom Microdialysis), mice were habituated to microdialysis cages for one more day. After this recovery period, a 2 mm 1000 kDa cutoff AtmosLM microdialysis probe (Eicom Microdialysis) was inserted through the guide cannula. A probe was connected to a microdialysis peristaltic pump with two channels (MAB20; SciPro), which was operated in a push pull mode. The perfusion buffer, 25% human albumin solution (Gemini Bio), was diluted to 4% with aCSF containing the following (in mM): 1.3 $CaCl_2$, 1.2 $MgSO_4$, 3 KCl, 0.4 KH_2PO_4, 25 $NaHCO_3$, and 122 NaCl, pH 7.35, on the day of use and filtered through 0.1 μm membrane. ISF was collected at 1 μl/min in a refrigerated fraction collector (SciPro).

Lactate assay. Lactate concentration in ISF was determined by YSI2700 biochemistry analyzer (YSI Life Sciences).

Sensorimotor battery and 1 h locomotor activity. All mice were evaluated on a battery of sensorimotor tests designed to assess balance (ledge and platform), strength (inverted screen), coordination (pole and inclined screens), and initiation of movement (walking initiation), as described previously (Wozniak et al., 2004; Grady et al., 2006). Locomotor activity was evaluated in all mice over a 1 h period using computerized photobeam instrumentation as described previously (Wozniak et al., 2004, 2007). General activity variables (total ambulations, vertical rearings), along with indices of emotionality, including time spent, distance traveled, and entries made in a 33 × 11 cm central zone, were analyzed.

Elevated plus maze. As described previously (Schaefer et al., 2000), the elevated plus maze (EPM) apparatus is a four-arm maze shaped like a plus sign. One set of the opposing arms have walls (closed arms) and the other set is not enclosed (open arms). The number of entries made, time spent, and distance traveled in each set of arms were quantified using a computerized, high-resolution photobeam system (Hamilton-Kinder). These three variables were also analyzed after normalizing the values to reflect percentages calculated out of the totals measured in both sets of arms.

Morris water maze. Spatial learning and memory were evaluated in the Morris water maze using a computerized tracking system (ANY-maze; Stoelting) and procedures that were similar to previously described methods (Wozniak et al., 2004, 2007). The protocol included cued, place, and probe trials and all trials were performed in a 120-cm-diameter pool

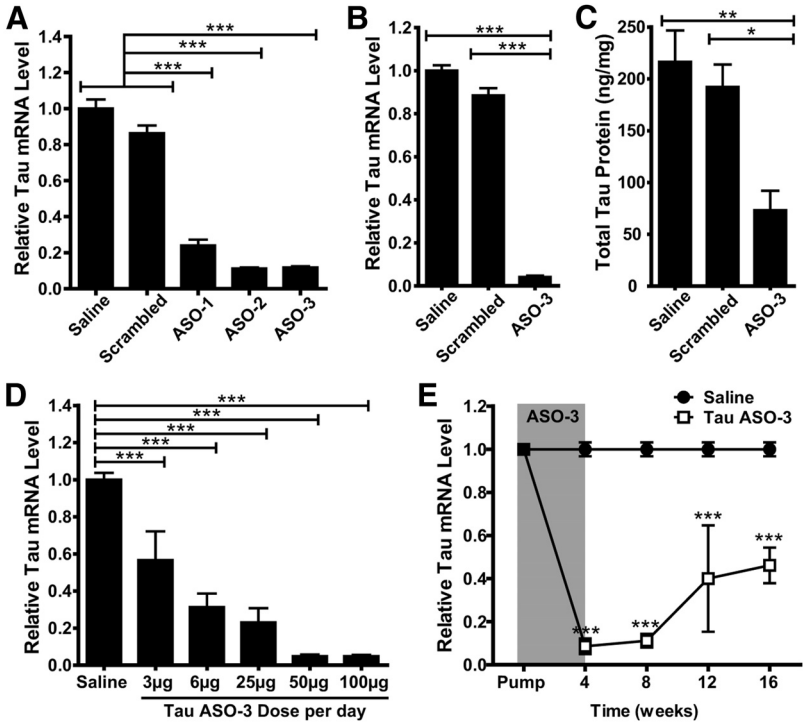

Figure 1. ASOs reduce tau mRNA and protein. ***A***, Saline, scrambled, or tau ASOs were infused into the right hippocampus of NT mice ($n = 4–6$ per group) and the area around the injection site was analyzed 1 week later for total tau mRNA levels. Tau $^{ASO-3}$ was very potent at reducing total tau mRNA. One-way ANOVA and Bonferroni *post hoc* analysis were used. ***B***, ***C***, Saline, scrambled, or Tau $^{ASO-3}$ was infused intracerebroventricularly (ICV) into NT mice at 100 μg/d for 1 month ($n = 4–7$). The right parietal cortex was analyzed for total tau mRNA levels (***B***) and the right ventral white matter was analyzed for total tau protein levels by ELISA (***C***). One-way ANOVA and Bonferroni *post hoc* analysis were used. ***D***, Saline or Tau $^{ASO-3}$ was delivered via ICV infusion with increasing concentrations of Tau $^{ASO-3}$ ($n = 3–13$). After 1 month, total tau mRNA levels were measured. One-way ANOVA and Bonferroni *post hoc* analysis were used. ***E***, Saline or Tau $^{ASO-3}$ was delivered via ICV infusion at 25 μg/d for 1 month. Total tau mRNA levels were analyzed at 4, 8, 12, and 16 weeks after pump implantation ($n = 3–5$). Two-way ANOVA and Bonferroni post hoc analysis were used. $^*p < 0.05$; $^{**}p < 0.01$; $^{***}p < 0.001$. Error bars represent SEM.

filled with opaque water. Cued trials were performed to identify nonassociative dysfunctions that might affect performance. This involved conducting four trials (60 s maximum) per day for two consecutive days with very few distal cues being present and with the platform location being moved for each trial to limit spatial learning. Three days later, place trials were initiated to assess spatial learning; mice were required to learn the single location of a submerged (nonvisible) platform in the presence of several salient distal spatial cues. The place trials were conducted for 5 consecutive days, each day consisting of 2 blocks of 2 trials (60 s maximum) separated by 2 h. Escape path length, latency, and swimming speeds were calculated for the cued and place trials. A probe trial lasting 60 s was conducted 1 h after the last trial of the place condition. This involved removing the platform and quantifying the time spent in the pool quadrant that had contained the platform (target) and each of the other quadrants and the number of crossings a mouse made over the exact location of where the platform had been (platform crossings). Spatial bias for the target quadrant was analyzed by comparing the time spent in it versus the times spent in each of the other quadrants.

Picrotoxin seizures and EEG recording. In vivo picrotoxin (PTX) reverse microdialysis experiments from awake and freely moving mice were developed with modifications to the previously described method (Cirrito et al., 2008). To record EEG activity, bipolar recording electrodes (Teflon-coated, stainless steel wire, 0.0055 inch coated OD, A-M Systems) were attached to the outside of the microdialysis guide cannula shaft using Elmer's Super-Fast Epoxy Resin. The electrodes extended ~1 mm beyond the tip of guide such that the tips of the electrodes would fall in the center of the 2 mm microdialysis probe membrane once inserted. The guide cannula with attached electrodes (BR-style; Bioanalytical Systems) was stereotaxically implanted in the left hippocampus under isoflurane anesthesia and cemented. Microdialysis probes (2 mm, BR-2, 30 kDa MWCO membrane; Bioanalytical Systems) were inserted into the hippocampus. The perfusion buffer comprised aCSF with 0.15% bovine serum albumin filtered through 0.1 μm membrane on the day of use. Once the microdialysis guide cannula and probe were placed into the left hippocampus, 12 h of basal EEG activity was measured using a P511K A.C. preamplifier (Grass Instruments), digitized with a DigiData 1322A data acquisition system (Molecular Devices), and recorded digitally with pClamp 9.2 (Molecular Devices). PTX (Sigma-Aldrich) was diluted to the indicated concentrations in 0.15% BSA-aCSF perfusion buffer and delivered at a flow rate of 1.0 μl/min, with the lowest dose given first. Each increasing dose was delivered for 90 min and EEG was measured continuously throughout drug delivery. EEG spike frequency was assessed for the last 60 min of each PTX dose and normalized to basal EEG of each mouse.

Experimental pentylenetetrazole seizures. Pentylenetetrazole (PTZ; Sigma) was dissolved in sterile PBS at a concentration of 5 mg/ml. A dose of 55 or 80 mg/kg was delivered intraperitoneally for the experiments shown in Figures 7 and 8, respectively. A quiet, isolated room was used for all seizures to minimize noise and/or visual distractions. Immediately after PTZ administration, each mouse was videotaped and 15 min later, the mouse was killed and the brain was snap-frozen for biochemical analyses. Seizures recorded on videotapes were scored in a blinded fashion for severity according to published scales (Löscher and Nolting, 1991; Racine, 1972). The seizure severity score used was as follows: 0 = normal behavior; 1 = immobility; 2 = spasm, tremble, or twitch; 3 = tail extension; 4 = forelimb clonus; 5 = generalized clonic activity; 6 = jumping or running seizures; 7 = full tonic extension; and 8 = death.

Statistics. The data were analyzed for statistical significance using GraphPad Prism 5 software. Two-tailed Student's *t* tests were used for total tau mRNA/protein and lactate analyses when only one comparison was being made and for analyzing tau mRNA/protein levels in multiple different brain regions. One-way ANOVA with Bonferroni *post hoc* analyses were used for total tau mRNA and protein expression when more than one comparison was needed and for the inverted screen task. Two-way ANOVA with Bonferroni *post hoc* analyses were used for the duration of action study and for ISF tau levels in multiple fractions. Two-way repeated-measures ANOVA (rmANOVA) with Bonferroni *post hoc* analyses were used to analyze Morris water maze, EPM trials, and PTX dose response. Specifically for the Morris water maze and EPM analyses, the Huynh-Feldt adjustment of α levels was used for all within-subjects effects containing more than two levels to protect against violations of sphericity/compound symmetry assumptions underlying rmANOVA models. The Kruskal–Wallis with Dunns *post hoc* analyses was used for the PTZ seizure severity analysis due to the categorical nature of the seizure severity scale. Linear regression analysis was used to analyze the CSF and brain tau correlations. Linear regression was used to generate the "best-fit" and 95% confidence interval lines seen on the graphs in Figures 6, 7, and 8, and the Spearman correlation was used to generate *r* and *p*-values for all total tau and EEG/seizure comparisons. Error bars in the figures represent SEM.

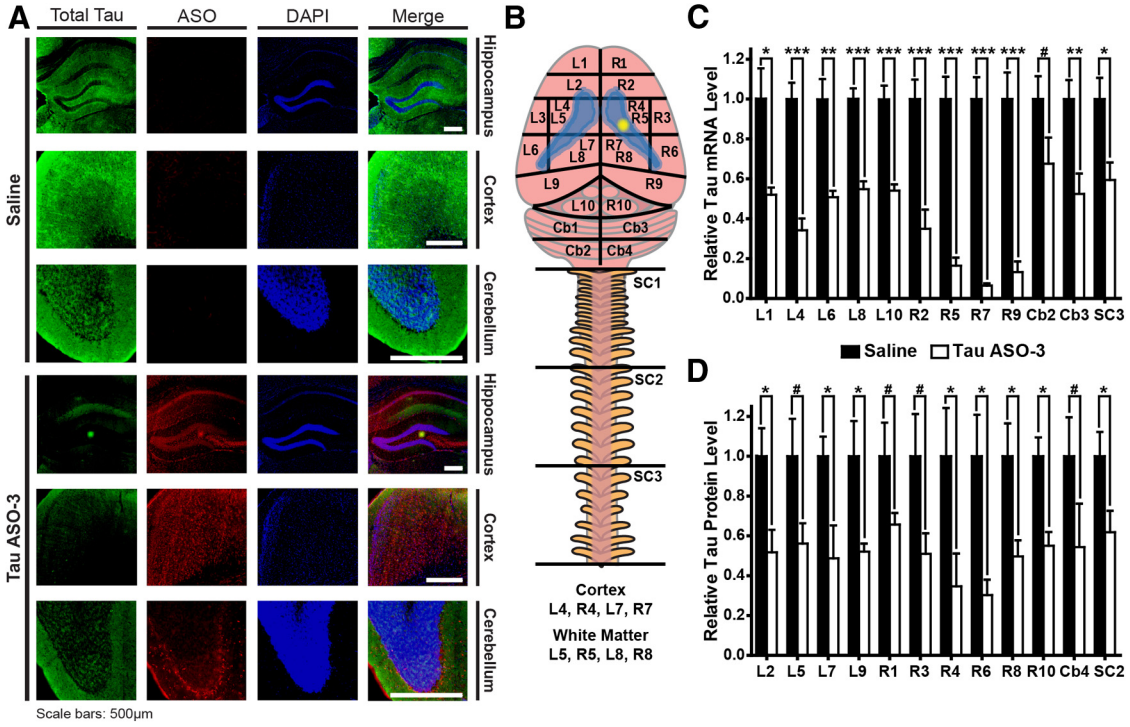

Figure 2. ASOs reduce tau mRNA and protein throughout the mouse CNS. ***A***, Saline or Tau^{ASO-3} was delivered by intracerebroventricular infusion at 25 μg/d into NT mice for 1 month. In mice collected 8 weeks after pump implantation, brain tissue was costained with a total tau antibody (green), an ASO antibody (red), and counterstained with DAPI (blue). Three brain regions—the hippocampus, frontal cortex, and cerebellum— on the contralateral side of the brain from the catheter (left hemisphere) were analyzed. Scale bars, 500 μm. ***B–D***, Using the same treatment paradigm as in ***A***, brains were dissected into regions as shown in ***B*** ($n = 4–6$). Lateral ventricles are highlighted in blue and the catheter position in yellow. Tau mRNA (***C***) and protein levels (***D***) were measured in each region. $^{\#}p < 0.1$, $^{*}p < 0.05$, $^{**}p < 0.01$, $^{***}p < 0.001$, two-tailed *t* test. Error bars represent SEM.

Results

Tau ASOs reduce endogenous tau mRNA and protein expression

To determine the functional effect of reducing tau mRNA and protein *in vivo*, we developed an ASO that reduces endogenous tau mRNA and protein in adult mice. After screening 80 ASOs for their ability to reduce tau mRNA in murine B16-F10 cells, we selected the three most potent ASOs to screen *in vivo*. We infused 50 μg of each tau ASO into the right hippocampus of adult nontransgenic (NT) mice using saline and a scrambled ASO as controls. One week after ASO infusion, the hippocampus surrounding the injection site was analyzed for total tau mRNA levels (Fig. 1*A*). All ASOs screened in the hippocampus provided >75% reduction of tau mRNA (ANOVA $F_{(4,22)} = 151.4$, $p < 0.0001$). The ASO Tau^{ASO-3} was then tested in a 1 month ICV Alzet osmotic pump infusion at 100 μg/d. Compared with the saline and scrambled ASO controls, those mice treated with Tau^{ASO-3} had substantially less total tau mRNA (ANOVA $F_{(2,14)} = 291.8$, $p < 0.0001$) and protein levels (ANOVA $F_{(2,13)} = 7.578$, $p = 0.007$; Fig. 1*B*,*C*). To test for general off-target ASO effects, we normalized tau mRNA to total RNA input and found no

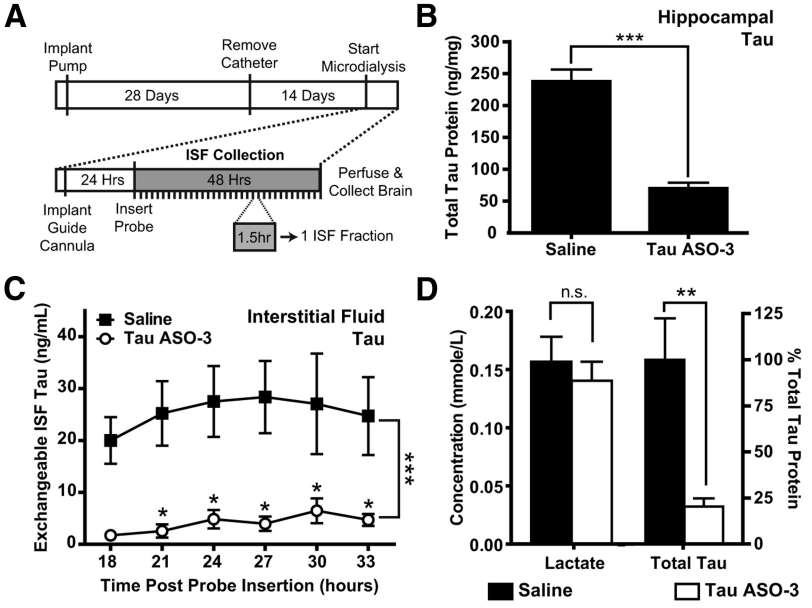

Figure 3. Total tau protein in the brain ISF is decreased. ***A***, Experimental paradigm. NT mice ($n = 4–6$) were treated with saline or 75 μg/d Tau^{ASO-3} via intracerebroventricular infusion for 1 month and the catheters then removed. After 14 d, a guide cannula and microdialysis probe were placed in the left hippocampus. ISF was collected for 48 h. Each ISF fraction comprised a 90 min collection time. ***B***, Total brain tau protein levels in the left hippocampus were measured, confirming that brain tau was reduced. Two-tailed *t* test was used. ***C***, Total tau protein levels were measured in several ISF fractions. Two-way ANOVA and Bonferroni *post hoc* analysis were used. ***D***, Fractions from 18–34 h were pooled for each animal to measure total tau protein levels and lactate as a control for probe function. The concentrations were calculated for the 1 μl/min flow rate. There was no significant decrease in lactate levels, demonstrating adequate probe function. Two-tailed t test was used. $^{*}p < 0.05$; $^{**}p < 0.01$; $^{***}p < 0.001$. Error bars represent SEM.

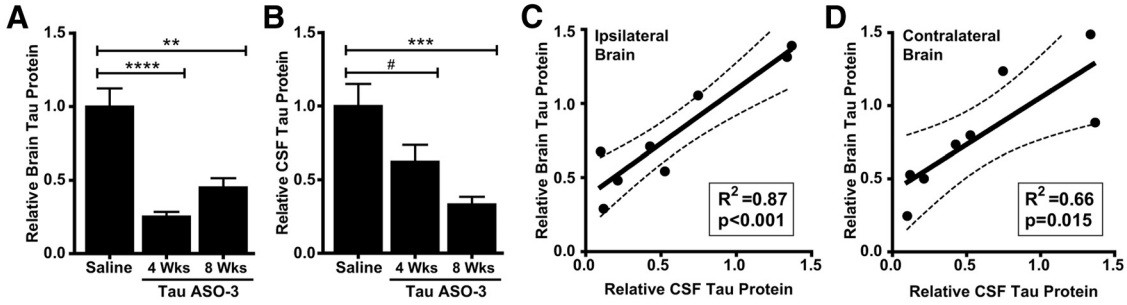

Figure 4. CSF tau protein levels are decreased and correlate with brain tau levels. ***A***, ***B***, NT mice were treated with saline or 25 μg/d Tau^{ASO-3} via intracerebroventricular infusion for 1 month. At 4 and 8 weeks after pump implantation, total tau protein levels in the brain ($n = 4–7$; ***A***) and CSF ($n = 8–10$; ***B***) were measured. One-way ANOVA and Bonferroni *post hoc* analysis were used. ***C***, ***D***, Total brain tau from the right (***C***) and left (***D***) sides of the brain were correlated with CSF tau levels for each mouse ($n = 8$). The best-fit line and 95% confidence bands were generated using linear regression analysis. $^{\#}p < 0.1$; $^{**}p < 0.01$; $^{***}p < 0.001$. Error bars represent SEM.

difference between tau mRNA results generated through standard GAPDH normalization or total RNA input (two-tailed *t* test: saline $t_{(12)} = 0.000$, $p = 1.000$; scrambled $t_{(10)} = 0.297$, $p = 0.773$; Tau^{ASO-3} $t_{(6)} = 1.317$, $p = 0.236$). To further test specificity for tau, we BLASTED the Tau^{ASO-3} sequence against the mouse genome and found that the closest match, neutral sphingomyelinase activation associated factor (Nsmaf), had 5 bp mismatches. When total Nsmaf mRNA levels were measured, no significant difference for saline, 100 μg/d of scrambled, or 100 μg/d of Tau^{ASO-3} treated mice was found (ANOVA $F_{(2,14)} = 1.914$, $p = 0.184$), reinforcing the specificity of Tau^{ASO-3} for murine tau.

To select the optimum dose for behavioral studies, we tested five doses of Tau^{ASO-3}. There was a dose-dependent decrease in total tau mRNA expression levels (ANOVA $F_{(5,28)} = 48.12$, $p < 0.0001$; Fig. 1*D*). The 25 μg/d dose was the lowest dose that provided >75% tau mRNA reduction and was selected for subsequent studies. In addition, to plan treatment paradigms for behavioral studies, we tested the duration of action of a 1 month ASO infusion. After infusing 25 μg/d Tau^{ASO-3} for 1 month, tau mRNA levels were measured in cohorts of mice at 4, 8, 12, and 16 weeks after pump implantation. Four weeks after ASO infusion had stopped (8 weeks after pump implantation), tau mRNA levels remained >80% decreased. Even at 12–16 weeks after pump implantation, tau mRNA remained decreased to >50% of the saline control (ANOVA $F_{(1,34)} = 225.7$, $p < 0.0001$; Fig. 1*E*). The long-term target knock-down results shown here are consistent with what others have reported for RNase-H-activating ASOs (Kordasiewicz et al., 2012), highlighting the long duration of action that RNase-H ASOs exhibit in tissue. This lengthy duration of action is likely due to a long half-life of the ASO itself (Yu et al., 2009; Kordasiewicz et al., 2012), allowing a 1 month infusion of 25 μg/d Tau^{ASO-3} to provide 4 months of tau mRNA reduction.

Tau ASOs reduce tau mRNA and protein throughout the brain and spinal cord

To determine the distribution of Tau^{ASO-3} after 1 month of ICV infusion of 25 μg/d, we used an antibody that recognizes the backbone chemistry of the ASO (Kordasiewicz et al., 2012). Staining for Tau^{ASO-3} demonstrated widespread, diffuse distribution of ASO in the brains of ASO-treated mice (Fig. 2*A*). Costaining for Tau^{ASO-3} and total tau demonstrated a clear link between the presence of ASO and lack of total tau in the contralateral frontal cortex, hippocampus, and cerebellum (Fig. 2*A*), showing that infusing Tau^{ASO-3} using ICV pumps can effectively distribute the ASO throughout the brain and reduce tau protein.

The immunofluorescence results showed a qualitative decrease in tau protein levels. To quantify more precisely the amount of tau mRNA and protein reduction in the CNS, we measured total tau mRNA and protein levels in multiple CNS regions 8 weeks after implantation of 1 month ICV pumps with 25 μg/d Tau^{ASO-3} (Fig. 2*B*). In both the mRNA and protein analyses, total tau levels were decreased in the left and right brain hemispheres and the spinal cord, confirming the widespread reduction of tau expression in the adult mouse CNS (Fig. 2*C*,*D*).

Tau protein levels are reduced in the brain ISF and CSF

To better understand the full effects of Tau^{ASO-3}, we examined tau protein levels in two additional CNS compartments: the brain ISF and CSF. Recently, reports have placed tau in the extracellular space under physiological conditions (Yamada et al., 2011; Pooler et al., 2013). To determine whether tau ASOs can decrease tau that is secreted into the ISF, we treated a cohort of mice with a 75 μg/d concentration of Tau^{ASO-3} or saline for 1 month with ICV pumps. At the end of ASO infusion, catheters and pumps were removed and microdialysis probes implanted into the left hippocampus 2 weeks later. We collected ISF for 48 h, with a new fraction being collected every 90 min (Fig. 3*A*). Immediately after ISF collection, the left hippocampus was dissected out and total tau levels were measured to confirm that brain tau protein was indeed reduced in the Tau^{ASO-3} cohort (two-tailed *t* test $t_{(10)} = 8.462$, $p < 0.0001$; Fig. 3*B*).

Total ISF tau protein levels were steady across time in both the saline and Tau^{ASO-3} groups and substantially reduced in the Tau^{ASO-3} treated cohort (ANOVA $F_{(1,36)} = 48.22$, $p < 0.0001$; Fig. 3*C*), allowing multiple fractions to be combined from the same mouse. These same eight fractions were pooled for each animal and total tau protein levels were again measured. In the Tau^{ASO-3}-treated group, ISF total tau protein levels were greatly reduced compared with the saline control (two-tailed *t* test $t_{(8)} = 9.283$, $p = 0.003$). ISF lactate levels were not significantly different between the saline and Tau^{ASO-3} groups (two-tailed *t* test $t_{(8)} = 0.6169$, $p = 0.555$). No difference in ISF lactate levels, which usually increase in response to synaptic transmission, suggests that a reduction in endogenous tau does not influence baseline neuronal activity (Bero et al., 2011).

To examine the correlation between brain and CSF tau levels, we treated a cohort of mice with 25 μg/d Tau^{ASO-3} or saline for 1 month. Half of the mouse brains were collected 4 weeks after pump implantation and the other 8 weeks after pump insertion. Immediately before collecting the brains, CSF was drawn from the cisterna magna of the mice, averaging 10 μl of CSF per mouse.

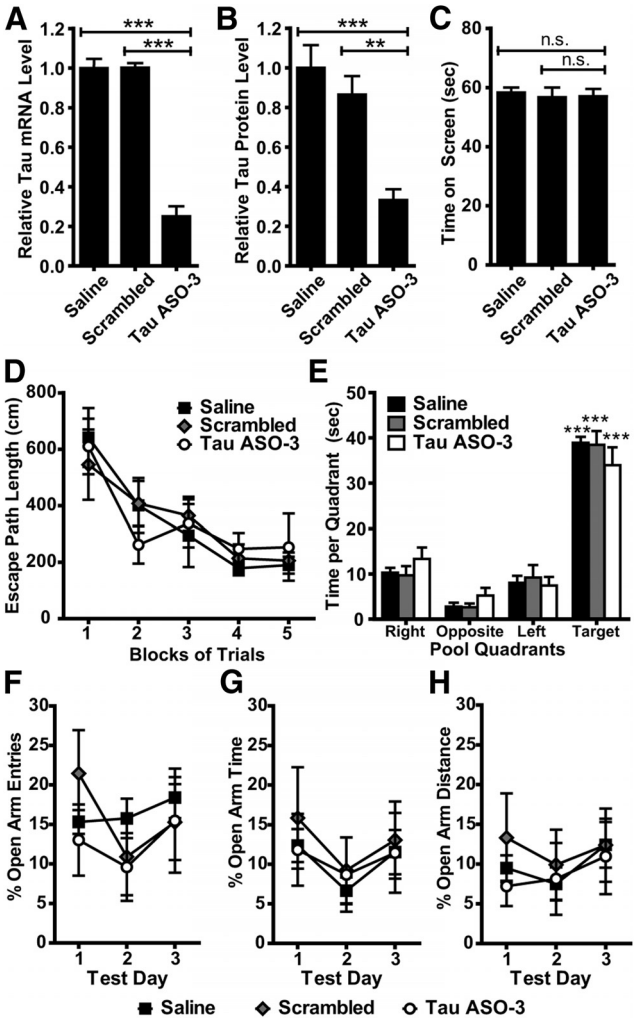

Figure 5. Tau reduction does not alter baseline behavior *in vivo*. ***A***, ***B***, NT mice ($n = 7–8$) were treated with saline, 25 μg/d scrambled ASO, or 25 μg/d Tau^{ASO-3} via intracerebroventricular infusion for 1 month. Pumps were removed and mice sent for a battery of behavioral tasks lasting a total of 1.5 months. Immediately after behavior testing, brain total tau mRNA (***A***) and protein (***B***) levels were measured. One-way ANOVA and Bonferroni *post hoc* analysis were used. ***C***, All three treatment groups performed similarly on the inverted screen task from the sensorimotor battery. One-way ANOVA and Bonferroni *post hoc* analysis were used. ***D***, ***E***, No significant differences were observed among the three treatment groups with regard to performance on the place trials in the Morris water maze (***D***) or spatial bias for the target quadrant during the probe trial (***E***). Two-way rmANOVA and Bonferroni *post hoc* analysis were used. ***F–H*** The three treatment groups also performed similarly on the EPM in terms of open arm entry percentage (***F***), percentage time spent in open arms (***G***), and open arm distance percentage (***H***), suggesting that tau reduction does not result in anxiety-related behavioral performance deficits. Two-way rmANOVA and Bonferroni *post hoc* analysis were used. $^{**}p < 0.01$; $^{***}p < 0.001$; $n = 7–8$. Error bars represent SEM.

As predicted, brain tau protein levels were decreased at both the first time point and the second (ANOVA $F_{(2,14)} = 20.96$, $p < 0.0001$; Fig. 4*A*). Interestingly, the CSF total tau was not reduced to the same extent as brain tau at the 4 week collection time, although by the 8 week time point, CSF tau was lower in the Tau^{ASO-3}-treated mice (ANOVA $F_{(2,24)} = 9.720$, $p = 0.0008$; Fig. 4*B*). Although the reason for this lag in CSF tau reduction is unknown, it may be in part due to a slow turnover of intracellular tau protein to the CSF pool, resulting in a continued decrease in CSF tau while brain tau levels begin to increase. Total brain and CSF tau protein levels were significantly correlated, both in the brain adjacent to the catheter (linear regression $R^2 = 0.867$, $F_{(1,6)} = 39.11$, $p = 0.0008$; Fig. 4*C*) and the contralateral frontal cortex (linear regression $R^2 = 0.657$, $F_{(1,6)} = 11.49$, $p = 0.0147$; Fig. 4*D*). These data, in addition to showing a reduction of extracellular tau, suggest that CSF tau levels may be an excellent predictor of brain tau levels in a Tau^{ASO-3} treatment paradigm.

Reducing tau mRNA and protein does not alter baseline behavior

Before assessing whether tau reduction can provide protection in experimental behavioral paradigms, we first analyzed the mice for any gross motor or cognitive behavioral abnormalities. Tau$^{-/-}$ mice appear normal on learning/memory tasks for up to 1 year (Roberson et al., 2007, 2011; Dawson et al., 2010; Ittner et al., 2010), with some minor parkinsonism motor phenotypes developing at ~12 months of age (Lei et al., 2012; Morris et al., 2013). These largely normal behavior phenotypes, however, could be in part due to developmental compensation. We treated a cohort of NT mice with saline, 25 μg/d scrambled control ASO, or 25 μg/d Tau^{ASO-3} for 1 month and conducted behavioral assessments for 1.5 months after pump removal. Total tau mRNA (ANOVA $F_{(2,19)} = 101.3$, $p < 0.0001$) and protein (ANOVA $F_{(2,19)} = 13.95$, $p = 0.0002$) levels were confirmed to be reduced only in mice treated with Tau^{ASO-3} (Fig. 5*A*,*B*). The mice with decreased tau levels performed similarly to both the saline and scrambled ASO control groups on all seven measures of the sensorimotor battery, including the inverted screen test (ANOVA $F_{(2,19)} = 0.116$, $p = 0.891$; Fig. 5*C*), suggesting that the Tau^{ASO-3} mice did not have any gross sensorimotor dysfunctions. Except for a possible hyperactivity in the Tau^{ASO-3} group, Tau^{ASO-3} mice also displayed similar behavior during the 1 h locomotor activity test. The Tau^{ASO-3} mice did not exhibit any significant performance deficits on the place (rmANOVA $F_{(2,76)} = 0.006$, $p = 0.994$) or probe (rmANOVA $F_{(2,76)} < 0.0001$, $p = 1.000$) trials in the water maze (Fig. 5*D*,*E*), thus providing evidence that their spatial learning and memory were intact. Analysis of the EPM data also showed that the Tau^{ASO-3} did not differ in levels of anxiety-related behaviors compared with the saline and scrambled ASO control groups (percentage of open arm entries rmANOVA $F_{(2,38)} = 0.284$, $p = 0.756$; percentage of open arm time rmANOVA $F_{(2,38)} = 0.134$, $p = 0.875$; percentage of open arm distance rmANOVA $F_{(2,38)} = 0.211$, $p = 0.754$; Fig. 5*F–H*). There was also no difference between groups in regard to the total distance traveled in the EPM (ANOVA $F_{(2,19)} = 0.639$, $p = 0.539$). Recognizing that the sample size tested was relatively small, the data suggest that, at least in the short term, reducing tau mRNA and protein in the adult mouse does not appear to result in behavioral impairments.

Reducing tau mRNA and protein protects against chemically induced seizures

To determine whether tau reduction is protective in an induced focal seizure model, we used reverse microdialysis to deliver the noncompetitive $GABA_A$ receptor antagonist PTX (Olsen, 2006) focally into the left hippocampus of NT male mice treated with saline, 25 μg/d scrambled ASO, or 12–25 μg/d Tau^{ASO-3} and simultaneously recorded the EEG activity at the site of PTX delivery. Because this treatment paradigm had not been used previously to study the protective effects of tau reduction, we included a cohort of untreated NT and tau$^{-/-}$ mice to serve as controls. Twelve hours of basal EEG activity were recorded, followed by continuous infusion of PTX into the left hippocampus with a stepwise increase in concentration every 90 min (4, 20, 100, and 500 μM). Untreated NT and saline-treated mice were com-

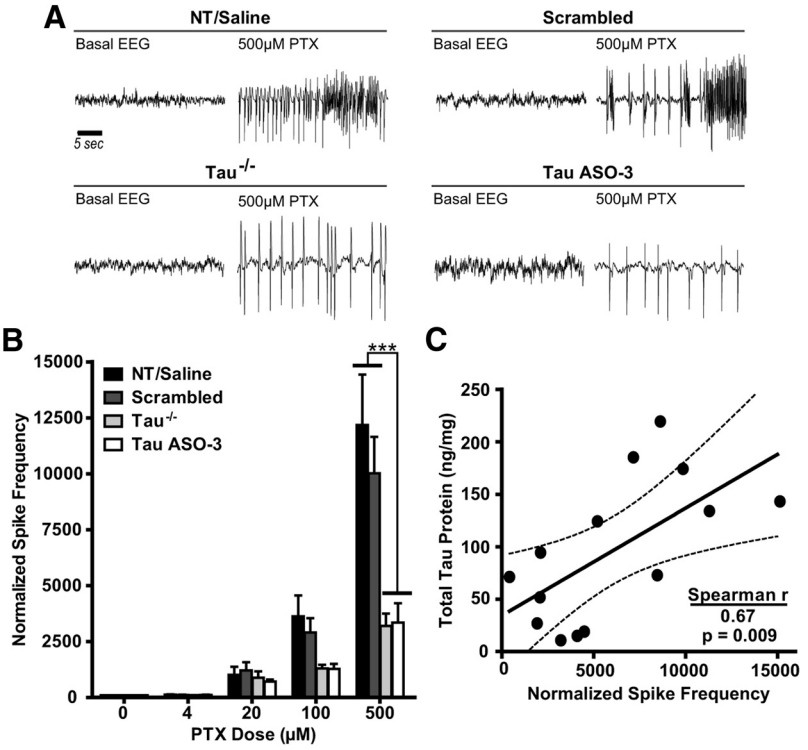

Figure 6. Tau reduction is protective against PTX-induced hyperexcitability in the hippocampus. ***A***, Increasing doses of PTX were infused into the left hippocampus of NT male mice treated with saline, 25 μg/d scrambled ASO, or 12–25 μg/d Tau$^{ASO\text{-}3}$ and into NT and tau$^{-/-}$ male mice with no catheter. Representative EEG traces from both baseline and 500 μm PTX are shown for NT/saline, scrambled ASO, Tau$^{-/-}$, and Tau$^{ASO\text{-}3}$ mice. ***B***, The spike frequency during the last hour of PTX infusion for each dose was calculated and normalized to baseline EEG. Untreated NT and saline-treated mice were combined due to no significant difference between the groups ($n = 4–8$). Two-way rmANOVA and Bonferroni *post hoc* analysis were used. ***C***, For those mice treated with saline, scrambled, and Tau$^{ASO\text{-}3}$ intracerebroventricular pumps, total tau levels in the left hippocampus were plotted against normalized spike frequency at the 500 μm PTX concentration (Spearman $r = 0.670$, $p = 0.0087$; $n = 14$). The best-fit line and 95% confidence bands were generated using linear regression analysis. ***$p < 0.001$. Error bars represent SEM.

bined due to no significant difference between the groups. The tau$^{-/-}$ mice showed a reduction in normalized spike frequency compared with the NT/saline group at the 500 μM PTX concentration, confirming the protective effect in tau-null mice in this new excitation paradigm (rmANOVA $F_{(3,72)} = 8.634$, $p = 0.0009$; Fig. 6*A*,*B*). The Tau$^{ASO\text{-}3}$-treated group also showed a strong protective effect compared with both the NT/saline and scrambled cohorts (Fig. 6*A*,*B*). Furthermore, total tau protein levels in the left hippocampus of pump-treated mice were highly correlated with normalized spike frequency at 500 μM PTX (Spearman correlation, $r_{(12)} = 0.670$, $p = 0.0087$; Fig. 6*C*). These PTX studies in adult mice support a direct correlation between lower tau protein levels and reduced neuronal hyperexcitability.

In addition to the focal increase in EEG activity, we tested the effects of tau reduction in a widely used seizure paradigm-intraperitoneal PTZ injections. PTZ seizures are considered a gold standard when testing the efficacy of anticonvulsant drugs in the early stages of development *in vivo* (Löscher, 2011). Three-month-old NT male mice were treated with saline, 25 μg/d scrambled ASO, or 25 μg/d Tau$^{ASO\text{-}3}$ for 1 month and then the pumps were removed. Three weeks later, 55 mg/kg of the GABA antagonist PTZ (Macdonald and Barker, 1977) was administered to the mice by intraperitoneal injection. The mice were videorecorded for 15 min and then immediately collected for total tau analyses (Fig. 7*A*). Any mouse that had >50% total tau mRNA levels was eliminated from the analysis of the Tau$^{ASO\text{-}3}$ group. Those mice treated with Tau$^{ASO\text{-}3}$ had less severe seizures than both the saline and scrambled ASO control groups (Kruskal–Wallis statistic = 16.26, $p = 0.0003$; Fig. 7*B*). Total tau mRNA (ANOVA $F_{(2,62)} = 281.5$, $p < 0.0001$) and protein (ANOVA $F_{(2,62)} = 45.73$, $p < 0.0001$) levels were confirmed to be reduced specifically in the Tau$^{ASO\text{-}3}$-treated group (Fig. 7*C*,*D*). As further confirmation that the effect of Tau$^{ASO\text{-}3}$ on seizures was secondary to tau reduction and was not an unknown effect of the ASO, we correlated the level of tau protein with seizure severity for individual animals. Indeed, seizure severity and tau protein levels correlated well in all tested mice (Spearman correlations, saline $r_{(24)} = 0.5889$, $p = 0.0016$; scrambled $r_{(19)} = 0.6795$, $p = 0.0007$; Tau$^{ASO\text{-}3}$ $r_{(18)} = 0.504$, $p = 0.0236$; Fig. 7*E*–*G*), providing evidence in a second inducible seizure model that a reduction in tau protein is protective against seizures.

Intrinsic variability in tau protein levels predicts susceptibility to chemically induced seizures

Due to the variability that has been seen with PTZ seizures (Mandhane et al., 2007), we were surprised that the correlation between seizure severity and tau levels persisted even in NT mice treated with only saline (Fig. 7*E*). This correlation suggests that, among the NT mouse population, normal endogenous tau levels predict susceptibility to neuronal hyperexcitability. It may be, however, that a more severe seizure results in an acute increase in brain tau protein expression. To test this possibility, we induced severe seizures in a separate cohort of untreated NT mice using a high dose of PTZ and analyzed total tau protein levels immediately afterward. There was no difference in tau protein levels in brain homogenate between those mice that underwent severe seizures secondary to PTZ injection compared with those mice that received a saline injection and did not have seizures (two-tailed *t* test $t_{(12)} = 0.354$, $p = 0.730$; Fig. 8*A*). Interestingly, in the PTZ-injected group, there was an inverse correlation between the time it took to reach a stage 8 seizure and the amount of endogenous tau protein measured. Those mice that had higher levels of endogenous tau protein progressed to severe seizures more quickly than those mice with lower tau (Spearman correlation $r_{(7)} = -0.887$, $p = 0.003$; Fig. 8*B*). These PTZ data show that the seizure itself does not increase tau protein acutely in brain tissues during the period of the seizure and, together with the Tau$^{ASO\text{-}3}$ PTX and PTZ seizure data, strongly suggest that those mice with higher levels of endogenous tau are inherently more susceptible to neuronal hyperexcitability.

Discussion

Using ASO technology directed against endogenous murine tau, total tau mRNA and protein levels were decreased throughout the brain and spinal cord of adult NT mice (Figs. 1,2). In addition, extracellular tau in the brain ISF (Fig. 3) and CSF (Fig. 4) was also

reduced after infusion of Tau$^{ASO\text{-}3}$ ASO. After tau was reduced in the adult mouse, no significant deviations from baseline were observed in a battery of motor and learning/memory behavior tasks (Fig. 5), demonstrating that short-term tau knock-down is well tolerated *in vivo*. In the setting of chemically induced seizures, tau reduction protected against seizure severity (Figs. 6,7), consistent with what has been reported with the genetic tau$^{-/-}$ mouse model. Further, we noted a significant correlation between total tau protein levels in the brain and seizure severity both in treated mice (Figs. 6,7) and in untreated mice (Fig. 8). These data strengthen the link between total tau expression levels and neuronal hyperexcitability regulation *in vivo* and demonstrate that the tau$^{-/-}$ effect on neuronal hyperexcitability is likely a tau-mediated event and not a developmental phenomenon.

The tau$^{-/-}$ genotype has been shown in numerous studies to be protective against excitotoxic insults (Roberson et al., 2007, 2011; Ittner et al., 2010), implicating tau in the physiological regulation of aberrant neuronal excitability. In addition, both a complete reduction and haploinsufficiency of tau significantly reduced seizures and extended survival in a well established genetic mouse model of epilepsy, Kv1.1$^{-/-}$ (Glasscock et al., 2010, 2012; Holth et al., 2013). These reports, in conjunction with previous *in vitro* data using tau knock-down ASOs to protect cells from glutamate-induced excitotoxicity (Pizzi et al., 1993) and our own *in vivo* tau knock-down data in two different seizure models, support the application of a tau-lowering therapy to regulate hyperexcitability in human patients. Compounds that provide protection against PTZ seizures *in vivo* have generally been successful in subsequent human clinical trials (Rogawski, 2006). Although many epilepsy patients respond to one or two anticonvulsants, 20–40% of patients remain untreated (Devinsky, 1999; Brodie et al., 2012). Therefore, a tau reduction approach may be an alternative therapy for this refractory population. Given the previous tau$^{-/-}$ protective findings in multiple seizure paradigms (Roberson et al., 2007, 2011; Holth et al., 2013), we predict that our findings of tau knock-down using two different GABA antagonists will also apply broadly to epilepsy *in vivo* models and to human epilepsy.

The finding that physiological endogenous tau levels in adult mice can affect susceptibility to hyperexcitability not only lends support to the idea that reducing tau may help lower seizure severity, but also implies that endogenous tau levels in humans may influence the risk of developing seizures. Although the exact reason for variability in tau protein expression between mice is unknown, other groups have shown similar variability in murine total tau levels (Holth et al., 2013). Further, tau mRNA and protein levels in human brains can vary by >2-fold (Lu et al., 2004; Kauwe et al., 2008; Trabzuni et al., 2012) and CSF total tau levels in control human subjects can differ substantially (Clifford et al., 2009; Fagan et al., 2009; Oka et al., 2013), perhaps due to variability in neuronal excretion rates of tau and different baseline tau levels in the brain. Higher levels of tau protein at baseline may not be detrimental, but, upon insult, increased tau expression may

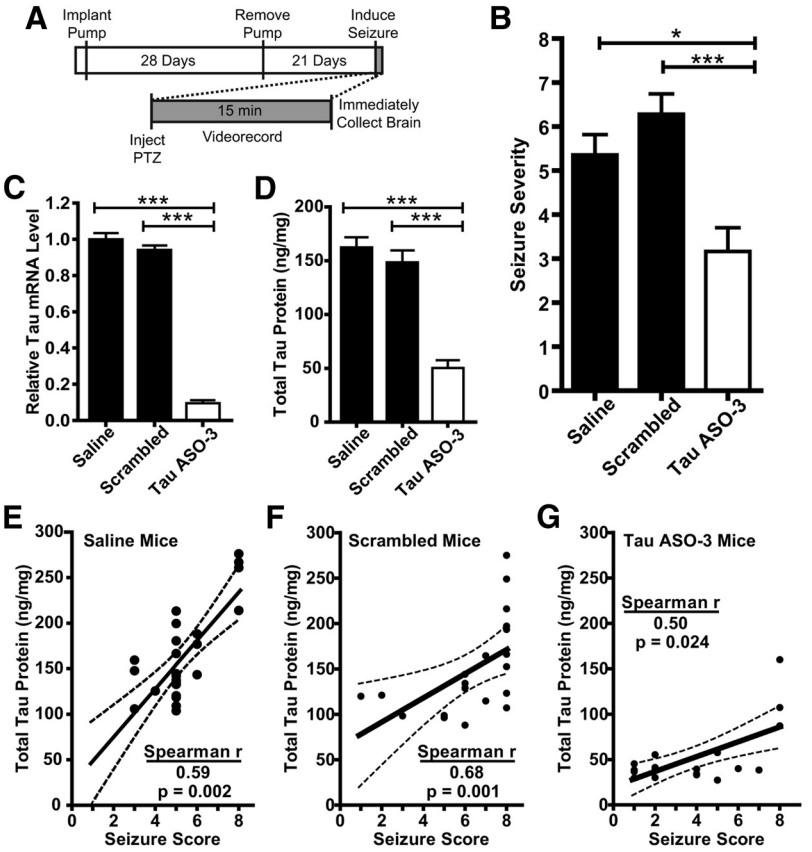

Figure 7. Tau reduction is protective against PTZ-induced global seizures. ***A***, Experimental paradigm. NT male mice were treated with saline, 25 μg/d scrambled ASO, or 25 μg/d Tau$^{ASO\text{-}3}$ for 1 month. Pumps were then removed and seizures induced 21 d later. Brains were collected immediately after the seizure. ***B***, PTZ (55 mg/kg) was given by intraperitoneal injection to saline-, scrambled ASO-, and Tau$^{ASO\text{-}3}$-treated mice and final seizure stage was scored blinded. Kruskal–Wallis and Dunn's *post hoc* analysis were used. ***C***, ***D***, Total tau mRNA (***D***) and protein (***E***) levels were confirmed to be down in only the Tau$^{ASO\text{-}3}$-treated group. One-way ANOVA and Bonferroni *post hoc* analysis were used. ***E***–***G***, Final seizure stage for each treated mouse plotted against the total tau protein levels. (saline: Spearman $r = 0.589$, $p = 0.002$; scrambled: Spearman $r = 0.680$, $p = 0.0007$; Tau$^{ASO\text{-}3}$: Spearman $r = 0.504$, $p = 0.024$). The best-fit line and 95% confidence bands were generated using linear regression analysis. $^{*}p < 0.05$; $^{**}p < 0.01$; $^{***}p < 0.001$; $n = 18–26$. Error bars represent SEM.

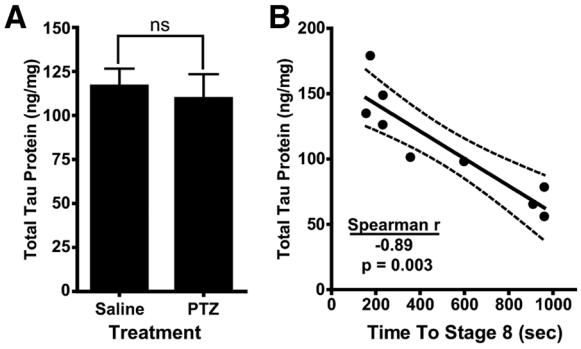

Figure 8. Total tau protein is inversely correlated with seizure latency. ***A***, A cohort of NT male mice ($n = 5–9$) were injected intraperitoneally with either saline or 80 mg/kg PTZ. Brains were collected immediately after mice reached a stage 8 seizure and total tau protein levels in right ventral white matter were measured. Two-tailed t test was used. ***B***, For each PTZ-injected mouse, the time to reach a stage 8 seizure was plotted against total tau protein (Spearman $r = -0.887$, $p = 0.003$). The best-fit line and 95% confidence bands were generated using linear regression analysis. Error bars represent SEM.

predispose human patients to injury-induced seizures. It is well documented that the incidence of seizures increases after different types of brain injury, including ischemic stroke (Camilo and Goldstein, 2004; Kwan, 2010) and traumatic brain injury (Annegers et al., 1998; Vespa et al., 2010). If human patients with higher baseline tau are more prone to developing seizures after an injury, being able to identify such patients through genetic studies of tau polymorphisms (Myers et al., 2007; Kauwe et al., 2008) or tau CSF levels (Palmio et al., 2009; Cruchaga et al., 2013) may help to risk stratify those patients and aid in determining who would benefit from a preventive antiepileptic therapy.

Tau knock-down has also been studied extensively in the presence of Aβ-deposition and proven to be protective against a growing number of Aβ-induced insults, including cognition (Roberson et al., 2007; Andrews-Zwilling et al., 2010; Ittner et al., 2010; Leroy et al., 2012), hyperexcitability (Roberson et al., 2007, 2011; Ittner et al., 2010; Suberbielle et al., 2013), decreased survival (Roberson et al., 2007, 2011; Ittner et al., 2010), axonal transport deficits (Vossel et al., 2010), cell-cycle reentry (Seward et al., 2013), and double-stranded breaks in DNA (Suberbielle et al., 2013). Several human amyloid precursor protein mouse lines and an ApoE4 mouse line have now been generated that display abnormal EEG and increased seizure frequency (Roberson et al., 2007; Ittner et al., 2010; Vogt et al., 2011; Hunter et al., 2012). Similarly, those with familial AD mutations, ApoE4 genotype, and sporadic late-onset AD also experience an increased incidence in seizures (Takao et al., 2001; Mendez and Lim, 2003; Harden, 2004; Velez-Pardo et al., 2004; Amatniek et al., 2006; Kauffman et al., 2010). This AD-associated excitotoxicity has been implicated in the pathogenesis of the disease (Olney et al., 1997; Mattson, 2004) and has recently been linked to an earlier onset of cognitive decline in AD patients (Vossel et al., 2013).

Because of the limitations in detecting abnormal EEG activity in large populations of AD patients, we currently rely heavily on animal models for predictions regarding hyperexcitability in the context of Aβ. In the human amyloid precursor protein J20 Aβ-depositing line, treatment with the anticonvulsant levetiracetam returned the baseline aberrant excitability back to NT levels and restored cognition (Sanchez et al., 2012), similar to what was seen with the tau $^{-/-}$ genetic cross (Roberson et al., 2007, 2011). This rescue in cognition by means of an anticonvulsant suggests that lowering the abnormal neuronal activity alone may have a positive impact on learning and memory. A similar pilot study was performed in human mildly cognitively impaired (MCI) patients, where patients were given either placebo or levetiracetam and then recall memory was tested using functional magnetic resonance imaging methods. Levetiracetam treatment significantly improved the recall performance of the MCI patients, again providing evidence that reducing the aberrant excitability in MCI and AD patients may help to restore cognition (Bakker et al., 2012). To test the hypothesis that decreasing aberrant hyperexcitability by means of tau reduction can in turn rescue cognitive decline, we have initiated tau-lowering ASO therapy in an Aβ-depositing mouse model of AD. We propose that tau may be involved in both AD-associated hyperexcitability and neuronal cell loss by means of tau aggregation and neurofibrillary tangle formation, making tau knock-down a strong therapeutic target for AD.

The human analog of the mouse tau ASO used here may be readily applicable to human patients. ASOs against superoxide dismutase 1 that extended survival in a rat model of amyotrophic lateral sclerosis (Smith et al., 2006) recently finished a phase I clinical trial in human patients. The CSF-delivered ASOs demonstrated excellent safety (Miller et al., 2013). Further, ASOs against survival motor neuron protein that also rescued rodent spinal muscular atrophy models (Hua et al., 2010; Passini et al., 2011; Porensky et al., 2012) are currently being used in phase II studies for children with spinal muscular atrophy. These studies and the growing success of ASOs in preclinical models (Kumar et al., 2000; Yokota et al., 2009; Lanford et al., 2010; DeVos and Miller, 2013b) suggest that the tau reduction strategy outlined here has real potential to be translated to the clinical setting for patients with epilepsy and perhaps tauopathies such as AD, progressive supranuclear palsy, and frontotemporal dementia.

References

Amatniek JC, Hauser WA, DelCastillo-Castaneda C, Jacobs DM, Marder K, Bell K, Albert M, Brandt J, Stern Y (2006) Incidence and predictors of seizures in patients with Alzheimer's disease. Epilepsia 47:867–872. CrossRef Medline

Andrews-Zwilling Y, Bien-Ly N, Xu Q, Li G, Bernardo A, Yoon SY, Zwilling D, Yan TX, Chen L, Huang Y (2010) Apolipoprotein E4 causes age- and Tau-dependent impairment of GABAergic interneurons, leading to learning and memory deficits in mice. J Neurosci 30:13707–13717. CrossRef Medline

Annegers JF, Hauser WA, Coan SP, Rocca WA (1998) A population-based study of seizures after traumatic brain injuries. N Engl J Med 338:20–24. CrossRef Medline

Bakker A, Krauss GL, Albert MS, Speck CL, Jones LR, Stark CE, Yassa MA, Bassett SS, Shelton AL, Gallagher M (2012) Reduction of hippocampal hyperactivity improves cognition in amnestic mild cognitive impairment. Neuron 74:467–474. CrossRef Medline

Barten DM, Cadelina GW, Hoque N, DeCarr LB, Guss VL, Yang L, Sankaranarayanan S, Wes PD, Flynn ME, Meredith JE, Ahlijanian MK, Albright CF (2011) Tau transgenic mice as models for cerebrospinal fluid tau biomarkers. J Alzheimers Dis 24:127–141. CrossRef Medline

Bennett CF, Swayze EE (2010) RNA targeting therapeutics: molecular mechanisms of antisense oligonucleotides as a therapeutic platform. Annu Rev Pharmacol Toxicol 50:259–293. CrossRef Medline

Bero AW, Yan P, Roh JH, Cirrito JR, Stewart FR, Raichle ME, Lee JM, Holtzman DM (2011) Neuronal activity regulates the regional vulnerability to amyloid-β deposition. Nat Neurosci 14:750–756. CrossRef Medline

Billingsley ML, Kincaid RL (1997) Regulated phosphorylation and dephosphorylation of tau protein: effects on microtubule interaction, intracellular trafficking and neurodegeneration. Biochem J 323:577–591. Medline

Brion JP, Passareiro H, Nunez J, Flament-Durand J (1985) Mise en evidence immunologique de la proteine tau au niveau des lesions de degenerescence neurofibrillaire de la maladie d'Alzheimer. Archives of Biologie, Bruxelles 95:229–235.

Brodie MJ, Barry SJ, Bamagous GA, Norrie JD, Kwan P (2012) Patterns of treatment response in newly diagnosed epilepsy. Neurology 78:1548–1554. CrossRef Medline

Buée L, Delacourte A (1999) Comparative biochemistry of tau in progressive supranuclear palsy, corticobasal degeneration, FTDP-17 and Pick's disease. Brain Pathol 693:681–693. Medline

Camilo O, Goldstein LB (2004) Seizures and epilepsy after ischemic stroke. Stroke 35:1769–1775. CrossRef Medline

Cheruvallath ZS, Kumar RK, Rentel C, Cole DL, Ravikumar VT (2003) Solid phase synthesis of phosphorothioate oligonucleotides utilizing diethyldithiocarbonate disulfide (DDD) as an efficient sulfur transfer reagent. Nucleosides Nucleotides Nucleic Acids 22:461–468. CrossRef Medline

Cirrito JR, Kang JE, Lee J, Stewart FR, Verges DK, Silverio LM, Bu G, Mennerick S, Holtzman DM (2008) Endocytosis is required for synaptic activity-dependent release of amyloid-beta in vivo. Neuron 58:42–51. CrossRef Medline

Clifford DB, Fagan AM, Holtzman DM, Morris JC, Teshome M, Shah AR, Kauwe JS (2009) CSF biomarkers of Alzheimer disease in HIV-associated neurologic disease. Neurology 73:1982–1987. CrossRef Medline

Cruchaga C, Kauwe JS, Harari O, Jin SC, Cai Y, Karch CM, Benitez BA, Jeng AT, Skorupa T, Carrell D, Bertelsen S, Bailey M, McKean D, Shulman JM, De Jager PL, Chibnik L, Bennett DA, Arnold SE, Harold D, Sims R, et al.

(2013) GWAS of cerebrospinal fluid tau levels identifies risk variants for Alzheimer's disease. Neuron 78:256–268. CrossRef Medline

Dawson HN, Cantillana V, Jansen M, Wang H, Vitek MP, Wilcock DM, Lynch JR, Laskowitz DT (2010) Loss of tau elicits axonal degeneration in a mouse model of AD. Neuroscience 169:516–531. CrossRef Medline

Devinsky O (1999) Patients with refractory seizures. N Engl J Med 340: 1565–1570. CrossRef Medline

DeVos SL, Miller TM (2013a) Direct intraventricular delivery of drugs to the rodent central nervous system. J Vis Exp 12:75. Medline

DeVos SL, Miller TM (2013b) Antisense oligonucleotides: treating neurodegeneration at the level of RNA. Neurotherapeutics 10:486–497. CrossRef Medline

Fagan AM, Head D, Shah AR, Marcus D, Mintun M, Morris JC, Holtzman DM (2009) Decreased cerebrospinal fluid Abeta(42) correlates with brain atrophy in cognitively normal elderly. Ann Neurol 65:176–183. CrossRef Medline

Glasscock E, Yoo JW, Chen TT, Klassen TL, Noebels JL (2010) Kv1.1 potassium channel deficiency reveals brain-driven cardiac dysfunction as a candidate mechanism for sudden unexplained death in epilepsy. J Neurosci 30:5167–5175. CrossRef Medline

Glasscock E, Qian J, Kole MJ, Noebels JL (2012) Transcompartmental reversal of single fibre hyperexcitability in juxtaparanodal Kv1.1-deficient vagus nerve axons by activation of nodal KCNQ channels. J Physiol 590: 3913–3926. CrossRef Medline

Grady RM, Wozniak DF, Ohlemiller KK, Sanes JR (2006) Cerebellar synaptic defects and abnormal motor behavior in mice lacking alpha- and beta-dystrobrevin. J Neurosci 26:2841–2851. CrossRef Medline

Harada A, Oguchi K, Okabe S, Kuno J, Terada S, Ohshima T, Sato-Yoshitake R, Takei Y, Noda T, Hirokawa N (1994) Altered microtubule organization in small-calibre axons of mice lacking tau protein. Nature 369:488–491. CrossRef Medline

Harden CL (2004) The apolipoprotein E epsilon (epsilon) 4 allele is important for trauma-related epilepsy. Epilepsy currents 4:29–30. CrossRef Medline

Holth JK, Bomben VC, Reed JG, Inoue T, Younkin L, Younkin SG, Pautler RG, Botas J, Noebels JL (2013) Tau loss attenuates neuronal network hyperexcitability in mouse and *Drosophila* genetic models of epilepsy. J Neurosci 33:1651–1659. CrossRef Medline

Hua Y, Sahashi K, Hung G, Rigo F, Passini MA, Bennett CF, Krainer AR (2010) Antisense correction of SMN2 splicing in the CNS rescues necrosis in a type III SMA mouse model. Genes Dev 24:1634–1644. CrossRef Medline

Hunter JM, Cirrito JR, Restivo JL, Kinley RD, Sullivan PM, Holtzman DM, Koger D, Delong C, Lin S, Zhao L, Liu F, Bales K, Paul SM (2012) Emergence of a seizure phenotype in aged apolipoprotein epsilon 4 targeted replacement mice. Brain Res 1467:120–132. CrossRef Medline

Iqbal K, Wisniewski HM, Grundke-Iqbal I, Korthals JK, Terry RD (1975) Chemical pathology of neurofibrils–neurofibrillary tangles of Alzheimer's presenile-senile dementia. J Histochem Cytochem 23:563–569. CrossRef Medline

Ittner LM, Ke YD, Delerue F, Bi M, Gladbach A, van Eersel J, Wölfing H, Chieng BC, Christie MJ, Napier IA, Eckert A, Staufenbiel M, Hardeman E, Götz J (2010) Dendritic function of tau mediates amyloid-β toxicity in Alzheimer's disease mouse models. Cell 142:387–397. CrossRef Medline

Kauffman MA, Consalvo D, Moron DG, Lereis VP, Kochen S (2010) ApoE epsilon4 genotype and the age at onset of temporal lobe epilepsy: a case-control study and meta-analysis. Epilepsy Res 90:234–239. CrossRef Medline

Kauwe JS, Cruchaga C, Mayo K, Fenoglio C, Bertelsen S, Nowotny P, Galimberti D, Scarpini E, Morris JC, Fagan AM, Holtzman DM, Goate AM (2008) Variation in MAPT is associated with cerebrospinal fluid tau levels in the presence of amyloid-beta deposition. Proc Natl Acad Sci U S A 105:8050–8054. CrossRef Medline

Kempf M, Clement A, Faissner A, Lee G, Brandt R (1996) Tau binds to the distal axon early in development of polarity in a microtubule- and microfilament-dependent manner. J Neurosci 16:5583–5592. Medline

Kordasiewicz HB, Stanek LM, Wancewicz EV, Mazur C, McAlonis MM, Pytel KA, Artates JW, Weiss A, Cheng SH, Shihabuddin LS, Hung G, Bennett CF, Cleveland DW (2012) Sustained therapeutic reversal of Huntington's disease by transient repression of huntingtin synthesis. Neuron 74: 1031–1044. CrossRef Medline

Kumar VB, Farr SA, Flood JF, Kamlesh V, Franko M, Banks WA, Morley JE (2000) Site-directed antisense oligonucleotide decreases the expression of amyloid precursor protein and reverses deficits in learning and memory in aged SAMP8 mice. Peptides 21:1769–1775. CrossRef Medline

Kwan J (2010) Stroke: predicting the risk of poststroke epilepsy-why and how? Nat Rev Neurol 6:532–533. CrossRef Medline

Lanford RE, Hildebrandt-Eriksen ES, Petri A, Persson R, Lindow M, Munk ME, Kauppinen S, Ørum H (2010) Therapeutic silencing of microRNA-122 in primates with chronic hepatitis C virus infection. Science 327:198–201. CrossRef Medline

Lei P, Ayton S, Finkelstein DI, Spoerri L, Ciccotosto GD, Wright DK, Wong BX, Adlard PA, Cherny RA, Lam LQ, Roberts BR, Volitakis I, Egan GF, McLean CA, Cappai R, Duce JA, Bush AI (2012) Tau deficiency induces parkinsonism with dementia by impairing APP-mediated iron export. Nat Med 18:291–295. CrossRef Medline

Leroy K, Ando K, Laporte V, Dedecker R, Suain V, Authelet M, Héraud C, Pierrot N, Yilmaz Z, Octave JN, Brion JP (2012) Lack of tau proteins rescues neuronal cell death and decreases amyloidogenic processing of APP in APP/PS1 mice. Am J Pathol 181:1928–1940. CrossRef Medline

Löscher W (2011) Critical review of current animal models of seizures and epilepsy used in the discovery and development of new antiepileptic drugs. Seizure 20:359–368. CrossRef Medline

Löscher W, Nolting B (1991) The role of technical, biological and pharmacological factors in the laboratory evaluation of anticonvulsant drugs. IV. Protective indices. Epilepsy Res 9:1–10. CrossRef Medline

Lovestone S, Reynolds CH (1997) The phosphorylation of tau: a critical stage in neurodevelopment and neurodegenerative processes. Science 78: 309–324. CrossRef Medline

Lu T, Pan Y, Kao SY, Li C, Kohane I, Chan J, Yankner BA (2004) Gene regulation and DNA damage in the ageing human brain. Nature 429: 883–891. CrossRef Medline

Macdonald RL, Barker JL (1977) Pentylenetetrazol and penicillin are selective antagonists of GABA-mediated post-synaptic inhibition in cultured mammalian neurones. Nature 267:720–721. CrossRef Medline

Mandhane SN, Aavula K, Rajamannar T (2007) Timed pentylenetetrazol infusion test: a comparative analysis with s.c.PTZ and MES models of anticonvulsant screening in mice. Seizure 16:636–644. CrossRef Medline

Mattson MP (2004) Pathways towards and away from Alzheimer's disease. Nature 430:631–639. CrossRef Medline

McKay RA, Miraglia LJ, Cummins LL, Owens SR, Sasmor H, Dean NM (1999) Characterization of a potent and specific class of antisense oligonucleotide inhibitor of human protein kinase C-alpha expression. J Biol Chem 274:1715–1722. CrossRef Medline

Mendez M, Lim G (2003) Seizures in elderly patients with dementia: epidemiology and management. Drugs Aging 20:791–803. CrossRef Medline

Miller TM, Pestronk A, David W, Rothstein J, Simpson E, Appel SH, Andres PL, Mahoney K, Allred P, Alexander K, Ostrow LW, Schoenfeld D, Macklin EA, Norris DA, Manousakis G, Crisp M, Smith R, Bennett CF, Bishop KM, Cudkowicz ME (2013) An antisense oligonucleotide against SOD1 delivered intrathecally for patients with SOD1 familial amyotrophic lateral sclerosis: a phase 1, randomised, first-in-man study. Lancet Neurol 12:435–442. CrossRef Medline

Morris M, Hamto P, Adame A, Devidze N, Masliah E, Mucke L (2013) Age-appropriate cognition and subtle dopamine-independent motor deficits in aged Tau knock-out mice. Neurobiol Aging 34:1523–1529. CrossRef Medline

Myers AJ, Pittman AM, Zhao AS, Rohrer K, Kaleem M, Marlowe L, Lees A, Leung D, McKeith IG, Perry RH, Morris CM, Trojanowski JQ, Clark C, Karlawish J, Arnold S, Forman MS, Van Deerlin V, de Silva R, Hardy J (2007) The MAPT H1c risk haplotype is associated with increased expression of tau and especially of 4 repeat containing transcripts. Neurobiol Dis 25:561–570. CrossRef Medline

Oka M, Hasegawa S, Matsushige T, Inoue H, Kajimoto M, Ishikawa N, Isumi H, Ichiyama T (2013) Tau protein concentrations in the cerebrospinal fluid of children with acute disseminated encephalomyelitis. Brain Dev In Press.

Olney JW, Wozniak DF, Farber NB (1997) Excitotoxic neurodegeneration in Alzheimer disease. New hypothesis and new therapeutic strategies. Arch Neurol 54:1234–1240. CrossRef Medline

Olsen RW (2006) Picrotoxin-like channel blockers of GABAA receptors. Proc Natl Acad Sci U S A 103:6081–6082. CrossRef Medline

Palmio J, Suhonen J, Keränen T, Hulkkonen J, Peltola J, Pirttilä T (2009)

Cerebrospinal fluid tau as a marker of neuronal damage after epileptic seizure. Seizure 18:474–477. CrossRef Medline

Passini MA, Bu J, Richards AM, Kinnecom C, Sardi SP, Stanek LM, Hua Y, Rigo F, Matson J, Hung G, Kaye EM, Shihabuddin LS, Krainer AR, Bennett CF, Cheng SH (2011) Antisense oligonucleotides delivered to the mouse CNS ameliorate symptoms of severe spinal muscular atrophy. Sci Transl Med 3:72ra18. CrossRef Medline

Pizzi M, Valerio A, Ribola M, Spano PF, Memo M (1993) A Tau antisense oligonucleotide decreases neurone sensitivity to excitotoxic injury. Neuroreport 4:823–826. CrossRef Medline

Pooler AM, Phillips EC, Lau DH, Noble W, Hanger DP (2013) Physiological release of endogenous tau is stimulated by neuronal activity. EMBO Rep 14:389–394. CrossRef Medline

Porensky PN, Mitrpant C, McGovern VL, Bevan AK, Foust KD, Kaspar BK, Wilton SD, Burghes AH (2012) A single administration of morpholino antisense oligomer rescues spinal muscular atrophy in mouse. Hum Mol Genet 21:1625–1638. CrossRef Medline

Racine RJ (1972) Modification of seizure activity by electrical stimulation. II. Motor seizure. Electroencephalogr Clin Neurophysiol 32:281–294. CrossRef Medline

Roberson ED, Scearce-Levie K, Palop JJ, Yan F, Cheng IH, Wu T, Gerstein H, Yu GQ, Mucke L (2007) Reducing endogenous tau ameliorates amyloid beta-induced deficits in an Alzheimer's disease mouse model. Science 316:750–754. CrossRef Medline

Roberson ED, Halabisky B, Yoo JW, Yao J, Chin J, Yan F, Wu T, Hamto P, Devidze N, Yu GQ, Palop JJ, Noebels JL, Mucke L (2011) Amyloid-β/Fyn-induced synaptic, network, and cognitive impairments depend on tau levels in multiple mouse models of Alzheimer's disease. J Neurosci 31:700–711. CrossRef Medline

Rogawski MA (2006) Diverse mechanisms of antiepileptic drugs in the development pipeline. Epilepsy Res 69:273–294. CrossRef Medline

Sanchez PE, Zhu L, Verret L, Vossel KA, Orr AG, Cirrito JR, Devidze N, Ho K, Yu GQ, Palop JJ, Mucke L (2012) Levetiracetam suppresses neuronal network dysfunction and reverses synaptic and cognitive deficits in an Alzheimer's disease model. Proc Natl Acad Sci U S A 109:E2895–E2903. CrossRef Medline

Schaefer ML, Wong ST, Wozniak DF, Muglia LM, Liauw JA, Zhuo M, Nardi A, Hartman RE, Vogt SK, Luedke CE, Storm DR, Muglia LJ (2000) Altered stress-induced anxiety in adenylyl cyclase type VIII-deficient mice. J Neurosci 20:4809–4820. Medline

Seward ME, Swanson E, Norambuena A, Reimann A, Cochran JN, Li R, Roberson ED, Bloom GS (2013) Amyloid-β signals through tau to drive ectopic neuronal cell cycle re-entry in Alzheimer's disease. J Cell Sci 26:1278–1286. CrossRef Medline

Smith RA, Miller TM, Yamanaka K, Monia BP, Condon TP, Hung G, Lobsiger CS, Ward CM, McAlonis-Downes M, Wei H, Wancewicz EV, Bennett CF, Cleveland DW (2006) Antisense oligonucleotide therapy for neurodegenerative disease. J Clin Invest 116:2290–2296. CrossRef Medline

Suberbielle E, Sanchez PE, Kravitz AV, Wang X, Ho K, Eilertson K, Devidze N, Kreitzer AC, Mucke L (2013) Physiologic brain activity causes DNA double-strand breaks in neurons, with exacerbation by amyloid-β. Nat Neurosci 16:613–621. CrossRef Medline

Takao M, Ghetti B, Murrell JR, Unverzagt FW, Giaccone G, Tagliavini F, Bugiani O, Piccardo P, Hulette CM, Crain BJ, Farlow MR, Heyman A (2001) Ectopic white matter neurons, a developmental abnormality that may be caused by the PSEN1 S169L mutation in a case of familial AD with myoclonus and seizures. J Neuropathol Exp Neurol 60:1137–1152. Medline

Trabzuni D, Wray S, Vandrovcova J, Ramasamy A, Walker R, Smith C, Luk C, Gibbs JR, Dillman A, Hernandez DG, Arepalli S, Singleton AB, Cookson MR, Pittman AM, de Silva R, Weale ME, Hardy J, Ryten M (2012) MAPT expression and splicing is differentially regulated by brain region: relation to genotype and implication for tauopathies. Hum Mol Genet 21:4094–4103. CrossRef Medline

Tucker KL, Meyer M, Barde YA (2001) Neurotrophins are required for nerve growth during development. Nat Neurosci 4:29–37. CrossRef Medline

Velez-Pardo C, Arellano JI, Cardona-Gomez P, Jimenez Del Rio M, Lopera F, De Felipe J (2004) CA1 hippocampal neuronal loss in familial Alzheimer's disease presenilin-1 E280A mutation is related to epilepsy. Epilepsia 45:751–756. CrossRef Medline

Vespa PM, McArthur DL, Xu Y, Eliseo M, Etchepare M, Dinov I, Alger J, Glenn TP, Hovda D (2010) Nonconvulsive seizures after traumatic brain injury are associated with hippocampal atrophy. Neurology 75:792–798. CrossRef Medline

Vogt DL, Thomas D, Galvan V, Bredesen DE, Lamb BT, Pimplikar SW (2011) Abnormal neuronal networks and seizure susceptibility in mice overexpressing the APP intracellular domain. Neurobiol Aging 32:1725–1729. CrossRef Medline

Vossel KA, Zhang K, Brodbeck J, Daub AC, Sharma P, Finkbeiner S, Cui B, Mucke L (2010) Tau reduction prevents Abeta-induced defects in axonal transport. Science 330:198. CrossRef Medline

Vossel KA, Beagle AJ, Rabinovici GD, Shu H, Lee SE, Naasan G, Hegde M, Gornes SB, Henry ML, Nelson AB, Seeley WW, Geschwind MD, Gorno-Tempini ML, Shih T, Kirsch HE, Garcia PA, Miller BL, Mucke L (2013) Seizures and epileptiform activity in the early stages of Alzheimer Disease. JAMA Neurol 8:1–9. CrossRef Medline

Weingarten MD, Lockwood AH, Hwo SY, Kirschner MW (1975) A protein factor essential for microtubule assembly. Proc Natl Acad Sci U S A 72:1858–1862. CrossRef Medline

Wozniak DF, Hartman RE, Boyle MP, Vogt SK, Brooks AR, Tenkova T, Young C, Olney JW, Muglia LJ (2004) Apoptotic neurodegeneration induced by ethanol in neonatal mice is associated with profound learning/memory deficits in juveniles followed by progressive functional recovery in adults. Neurobiol Dis 17:403–414. CrossRef Medline

Wozniak DF, Xiao M, Xu L, Yamada KA, Ornitz DM (2007) Impaired spatial learning and defective theta burst induced LTP in mice lacking fibroblast growth factor 14. Neurobiol Dis 26:14–26. CrossRef Medline

Yamada K, Cirrito JR, Stewart FR, Jiang H, Finn MB, Holmes BB, Binder LI, Mandelkow EM, Diamond MI, Lee VM, Holtzman DM (2011) In vivo microdialysis reveals age-dependent decrease of brain interstitial fluid tau levels in P301S human tau transgenic mice. J Neurosci 31:13110–13117. CrossRef Medline

Yokota T, Lu QL, Partridge T, Kobayashi M, Nakamura A, Takeda S, Hoffman E (2009) Efficacy of systemic morpholino exon-skipping in Duchenne dystrophy dogs. Ann Neurol 65:667–676. CrossRef Medline

Yu RZ, Lemonidis KM, Graham MJ, Matson JE, Crooke RM, Tribble DL, Wedel MK, Levin AA, Geary RS (2009) Cross-species comparison of in vivo PK/PD relationships for second-generation antisense oligonucleotides targeting apolipoprotein B-100. Biochem Pharmacol 77:910–919. CrossRef Medline

Conclusions

This research showed that endogenous tau reduction using ASOs results in >70% reduction in tau, with good spread throughout the brain and spinal cord. Furthermore, this reduction did not change the behavior of the mice compared to controls. It did, however, have a protective effect against chemically-induced seizures, consistent with findings from tau knock-out models. This finding demonstrates that tau levels affect susceptibility to hyperexcitability and that by lowering tau we can lower seizure severity.

Many other publications have focused on Aβ's role in neuronal excitotoxicity and seizures (Palop & Mucke 2010; Busche et al. 2008; Busche et al. 2012; Menéndez 2005; Minkeviciene et al. 2009; Westmark et al. 2008), but here we showed that tau also plays a role. Our findings imply that endogenous tau levels in humans with AD may influence their risk of developing seizures and that by reducing their tau levels, we may be able to rescue some of the cognitive deficits associated with neuronal hyperexcitability.

Our experiment does not provide any evidence as to if this decrease in tau needs to happen before cognitive deficits occur, or if some level of recovery is possible after impairments are evident. Testing has been done in MCI patients to see if levetiracetam, an anticonvulsant, helps with recall. Patients were tested using functional magnetic resonance imaging, and it was found that treatment with levetiracetam did improve recall performance in MCI patients.

In future experiments, we would test to see if reducing Aβ and APP has a similar effect on seizures and if by reducing these we can rescue cognitive decline in AD mouse models.

Research into the use of ASOs as a tau-lowering agent continued after the success of this study. Further research first progressed into PS19 mouse models (DeVos et al. 2017), which is a transgenic mouse model expressing human tau (Yoshiyama et al. 2007). For this research, human tau ASOs were designed to specifically target the coding 1N4R transgene of human tau expressed in the PS19 mouse model (DeVos et

al. 2017). As with our previous research, the human tau ASO used here had good spread through the murine brain and demonstrated a long duration of effect. PS19 mice show age-dependent neuronal and hippocampal loss starting at 9 months. ASO treatment prevented this loss and reduced tau “seeding,” which is the prion-like capability of hyperphosphorylated tau to spread from cell-to-cell transmitting its aberrant pathology. Survival rates for the PS19 mice were also increased (DeVos et al. 2017).

After their success in mice, DeVos et al. also treated *Cynomologus* monkeys. They again found that the ASO had good spread through an intrathecal delivery method and both tau mRNA and protein levels were decreased (DeVos et al. 2017).

The first human trials using ASO treatment to lower tau began in 2017 and is expected to run through 2022 (Ionis Pharmaceuticals, Inc 2017).

Chapter 4: Genetic suppression of transgenic APP rescues hypersynchronous network activity in a mouse model of AD

As discussed in the previous chapter, AD is associated with an elevated risk of seizures. For EOAD, this risk increases by 87-fold, whereas LOAD only has a 3-fold increased risk (Amatniek et al. 2006). Seizures are aberrant electrical activity and likely contribute to cognitive decline. Previous studies on mouse models showed that treatment with the antiepileptic drug levetiracetam improved spatial navigation and decreased anxiety (Sanchez et al. 2012).

Previous studies and the prominence of the Aβ phenotype have led to the hypothesis that Aβ has a mechanistic link between AD and seizures. The majority of Aβ mouse models also produce high levels of APP, making it difficult to tell if Aβ or APP is more influential in seizure activity.

For this experiment, we sought to make a distinction between APP and Aβ's role in seizure activity. By using tet-off responsive systems for the translation of the APP gene, we were able to control the level of APP production and test subsequent EEG activity. APP suppression was performed at different age time points to see if production of APP at a young age produced different results than production starting in older mice. Susceptibility to chemically-induced seizures was also looked at using picrotoxin to see if APP suppression altered animals' response. To test Aβ's role in seizure we used a γ-secretase inhibitor to see if decreasing the level of Aβ had any effect on EEG activity.

For this experiment, I was responsible for creating the wired EEG implants and determining how dual cannulas could be implanted into the mouse brain simultaneously. I performed the surgical procedures relating to EEG cannula implantation, and microdialysis, as well as setting up the mice for proper sample collection for each. I also ensured the EEG and microdialysis animals were given doxycycline chow and γ-secretase inhibitor at appropriate time points.

This paper has been cited in 85 other publications, including publications in high-influence journals such as Science (impact factor 37.205), Nature Medicine (impact factor 32.621), Lancet Neurology (impact factor 27.144), and Molecular Psychiatry (impact factor 13.204).

Neurobiology of Disease

Genetic Suppression of Transgenic APP Rescues Hypersynchronous Network Activity in a Mouse Model of Alzeimer's Disease

Heather A. Born,[1] Ji-Yoen Kim,[1] Ricky R. Savjani,[1,8] Pritam Das,[9] Yuri A. Dabaghian,[6,10] Qinxi Guo,[7] Jong W. Yoo,[2] Dorothy R. Schuler,[11] John R. Cirrito,[11] Hui Zheng,[1,3,4,7] Todd E. Golde,[12] Jeffrey L. Noebels,[1,2,4] and Joanna L. Jankowsky[1,2,5,7]

[1]Department of Neuroscience, [2]Department of Neurology, [3]Department of Molecular and Cellular Biology, [4]Department of Human and Molecular Genetics, [5]Department of Neurosurgery, [6]the Jan and Dan Duncan Neurological Research Institute, and [7]the Huffington Center on Aging, Baylor College of Medicine, Houston, Texas 77030, [8]Texas A&M Health Science Center, College Station, Texas 77843, [9]Department of Neuroscience, Mayo Clinic, Jacksonville, Florida 32224, [10]Department of Computational and Applied Mathematics, Rice University, Houston, Texas 77251, [11]Department of Neurology, Washington University School of Medicine, St. Louis, Missouri 63110, and [12]Department of Neuroscience, University of Florida, Gainesville, Florida 32610

Alzheimer's disease (AD) is associated with an elevated risk for seizures that may be fundamentally connected to cognitive dysfunction. Supporting this link, many mouse models for AD exhibit abnormal electroencephalogram (EEG) activity in addition to the expected neuropathology and cognitive deficits. Here, we used a controllable transgenic system to investigate how network changes develop and are maintained in a model characterized by amyloid β (Aβ) overproduction and progressive amyloid pathology. EEG recordings in tet-off mice overexpressing amyloid precursor protein (APP) from birth display frequent sharp wave discharges (SWDs). Unexpectedly, we found that withholding APP overexpression until adulthood substantially delayed the appearance of epileptiform activity. Together, these findings suggest that juvenile APP overexpression altered cortical development to favor synchronized firing. Regardless of the age at which EEG abnormalities appeared, the phenotype was dependent on continued APP overexpression and abated over several weeks once transgene expression was suppressed. Abnormal EEG discharges were independent of plaque load and could be extinguished without altering deposited amyloid. Selective reduction of Aβ with a γ-secretase inhibitor has no effect on the frequency of SWDs, indicating that another APP fragment or the full-length protein was likely responsible for maintaining EEG abnormalities. Moreover, transgene suppression normalized the ratio of excitatory to inhibitory innervation in the cortex, whereas secretase inhibition did not. Our results suggest that APP overexpression, and not Aβ overproduction, is responsible for EEG abnormalities in our transgenic mice and can be rescued independently of pathology.

Key words: **amyloid precursor protein; EEG; epilepsy; seizure; sharp wave discharge; transgene suppression**

Introduction

A growing body of evidence suggests that Alzheimer's disease (AD) increases the risk for seizures above the rise connected with aging. Late-onset sporadic AD is associated with a threefold increase in seizure incidence compared with the general population, whereas early-onset familial AD is linked to an astonishing 87-fold rise (Amatniek et al., 2006). Seizure disorders and epilepsy are especially pronounced in families with presenilin mutations, in which nearly 30% of patients display this comorbidity, rising to nearly 75% in cases of particularly aggressive variants with onset before age 40 (Snider et al., 2005; Larner and Doran, 2006; Jayadev et al., 2010). Recent studies suggest that electrical imbalance may contribute to cognitive deficits in AD and serve as a target for clinical intervention (Palop and Mucke, 2009). Consistent with this idea, mouse models for AD show improved spatial navigation and diminished anxiety after treatment with the antiepileptic drug levetiracetam (Sanchez et al., 2012). Similar benefit from levetiracetam was observed in a small pilot study of patients with mild cognitive impairment (Bakker et al., 2012).

The mechanism by which AD increases seizure risk has only recently been explored using mouse models for the disease. Spontaneous seizures and sharp wave discharges (SWDs) have been observed in several transgenic models expressing mutations in

Received Dec. 10, 2013; revised Jan. 10, 2014; accepted Jan. 30, 2014.

Author contributions: H.A.B., J.-Y.K., and J.L.J. designed research; H.A.B., J.-Y.K., P.D., J.W.Y., D.R.S., and J.R.C. performed research; Q.G., H.Z., and T.E.G. contributed unpublished reagents/analytic tools; H.A.B., J.-Y.K., R.R.S., P.D., Y.A.D., J.R.C., and J.L.N. analyzed data; H.A.B. and J.L.J. wrote the paper.

This work was funded by the National Institutes of Health (Office of the Director New Innovator Award DP2 OD001734 to J.L.J.). H.A.B. was supported by the National Institute of Aging Biology of Aging (Training Grant T32 AG000183) and by a gift from the family of Mr. Robert L. Cook. We thank Rich Paylor for sharing telemetry equipment used in this study; Cynthia Evans for creative support of our vivarium needs; Corey Reynolds and the BCM Mouse Phenotyping Core for help with initial telemetry recordings; Philip Jones for chemical analysis of inhibitor syntheses; and Anna Gumpel, Carolyn Allen, Yuanyuan Zhang, Bryan Song, and Anna Kuperman for careful oversight of the mouse colony.

The authors declare no competing financial interests.

Correspondence should be addressed to Joanna L. Jankowsky, Baylor College of Medicine, BCM295, One Baylor Plaza, Houston, TX 77030. E-mail: jankowsk@bcm.edu.

DOI:10.1523/JNEUROSCI.5171-13.2014

 0270-6474/14/343826-15$15.00/0

amyloid precursor protein (APP). The seizure phenotype is most often noted in models carrying the Swedish mutation, including Tg2576 (Westmark et al., 2008), APP23 (Lalonde et al., 2005), hAPPJ20 (Palop et al., 2007; Sanchez et al., 2012; Verret et al., 2012; Corbett et al., 2013), and APP/PS1dE9 (Minkeviciene et al., 2009; Ziyatdinova et al., 2011). The prominent amyloid phenotype of these models has pointed to amyloid β (Aβ) as the mechanistic link connecting AD with seizures (Palop and Mucke, 2010). Although bath application of exogenous Aβ generally diminishes synaptic plasticity, it conversely increases electrical activity of excitatory neurons (Minkeviciene et al., 2009). Hippocampal neurons in transgenic APP mice display abnormal spontaneous activity well before plaque formation (Busche et al., 2012), with hyperactive foci persisting at the periphery of amyloid deposits in later stages of disease (Busche et al., 2008). In turn, this hyperactivity may increase synaptic exocytosis of Aβ (Kamenetz et al., 2003; Cirrito et al., 2005; Bero et al., 2011), placing Aβ at the center of a pathological feedback loop (Noebels, 2011).

Aβ may not be the only contributor to epileptogenesis in AD and its mouse models. Patients with APP duplication are at greater risk for seizure (Cabrejo et al., 2006), as are Down syndrome patients with dementia (Menéndez, 2005). Many AD mouse models also produce high levels of APP, making it difficult to distinguish whether Aβ is solely responsible for seizure activity or if other APP fragments may also contribute. Moreover, unlike most AD patients, transgenic mice overexpress APP during cortical development, when the protein's synaptogenic properties may have unanticipated effects on circuit connectivity (Young-Pearse et al., 2008; Wang et al., 2009; Zheng and Koo, 2011). Because of their intrinsic relationship, separating the impact of APP from that of Aβ and amyloid has been experimentally challenging. Here, we used a controllable APP-transgenic model to separate these factors and evaluate how APP overexpression, Aβ overproduction, and plaque formation each contribute to network hyperactivity.

Materials and Methods

Mice

We studied tetracycline-responsive APP-transgenic mice (APP/TTA) expressing a chimeric mouse APP with a humanized Aβ domain encoding the Swedish and Indiana mutations (MMRRC #34845; Jankowsky et al., 2005) that had been mated to CaMKIIα-tTA line B mice expressing the tetracycline transactivator under control of the CaMKIIα promoter (#3010; Jackson Laboratories; Mayford et al., 1996). Single-transgenic (TTA only) and nontransgenic (NTG) cagemates were used as controls. Each line had been independently backcrossed to C57BL/6J for >20 generations before being intercrossed to generate stud males that were bred with C57BL/6J females to generate animals for study (Rodgers et al., 2012). Animals were housed on a 12 h/12 h or 13 h/11 h day/night cycle and were used for study between 3 and 12 months of age.

APP/PS1 double knock-in mice were created by crossing APP knock-in mice encoding a humanized Aβ domain flanked by the Swedish and London mutations with PS1 knock-in mice encoding the M146V mutation (Guo et al., 1999; Köhler et al., 2005). Both lines were maintained on a C57BL/6 J background and were 23–24 months of age at the time of study. All studies were gender balanced. All animal experiments were performed using protocols that were reviewed and approved by the Institutional Care and Use Committee at Baylor College of Medicine.

Chronic EEG recording and analysis

Direct EEG recording. One cohort of APP/TTA, TTA, and NTG mice were implanted for baseline EEG recordings using wired, two-lead subdural EEG. After anesthesia with Avertin, subdural recording electrodes were implanted bilaterally over the parietal cortices. Mice were allowed to recover for at least 24 h before recording. EEG signal was recorded over 3 3 h sessions using the Stellate Harmonie system (Natus Medical). Data were sampled at 200 Hz over a frequency range of 0.3–70 Hz. Recordings were analyzed manually for SWDs and seizures by a blinded observer.

Estimating the specificity and sensitivity of single-lead EEG recordings. For the semiquantitative experiments we had in mind, we needed an EEG system that would deliver high-throughput, chronic recording capability. Telemetric recording systems provided these advantages, but at the cost of spatial resolution: mouse-sized radiofrequency transmitters carried only one recording lead rather than the two or more used by traditional EEG equipment. To validate the accuracy of EEG data obtained from a single lead, we reanalyzed the recordings made with our dual-lead wired setup to count the number of SWDs detected by one lead against the number detected by both. This provided a rough estimate of the percentage of bilateral events that would be accurately detected by a single recording electrode, along with a measure of the number of false positives that would be detected in a single lead but not present bilaterally. We found that, as the number of SWDs increased, so also did the percentage of SWDs recorded bilaterally, such that for data beyond ~30 spikes/h, >90% of all spikes identified by one electrode were seen in both (Fig. 1). Because most of our APP/TTA recordings fell at or above this SWD frequency, we transitioned to telemetry for all subsequent EEG recordings.

Telemetric EEG and locomotor recording. All subsequent EEG experiments used wireless ETA-F10 transmitters (Data Sciences International) for chronic EEG recording and locomotor monitoring. After anesthesia with isoflurane, a 1 cm midline sagittal incision was made starting above the interaural line and extending along the neck to create a pocket for subcutaneous placement of the transmitter along the dorsal flank of the animal. The recording electrode (stereotaxic coordinates relative to bregma: +2.5 mm, −2.5 mm) and ground electrode (−1.0 mm, +1.0 mm) were implanted subdurally through small holes drilled in the skull and held in place with dental cement. Mice were provided with ketoprofen analgesic for 3 d after surgery and allowed to recover for 10 d before recording.

Mice remained in their home cage during overnight recording sessions. EEG signal was collected through radiofrequency receivers placed under each cage. Locomotor activity was also interpolated from this signal by monitoring changes in signal strength between the transmitter and receiver as the animal moved about the cage. Using this system, a movement count was triggered whenever the signal change exceeded a prespecified threshold. Locomotor data are therefore reported as arbitrary activity counts per hour. Locomotor data were acquired at a sampling rate of 16 Hz; EEG data between 1 and 200 Hz were acquired at a sampling rate of 1 kHz using the Dataquest A.R.T. system, versions 2.1 and 4.0 (Data Sciences International).

Automated EEG analysis. Three overnight recordings made over the course of a week were averaged to determine the baseline frequency of SWDs per hour for each mouse. EEG recordings were analyzed to include a balanced number of daylight and nighttime hours for a total of 12 h per session (from 3:00 to 9:00 A.M. and from 4:00 to 10:00 P.M.). EEG signal was filtered using a band pass of 0.3–70 Hz. Automated analysis of SWDs was done using Neuroscore software version 2.1 (Data Science International). The baseline threshold for each recording was manually determined as the best fit line that includes the majority of the EEG trace using the period between 12:00 and 1:00 A.M. when a low frequency of SWDs was observed. To be counted as a SWD, an electrical event must be brief in duration (5–15 ms) and have a peak amplitude 2.5× greater than the average baseline range. The ETA-F10 transmitters also acquired data on animal movement during recording, which was analyzed using Neuroscore to report activity counts per hour.

Power, entropy, and autocorrelation analyses

Two time points were analyzed for each animal, once before (baseline) and once after 4 weeks of transgene suppression. Analysis of each condition was limited to data collected during a single 6 h session spanning 1 dark-light transition (3:00–9:00 A.M.). Data were not filtered before analysis. One animal was excluded from each genotype due to noise in

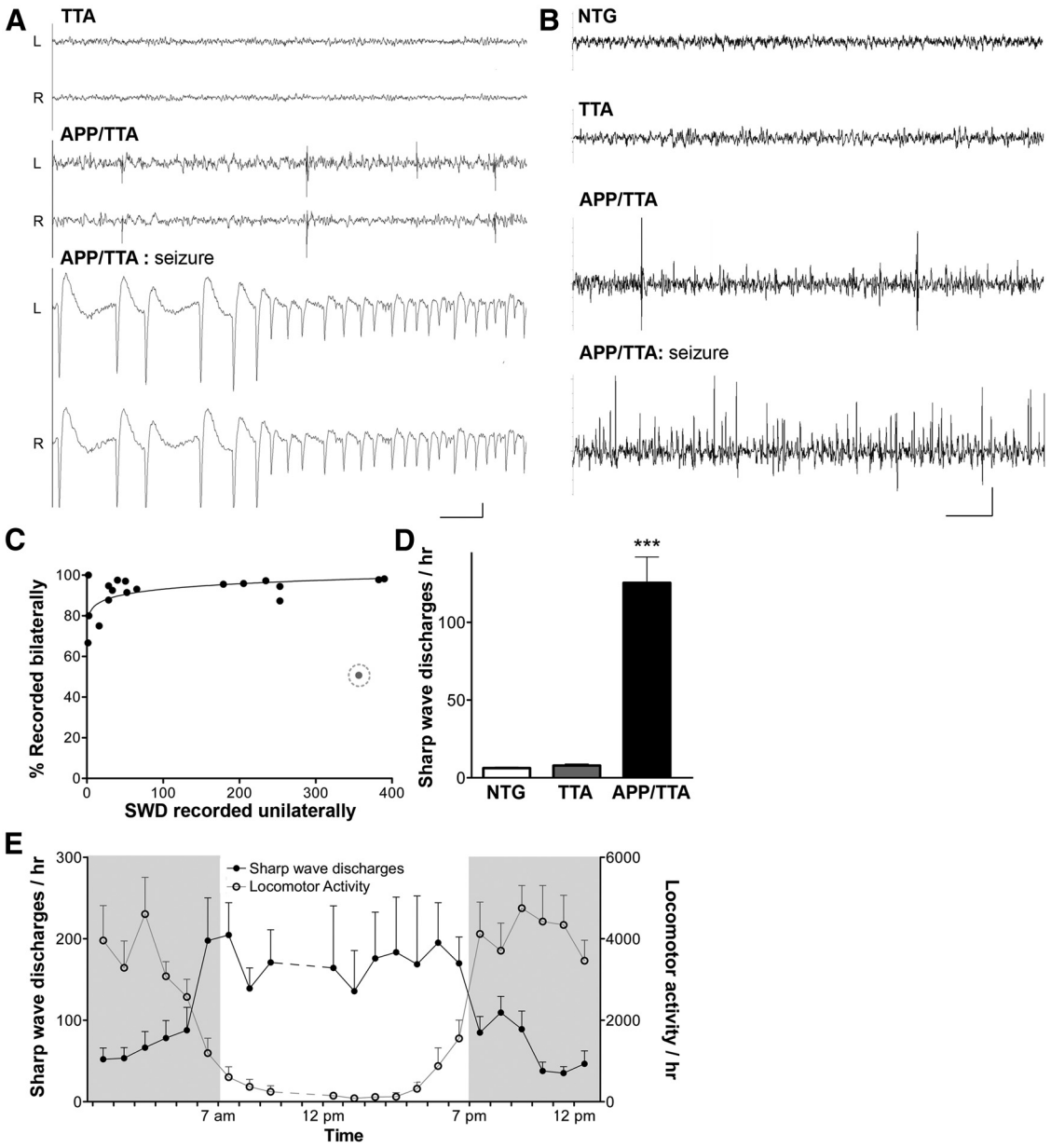

Figure 1. EEG recording reveals abnormal SWDs in tet-off APP-transgenic mice. ***A***, ***B***, EEG recordings made via wired dual-lead electrodes (***A***) or by wireless radiofrequency transmitters (***B***) uncovered frequent SWDs and irregular seizure episodes in APP/TTA mice. Scale bars: ***A***, 0.5 mV and 2 s; ***B***, 0.4 mV and 2 s. ***C***, Recordings made with dual-lead electrodes were used to assess the percentage of spikes that would be counted in error by moving to a single-lead setup. The graph illustrates the percentage of SWDs recorded bilaterally as a function of SWDs recorded unilaterally. As the number of spikes increased, so also did the percentage of spikes recorded bilaterally. One data point (circled) was identified as an outlier and excluded from analysis. ***D***, APP/TTA mice display a significantly higher number of SWDs/h than age-matched NTG and TTA controls. ***$p < 0.001$. ***E***, SWD frequency was inversely related to locomotor activity in APP/TTA mice. Black circles, SWDs; open circles, locomotor activity.

the signal that invalidated full-spectrum analyses, but this did not affect measurement of large-amplitude SWDs.

To characterize the spectral properties of the EEG signal in the WT and AD mice, we first normalized each signal by its SD and then computed the Fourier transform for each recording with an 8 s (8000 points) time window using the standard MATLAB Signal Processing toolbox (MathWorks). We calculated the normalized signal amplitude as a function of frequency between 0 and 300 Hz across the entire 6 h window. The results were then averaged for control and APP/TTA groups with no additional smoothing. Because the data were normalized before transformation, values are expressed as arbitrary units rather than mV^2.

To characterize the entropy of peak timing in the EEG signal, we first isolated peak values >3 SD of the mean signal amplitude. These points were characterized by the time at which they occurred in the recording and used to calculate nearest-neighbor interpeak intervals. We next performed a sliding analysis of the data using a 17 s (17,000 points) window at a time. For each window, we plotted the distribution of interpeak intervals and from this calculated the entropy of the distribution according to the following equation:

$$H = -\sum_x P(x) \log_2 P(x),$$

The window was then shifted by 0.1 s (100 points) and the entropies recomputed. By scanning the entire time axis in this way, we obtained entropy as a function of time. The results were averaged for each genotype and used to compute the entropy distributions shown in Figure 3. Both the amplitude threshold for defining signal peaks and the time

window used for scanning the data were tested at multiple values and yielded similar results to the 3 SD/17 s analysis shown here.

Autocorrelation within the signal was tested for time lags ranging from 0 to 10 s (10,000 points) using MATLAB Signal Processing and Econometrics toolboxes. Group averages at each time lag were calculated and graphed as mean and SE.

Doxycycline treatment

To measure the effect of transgenic APP suppression on SWD frequency, one cohort of mice was treated with doxycycline (DOX) for 4–5 weeks after completion of baseline EEG recordings (F5903 50 mg/kg DOX in TestDiet 5001 rodent chow; Purina).

A separate cohort of animals was used to measure the effect of delaying transgenic APP expression until adulthood on EEG activity. Mice used for adult onset studies were reared on DOX chow to suppress APP overexpression for the first 6 weeks of life, as described previously (Rodgers et al., 2012). At 6 weeks of age, mice were returned to unmedicated chow to initiate expression of transgenic APP. Thereafter, the transgene was continuously expressed until EEG testing.

In vivo microdialysis

The effect of DOX treatment on soluble Aβ levels was determined using a separate cohort of mice implanted for microdialysis of interstitial fluid (ISF). Mice were unilaterally implanted with a 38 kDa MW cutoff microdialysis probe (2 mm BR-style; Bioanalytical Systems) placing the probe tip into the hippocampus at a 12 degree angle −3.1 mm from bregma, −2.5 mm from midline, and 3.2 mm below the dura (Cirrito et al., 2003; Cirrito et al., 2011). Microdialysis perfusion buffer consisted of 4% albumin in artificial CSF at a flow rate of 1.0 μl/min. Animals were allowed to recover for 6–8 h after probe insertion, and then 6 ISF Aβ measurements were taken over a 6 h period. The mean concentration of exchangeable Aβ during this 6 h period was defined as the baseline ISF Aβ concentration for each mouse. After basal Aβ levels were determined, mice were administered DOX through their chow as above and microdialysis samples were taken into a refrigerated fraction collector every 1–3 h for the following 4 d. After the final collection, samples were assayed for $A\beta_{x\text{-}40}$ and $A\beta_{x\text{-}42}$ by sandwich ELISA using an $A\beta_{40}$ (mHF2)- or $A\beta_{42}$-specific antibody (mHJ7.4) to capture the peptide, followed by a biotinylated central domain anti-Aβ antibody (mHJ5.1) for detection (Cirrito et al., 2011). The concentration of ISF Aβ in each sample was normalized to the baseline Aβ concentration for each mouse. At the end of the experiment, the brains were harvested and processed for histological verification of probe placement.

γ-Secretase inhibition

To test the efficacy of γ-secretase inhibition on steady-state levels of Aβ in our mice, we administered young, predeposit APP/TTA mice (5–6 weeks of age) either a single intraperitoneal dose of LY411575 or 1 week of medicated chow. For acute treatment, the drug was dissolved in DMSO at 100 mg/ml, diluted in corn oil to the appropriate concentration, and injected intraperitoneally to deliver 0, 2.5, 5, 10, or 20 mg/kg. Mice were harvested 3–4 h after injection. Dosing for subchronic treatment was assessed by feeding mice chow compounded with LY411575 at 50 mg/kg to deliver 5 or 10 mg/kg/d. Mice were harvested after 1 week of treatment. From these dose–response studies, we decided to use a step-down regimen in the aged cohort to test the effect of γ-secretase inhibition on EEG activity. After baseline recordings, aged APP/TTA and control mice were treated for 2 weeks with LY411575 compounded at a concentration of 50 mg/kg into Purina TestDiet 5001 chow to deliver 10 mg/kg/d. After 2 weeks of treatment at 10 mg/kg/d, dosing was decreased to 5 mg/kg/d for the remainder of the experiment.

Aβ ELISA

To measure the dose response of LY411575 on soluble Aβ levels, tissue was harvested from mice treated acutely or subchronically with LY411575 as described in γ-Secretase inhibition, above. Frozen hemiforebrain samples were homogenized by sonication in 7.5 volumes of TBS containing 1% Triton X-100 and 1× protease inhibitor mixture as described previously (Jankowsky et al., 2007). Aβ levels were determined by end-specific sandwich ELISAs using monoclonal antibody 2.1.3 for capture (human Aβx-42 specific) and HRP-conjugated monoclonal antibody Ab9 (human Aβ1–16 specific) for detection or monoclonal antibody Ab9 for capture and HRP-conjugated monoclonal antibody 13.1.1 (human Aβx-40 specific) for detection (Levites et al., 2006a; Levites et al., 2006b). All values were calculated as picomoles per gram based on the initial weight of brain tissue.

Seizure induction

To determine whether APP overexpression altered the threshold for chemical seizure induction, mice were implanted with ETA-F10 transponders as described in Telemetric EEG and locomotor recording, above and recorded for pretreatment values before convulsant exposure. Picrotoxin (P1675; Sigma) was dissolved in sterile saline and injected subcutaneously at 1.75 mg/kg. Mice were videotaped during EEG recording for 1 h after injection. A separate cohort of mice was treated with kainic acid (BML-EA123; VWR) injected subcutaneously at 35 mg/kg and recorded for 1 h after injection. Video recordings were reviewed to determine: (1) the latency to seizure onset, (2) the total number of seizures induced, and (3) the severity of each seizure. Behavioral changes were scored according to the Racine scale, with 0 = normal activity; 1 = hypoactivity; 2 = head or forelimb clonus; 3 = whole-body clonus, rearing and falling, or wild running; 4 = tonic-clonic seizures; and 5 = death (Racine, 1972; Ferraro et al., 1999). EEG recordings were analyzed for latency to onset and number of seizures.

Tissue harvest

Animals were killed at the end of each experiment and brain tissue was collected through one of two methods. For the first method, one hemisphere was frozen for biochemical analyses and the other hemisphere was immersion fixed for 48 h at 4°C in 4% paraformaldehyde/1× PBS. For the second method, mice were transcardially perfused with PBS containing 10 U/ml heparin followed by 4% paraformaldehyde/1× PBS and postfixed for 24 h at 4°C in 4% paraformaldehyde/1× PBS.

Immunoblotting

Frozen hemi-forebrain or cortical tissue was homogenized by sonication in 7.5 volumes of 2% SDS and then diluted with an equal volume of 2×-concentrated RIPA buffer minus SDS (2× PBS, 1% deoxycholate, 1% NP40, 5 mM EDTA, plus protease inhibitors) to yield a 6.7% homogenate in 1× RIPA buffer. Approximately 35 μg of protein from this homogenate was separated using 10.5–14% Tris-glycine gels (Bio-Rad) for quantitation of protein levels. After transfer to nitrocellulose (iBlot; Invitrogen), blots were blocked for 1 h in 5% nonfat dry milk before being incubated with one or more primary antibodies: mouse anti-human APP/Aβ antibody 6E10 (catalog #9300-02, 1:5000; Signet), rabbit anti-CT15 (1:4000; a gift from Eddie Koo). Chicken anti-GAPDH polyclonal antibody (catalog #Ab2302, 1:5000; Millipore) was used as a loading control. Binding was detected with HRP-labeled secondary antibodies and developed with ECL reagent (Millipore). Chemiluminescence was measured with a Fuji LAS-4000 mini CCD system and quantified using MultiGauge software.

Histology

Immersion-fixed hemibrains were cryoprotected with 30% sucrose at 4°C before being frozen and sectioned at 35 μm using a freezing sliding microtome. Sections were stored in cryoprotectant at −20°C until use.

Campbell–Switzer silver stain. Amyloid was detected from a 1 in 24 series of sections using the Campbell–Switzer silver stain. A detailed protocol for this stain can be found online at the NeuroScience Associates website (http://www.neuroscienceassociates.com/Documents/Publications/campbell-switzer_protocol.htm).

Aβ immunohistochemistry. A 1 in 24 series of sections was pretreated with 88% formic acid for 1 min at room temperature, rinsed several times with TBS, and blocked with TBS plus 0.1% Triton-X (TBST) containing 1.5% normal goat serum before being incubated overnight at 4°C with rabbit anti-APP/Aβ antibody diluted in blocking solution (catalog #44-344, 1:500; Zymed). After washing with TBS, sections were incubated for 1 h with biotin-conjugated goat anti-rabbit secondary antibody (Vectastain Elite Rabbit IgG ABC Kit, 1:500; Vector Laboratories), followed

by HRP-avidin conjugate diluted 1:100 in TBS for 30 min, and then developed with DAB.

Vesicular glutamate transporter 1/vesicular GABA transporter immunofluorescence. Sections were rinsed with TBS to remove antifreeze and blocked with TBS plus 0.1% Triton X-100 containing 5% normal goat serum followed by overnight incubation at 4°C in primary antibody diluted in blocking solution (rabbit antivesicular glutamate transporter 1 [vGLUT1], catalog #135-303, 1:2000; Synaptic Systems and guinea pig antivesicular GABA transporter [vGAT], catalog #131-004, 1:750; Synaptic Systems). After washes with TBS, sections were incubated with Alexa Fluor 488-conjugated goat anti-rabbit antibody (catalog #A11034, 1:500; Invitrogen) and Alexa Fluor 594-conjugated goat anti-guinea pig antibodies (catalog #A11076, 1:750; Invitrogen).

Quantification of vGLUT1/vGAT. Sagittal sections located ~1–1.5 mm from midline were selected for analysis based on landmarks in hippocampus, lateral ventricle, and striatum. A total of 4–5 sections were imaged per animal. Fluorescent images were collected from nonoverlapping fields within cortex (L2/3 above CA1 and L5 above lateral ventricle). A single optical plane of 0.977 μm in depth was collected in red (vGAT) and green (vGLUT) channels using an ApoTome structured illumination device (Carl Zeiss) at 40× magnification (222.2 × 166.4 μm per field). We used a custom script written in MATLAB (R2012b) to batch process two-channel fluorescence images in an unbiased and automated way. Grayscale images were binarized using Otsu's method to divide the dataset into signal and background so that the variance in each of the resulting subsets is mimimized. In this case, the method uses variance minimization to define the cutoff between immunopositive pixels and background. The script then calculates the area occupied by vGLUT- or vGAT-positive pixels in each image normalized to the total area of the field. We have posted a modified version of the script on MATLAB's file exchange site (http://www.mathworks.com/matlabcentral/fileexchange/39591).

Statistics

EEG power, entropy, and autocorrelation analyses were analyzed by repeated-measures ANOVA using MATLAB; reported *p*-values represent the main effect of genotype. All other statistical analyses were done using GraphPad Prism 5.0. Comparisons between two groups were analyzed using Student's *t* test. Comparisons involving more than two groups were analyzed using one-way or two-way ANOVA followed by Bonferroni *post hoc* tests. Unless indicated (and with the exception of power, entropy, and autocorrelation analyses), all reported *p*-values are for *post hoc* comparisons. All graphs display group mean ± SEM.

Results

Tet-off APP mice display EEG abnormalities similar to other APP-transgenic models

A growing number of studies have documented abnormal electrical activity in APP-transgenic models for Alzheimer's disease (Lalonde et al., 2005; Palop et al., 2007; Westmark et al., 2008; Minkeviciene et al., 2009; Ziyatdinova et al., 2011; Sanchez et al., 2012; Verret et al., 2012; Corbett et al., 2013). These models differ in the APP mutations they encode, the coexpressed transgenes, and the promoters used to drive expression. We were therefore optimistic that their shared APP overexpression is salient to the EEG phenotype and that we might also find EEG abnormalities in our tetracycline-controllable APP-transgenic mice. These mice express mouse APP with a humanized Aβ domain harboring the Swedish and Indiana familial mutations (tetO-APP line 102) under control of the CaMKIIα-TTA driver (APP/TTA; Jankowsky et al., 2005). We used traditional wire-lead EEG recordings (Stellate Systems) to measure electrical activity in the brains of bigenic APP/TTA animals and their single-transgenic and NTG siblings at an age when we knew the bigenic mice would harbor amyloid pathology (7–9 months). As described for other APP-transgenic models, we detected frequent SWDs and irregular seizure episodes in the APP/TTA mice (19/21 exhibit >30 SWDs/h), whereas both of these features were absent from traces recorded in controls (0/15 mice exhibit >30 SWDs/h; Fig. 1).

Although wired EEG recordings are the gold standard for localizing the origin and spread of seizure activity, our system was limited in throughput. To conduct a quantitative analysis of EEG abnormalities in our model and then follow their response to various interventions, we moved to a wireless radiofrequency telemetry system that enabled us to perform continuous home-cage EEG recordings from up to eight mice at a time. Consistent with the qualitative observation from wired EEG recordings, quantitative analysis of wireless telemetry sessions confirmed that APP/TTA mice display a significantly higher number of SWDs/h than age-matched NTG and TTA controls (NTG = 6.24 ± 0.62; TTA = 7.84 ± 1.12, APP/TTA = 125.40 ± 16.62, $p < 0.001$, $n = 4$–11 mice/genotype; Fig. 1). We found no differences in the EEG properties of NTG and TTA mice and decided to combine both genotypes into balanced control groups for subsequent experiments.

We also assessed locomotor activity during our EEG sessions using information collected by the telemetry device. We found an inverse correlation between SWD frequency and ambulation such that SWD frequency was highest during daylight hours, when the mice are the least physically active and more likely to be asleep (Fig. 1).

Genetic suppression of transgenic APP normalizes cortical EEG activity

One advantage of using the tet-off APP model is that we can exercise temporal control over transgenic APP expression using orally administered DOX. Transgene expression can be reduced by >90% using moderate doses of DOX compounded into the chow (Jankowsky et al., 2005; Wang et al., 2011; Rodgers et al., 2012). In the present experiments, chow provided by a different vendor was slightly less effective but still reduced transgenic APP levels by ~80%. Transgenic APP was reduced by 77 ± 0.09% within 2 d of DOX administration and remained at 82 ± 0.02% suppression 4 weeks later (n = 3–5 mice/time point; Fig. 2). We next performed *in vivo* microdialysis of hippocampal interstitial fluid to confirm that Aβ levels declined in parallel with transgenic APP expression. Baseline levels of Aβ40 and Aβ42 were 231.1 ± 30.1 pg/ml and 25.42 ± 3.7 pg/ml, respectively (n = 5), but dropped by nearly half to 48.0 ± 5.4% (Aβ40) and 55.6 ± 5.3% (Aβ42) within 2 d after the mice began DOX treatment (Fig. 2). We suspect that compensatory release of exchangeable Aβ from nearby amyloid plaques may have limited the reduction of interstitial Aβ relative to full-length APP (Hong et al., 2011). Nonetheless, both transgenic APP and transgene-derived Aβ were significantly decreased within 2 d of DOX treatment. Despite the significant reduction in Aβ release, amyloid load was unchanged by DOX treatment. We have used this model in past studies to demonstrate that transgene suppression arrests amyloid growth indefinitely (Jankowsky et al., 2005; Wang et al., 2011). Plaque load neither progresses nor abates, so DOX treatment provides a way of reducing transgenic APP and soluble/exchangeable forms of Aβ without altering deposited amyloid.

Once baseline EEG recordings were completed, we switched all of the mice to DOX chow and continued weekly EEG recordings for another 4–5 weeks (Fig. 2). We found that SWD frequency steadily decreased in the APP/TTA mice, but over a time frame considerably longer than that of transgene suppression. After 2 weeks of DOX treatment, the SWD frequency in APP/TTA mice was significantly lower than baseline

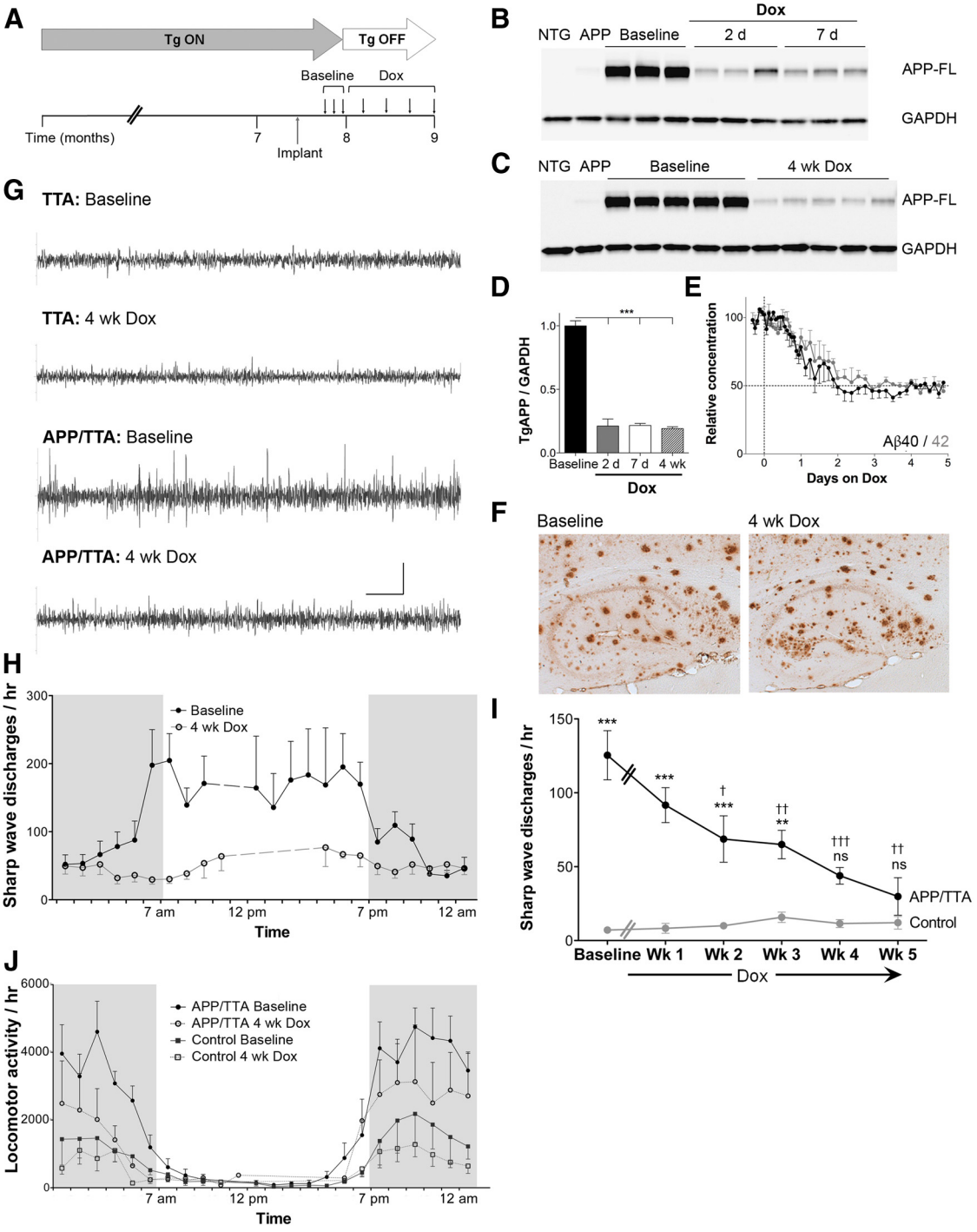

Figure 2. Transgene suppression reduces the frequency of SWDs in APP/TTA mice. ***A***, Mice were implanted with radiofrequency transmitters at 7– 8 months of age. After baseline recordings were completed, all mice were treated with DOX while continuing weekly EEG recordings. ***B***, ***C***, Western blotting for transgenic APP (6E10) confirmed that untreated APP/TTA mice expressed high levels of transgenic protein. Expression was substantially decreased within 2 d of DOX treatment and remained low at the end of the experiment 4 –5 weeks later. ***D***, Quantification of the Western blots shown in ***B*** and ***C***. Transgenic APP has been normalized to GAPDH and all values are expressed relative to baseline expression in untreated bigenic animals. $***p < 0.001$. ***E***, *In vivo* microdialysis showed that ISF Aβ reached new steady-state levels within days after transgene suppression. Black circles, Aβ40; gray circles, Aβ42. ***F***, Tissue sections immunostained for Aβ confirmed that plaque loads were similar in untreated and DOX-treated APP/TTA mice used for EEG analysis. ***G***, EEG abnormalities in APP/TTA mice were substantially reduced after 4 weeks of transgene suppression. Scale bar, 0.4 mV, 5 s. ***H***, Comparison of SWD frequency over time in APP/TTA mice before and after 4 weeks of transgene suppression revealed that the decrease in SWD frequency was most pronounced during daylight hours. Filled circles, baseline; open circles, DOX 4 weeks. ***I***, Rate of SWDs in APP/TTA mice declined steadily from the start of treatment and became statistically indistinguishable from controls after 4 weeks of transgene suppression. Black circles, APP/TTA; gray circles, Control. $**p < 0.01$, $***p < 0.001$ vs Control; $†p < 0.05$, $††p < 0.01$, $†††p < 0.001$ vs Baseline. ***J***, Locomotor activity measured during EEG recordings suggests that nighttime movement is slightly diminished in both genotypes by DOX treatment. Circles, APP/TTA; squares, Control; filled symbols, Baseline; open symbols, DOX 4 weeks.

(baseline: 125.4 ± 16.6; DOX 2 weeks: 68.7 ± 15.6 SWDs/h; $p < 0.05$; $n = 11$ mice). After 4 weeks of DOX treatment, the frequency of SWD in APP/TTA mice was statistically indistinguishable from controls (DOX 4 weeks, APP/TTA: 43.9 ± 5.6; Control: 11.5 ± 2.7 SWDs/h; DOX 5 weeks, APP/TTA: 29.9 ± 12.7; Control: 12.1 ± 4.3 SWDs/h, $p > 0.05$, $n = 9–11$ mice/genotype). The change was most apparent during daylight hours, when SWD frequency was highest in the untreated mice. In contrast, the rate of SWDs in our control group (a balanced mix of NTG and TTA) was already low at baseline and did not change with DOX treatment.

The presence of SWDs is just one feature of the EEG signal that distinguishes APP-transgenic mice from controls. Past studies have shown significant irregularities in the power spectrum of EEG signals from APP-transgenic animals, noting that a subset of mice display dramatic changes in amplitude at selected wavelengths (Verret et al., 2012). We were particularly keen to determine whether similar differences existed in the APP/TTA mice and, if so, whether they were normalized by transgene suppression. We examined three features of the EEG signals that broadly defined their underlying structure: (1) the power spectrum across wavelengths, (2) the entropy of interpeak intervals, and (3) signal autocorrelation. In agreement with past studies, we found that the power spectrum differed significantly between genotypes during baseline recordings. Power curves from APP/TTA and control mice were readily distinguished by their profiles and their peaks. Although control animals displayed peak power levels in the delta range (2.6–3.8 Hz, peak at 3.1, $n = 8$), the spectra of APP/TTA mice reached maximal power at frequencies in the theta range (5.9–8.5 Hz, peak at 7.6; $n = 10$) and the overall distribution of the two groups was significantly different ($p = 0.014$, Fig. 3). In contrast, the power spectra after DOX treatment were nearly indistinguishable ($p = 0.62$). Both groups had peak power levels in the delta to low theta range (Control: 2.2–6.8 Hz, APP/TTA: 2.6–6.8 Hz). Transgene suppression thus rebalanced the power of the EEG signal across the entire range of frequencies.

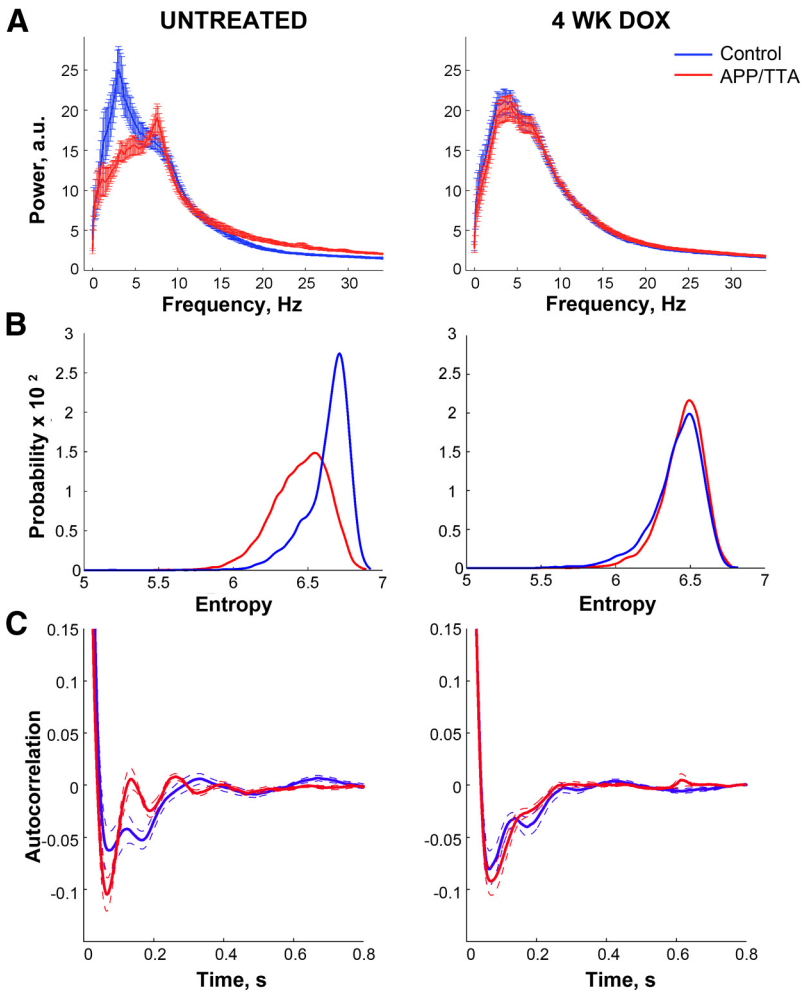

Figure 3. Transgene suppression normalizes the power spectrum, entropy, and autocorrelation of EEG signal in APP/TTA mice. ***A***, Spectral analysis of the EEG signal revealed a shift toward higher power in the theta range and diminished power in the delta range of untreated APP/TTA mice compared with controls. After 4 weeks of transgene suppression, the power distribution was identical between genotypes. ***B***, Interpeak timing in untreated APP/TTA mice has a lower entropy distribution compared with control mice, suggesting that their electrical activity is less stochastic than normal. The entropy distribution returns to control levels after 4 weeks of transgene suppression. ***C***, Autocorrelation within the EEG signal is lower in untreated APP/TTA mice than controls, indicating that the signal is intrinsically more structured. This, too, returns to control levels after DOX treatment. Red, APP/TTA; blue, Control.

EEG signals reveal a continuous ebb and flow of neuronal activity that occurs at a level far below overt SWD. The amplitude of "chatter" in the signal rises and falls hundreds or thousands of times each minute in both healthy controls and transgenic animals. Under normal conditions, these movements approximate random variation with little or no periodicity to the signal. This characteristic is mathematically defined by its entropy. EEG signals with regular, repeating patterns have lower entropy than signals that vary randomly, reflecting a higher degree of rhythmic synchronization in the network. Consistent with this characterization, we found that the entropy of peak timing in baseline recordings from APP/TTA was significantly lower than in control mice. Although the absolute numbers are immaterial (they vary with the peak threshold and time window used to measure interpeak intervals), the overall shape of the entropy probability distribution for untreated APP/TTA mice was much lower and broader than the corresponding control values ($p = 0.033$; Fig. 3). This finding was supported by characterization of autocorrelation in the signal, which provides another way of detecting regular structure in complex data. At short time lags, the signal from untreated APP/TTA mice showed a greater degree of negative autocorrelation than controls ($p = 0.021$; Fig. 3). In other words, the EEG amplitude could be more predictably expected to increase within 50–100 ms after it had fallen (and vice versa) in APP/TTA mice than in controls. However, both entropy and autocorrelation returned to control levels after 4 weeks of transgene suppression ($p = 0.48$ and $p = 0.32$, respectively). These findings indicate that the EEG abnormalities observed in untreated APP/TTA mice were de-

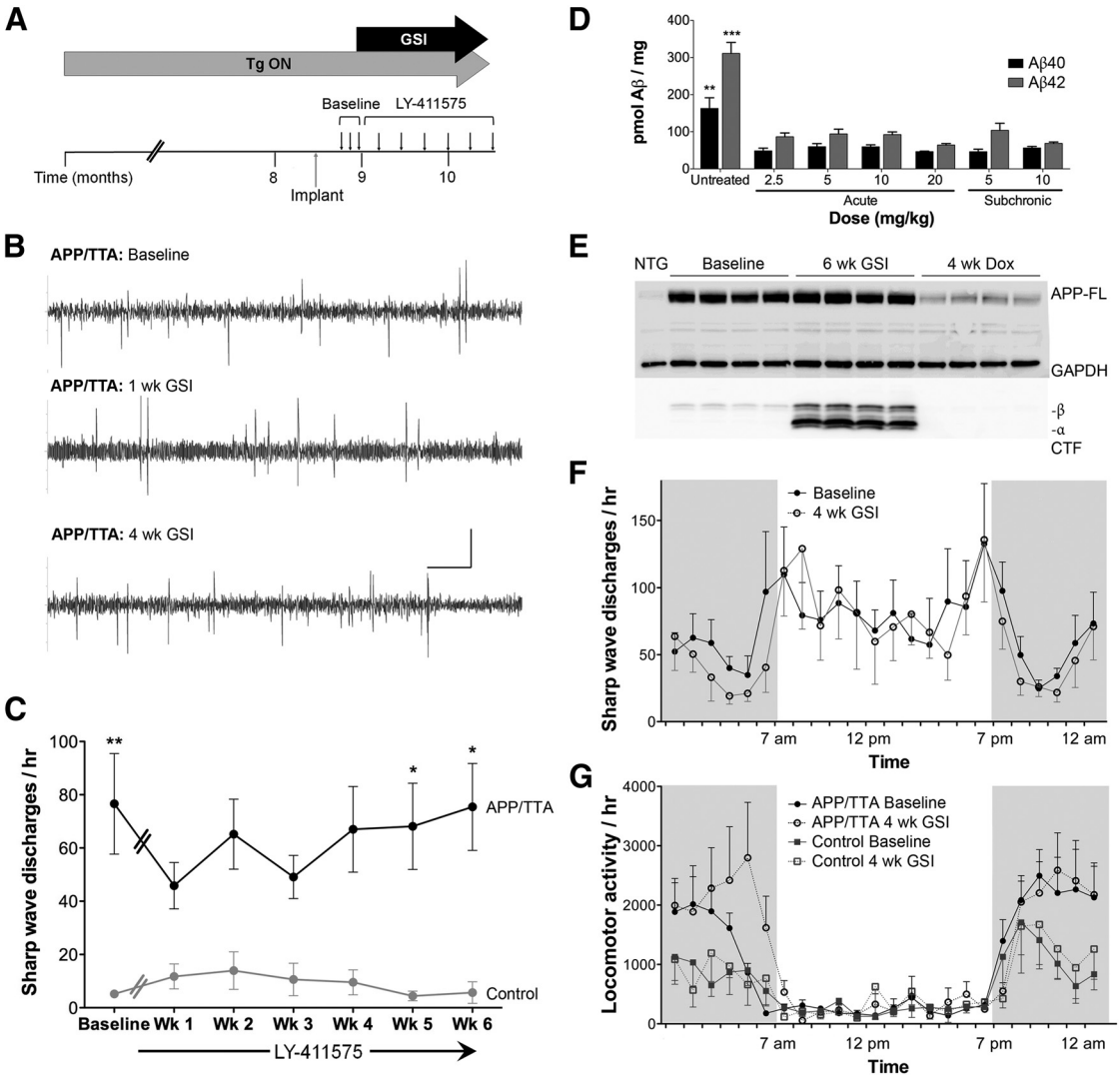

Figure 4. Selective Aβ reduction does not diminish SWD frequency in APP/TTA mice. ***A***, Mice were implanted at 8–9 months for baseline EEG recordings before GSI treatment with continued weekly recordings. ***B***, EEG recordings made before and during GSI treatment show that SWDs in APP/TTA mice were unchanged after 4 weeks of selective Aβ reduction. Scale bar, 0.4 mV, 5 s. ***C***, EEG analysis confirmed that the rate of SWDs in APP/TTA mice did not change during treatment and remained statistically different from controls after 6 weeks of GSI treatment. Black, APP/TTA; gray, Controls. $*p < 0.05$, $**p < 0.01$, $***p < 0.001$. ***D***, Dose–response analysis for LY411575 in young, predeposit APP/TTA mice revealed that both acute and chronic treatment reduced Aβ levels in the brain. $**p < 0.01$, $***p < 0.001$. ***E***, Western blotting with 6E10 shows that expression of full-length transgenic APP is maintained during GSI treatment, however, the levels of C-terminal fragment (CTF) increase as expected after γ-secretase inhibition. ***F***, Analysis of SWD frequency over time reveals that the circadian pattern of EEG activity in APP/TTA mice was unchanged by GSI treatment. Filled circles, Baseline; open circles, GSI 4 weeks. ***G***, Locomotor hyperactivity was also unchanged by GSI treatment. Circles, APP/TTA; squares, Control; filled symbols, Baseline; open symbols, GSI 4 weeks.

pendent on continued expression of transgenic APP, but were independent of deposited amyloid.

γ-Secretase inhibitor treatment does not rescue EEG abnormalities in tet-off APP mice

The rescue of EEG abnormalities by transgene suppression suggested that either APP itself or one of its cleavage products was responsible for establishing aberrant hyperexcitability in our tet-off APP mice. Based on its proposed role in Alzheimer's disease, we initially suspected that Aβ provoked this cortical hyperactivity. To test whether reducing Aβ would be sufficient to attenuate EEG abnormalities, we treated mice with a potent γ-secretase inhibitor (GSI), LY411575, which selectively decreased Aβ production without affecting full-length APP expression. We first measured the dose–response curve for this drug using brain Aβ levels as a readout of efficacy. We treated predeposit APP/TTA mice (5 weeks of age, $n = 4–6$ per dose) with a single intraperitoneal injection of 0, 2.5, 5, 10, or 20 mg/kg and harvested 3–4 h later. A second group of mice was chronically treated for 1 week by compounding the drug into chow at concentrations that would deliver 5 or 10 mg/kg/d orally. The reduction in steady-state Aβ levels attained by acute dosing suggested that maximal efficacy was reached by 2.5 mg/kg; however, the Aβ levels measured after 1 week of chronic treatment suggested that 10 mg/kg/d achieved slightly better reduction for Aβ42 than 5 mg/kg/d (Fig. 4).

With information gained from this initial dosing study, we began baseline EEG recordings in a new cohort of 8- to 9-month-old mice before beginning treatment with LY411575. We treated the mice with chow formulated to provide 10 mg/kg/d for the first 2 weeks of treatment, followed by 5 mg/kg/d to reduce mortality for an additional 4 weeks. To our surprise, we found no apparent

differences in SWD frequency during GSI treatment. Unlike what we had observed after transgene suppression, the number of SWDs/h remained stable in GSI-treated APP/TTA mice over successive weeks of recording ($p > 0.05$, $n = 8$–10; Fig. 4). Neither the circadian pattern of SWDs nor locomotor hyperactivity was altered after 4 weeks of GSI treatment. Even after 6 weeks of GSI treatment, SWD frequency remained identical to baseline ($p > 0.05$, Student's t test). Similarly, sibling controls showed no difference from baseline throughout the 6 week GSI treatment ($p > 0.05$, $n = 3$–6/time point). During treatment, all of the mice developed side effects characteristic of GSI treatment, including changes in pigmentation and patchy hair loss. After harvesting the mice, we confirmed that the dose of GSI we used was adequate to dramatically increase APP C-terminal fragments, suggesting that it had reached therapeutic levels in the brain. We conclude that GSI was sufficient to significantly reduce Aβ production, but failed to rescue EEG abnormalities and locomotor hyperactivity. Contrary to our initial expectations, these data suggest that APP itself or a fragment other than Aβ is responsible for EEG abnormalities in the tet-off APP mice.

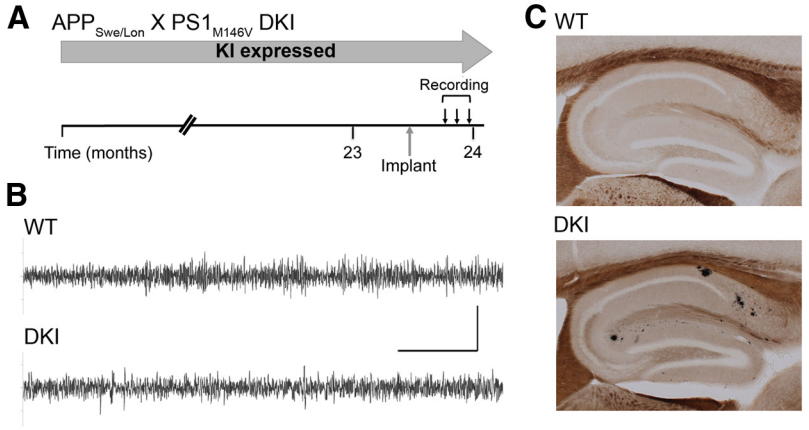

Figure 5. APP/PS1 DKI mice show normal EEG activity despite elevated Aβ production. ***A***, $APP_{Swe/Lon}/PS1_{M146V}$ mice and age-matched WT animals were implanted with transmitters for EEG recording at 23–24 months of age. ***B***, SWDs are not evident in aged DKI animals. Scale bar, 0.4 mV, 5 s. ***C***, Silver histology indicates that early amyloid pathology was present by the time of EEG recording.

Overproduction of Aβ is not sufficient to generate EEG abnormalities in double knock-in APP/PS1 mice

As a counterpoint to GSI treatment, which selectively suppresses Aβ overproduction while maintaining APP overexpression, we recorded EEGs from mice that have elevated levels of Aβ with endogenous levels of APP expression. We implanted EEG transmitters in homozygous $APP_{Swe/Lon}/PS1_{M146V}$ double knock-in (DKI) mice and their WT siblings at 23–24 months of age and recorded EEG activity during 7 sessions over 2 weeks (Fig. 5). This model displays early behavioral alterations (2–3 months) but fairly late amyloid deposition, with initial plaques apparent between 18 and 22 months of age (Guo et al., 2012; Guo et al., 2013). Although we recorded twice as many baseline sessions for the DKI mice as we had for the tet-off APP mice, we observed no EEG abnormalities and no increase in SWD frequency from controls (WT = 1.18 ± 0.17; DKI = 2.34 ± 0.69 SWDs/h, $p > 0.05$, Student's t test with Welch's correction, $n = 4$–5/genotype). We harvested the mice after recording to ascertain the presence of amyloid pathology expected from this model by 24 months of age. Although the plaque burden was considerably lower than in the tet-off APP mice, silver-positive plaques were detected in the hippocampus and cortex of all DKI mice we examined. This suggests that, in the absence of APP overexpression, Aβ overproduction is not sufficient to alter network excitability and lends further support to the hypothesis that full-length APP or another cleavage fragment underlies EEG abnormalities in the tet-off APP animals.

Increased susceptibility to chemically induced seizures is not attenuated by diminishing spontaneous hyperactivity

Because the tet-off APP mice exhibit spontaneous EEG abnormalities, we wanted to test whether they were also more vulnerable to chemically induced seizures, as demonstrated for other APP-transgenic models (Del Vecchio et al., 2004; Palop et al., 2007; Westmark et al., 2008). We implanted APP/TTA and control animals with transmitters at 6–7 months of age to monitor the seizure induction both electrographically and behaviorally. We measured the time to seizure onset, the number of seizures evoked, and the behavioral severity using a modified Racine scale (Racine, 1972; Ferraro et al., 1999). We began by testing susceptibility to the noncompetitive $GABA_A$ antagonist picrotoxin, which has a similar mechanism of action as pentylenetetrazol, the agent most commonly used in past studies with APP-transgenic mice. We determined that 1.75 mg/kg subcutaneously was just below the threshold for convulsive seizures in NTG animals, so we used this dose for EEG/behavioral studies in APP/TTA mice. The APP/TTA mice showed a significantly stronger response to picrotoxin than control animals for all measures we evaluated ($p < 0.05$, Student's t test, $n = 6$ mice/genotype; Fig. 6). Control animals developed modest EEG abnormalities in response to picrotoxin, but no electrographic seizures and only mild behavioral effects such as a flattened posture or prolonged immobility. In contrast, all of the APP/TTA mice progressed to tonic-clonic seizures within an hour, suggesting that they have an impairment in GABAergic inhibition.

We then tested whether this heightened susceptibility extended to other convulsants with different mechanisms of action. We selected kainic acid as a well studied agonist of ionotropic glutamate receptors and a good counterpoint to our experiments with picrotoxin. We determined that 35 mg/kg was just below the convulsive dose for kainic acid in NTG controls. To our surprise, APP/TTA transgenic animals were no more susceptible to kainic acid than controls ($p > 0.05$, Student's t test, $n = 5$ mice/genotype; Fig. 6). Kainate induced electrographic and behavioral seizures in some, but not all, mice of both genotypes. These data demonstrate that spontaneous electrographic hyperactivity does not automatically predispose the network to chemically induced seizures and suggests that the two neurotransmitter systems may be differentially altered by APP overexpression.

We were next curious to test whether allaying spontaneous EEG abnormalities in the tet-off APP mice would normalize their susceptibility to picrotoxin. We treated 6-month-old APP/TTA mice with DOX for 5 weeks before implanting them with transmitters and challenging them with picrotoxin. Despite the expected decline in SWD frequency, the DOX-treated APP/TTA mice were still significantly more susceptible to picrotoxin than

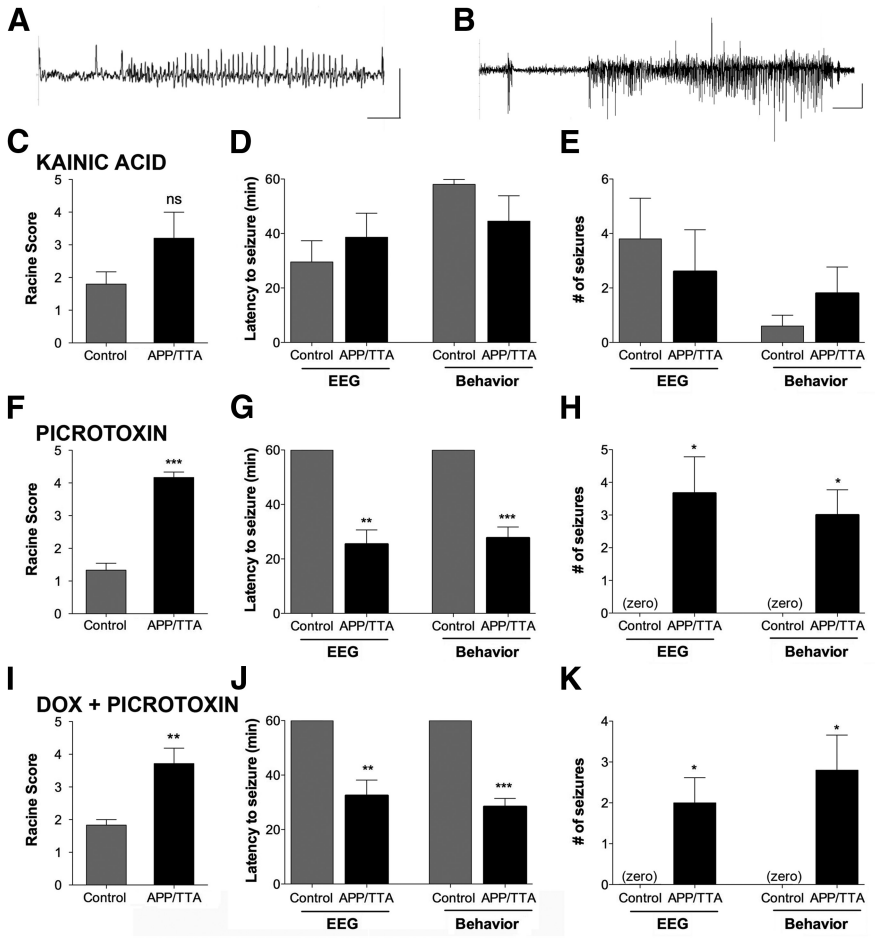

Figure 6. APP/TTA and control mice were challenged with kainic acid (***A, C, D, E***) or picrotoxin (***B, F, G, H***) and scored for seizure induction by EEG and behavioral observation. A separate cohort was treated with DOX for 5 weeks before picrotoxin challenge (***I–K***). ***A***, ***B***, Example EEG traces from APP/TTA mice challenged with kainic acid or picrotoxin. Scale bars: ***A***, 0.4 mV, 1 s; ***B***, 0.4 mV, 5 s. ***C, F, I***, Seizure severity was scored using a modified Racine scale. ***D, G, J***, Latency to first seizure. ***E, H, K***, Total number of seizures observed in the first hour after drug challenge. $*p < 0.05$, $**p < 0.01$, $***p < 0.001$.

similarly treated controls by every metric we tested ($p < 0.05$, Student's t test, $n = 5$–7 mice/genotype). These data suggest that increased sensitivity to acute GABA inhibition is mechanistically distinct from spontaneous SWDs and that cellular changes that diminish the likelihood of spontaneous SWDs are insufficient to protect against induced seizure.

APP overexpression alters the excitatory to inhibitory balance in the cortex

The sensitivity of APP/TTA mice to both spontaneous SWDs and acute GABAergic inhibition prompted us to test whether there may be underlying changes in the excitatory to inhibitory balance. We examined the relative levels of glutamatergic to GABAergic innervation by measuring the density of synaptic immunostaining for their respective vesicular neurotransmitter transporters, vGLUT and vGAT. Because our EEG recordings were taken above parietal cortex, we focused our histological analyses on this region and specifically on the main neuronal cell body layers 2/3 and 5. Within layer 5, the area occupied by vGLUT staining was significantly lower in APP/TTA mice than in controls ($p < 0.05$; $n = 4$–5 mice/group; Fig. 7). vGLUT density was restored to control levels by 4–5 weeks of transgene suppression, but was not rescued by GSI treatment, which is consistent with our EEG findings. In contrast, vGLUT staining within layer 2/3 was not significantly altered by transgene expression or treatment.

Changes in vGAT staining were opposite to those in vGLUT. In layer 5, the area of vGAT staining increased with APP overexpression ($p < 0.01$ vs control) but decreased to control levels after transgene suppression. vGAT staining in layer 2/3 showed a similar pattern: although the increase in vGAT with transgene expression was not significant, the drop after suppression was ($p < 0.01$ vs untreated). vGAT levels after GSI treatment fell in between those of untreated and DOX-treated animals, but were not significantly changed from untreated APP/TTA mice.

Together, these analyses revealed that continued overexpression of APP caused a significant reduction in the ratio of vGLUT:vGAT within layer 5 ($p < 0.01$ vs control) and a parallel trend in layer 2/3. Transgene suppression restored the excitatory/inhibitory ratio to control levels, whereas GSI treatment did not.

Suppression of APP overexpression during postnatal development delays the onset of EEG abnormalities in APP/TTA mice

Our EEG recordings after transgene suppression suggested that spontaneous SWDs were dependent on continued expression of mutant APP, but told us little about how network hyperexcitability arose in the first place. Our past studies with the tet-off mice demonstrated that APP overexpression during postnatal brain development had a lifelong impact on locomotor hyperactivity (Rodgers et al., 2012). To test whether delaying the expression of transgenic APP might also prevent network hyperexcitability, we reared a naive cohort of APP/TTA and control mice on DOX from postnatal day 2 (P2) until P42 to withhold APP overexpression until the brain was fully developed. At 6 weeks of age (P42), the mice were switched to normal chow to activate expression of transgenic APP (Fig. 8). At times ranging from 1 to 9 months later, we implanted the mice with EEG transmitters and recorded baseline cortical activity. We were thus able to compare the appearance of EEG abnormalities in juvenile- and adult-onset mice that were matched for duration of transgenic APP expression. Although the juvenile-onset APP/TTA mice showed higher-than-normal SWD frequency from the earliest ages we could examine (3 months), the adult-onset mice displayed no EEG abnormalities after 1, 3, or 6 months of transgene expression. However, by 9 months of APP overexpression, SWD frequency rose dramatically, reaching rates similar to those observed in juvenile-onset animals ($n = 5$–11 mice/treatment/age; Fig. 8). Despite the initial protection afforded by delaying APP exposure, these mice ultimately developed EEG abnormalities that were as severe as those in animals exposed to transgenic APP as juveniles. The contrast between the early appearance of SWDs in juvenile-onset mice and the substantial delay of SWDs in adult-onset animals suggests

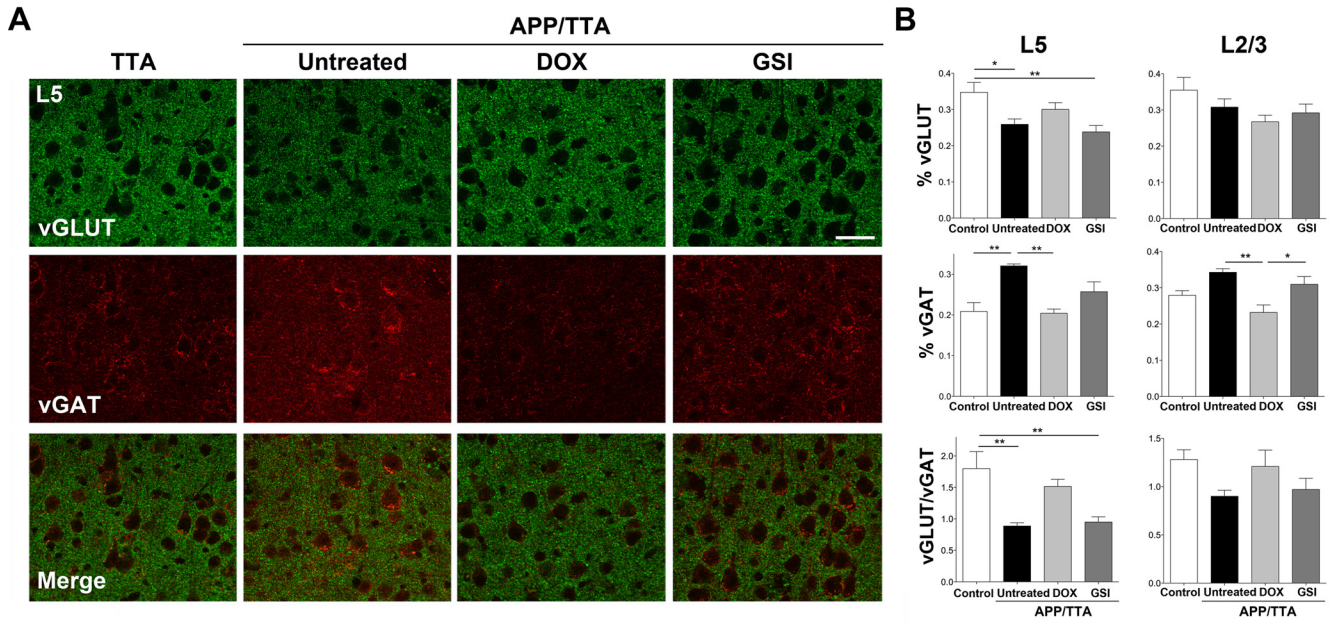

Figure 7. Transgene suppression restores cortical markers of glutamatergic and GABAergic innervation to control levels. ***A***, Tissue from TTA and APP/TTA mice used for EEG recording was coimmunostained for vGLUT1 and vGAT. Images show cortex layer 5 from untreated TTA (control) mice along with untreated, DOX-treated, and GSI-treated APP/TTA mice. Scale bar, 50 μm. ***B***, Percent area occupied by vGLUT1 and vGAT staining within layers 2/3 and 5 was measured using a custom MATLAB script. Untreated APP/TTA mice had a lower density of vGLUT1 and higher density of vGAT in layer 5 than control animals, with a similar trend in layer 2/3. Transgene suppression restored these excitatory/inhibitory markers to control levels, whereas GSI had no effect. $*p < 0.05$, $**p < 0.01$.

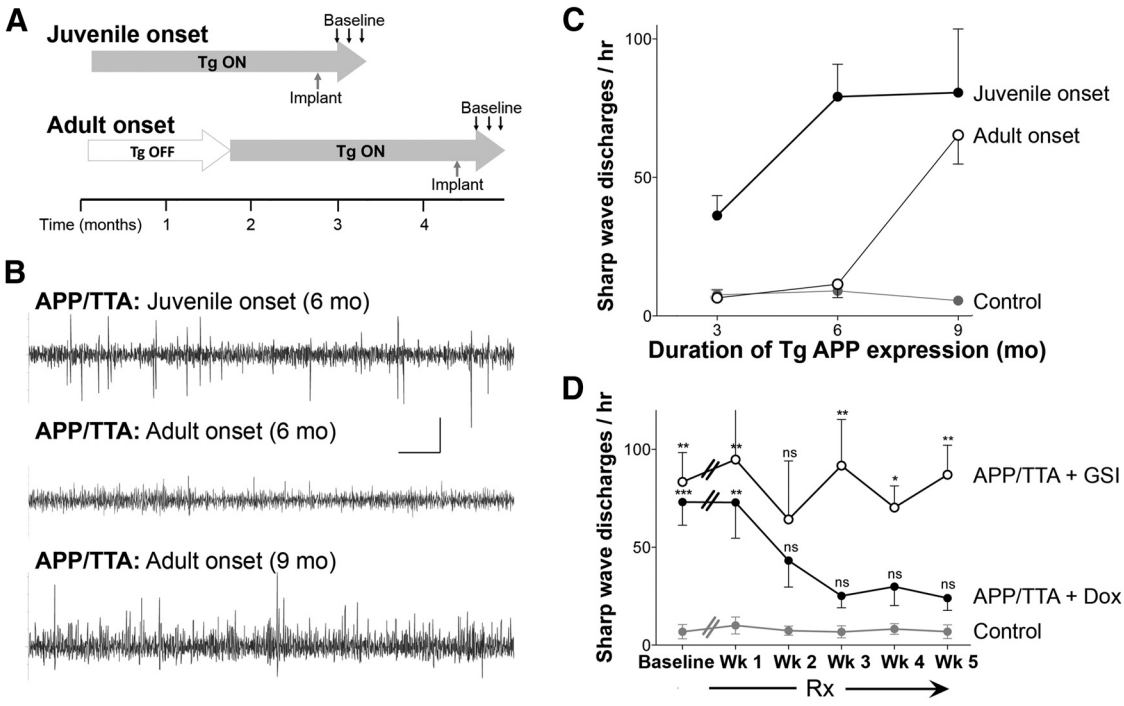

Figure 8. Delaying the onset of APP overexpression protects against early EEG abnormalities. ***A***, EEG activity was compared between juvenile-onset mice that express transgenic APP from birth and adult-onset mice in which APP overexpression was delayed with DOX until the mice reached 6 weeks of age. ***B***, SWDs were common in juvenile-onset APP/TTA mice at both 6 and 9 months of age, but were found in adult-onset mice only after 9 months of APP overexpression. Scale bar, 0.4 mV, 5 s. ***C***, Transgenic APP expression from birth resulted in elevated SWD frequency by the earliest ages we could examine (3 months), whereas mice with delayed transgene expression develop SWDs considerably later (9 months). Filled circles, juvenile onset; open circles, adult onset. ***D***, After 9 months of APP overexpression, adult onset mice were treated either with DOX or with GSI for 5 weeks. The frequency of SWDs decreased to control levels within 2 weeks of transgene suppression, but did not change significantly with secretase inhibition. Filled circles, DOX; open circles, GSI. $*p < 0.05$, $**p < 0.01$.

that postponing transgenic APP expression either provides initial, but not indefinite, protection from mutant APP and its cleavage products or that the two models may reach the same phenotype by distinct mechanisms.

We next examined whether SWDs, once present, were dependent on continued APP overexpression in adult-onset mice, as they had been in mice that expressed APP from birth. After completing baseline EEG recordings in adult-onset mice that had

overexpressed APP for 9 months, we started DOX treatment and continued weekly recording. We found that SWD frequency decreased to rates that were statistically indistinguishable from controls within 2 weeks of transgene suppression ($p > 0.05$, $n = 5$–9 mice/genotype; Fig. 8). We further tested whether selective reduction of soluble Aβ could abate SWDs by treating adult-onset mice with GSI. However, similar to our findings in juvenile-onset mice, GSI treatment had no effect on SWD frequency ($p > 0.05$; $n = 3$ mice; Fig. 8). This finding suggests that, regardless of when they appear, network changes that support spontaneous SWDs are actively maintained by the continued overexpression of APP rather than by the overproduction of Aβ.

Discussion

We set out to distinguish whether soluble Aβ, deposited amyloid, or APP itself was responsible for the epileptiform phenotype reported in transgenic models of Alzheimer's disease. In the process, we discovered that the cause of network hyperexcitability was more complex than we expected and was not due directly to either Aβ or amyloid. We found that juvenile APP overexpression predisposed the adult brain to hypersynchronous discharge. Delaying APP overexpression for just 6 weeks protected against epileptiform activity for >6 months, but spontaneous hyperexcitability ultimately emerged as amyloid pathology became severe. Surprisingly, whether epileptiform events were provoked by the development or degeneration, plaques themselves do not appear to govern network activity. Instead, we find that APP itself—or one of its processed fragments—determines the persistence of hyperactivity. Reducing the level of transgenic APP, but not that of Aβ, restored network activity to normal even while significant amyloid pathology remained. Phenotypic rescue took longer than was needed to arrest transgene expression, suggesting that APP overexpression elicited network alterations through an indirect mechanism. Consistent with this idea, markers of excitatory and inhibitory innervation revealed an imbalance in the cortical network that supported EEG abnormalities but was restored to normal after APP suppression.

Our study is the first to test directly the proposed link between soluble Aβ species and seizures (Palop and Mucke, 2010). In contrast to what we had expected, diminishing Aβ with GSI failed to reduce the frequency of SWDs. One concern we had in interpreting these data was that GSI treatment failed to completely eliminate soluble Aβ from the brain, raising the possibility that the residual Aβ was sufficient to maintain SWDs. However, transgene suppression was less efficient at lowering soluble Aβ than GSI yet fully suppressed the SWD phenotype, arguing against this explanation. Instead, our findings suggest that Aβ is not the primary cause of epileptiform discharge in APP-transgenic models. This conclusion is further supported by the absence of EEG abnormalities in aged APP/PS1 knock-in mice with elevated Aβ production and late-onset plaque formation. Together, these findings suggest that other fragments, or even full-length APP itself, may be responsible for network disruption in APP-transgenic models. APP overexpression might promote network hyperexcitability by exacerbating a physiological function of the endogenous protein, such as neurogenesis, neurite outgrowth, or synapse formation (Zheng and Koo, 2011; Hoe et al., 2012). Endogenous APP expression is highest during synaptogenesis between 2 and 6 weeks of age (Hoe et al., 2012; Westmark, 2013), a time that may be when the developing network is the most sensitive to APP overexpression. Consistent with this idea, we find that mice exposed to transgenic APP as juveniles developed epileptiform activity much earlier than animals in which APP expression was delayed until adulthood. This result suggests that APP overexpression during postnatal development makes the brain more susceptible to hypersynchronous activity in the adult.

Although juvenile APP exposure was sufficient to prime network hyperactivity, continued APP overexpression was necessary to maintain it. Intriguingly, even though transgenic APP was reduced by 80% within days of DOX treatment, it took several weeks for SWD frequency to fully decline. The temporal disparity suggests that the mechanism supporting spontaneous discharge is not a simple on/off process. Our histological data suggest that APP overexpression alters the pattern of cortical innervation, although it is unclear whether it acts directly on synapse formation during development or indirectly as a consequence of later neuronal hyperactivity. The direction of this shift, toward elevated GABAergic and diminished glutamateric innervation, intuitively contradicts the observed hypersynchronous phenotype; however, past work has shown that increased GABAergic signaling can synchronize neuronal firing in the cortex and trigger epileptiform activity (Cobb et al., 1995; Klaassen et al., 2006). Alternatively, the shift in innervation may be a compensatory attempt to dampen network hyperactivity caused by APP overexpression (Palop et al., 2007). Whether causal or reactive, the levels of GABAergic and glutamatergic innervation returned to control levels once transgenic APP was removed from the system. The level of APP expression may thus act as a rheostat on synaptic balance in the brain.

Although spontaneous discharge eventually subsided after APP suppression, bigenic mice remained susceptible to chemically induced seizures. APP/TTA mice were more sensitive to picrotoxin than controls regardless of whether APP expression was active or not, suggesting that some aspects of the network may remain permanently altered by juvenile APP exposure. Past studies in other APP-transgenic models have identified a similar vulnerability to pentylenetetrazol (Del Vecchio et al., 2004; Palop et al., 2007; Westmark et al., 2008; Roberson et al., 2011). Intriguingly, APP/TTA mice were identical to controls for kainate susceptibility, revealing an unexpected degree of selectivity in seizure sensitivity. Recent work suggests that tonic hyperpolarization of cortical interneurons contribute to network excitability in J20 mice (Verret et al., 2012), whereas other APP-transgenic models display overt degeneration of inhibitory neurons (Ramos et al., 2006; Baglietto-Vargas et al., 2010; Takahashi et al., 2010; Loreth et al., 2012). Together, these results support a permanent reduction in GABAergic function caused by developmental exposure to APP overexpression.

How could it be that some aspects of GABAergic dysfunction remain amenable to APP suppression, whereas other changes were permanent? Our experiments do not speak to this distinction directly, but we may gain insight from comparing the phenotypes that changed with those that did not. Both SWD and the theta/delta imbalance were abated by reducing APP levels, but increased sensitivity to picrotoxin was not. Parvalbumin-positive interneurons have been linked to the spontaneous EEG features in APP-transgenic mice and are believed to drive theta oscillations in the healthy brain (Hangya et al., 2009; Cutsuridis and Hasselmo, 2012; Verret et al., 2012). In contrast, other classes of GABAergic interneurons appear to be involved in synchronous discharge caused by picrotoxin (Hiscock et al., 1996). This raises the possibility that APP exposure may have distinct consequences on different classes of interneurons depending on when the transgene is expressed.

The final experiment of our study demonstrated that the timing of APP expression has a significant impact on the resulting phenotype. We had shown previously that postponing transgenic

APP expression until 6 weeks of age attenuated locomotor hyperactivity in the adult (Rodgers et al., 2012). Here, we show that postponing transgene expression also delayed the appearance of EEG abnormalities. Ultimately, the adult-onset mice developed SWDs similar to those seen at earlier ages after juvenile APP expression, but only after severe amyloid accumulation. This disparity suggests there may be two ways to reach the same phenotypic outcome. In one case, APP overexpression during postnatal development alters network formation to favor hyperexcitability; in the other, pathological damage degrades the network to a point where it becomes vulnerable to synchronization. In both settings, SWDs only persist as long as APP overexpression continues. We therefore propose a "two-hit" model in which either developmental alterations or pathological damage make cortical circuits permissive for synchrony, but then require APP overexpression to trigger recurrent SWDs. From our experiments, we cannot identify the precise fragment responsible, but our GSI findings rule out AICD, P3, CTFα, and CTFβ, because all four would be affected by the loss of γ-processing. Although our data do not speak to the mechanism by which APP overexpression triggers SWDs, past work in other models suggest a possible explanation. In particular, BACE1-null mice display seizure abnormalities similar to those described in APP-transgenic mice (Kobayashi et al., 2008; Hitt et al., 2010; Hu et al., 2010). Moreover, expression of mutant APP on the BACE-null background exacerbates the seizure phenotype (Kobayashi et al., 2008), which suggests that neither sAPPβ nor CTFβ contribute to SWDs in APP/TTA mice. Instead, high levels of full-length APP in the transgenic mice may commandeer a disproportionate fraction of the cell's limited BACE pool, thereby reducing its ability to process other substrates critical for neuronal function. BACE normally cleaves several proteins involved in regulating neuronal activity, including the accessory subunits for voltage-gated ion channels and neuregulin, both of which play important roles in GABAergic neurons (Wong et al., 2005; Kim et al., 2007; Kim et al., 2011; Fleck et al., 2012; Sachse et al., 2013). NaVβ2 controls membrane localization of the sodium channel NaV1.1 to facilitate electrical excitability (Kovacs et al., 2010; Huth and Alzheimer, 2012), whereas neuregulin 1 stimulates GABA release (Wen et al., 2010). Reduction of either protein promotes epileptogenesis (Yu et al., 2006; Cheah et al., 2012; Tan et al., 2012). With multiple activity-regulating proteins dependent on BACE processing, any process that impairs this function could alter the normal balance of excitability in the brain.

Our findings may also offer a new perspective on the association between seizures and AD in the clinical literature. Epidemiological studies have revealed that seizure risk is increased 87-fold in patients with early-onset AD (Amatniek et al., 2006). Seizure risk in patients with late-onset AD drops to only threefold, offset in part because seizure risk for the entire population increases with age. The risk disparity suggests that there may be different mechanisms underlying the predisposition for seizure in each population. Inherited mutations may exert Aβ-independent effects during circuit formation that predispose the network to hypersynchrony. Absent this developmental influence, patients with late-onset disease may be more resistant to seizures until the network becomes severely damaged. In both cases, lowering Aβ may alleviate the pathological and cognitive progression of AD, but our data suggest that this peptide may be the wrong target for alleviating hypersynchrony.

References

Amatniek JC, Hauser WA, DelCastillo-Castaneda C, Jacobs DM, Marder K, Bell K, Albert M, Brandt J, Stern Y (2006) Incidence and predictors of seizures in patients with Alzheimer's disease. Epilepsia 47:867–872. CrossRef Medline

Baglietto-Vargas D, Moreno-Gonzalez I, Sanchez-Varo R, Jimenez S, Trujillo-Estrada L, Sanchez-Mejias E, Torres M, Romero-Acebal M, Ruano D, Vizuete M, Vitorica J, Gutierrez A (2010) Calretinin interneurons are early targets of extracellular amyloid-β pathology in PS1/AβPP Alzheimer mice hippocampus. J Alzheimers Dis 21:119–132. CrossRef Medline

Bakker A, Krauss GL, Albert MS, Speck CL, Jones LR, Stark CE, Yassa MA, Bassett SS, Shelton AL, Gallagher M (2012) Reduction of hippocampal hyperactivity improves cognition in amnestic mild cognitive impairment. Neuron 74:467–474. CrossRef Medline

Bero AW, Yan P, Roh JH, Cirrito JR, Stewart FR, Raichle ME, Lee JM, Holtzman DM (2011) Neuronal activity regulates the regional vulnerability to amyloid-β deposition. Nat Neurosci 14:750–756. CrossRef Medline

Busche MA, Eichhoff G, Adelsberger H, Abramowski D, Wiederhold KH, Haass C, Staufenbiel M, Konnerth A, Garaschuk O (2008) Clusters of hyperactive neurons near amyloid plaques in a mouse model of Alzheimer's disease. Science 321:1686–1689. CrossRef Medline

Busche MA, Chen X, Henning HA, Reichwald J, Staufenbiel M, Sakmann B, Konnerth A (2012) Critical role of soluble amyloid-β for early hippocampal hyperactivity in a mouse model of Alzheimer's disease. Proc Natl Acad Sci U S A 109:8740–8745. CrossRef Medline

Cabrejo L, Guyant-Maréchal L, Laquerrière A, Vercelletto M, De la Fournière F, Thomas-Antérion C, Verny C, Letournel F, Pasquier F, Vital A, Checler F, Frebourg T, Campion D, Hannequin D (2006) Phenotype associated with APP duplication in five families. Brain 129:2966–2976. CrossRef Medline

Cheah CS, Yu FH, Westenbroek RE, Kalume FK, Oakley JC, Potter GB, Rubenstein JL, Catterall WA (2012) Specific deletion of NaV1.1 sodium channels in inhibitory interneurons causes seizures and premature death in a mouse model of Dravet syndrome. Proc Natl Acad Sci U S A 109:14646–14651. CrossRef Medline

Cirrito JR, May PC, O'Dell MA, Taylor JW, Parsadanian M, Cramer JW, Audia JE, Nissen JS, Bales KR, Paul SM, DeMattos RB, Holtzman DM (2003) In vivo assessment of brain interstitial fluid with microdialysis reveals plaque-associated changes in amyloid-β metabolism and half-life. J Neurosci 23:8844–8853. Medline

Cirrito JR, Yamada KA, Finn MB, Sloviter RS, Bales KR, May PC, Schoepp DD, Paul SM, Mennerick S, Holtzman DM (2005) Synaptic activity regulates interstitial fluid amyloid-β levels in vivo. Neuron 48:913–922. CrossRef Medline

Cirrito JR, Disabato BM, Restivo JL, Verges DK, Goebel WD, Sathyan A, Hayreh D, D'Angelo G, Benzinger T, Yoon H, Kim J, Morris JC, Mintun MA, Sheline YI (2011) Serotonin signaling is associated with lower amyloid-β levels and plaques in transgenic mice and humans. Proc Natl Acad Sci U S A 108:14968–14973. CrossRef Medline

Cobb SR, Buhl EH, Halasy K, Paulsen O, Somogyi P (1995) Synchronization of neuronal activity in hippocampus by individual GABAergic interneurons. Nature 378:75–78. CrossRef Medline

Corbett BF, Leiser SC, Ling HP, Nagy R, Breysse N, Zhang X, Hazra A, Brown JT, Randall AD, Wood A, Pangalos MN, Reinhart PH, Chin J (2013) Sodium channel cleavage is associated with aberrant neuronal activity and cognitive deficits in a mouse model of Alzheimer's disease. J Neurosci 33:7020–7026. CrossRef Medline

Cutsuridis V, Hasselmo M (2012) GABAergic contributions to gating, timing, and phase precession of hippocampal neuronal activity during theta oscillations. Hippocampus 22:1597–1621. CrossRef Medline

Del Vecchio RA, Gold LH, Novick SJ, Wong G, Hyde LA (2004) Increased seizure threshold and severity in young transgenic CRND8 mice. Neurosci Lett 367:164–167. CrossRef Medline

Ferraro TN, Golden GT, Smith GG, St Jean P, Schork NJ, Mulholland N, Ballas C, Schill J, Buono RJ, Berrettini WH (1999) Mapping loci for pentylenetetrazol-induced seizure susceptibility in mice. J Neurosci 19:6733–6739. Medline

Fleck D, Garratt AN, Haass C, Willem M (2012) BACE1 dependent neuregulin processing: review. Curr Alzheimer Res 9:178–183. CrossRef Medline

Guo Q, Fu W, Sopher BL, Miller MW, Ware CB, Martin GM, Mattson MP

(1999) Increased vulnerability of hippocampal neurons to excitotoxic necrosis in presenilin-1 mutant knock-in mice. Nat Med 5:101–106. CrossRef Medline

Guo Q, Zheng H, Justice NJ (2012) Central CRF system perturbation in an Alzheimer's disease knockin mouse model. Neurobiol Aging 33:2678–2691. CrossRef Medline

Guo Q, Li H, Cole AL, Hur JY, Li Y, Zheng H (2013) Modeling Alzheimer's disease in mouse without mutant protein overexpression: cooperative and independent effects of Aβ and tau. PLoS One 8:e80706. CrossRef Medline

Hangya B, Borhegyi Z, Szilágyi N, Freund TF, Varga V (2009) GABAergic neurons of the medial septum lead the hippocampal network during theta activity. J Neurosci 29:8094–8102. CrossRef Medline

Hiscock JJ, MacKenzie L, Willoughby JO (1996) Fos induction in subtypes of cerebrocortical neurons following single picrotoxin-induced seizures. Brain Res 738:301–312. CrossRef Medline

Hitt BD, Jaramillo TC, Chetkovich DM, Vassar R (2010) BACE1$^{-/-}$ mice exhibit seizure activity that does not correlate with sodium channel level or axonal localization. Mol Neurodegener 5:31. CrossRef Medline

Hoe HS, Lee HK, Pak DT (2012) The upside of APP at synapses. CNS Neurosci Ther 18:47–56. CrossRef Medline

Hong S, Quintero-Monzon O, Ostaszewski BL, Podlisny DR, Cavanaugh WT, Yang T, Holtzman DM, Cirrito JR, Selkoe DJ (2011) Dynamic analysis of amyloid β-protein in behaving mice reveals opposing changes in ISF versus parenchymal Aβ during age-related plaque formation. J Neurosci 31:15861–15869. CrossRef Medline

Hu X, Zhou X, He W, Yang J, Xiong W, Wong P, Wilson CG, Yan R (2010) BACE1 deficiency causes altered neuronal activity and neurodegeneration. J Neurosci 30:8819–8829. CrossRef Medline

Huth T, Alzheimer C (2012) Voltage-dependent Na+ channels as targets of BACE1-implications for neuronal firing and beyond. Curr Alzheimer Res 9:184–188. CrossRef Medline

Jankowsky JL, Slunt HH, Gonzales V, Savonenko AV, Wen JC, Jenkins NA, Copeland NG, Younkin LH, Lester HA, Younkin SG, Borchelt DR (2005) Persistent amyloidosis following suppression of Aβ production in a transgenic model of Alzheimer's disease. PLoS Med 2:e355. CrossRef Medline

Jankowsky JL, Younkin LH, Gonzales V, Fadale DJ, Slunt HH, Lester HA, Younkin SG, Borchelt DR (2007) Rodent Aβ modulates the solubility and distribution of amyloid deposits in transgenic mice. J Biol Chem 282:22707–22720. CrossRef Medline

Jayadev S, Leverenz JB, Steinbart E, Stahl J, Klunk W, Yu CE, Bird TD (2010) Alzheimer's disease phenotypes and genotypes associated with mutations in presenilin 2. Brain 133:1143–1154. CrossRef Medline

Kamenetz F, Tomita T, Hsieh H, Seabrook G, Borchelt D, Iwatsubo T, Sisodia S, Malinow R (2003) APP processing and synaptic function. Neuron 37:925–937. CrossRef Medline

Kim DY, Carey BW, Wang H, Ingano LA, Binshtok AM, Wertz MH, Pettingell WH, He P, Lee VM, Woolf CJ, Kovacs DM (2007) BACE1 regulates voltage-gated sodium channels and neuronal activity. Nat Cell Biol 9:755–764. CrossRef Medline

Kim DY, Gersbacher MT, Inquimbert P, Kovacs DM (2011) Reduced sodium channel NaV1.1 levels in BACE1-null mice. J Biol Chem 286:8106–8116. CrossRef Medline

Klaassen A, Glykys J, Maguire J, Labarca C, Mody I, Boulter J (2006) Seizures and enhanced cortical GABAergic inhibition in two mouse models of human autosomal dominant nocturnal frontal lobe epilepsy. Proc Natl Acad Sci U S A 103:19152–19157. CrossRef Medline

Kobayashi D, Zeller M, Cole T, Buttini M, McConlogue L, Sinha S, Freedman S, Morris RG, Chen KS (2008) BACE1 gene deletion: impact on behavioral function in a model of Alzheimer's disease. Neurobiol Aging 29:861–873. CrossRef Medline

Köhler C, Ebert U, Baumann K, Schroder H (2005) Alzheimer's disease-like neuropathology of gene-targeted APP-SLxPS1mut mice expressing the amyloid precursor protein at endogenous levels. Neurobiol Dis 20:528–540. CrossRef Medline

Kovacs DM, Gersbacher MT, Kim DY (2010) Alzheimer's secretases regulate voltage-gated sodium channels. Neurosci Lett 486:68–72. CrossRef Medline

Lalonde R, Dumont M, Staufenbiel M, Strazielle C (2005) Neurobehavioral characterization of APP23 transgenic mice with the SHIRPA primary screen. Behav Brain Res 157:91–98. CrossRef Medline

Larner AJ, Doran M (2006) Clinical phenotypic heterogeneity of Alzheimer's disease associated with mutations of the presenilin-1 gene. J Neurol 253:139–158. CrossRef Medline

Levites Y, Das P, Price RW, Rochette MJ, Kostura LA, McGowan EM, Murphy MP, Golde TE (2006a) Anti-Aβ42- and anti-Aβ40-specific mAbs attenuate amyloid deposition in an Alzheimer disease mouse model. J Clin Invest 116:193–201. CrossRef Medline

Levites Y, Smithson LA, Price RW, Dakin RS, Yuan B, Sierks MR, Kim J, McGowan E, Reed DK, Rosenberry TL, Das P, Golde TE (2006b) Insights into the mechanisms of action of anti-Aβ antibodies in Alzheimer's disease mouse models. FASEB J 20:2576–2578. CrossRef Medline

Loreth D, Ozmen L, Revel FG, Knoflach F, Wetzel P, Frotscher M, Metzger F, Kretz O (2012) Selective degeneration of septal and hippocampal GABAergic neurons in a mouse model of amyloidosis and tauopathy. Neurobiol Dis 47:1–12. CrossRef Medline

Mayford M, Bach ME, Huang YY, Wang L, Hawkins RD, Kandel ER (1996) Control of memory formation through regulated expression of a CaMKII transgene. Science 274:1678–1683. CrossRef Medline

Menéndez M (2005) Down syndrome, Alzheimer's disease and seizures. Brain Dev 27:246–252. CrossRef Medline

Minkeviciene R, Rheims S, Dobszay MB, Zilberter M, Hartikainen J, Fülöp L, Penke B, Zilberter Y, Harkany T, Pitkänen A, Tanila H (2009) Amyloid β-induced neuronal hyperexcitability triggers progressive epilepsy. J Neurosci 29:3453–3462. CrossRef Medline

Noebels J (2011) A perfect storm: converging paths of epilepsy and Alzheimer's dementia intersect in the hippocampal formation. Epilepsia 52:39–46. CrossRef Medline

Palop JJ, Mucke L (2009) Epilepsy and cognitive impairments in Alzheimer disease. Arch Neurol 66:435–440. CrossRef Medline

Palop JJ, Mucke L (2010) Amyloid-β-induced neuronal dysfunction in Alzheimer's disease: from synapses toward neural networks. Nat Neurosci 13:812–818. CrossRef Medline

Palop JJ, Chin J, Roberson ED, Wang J, Thwin MT, Bien-Ly N, Yoo J, Ho KO, Yu GQ, Kreitzer A, Finkbeiner S, Noebels JL, Mucke L (2007) Aberrant excitatory neuronal activity and compensatory remodeling of inhibitory hippocampal circuits in mouse models of Alzheimer's disease. Neuron 55:697–711. CrossRef Medline

Racine RJ (1972) Modification of seizure activity by electrical stimulation. II. Motor seizure. Electroencephalogr Clin Neurophysiol 32:281–294. CrossRef Medline

Ramos B, Baglietto-Vargas D, del Rio JC, Moreno-Gonzalez I, Santa-Maria C, Jimenez S, Caballero C, Lopez-Tellez JF, Khan ZU, Ruano D, Gutierrez A, Vitorica J (2006) Early neuropathology of somatostatin/NPY GABAergic cells in the hippocampus of a PS1xAPP transgenic model of Alzheimer's disease. Neurobiol Aging 27:1658–1672. CrossRef Medline

Roberson ED, Halabisky B, Yoo JW, Yao J, Chin J, Yan F, Wu T, Hamto P, Devidze N, Yu GQ, Palop JJ, Noebels JL, Mucke L (2011) Amyloid-β/Fyn-induced synaptic, network, and cognitive impairments depend on tau levels in multiple mouse models of Alzheimer's disease. J Neurosci 31:700–711. CrossRef Medline

Rodgers SP, Born HA, Das P, Jankowsky JL (2012) Transgenic APP expression during postnatal development causes persistent locomotor hyperactivity in the adult. Mol Neurodegener 7:28. CrossRef Medline

Sachse CC, Kim YH, Agsten M, Huth T, Alzheimer C, Kovacs DM, Kim DY (2013) BACE1 and presenilin/γ-secretase regulate proteolytic processing of KCNE1 and 2, auxiliary subunits of voltage-gated potassium channels. FASEB J 27:2458–2467. CrossRef Medline

Sanchez P, Zhu L, Verret L, Vossel K, Orr A, Cirrito J, Devidze N, Ho K, Yu G, Palop J, Mucke L (2012) Levetiracetam suppresses neuronal network dysfunction and reverses synaptic and cognitive deficits in an Alzheimer's disease model. Proc Natl Acad Sci U S A 109):E2895–E2903. CrossRef

Snider BJ, Norton J, Coats MA, Chakraverty S, Hou CE, Jervis R, Lendon CL, Goate AM, McKeel DW Jr, Morris JC (2005) Novel presenilin 1 mutation (S170F) causing Alzheimer disease with Lewy bodies in the third decade of life. Arch Neurol 62:1821–1830. CrossRef Medline

Takahashi H, Brasnjevic I, Rutten BP, Van Der Kolk N, Perl DP, Bouras C, Steinbusch HW, Schmitz C, Hof PR, Dickstein DL (2010) Hippocampal interneuron loss in an APP/PS1 double mutant mouse and in Alzheimer's disease. Brain Struct Funct 214:145–160. CrossRef Medline

Tan GH, Liu YY, Hu XL, Yin DM, Mei L, Xiong ZQ (2012) Neuregulin 1 represses limbic epileptogenesis through ErbB4 in parvalbumin-expressing interneurons. Nat Neurosci 15:258–266. CrossRef Medline

Verret L, Mann EO, Hang GB, Barth AM, Cobos I, Ho K, Devidze N, Masliah

E, Kreitzer AC, Mody I, Mucke L, Palop JJ (2012) Inhibitory interneuron deficit links altered network activity and cognitive dysfunction in Alzheimer model. Cell 149:708–721. CrossRef Medline

Wang A, Das P, Switzer RC 3rd, Golde TE, Jankowsky JL (2011) Robust amyloid clearance in a mouse model of Alzheimer's disease provides novel insights into the mechanism of amyloid-β immunotherapy. J Neurosci 31:4124–4136. CrossRef Medline

Wang Z, Wang B, Yang L, Guo Q, Aithmitti N, Songyang Z, Zheng H (2009) Presynaptic and postsynaptic interaction of the amyloid precursor protein promotes peripheral and central synaptogenesis. J Neurosci 29: 10788–10801. CrossRef Medline

Wen L, Lu YS, Zhu XH, Li XM, Woo RS, Chen YJ, Yin DM, Lai C, Terry AV Jr, Vazdarjanova A, Xiong WC, Mei L (2010) Neuregulin 1 regulates pyramidal neuron activity via ErbB4 in parvalbumin-positive interneurons. Proc Natl Acad Sci U S A 107:1211–1216. CrossRef Medline

Westmark CJ (2013) What's hAPPening at synapses? The role of amyloid β-protein precursor and β-amyloid in neurological disorders. Mol Psychiatry 18:425–434. CrossRef Medline

Westmark CJ, Westmark PR, Beard AM, Hildebrandt SM, Malter JS (2008) Seizure susceptibility and mortality in mice that over-express amyloid precursor protein. Int J Clin Exp Pathol 1:157–168. Medline

Wong HK, Sakurai T, Oyama F, Kaneko K, Wada K, Miyazaki H, Kurosawa M, De Strooper B, Saftig P, Nukina N (2005) β Subunits of voltage-gated sodium channels are novel substrates of β-site amyloid precursor protein-cleaving enzyme (BACE1) and γ-secretase. J Biol Chem 280: 23009–23017. CrossRef Medline

Young-Pearse TL, Chen AC, Chang R, Marquez C, Selkoe DJ (2008) Secreted APP regulates the function of full-length APP in neurite outgrowth through interaction with integrin β1. Neural Dev 3:15. CrossRef Medline

Yu FH, Mantegazza M, Westenbroek RE, Robbins CA, Kalume F, Burton KA, Spain WJ, McKnight GS, Scheuer T, Catterall WA (2006) Reduced sodium current in GABAergic interneurons in a mouse model of severe myoclonic epilepsy in infancy. Nat Neurosci 9:1142–1149. CrossRef Medline

Zheng H, Koo EH (2011) Biology and pathophysiology of the amyloid precursor protein. Mol Neurodegener 6:27. CrossRef Medline

Ziyatdinova S, Gurevicius K, Kutchiashvili N, Bolkvadze T, Nissinen J, Tanila H, Pitkänen A (2011) Spontaneous epileptiform discharges in a mouse model of Alzheimer's disease are suppressed by antiepileptic drugs that block sodium channels. Epilepsy Res 94:75–85. CrossRef Medline

Conclusion

The results of this study were not what we expected to see, and in fact suggest a much more complicated relationship between APP, Aβ, and seizures. APP mice were found to have abnormal EEG measurements, as expected, which were normalized when APP was suppressed with DOX. This same normalization was not found when Aβ was inhibited though, suggesting that APP or something other than Aβ is responsible for the observed EEG abnormalities. We also found that Aβ overproduction on its own without APP overproduction was not enough to alter network excitability.

Surprisingly, mice that had previously overexpressed APP and had subsequent DOX dosing still showed higher susceptibility to chemically-induced seizures than control mice, showing that some aspects of the CNS may be permanently altered. To explain this finding, we looked into the excitatory and inhibitory balance in the experimental and control murine cortexes. We found that APP overexpression results in changes to GABAergic inhibition. Our experiments were not able to conclude why some changes were permanent while others transitory with the suppression or overexpression of APP.

The different risk levels for EOAD and LOAD suggest that each population has different mechanisms underlying their seizure predisposition. By changing the time of APP expression in the mice, our experiment suggests that inherited mutations may have independent effects from Aβ that predispose patients to seizures, whereas those with LOAD may have a resistance to seizures. This protective effect is diminished with neurodegeneration though. Our work shows that in either case, Aβ is not a good target for suppressing aberrant electrical activity.

As briefly discussed in the paper, Down syndrome patients are at a greater risk for seizures (Menéndez 2005). Down syndrome, also referred to as Trisomy 21, is a heterogenous disorder that is caused by the presence of an extra copy of chromosome 21 (Choong et al. 2015). This extra chromosome leads to the overproduction of APP and subsequently to an increase in amyloidogenic fragments (Menéndez 2005). As a result, an estimated 90% of all Down syndrome patients develop AD and virtually all

have AD pathology present by age 40 (Wisniewski et al. 1985; McCarron et al. 2014; Margallo-Lana et al. 2007).

The research presented here provides some interesting potential insights into the brain abnormalities associated with Down syndrome. As with the mouse models used here, Down syndrome patients also have an abnormal power spectrum (Menéndez 2005) indicative of hypersynchronicity.

As stated, the findings from this paper showed that susceptibility to seizures and abnormal network excitability was not due to Aβ overproduction but was more closely linked to the overexpression of APP. We also found that exposure to APP overproduction in juvenile mice predisposed them to hypersynchronicity. By delaying APP production, we were able to prevent the development of these abnormalities. As Down syndrome patients overexpress APP throughout their life, it seems likely that this model is a good comparison to explore the abnormalities resulting from this condition.

Furthermore, Down syndrome is also associated with excessive inhibition (Belichenko et al. 2009; Stagni et al. 2015), which we also observed in the APP/TTA mouse model.

Extrapolating out from these findings, it may be possible to prevent the network excitability and increased incidence of seizures seen with Down syndrome by delaying or decreasing the production of APP. With the advent of new genetic therapies, this could be achieved through selective silencing of APP with antisense oligonucleotide therapies or RNA interference, which are being tested in other diseases such as Amyotrophic lateral sclerosis (ALS) (van Zundert & Brown 2017) and Huntington's disease (Bennett 2018). APP expression could also be silenced through viral vectors or the Clustered Regularly Interspaced Short Palindromic Repeats/Cas (CRISPER/CAS) system (Ingusci et al. 2019).

The disadvantages of all these approaches are that they only target one gene, and Down syndrome is caused by the duplication of an entire chromosome, so these methods would have limited therapeutic effect. To that end, there is research being done to selectively repress the entire duplicate chromosome (Chiang et al. 2018).

In the past few years, our research has been further progressed by other researchers. Duffy et al. showed that Tg2576 mice show increased excitability in the entorhinal cortex as young as 2 months of age, prior to plaque deposition (Duffy et al. 2015).

Another study in 2017 was done on triple-transgenic mice with human APP, tau, and PS1 mutations to see if passive immunization with anti-human APP/Aβ monoclonal antibody would ameliorate seizure susceptibility (Kazim et al. 2017). They found this mouse model exhibited enhanced seizure susceptibility by three weeks of age, before plaque or neurofibrillary pathologies. Administration of 6E10 significantly reduced the incidence of seizures (Kazim et al. 2017). This study supports our previous findings that APP plays an important role in the hypersynchronicity and higher incidence of seizures in AD mouse models and takes the research that I completed a step further by including human tau expression.

Chapter 5: Genetic modulation of soluble Aβ rescues cognitive and synaptic impairment in a mouse model of AD

The role of Aβ in AD is still highly debated. As discussed earlier, it is not yet known if Aβ plaques are harmful or perhaps play a protective role in reducing the amount of soluble Aβ that is known to be toxic to cells. There have been few studies done to compare the contribution of each Aβ type to cognitive impairment in mouse models of AD.

The research completed in this study sought to discover if reducing soluble Aβ levels while not affecting Aβ plaque levels in mice would have any beneficial effects on their cognition. In order to halt the production of Aβ, APP transgenic mice were bred to have a tet-off responsive system for the translation of the APP gene. This allowed us to control the production of Aβ in the mice.

Through behavioral testing, immunohistochemistry, and microdialysis, we were able to quantify if there was behavioral rescue and a reduction in soluble Aβ burden when APP production was halted. My role in this study was to perform the microdialysis surgery on the mice, collect the *in vivo* ISF samples from the mice, ensure they were dosed with doxycycline at appropriate times and received enough to decrease their APP production by 90-95%, and harvest the brains for histological and immunohistochemistry testing.

This paper has been cited in 66 other publications, including publications in high-influence journals such as the Journal of Experimental Medicine (impact factor 10.790), and Current Biology (impact factor 9.251), and Neuron (impact factor 14.318).

Neurobiology of Disease

Genetic Modulation of Soluble Aβ Rescues Cognitive and Synaptic Impairment in a Mouse Model of Alzheimer's Disease

Stephanie W. Fowler,[1]* Angie C. A. Chiang,[1]* Ricky R. Savjani,[1,3] Megan E. Larson,[4] Mathew A. Sherman,[4] Dorothy R. Schuler,[5] John R. Cirrito,[5] Sylvain E. Lesné,[4] and Joanna L. Jankowsky[1,2]

[1]Departments of Neuroscience and [2]Neurology and Neurosurgery, Huffington Center on Aging, Baylor College of Medicine, Houston, Texas 77030, [3]Texas A&M Health Science Center, College Station, Texas 77843, [4]Department of Neuroscience, N. Bud Grossman Center for Memory Research and Care, and Institute for Translational Neuroscience, University of Minnesota, Minneapolis, Minnesota 55454, and [5]Department of Neurology, Washington University School of Medicine, St. Louis, Missouri 63110

An unresolved debate in Alzheimer's disease (AD) is whether amyloid plaques are pathogenic, causing overt physical disruption of neural circuits, or protective, sequestering soluble forms of amyloid-β (Aβ) that initiate synaptic damage and cognitive decline. Few animal models of AD have been capable of isolating the relative contribution made by soluble and insoluble forms of Aβ to the behavioral symptoms and biochemical consequences of the disease. Here we use a controllable transgenic mouse model expressing a mutant form of amyloid precursor protein (APP) to distinguish the impact of soluble Aβ from that of deposited amyloid on cognitive function and synaptic structure. Rapid inhibition of transgenic APP modulated the production of Aβ without affecting pre-existing amyloid deposits and restored cognitive performance to the level of healthy controls in Morris water maze, radial arm water maze, and fear conditioning. Selective reduction of Aβ with a γ-secretase inhibitor provided similar improvement, suggesting that transgene suppression restored cognition, at least in part by lowering Aβ. Cognitive improvement coincided with reduced levels of synaptotoxic Aβ oligomers, greater synaptic density surrounding amyloid plaques, and increased expression of presynaptic and postsynaptic markers. Together these findings indicate that transient Aβ species underlie much of the cognitive and synaptic deficits observed in this model and demonstrate that significant functional and structural recovery can be attained without removing deposited amyloid.

Key words: **amyloid; amyloid precursor protein; APP; oligomer; tetracycline transactivator; TTA**

Introduction

Amyloid-β (Aβ) peptides produced by the cleavage of the amyloid precursor protein (APP) are a major focus of drug development for Alzheimer's disease (AD). However, there is little consensus about what form of Aβ–monomer, small soluble assemblies, or aggregated deposits–should be targeted therapeutically. Initial testing in animal models suggested that cognitive protection could be achieved by lowering all forms of Aβ by preventative active immunization (Janus et al., 2000; Morgan et al., 2000), while subsequent studies using passive immunization or γ-secretase inhibitors (GSIs) suggested that decreasing soluble Aβ and oligomeric assemblies was sufficient to restore cognitive function (Dodart et al., 2002; Kotilinek et al., 2002; Comery et al., 2005; Lee et al., 2006). However, many of these studies either tested before amyloid formation (Martone et al., 2009; Fukumoto et al., 2010; Balducci et al., 2011; Mitani et al., 2012; Zago et al., 2012), or used chronic treatments that affected plaque burden (Wilcock et al., 2004, 2006; Hartman et al., 2005; Chang et al., 2011). To date, only a limited number of studies have sought to distinguish the contribution made by different pools of Aβ to cognitive impairments in mouse models of AD (Dodart et al., 2002; Comery et al., 2005; Lee et al., 2006; Melnikova et al., 2013; Mitani et al., 2013). However, most of these studies relied on a single behavioral measure to evaluate cognitive efficacy, and none examined recovery at the level of neuronal structure or function.

Both soluble and insoluble forms of Aβ can dramatically affect neuronal structure and function. Axons passing near amyloid plaques develop large distended swellings of ubiquitinated aggregates separated by domains that are abnormally thin and tortuous (Le et al., 2001; D'Amore et al., 2003; Stokin et al., 2005). In

Received Feb. 8, 2014; revised April 4, 2014; accepted April 29, 2014.

Author contributions: S.W.F., A.C.A.C., S.E.L., and J.L.J. designed research; S.W.F., A.C.A.C., M.E.L., M.A.S., D.R.S., J.R.C., and S.E.L. performed research; S.W.F., A.C.A.C., R.R.S., M.E.L., M.A.S., J.R.C., S.E.L., and J.L.J. analyzed data; S.W.F., A.C.A.C., S.E.L., and J.L.J. wrote the paper.

This work was funded by a National Institutes of Health Office of the Director New Innovator Award DP2 OD001734 and by a gift from the Robert A. and Rene E. Belfer Family Foundation (J.L.J.). A.C.A.C. was supported by National Institute of Aging Biology of Aging training grant T32 AG000183 and by a Gates Millennium Scholarship. S.E.L., M.A.S., and M.E.L. are supported by the National Institute of Health (R00-AG031293, R01-NS033249) and by startup funds from the University of Minnesota Medical Foundation. We thank Bryan Song and Yuanyuan Zhang for animal care, Rich Paylor for advice on behavioral testing, Phil Jones for chemical analysis of the commercial GSI synthesis, and Kim Tolias and Shalaka Mulherkar for advice and reagents to analyze cofilin changes.

*S.W.F. and A.C.A.C. contributed equally to this work.

The authors declare no competing financial interests.

Correspondence should be addressed to Joanna L. Jankowsky, Baylor College of Medicine, BCM295, One Baylor Plaza, Houston, TX 77030. E-mail: jankowsk@bcm.edu.

DOI:10.1523/JNEUROSCI.0572-14.2014

 0270-6474/14/347871-15$15.00/0

addition to these gross morphological changes in neighboring neurons, amyloid formation is associated with alterations in both local and long-distance neuronal signaling. Amyloid-bearing animals show diminished signal transmission between hemispheres with reduced response precision (Stern et al., 2004). Subsets of neurons in the vicinity of fibrillar deposits become hyperactive, while neighboring astrocytes develop spontaneous calcium waves uncoupled from local network activity (Busche et al., 2008; Kuchibhotla et al., 2008, 2009). The physical response to soluble oligomeric Aβ is considerably more subtle than the reaction to insoluble deposits, although no less consequential. Mounting evidence suggests that oligomeric Aβ in forms ranging from dimers and trimers to larger oligomers and protofibrils can be potently synaptotoxic (Wilcox et al., 2011; Larson and Lesne, 2012). *In vitro* application of naturally secreted oligomeric preparations causes rapid loss of dendritic spines and deficits in synaptic plasticity, while intracranial injection of similar preparations impairs learning and memory (Wilcox et al., 2011; Larson and Lesne, 2012). Together, these studies suggest a complex relationship between soluble and insoluble forms of Aβ, alterations in neuronal structure and function, and resulting cognitive decline.

We sought to dissect this relationship using a unique mouse model in which the expression of transgenic APP and consequent overproduction of Aβ could be arrested by treatment with doxycycline (dox). In past work, we have shown that suppressing transgenic APP expression after amyloid onset stops further plaque deposition while having little effect on pre-existing amyloid (Jankowsky et al., 2005; Wang et al., 2011). Here, we use this system to test the potential for synaptic and cognitive recovery following acute reduction of transgenic APP/Aβ in the continued presence of amyloid plaques. By modulating the levels of APP and soluble Aβ independently from amyloid load, we demonstrate significant functional and structural restoration, suggesting that substantial therapeutic benefit may be possible by reducing further production of Aβ without removing amyloid that has already formed.

Materials and Methods

Mice

The tet-responsive APP transgenic line 102 (tetO-APPswe/ind 102; MMRRC stock # 034845-JAX; Jankowsky et al., 2005) and the tet-activator line B CaMKIIα-tTA (Jackson Laboratories #3010; Mayford et al., 1996) were independently backcrossed to C57BL/6J for >25 generations before being intercrossed for these studies. The resulting double transgenic male offspring were then mated with wild-type FVB females to produce experimental cohorts on a FVBB6 F1 background.

Dox administration. All mice used in this study were raised on dox to suppress transgene expression during postnatal development. We have previously shown this strategy to ameliorate locomotor hyperactivity and normalize body weight of double transgenic animals, permitting reliable cognitive testing (Rodgers et al., 2012). Offspring were started on dox 1–3 d after birth by placing nursing mothers on medicated chow, formulated to 50 mg/kg dox (Purina Mills TestDiet #5APL). At weaning, mice were maintained on dox until 6 weeks of age (Purina Mills TestDiet #5SBA).

All mice were returned to regular chow for the following 6 months, allowing APP/tetracycline transactivator (TTA) animals to develop a moderate amyloid load. To test the potential cognitive benefit of short-term APP suppression, at 7.5 months half of the mice were treated with dox for 2 weeks before behavioral testing and were maintained on dox until harvest.

During the course of this study, we discovered that the lot of chow we had purchased for postnatal treatment provided submaximal transgene suppression (80% suppression rather than the 90–95% we expected at this dose), so therapeutic administration at 7.5 months was done by administering dox in the drinking water at a dose of 50 μg/ml supplemented with 5% sucrose to mask the bitter taste.

GSI administration. A separate cohort of age-matched mice that had also expressed transgenic APP for 6 months was treated with GSI to confirm that behavioral recovery attained by transgene suppression with dox was due to reduction of Aβ. LY411575 was administered either in drinking water at a concentration of 40 μg/ml (GSI stock dissolved at 100 mg/ml in DMSO/ethanol to yield a working solution containing 1% DMSO and 0.8% ethanol) or through the chow at a concentration of 25 mg/kg (BioServ Rodent Diet #156166), in both cases to deliver an estimated dose of 5 mg/kg/d. Behavioral analysis began 5 d after treatment started.

Behavioral assays

Behavioral testing began at 8 months of age and included open field, Morris water maze (MWM), radial arm water maze (RAWM), and contextual fear conditioning (CFC). Animals were handled for 3 d before the start of behavioral testing. Locomotor activity was assessed on day 1, followed by MWM training on days 2–10, and RAWM training on day 11. Mice were allowed a 2 d rest period before fear conditioning training on day 14, which was followed by a retention test 24 h later. All animal experiments were reviewed and approved by the Baylor College of Medicine Institutional Care and Use Committee.

Open-field assessment. Locomotor activity was assessed in white acrylic open-top boxes (46 × 46 × 38 cm) in a room lit by indirect white light. Activity was recorded for 30 min and analyzed using the ANY-maze Video Tracking System (Stoelting).

MWM. MWM testing was conducted in a circular tank measuring 58 cm high and 122 cm in diameter. The water level was 20 cm from the top of the tank and made opaque using nontoxic white paint. Water temperature was maintained between 21 and 23°C. The room was lit with indirect white light and trials were recorded and tracked using ANY-maze Video Tracking System.

Before the start of acquisition training, mice received 1 d of training in a straight swim channel to acclimate them to the water and check for motor deficits. Mice received eight trials with a 15 min intertrial interval (ITI) in a channel constructed of white acrylic and measuring 107 × 56 ×14 cm, which was placed in the center of pool. Visible cues were removed from the room during straight swim shaping trials. Mice were allowed 60 s to reach a submerged platform on the opposite side of the channel. Mice that failed to reach the platform were guided to the location by the experimenter. Mice were allowed to stay on the platform for 15 s before being removed from the water, dried, and returned to their home cage under an infrared lamp between trials.

Acquisition training in the MWM consisted of four trials per day with a 15 min ITI. Each training session ended with a short-term memory probe. A square platform (10 × 10 cm) covered in nylon mesh for traction was located 1 cm below the surface in the NE quadrant of the maze, half way between the side and the center of the pool. Mice were placed in the maze facing the wall at each of four cardinal start locations and allowed 60 s to locate the hidden platform. As with straight swim, animals that failed to locate the platform in the allotted time were gently guided there by the experimenter. Mice were allowed to stay on the platform for 15 s before being returned to their home cage between trials. Following the 4 training trials, the platform was removed from the maze for an immediate probe trial. Animals were placed in the tank half way between the cardinal points (SW, NW, SE, and NE) and allowed 45 s to navigate the maze. Proximity to target, percentage time, and percentage path spent in each quadrant were calculated along with the number of times the animal crossed the platform location compared with the other three potential platform locations (in the SW, NW, and SE quadrants). Mice were trained to a performance criterion during probe trials of ≥35% path in the correct quadrant and at least 40% of total platform crossings over the correct site compared with other possible platform locations.

When mice reached criterion, they were retired from further MWM training, but given a final long-term memory probe 24 h after reaching criterion. Mice were trained for a maximum of 7 d. After all mice either reached criterion or completed 7 d of training, each was given one additional "refresher" day of training (four trials) with probe test to ensure

equivalent performance between groups before starting RAWM training. During this refresher training, performance in our cohorts was identical both between genotypes ($F_{(2,52)} = 0.34$, $p > 0.05$) and treatment groups ($F_{(1,52)} = 0.74$, $p > 0.05$). Thus, this procedure ensured that all mice were trained to a similar performance level before moving onto RAWM testing in the same room.

RAWM. The day following MWM refresher training, mice received 1 d of RAWM training consisting of eight trials with a 15 min ITI. The RAWM was created by installing clear Plexiglas triangular inserts into the existing water maze pool (41.25 cm on each side × 50 cm high), which resulted in six open arms joined at the center. Each arm measured 20 cm wide × 34 cm long, and the water was maintained at a depth of 38 cm. The platform was located 3 cm from the end of one arm and submerged 1 cm below the water's surface. Mice were placed into a different arm at the beginning of each trial, with the order of starting positions pseudorandomly selected before training such that no trial began in an arm adjacent to the previous start position. Mice were allowed 60 s to navigate the maze. If a mouse failed to locate the platform in the allotted time, it was gently guided to there by the experimenter and allowed to remain on the platform for 15 s before being returned to its home cage between trials. Latency to locate the platform, swim path length, and number of working memory errors (re-entries into a previously visited arm) were calculated for each trial. Trial 1 scores were excluded from analysis due to the inflated error rate as animals learned the new procedure. Data from trials 2–8 was averaged to provide a performance index for overall RAWM learning. After the final training trial, animals were tested with a short-term probe trial in which the platform was removed and animals were allowed 45 s to navigate the maze. Percentage time and path spent in the target arm were calculated and compared among treatment groups.

CFC. Two days after RAWM testing, mice were trained in CFC using a near-infrared video fear conditioning system (Med Associates). Conditioning boxes (30.5 × 24 × 21 cm) with a stainless steel grid floor were located inside sound-attenuating chambers and indirectly lit from above. Movement was recorded by a video camera mounted inside the sound-attenuating chamber and analyzed using Video Freeze software (Med Associates). Motion threshold was set to 19 arbitrary units (a.u.) and the minimum freeze duration to 1 s. Chambers and grid floors were cleaned with a 20% ethanol solution after each trial.

During conditioning, mice were allowed to freely explore the chambers for 2 min before receiving a 1 s 0.8 mA footshock. After a 2 min interval, mice received a second 1 s 0.8 mA footshock. Mice remained in the chamber for 1 min after second footshock before being returned to their home cage. Twenty-four hours later, animals were returned to the same conditioning box for a 5 min retention test. The duration of immobility was recorded and used as an index of learning.

Tissue harvest

One week after behavioral testing was completed, mice were killed by sodium pentobarbital overdose and transcardially perfused with ice-cold PBS containing 10 μg/ml heparin. Brains were removed and hemisected along the midline. One hemisphere was dissected to isolate the cortex and hippocampus, which were snap frozen for biochemistry, and the other hemisphere was immersion fixed in 4% PFA at 4°C for 48 h. Brains were cryoprotected in 30% sucrose at 4°C. Tissue was sectioned at 35 μm in the sagittal plane using a freezing sliding microtome, then stored in cryoprotectant (0.1 M phosphate buffer, pH 7.4, 30% ethylene glycol, and 25% glycerol) at −20°C until use.

Histology

Campbell–Switzer silver stain. A detailed protocol for this stain can be found at the NeuroScience Associates website (http://www.neurosciencesassociates.com/Documents/Publications/campbell-switzer_protocol.htm).

Thioflavine-S histology. A 1/12 series of sections spaced at 420 μm intervals were stained for thioflavine. Sagittal 35 μm sections were rinsed, mounted onto SuperFrost Plus slides, and dried overnight. Sections were rehydrated in running tap water, incubated for 10–15 min in 0.25% potassium permanganate, followed by 5 min in 1% potassium metabisulfite/1% oxalic acid, before staining in 0.02% thioflavine-S (Sigma #T1892) for 8 min. Staining was differentiated in 80% ethanol, followed by running tap water. Sections were dehydrated through xylene and coverslipped with Permount.

Synaptophysin immunofluorescence and thioflavine-S histology. A 1/24 series of sections spaced at 840 μm intervals were immunostained for synaptophysin and counterstained for thioflavine. Sagittal 35 μm sections were rinsed, blocked in TBS plus 0.3% Triton X-100 (TBST) and 5% normal goat serum for 1 h at room temperature, and stained with rabbit anti-synaptophysin antibody (#AB9272; Millipore) diluted 1:1000 in blocking solution overnight at 4°C. Sections were then washed with TBS and incubated with Alexa 568-conjugated secondary antibody (goat anti-rabbit IgG #A11011; Invitrogen) diluted 1:500 in block at room temperature for 1 h. Sections were washed with TBS before being counterstained with 0.002% thioflavine-S (#T1892; Sigma) diluted in TBS at room temperature for 8 min. After two 1 min washes in 50% ethanol followed by several washes in TBS, sections were mounted on SuperFrost Plus slides and coverslipped with Vectashield mounting medium (Vector Laboratories).

Aβ immunohistochemistry. A 1/12 series of sections spaced at 420 μm intervals were rinsed with TBS, pretreated with 88% formic acid for 1 min at room temperature, and blocked with TBST containing 5% normal goat serum before overnight incubation at 4°C with rabbit anti-human Aβ antibody (#71-5800; Zymed/Invitrogen) diluted 1:500 in blocking solution. After several washes in TBS, sections were incubated with biotin-conjugated goat anti-rabbit secondary (Vectastain Elite ABC Kit, Rabbit IgG; Vector Laboratories) diluted 1:500 in blocking solution for 1 h at room temperature followed by HRP-avidin conjugate diluted 1:50 in TBS for 30 min at room temperature. Sections were developed with DAB (#D4418; Sigma), then mounted, dehydrated, and coverslipped with Permount.

Quantification of amyloid burden. Amyloid burden was quantified using a custom macro written for Zeiss AxioVision 4.8 software as described previously (Wang et al., 2011). Color thresholds were used to identify amyloid plaques in high-resolution digital scans of Aβ immunostained and thioflavine-S stained sections using a custom macro written with Zeiss AxioVision software. Background staining and shading artifacts were manually excluded from the analyses. The region of interest was specified by outlining the cortex or hippocampus and the area above threshold computed relative to total area. Three (Aβ immunostain) or six sections (thioflavine-S) spaced at 420 μm intervals were measured for each animal.

Quantification of synaptophysin. The area of synaptophysin immunostaining surrounding thioflavine-S-positive fibrillar plaques was measured using a custom script written in MATLAB (R2012b) to batch process two-channel fluorescence images in an unbiased and automated way. Two tissue sections spanning the frontal cortex were selected for analysis from each animal. Two nonoverlapping fields of view each centered on an isolated plaque of 43.56 μm average diameter were photographed for each section. A single optical plane of 0.98 μm in depth was collected from each field in the red (synaptophysin) and green (thioflavine) channels using an ApoTome structured illumination device (Carl Zeiss). At 40× magnification each field spanned an area of 222.2 × 166.4 μm.

The first step in the automated script removed the area occupied by the thioflavine-positive plaque from the region of interest that would be used be used to measure synaptophysin. To accomplish this in an unbiased fashion, we binarized the grayscale thioflavine images using Otsu's method. The Otsu method works by calculating the threshold at which to divide the dataset into signal and background so that the variance in each of the resulting subsets is minimized. In this case, the method uses variance minimization to define the cutoff between thioflavine-positive pixels and thioflavine-negative pixels. Pixels above background defined the area of the plaque and were used as a mask to remove this region from the corresponding synaptophysin image. The masked synaptophysin images were then also binarized, again applying Otsu's method for determining the optimal threshold between signal and background. The script then calculated the area occupied by synaptophysin-positive pixels in each image, normalizing to the total area remaining after the region of thioflavine staining was removed. We have posted the script on MATLAB's

File Exchange (http://www.mathworks.com/matlabcentral/fileexchange/39591).

Immunoblotting

APP, synapsin, and PSD95. Frozen cortical samples were prepared for Western blotting by sonication in 2% SDS plus 1× protease inhibitor cocktail (Sigma P8340) and then diluted 1:1 with 2× SDS-free RIPA buffer (2× PBS, 1% deoxycholate, 1% NP40, and 5 mM EDTA). For APP, ~50 μg of the resulting homogenate was separated on a 10.5–14% Tris-HCl gel (Bio-Rad Criterion) and transferred to nitrocellulose. For synapsin and PSD95, 25 μg of cortical homogenate was separated on a 4–15% Tris-HCl gel and transferred to nitrocellulose. Membranes were blocked in PBS plus 0.1% Tween 20 and 5% nonfat dry milk for 1 h at room temperature. APP/Aβ antibody 6E10 and PSD95 was used to probe the upper part of the blot; GAPDH was used to probe the lower part as a loading control. HRP-labeled secondary antibodies [goat anti-mouse IgG diluted 1:5000 (#115-035-003; Jackson ImmunoResearch) and goat anti-chicken IgG diluted 1:10,000 (#14-24-06; Kirkegaard & Perry Laboratories)] were used to detect binding, and developed with Immobilon ECL Reagent (#WBKLS0100; Millipore). Chemiluminescence was measured with a Fuji miniLAS-4000 system and quantified using MultiGauge software. After imaging, the blot was stripped by incubation for 30 min at 50°C in 50 mM Tris-HCl, 2% SDS, and 0.7% β-mercaptoethanol and the upper portion reprobed for synapsin as above.

ADF/cofilin and PAK1. Frozen cortical samples were prepared for Western blotting by cellular fractionation described below. Approximately 50 μg of the intracellular fraction was separated on a 4–15% Tris-HCl gel and transferred to nitrocellulose. Phosphorylated cofilin and PAK1 was probed first using rabbit anti-phospho-cofilin (1:500; #3311; Cell Signaling Technology) or rabbit anti-phospho-PAK1 (1:1000; #2601; Cell Signaling Technology) in conjunction with chicken anti-GAPDH (1:10,000; #AB3202; Millipore) as a loading control. After chemiluminescence was measured, blots were stripped as described above and reprobed for total levels of protein using rabbit anti-cofilin diluted 1:1000 (#5175; Cell Signaling Technology) or rabbit anti-PAK1 (1:1000; #2602; Cell Signaling Technology).

Oligomeric Aβ. Frozen cortical samples were fractionated by a four-step extraction method. Extraction began by mechanical homogenization in 250 μl of 50 mM Tris-HCl, pH 7.6, 0.01% NP-40, 150 mM NaCl, 2 mM EDTA, 0.1% SDS, and 1× PPP [1 mM phenylmethylsulfonyl fluoride, 2 mM 1,10-phenanthroline monohydrate, and 1× protease inhibitor cocktail] using five passes through a 1 ml syringe with a 20 gauge needle. Soluble, extracellular-enriched proteins were collected from the supernatant of this extract following 10 min at 800 × *g*, 4°C. The remaining pellet was then mechanically dissociated by trituration with an Eppendorf micropipette in 250 μl of 50 mM Tris-HCl, pH 7.4, 150 mM NaCl, 0.1% Triton X-100, and 1× PPP. Cytoplasmic proteins were collected from the supernatant of this extract following 90 min at 16,100 × *g*, 4°C. The remaining pellet was then triturated with a micropipette followed by passive lysis on a rotating platform for 15 min at 4°C in 250 μl of 50 mM Tris-HCl, pH 7.4, 150 mM NaCl, 0.5% Triton X-100, 1 mM EGTA, 3% SDS, 1% deoxycholate, and 1× PPP. Membrane-enriched proteins were collected from the supernatant of this extract following 90 min at 16,100 × *g*, 4°C. The membrane-enriched fraction was clarified by 60 min at 100,000 × *g*. Each fraction was depleted of endogenous immunoglobulins by sequential incubation for 1 h at 4°C with 50 μl of protein A-Sepharose, Fast Flow followed by 50 μl of protein G-Sepharose, Fast Flow (GE Healthcare Life Sciences). All supernatants were clarified by 90 min at 16,100 × *g* before Western blot analysis.

One hundred micrograms of protein per sample was electrophoresed on 10–20% SDS-polyacrylamide Tris-tricine gels (Bio-Rad). Proteins were transferred to nitrocellulose and membranes boiled in PBS for 5 min. Membranes were blocked in TBSTw containing 5% bovine serum albumin (#A3803; Sigma, >98% grade) for 2 h at room temperature, and probed with either 6E10 (#SIG-39320; Covance) or biotinylated-6E10 (#SIG-39340; Covance) diluted 1:2500 in blocking solution. A duplicate set of gels loaded with 50 μg or 20 μg protein was blotted and probed for α-synuclein (extracellular fraction; Covance #SIG-39720 diluted 1:5,000) or actin (membrane fraction; Sigma #A2066 diluted 1:10,000) as internal controls to demonstrate equal protein concentrations across samples. Primary antibodies were detected using anti-IgG conjugated with either biotin or infrared dyes (LI-COR Biosciences). When biotin-conjugated antibodies were used, DyLight800-conjugated NeutrAvidin (#22853; Thermo Scientific) was added to amplify the signal. Blots were imaged with an Odyssey detection system (LI-COR Biosciences). Densitometry analyses were performed using OptiQuant software (Packard Bioscience) or Image Studio software (LI-COR Biosciences).

Dot blotting

Two micrograms of extracellular-enriched or membrane-associated protein lysates were mixed with sterile filtered deionized water in a total volume of 2.5 μl. Each sample was then adsorbed onto a nitrocellulose membrane until dry. Following a brief activation in 10% methanol/TBS, the membrane was boiled in PBS to enhance antigen detection as previously described (Sherman and Lesné, 2011). Membranes were blocked in TBS containing 5% bovine serum albumin for 60 min, then moved to primary antibody 6E10 (1:2500) and A11 (1:2000; a kind gift from Rakez Kayed, University of Texas Medical Branch, Galveston, TX) for overnight incubation at 4°C. Following several washes, anti-mouse IgG-IR800 (1:100,000) and anti-rabbit IgG-IR680 (1:150,000) secondary antibodies were used for detection with a Li-Cor Odyssey imager. All steps were performed without detergent to enhance A11 binding of oligomeric species as previously reported (Lesné et al., 2006).

Immunoprecipitation

Two hundred micrograms of protein extract was diluted to 1 ml with dilution buffer (50 mM Tris-HCl, pH 7.4, and 150 mM NaCl) and incubated with 5 μg of 6E10 overnight at 4°C. The following day, 50 μl of Protein G-Sepharose, Fast Flow (GE Life Sciences) was added [mixed 1:1 (v:v) with immunoprecipitation (IP) buffers A and B; Sherman and Lesné, 2011] and incubated at 4°C for 2 h. The beads were washed twice in 1 ml of dilution buffer and proteins were eluted by boiling in 30 μl of SDS-PAGE loading buffer.

In vivo *microdialysis.* Mice were unilaterally implanted with a 38 kDa molecular weight cutoff microdialysis probe (2 mm BR-style; Bioanalytical Systems) by placing the probe tip into the hippocampus at a 12 degree angle −3.1 mm from bregma, −2.5 mm from midline, and 3.2 mm below the dura (Cirrito et al., 2003, 2011). Microdialysis perfusion buffer consisted of 4% albumin in artificial CSF at a flow rate of 1.0 μl/min. Animals were allowed to recover for 6–8 h after probe insertion, then six interstitial fluid (ISF) Aβ measurements were taken over a 6 h period. The mean concentration of exchangeable Aβ during this 6 h period was defined as the baseline ISF Aβ concentration for each mouse. After baseline Aβ levels were established, mice were treated with dox at a concentration of 50 μg/ml in their drinking water for 4 d. During this time, microdialysis samples were continuously collected every 1–3 h into a refrigerated fraction collector. Following the final collection, samples were assayed for Aβx-40 and Aβx-42 by sandwich ELISA using an Aβ40 (mHJ2) or Aβ42-specific antibody (mHJ7.4) to capture the peptide followed by a biotinylated central domain anti-Aβ antibody (mHJ5.1) for detection (Cirrito et al., 2011). The concentration of ISF Aβ in each sample was normalized to the baseline Aβ concentration for each mouse. At the end of the experiment, the brains were harvested and processed for histological verification of probe placement.

Statistical analysis

Data were analyzed using one-way or two-way ANOVA or *t* test where appropriate. All *post hoc* comparisons were conducted using Bonferroni correction. Statistical tests for behavioral experiments were conducted using SPSS Statistics 20 (IBM). Statistical tests for biochemical and histological experiments were conducted using Prism 6.0 (GraphPad). Graphs were created using Prism 6.0 and display group means ± SEM.

Results

Dox rapidly suppresses transgenic APP expression, decreases exchangeable Aβ levels, and stabilizes amyloid load

We studied a temporally controlled transgenic mouse model in which the TTA activates expression of human $APP_{swe/ind}$ within

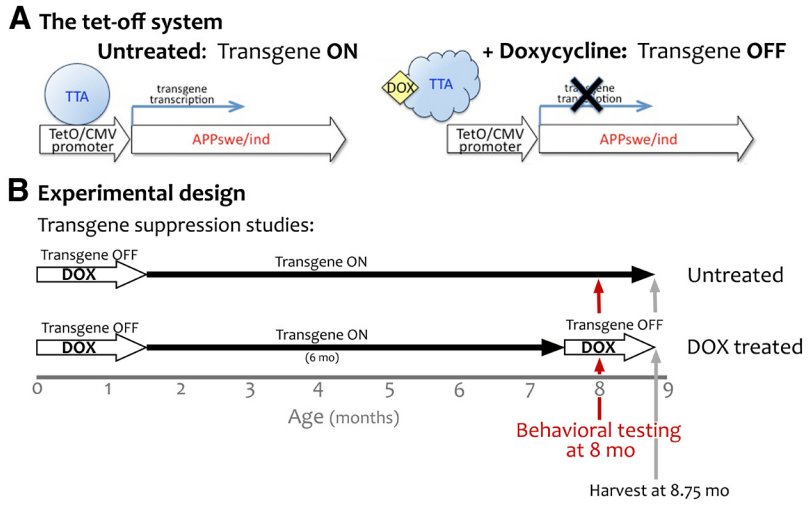

Figure 1. Using the tet-off system to initiate APP/Aβ overexpression in the adult and therapeutically suppress it after amyloid onset. ***A***, Under normal conditions, TTA binds to its recognition sequence in the hybrid tetO/CMV promoter to activate transcription of the downstream transgene (APPswe/ind). Upon binding dox, TTA undergoes a conformational switch that prevents DNA binding and stops further transcription of transgenic mRNA. ***B***, The tet-off APP model uses the CaMKIIα promoter to control the expression of TTA, thereby limiting transgenic APP to the forebrain. Under normal conditions, expression from this promoter begins during late embryogenesis and transgenic APP is present at high levels by birth. In the current experiments, dox was used to delay transgene expression until adulthood (P41–P43). Transgenic APP expression was initiated at 6 weeks of age by removing dox from the diet, and remained active for the next 6 months. Therapeutic intervention to suppress further transgene expression with dox or prevent Aβ release with GSI began at 7.5 months of age. One cohort of dox-treated mice was harvested after just 2 weeks of treatment to establish the amyloid load present at the outset of behavioral testing. Behavioral testing in the remaining dox-treated animals continued for another 3 weeks; afterward all mice were harvested for histology and biochemical analysis.

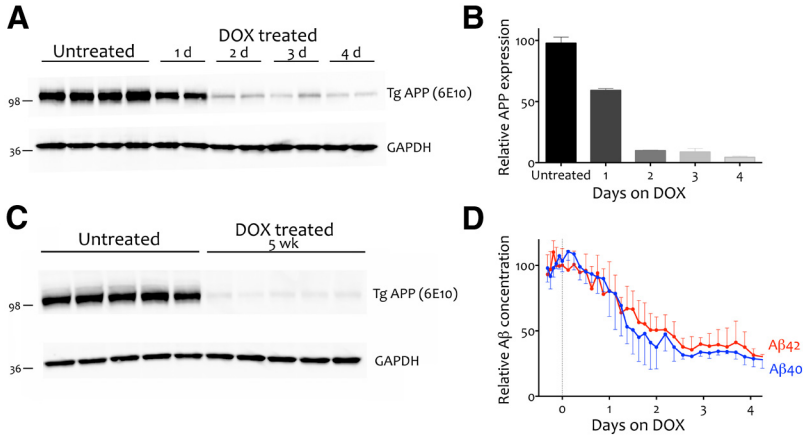

Figure 2. Dox treatment induces rapid, persistent suppression of transgenic APP and a concomitant decrease in ISF Aβ concentration. ***A***, Western blot showing APP suppression in APP/TTA mice following 1–4 d of dox treatment. Anti-Aβ antibody 6E10 was used to detect transgenic APP in cortical homogenates. GAPDH was probed as an internal control. ***B***, Quantification of the immunoblot shown in ***A*** reveals that transgenic APP levels are reduced by 40% within 1 d of dox treatment and by 90% within 2 d. ***C***, Immunoblot analysis of transgenic APP in cortical homogenates from behaviorally tested mice demonstrates that transgene suppression was maintained at >90% throughout cognitive testing ($n = 5$ per condition). ***D***, Microdialysis of hippocampal ISF reveals that following a 1 d delay, Aβ concentration dropped at approximately the same rate and to a similar extent as transgenic APP. The concentration of both Aβ40 (blue; $n = 5$) and Aβ42 (red; $n = 4$) were decreased by >50% within 2 d of dox treatment and 70% by 3 d.

forebrain neurons. In this system, TTA acts as an artificial transcription factor specific for the tetO promoter controlling transgenic APP. On administration of dox, TTA undergoes a conformational change that prevents it from binding DNA and thereby arrests further expression of transgenic APP (Fig. 1*A*). We took advantage of this system to test whether acutely reducing production of transgenic APP and Aβ is sufficient to rescue cognitive impairments after the onset of amyloid deposition. Because we have previously shown that APP overexpression during postnatal development causes severe locomotor hyperactivity (Rodgers et al., 2012), here we used mice in which transgene expression was delayed until adulthood (Fig. 1*B*). Transgene expression was initiated at 6 weeks of age and continued for an additional 6 months to produce moderate amyloid deposition in APP/TTA double transgenic mice by the age of behavioral testing. In past work we have shown that amyloid formed during this period of APP overexpression persists for >18 months after transgene suppression (Jankowsky et al., 2005; Wang et al., 2011; J.L. Jankowsky, unpublished data).Together, this model provides a way to controllably arrest further production of transgenic APP and soluble Aβ without affecting pre-existing amyloid.

We first examined the rate and efficiency of transgenic APP suppression in the tet-off model using mice of approximately the same age as our behaviorally tested animals, but which were killed within 1–4 d of starting dox treatment. Western blotting of transgenic APP levels across days revealed that APP expression was reduced by 40% within 24 h of dox treatment and reached 90% suppression at 48 h (Fig. 2*A*,*B*). We confirmed that APP suppression could be chronically maintained at this level by measuring transgenic APP expression in behaviorally tested animals treated for 5 weeks on dox, as shown by comparing APP expression in mice that were harvested after 5 weeks of differential treatment (Fig. 2*C*). These mice showed the same degree of suppression as animals harvested after 2 d on dox, with transgenic APP levels < 10% that of untreated mice ($t = 102.1$, df = 8, $p < 0.001$). These results indicate that APP suppression had stabilized at >90% before behavioral testing and remained at this level throughout our experiments.

We then used *in vivo* microdialysis to ascertain that soluble Aβ levels in hippocampal ISF were reduced by dox treatment along with transgenic APP (Fig. 2*D*; Cirrito et al., 2003). Before dox treatment, Aβ40 levels averaged 742 ± 106 pg/ml ($n = 5$) and Aβ42 140 ± 24 pg/ml ($n = 4$). The concentration of both peptides quickly declined with dox treatment. Exchangeable ISF Aβ40 and Aβ42 levels dropped by >50% within 48 h of dox treatment (*post hoc* test, $p < 0.001$), and reached nearly 70% suppression compared with baseline ISF Aβ levels by 72 h (*post hoc* test, $p < 0.0001$). The difference between the extent of APP reduction and that of Aβ is likely due to the continued release of peptide from nearby plaques even after further production is suppressed. Recent work suggests that the concentration of ISF Aβ is deter-

mined by a combination of existing peptide in exchange with insoluble aggregates and *de novo* synthesis (Hong et al., 2011; Takeda et al., 2013). Consistent with this explanation, when the reduction of Aβ was tested in young, predeposit animals from a line similar to the one studied here, both transgenic APP and PBS-soluble Aβ42 dropped by >95% after transgene suppression (Jankowsky et al., 2005). Thus, dox treatment may be equally effective at reducing new Aβ synthesis as transgenic APP, but the impact on ISF Aβ is likely offset by peptide shedding from pre-existing aggregates. In this regard, the outcome of transgene suppression is precisely what has been demonstrated in noncontrollable models using pharmacologic secretase inhibitors (Hong et al., 2011).

Although transgenic APP and ISF Aβ levels quickly declined with dox treatment, our past work with this system has shown that suppressing APP expression halts amyloid growth without plaque clearance (Jankowsky et al., 2005; Wang et al., 2011). Given this, we predicted that dox-treated animals would approximately maintain the same amyloid burden as age-matched untreated controls, at least for short periods of time. We confirmed that the area of total amyloid detected by silver staining or Aβ immunohistochemistry (fibrillar + diffuse; Fig. 3*A*,*B*), and specifically that of fibrillar amyloid detected by thioflavine-S staining (Fig. 3*C*), was identical in dox-treated and untreated mice following 2 weeks of differential treatment ($p > 0.05$ for both cortex and hippocampus; Fig. 3*D*). We then designed our behavioral experiments based on this time frame so that the two groups began testing with identical plaque burden. Over the next 3 weeks of differential treatment, fibrillar amyloid remained unchanged in both cortex and hippocampus and was indistinguishable between treatment groups at the end of behavioral testing (two-way ANOVA, main effect of treatment, $F_{(1,26)} = 0.653$, main effect of time, $F_{(1,26)} = 0.004$, both $p > 0.05$). Total amyloid load detected by Aβ immunostaining increased more noticeably between 2 and 5 weeks of differential treatment due to accumulation of diffuse deposits in untreated mice. We have previously shown that amyloid deposition in tet-off APP mice occurs rapidly at this stage of pathology, and the significant rise observed here over just a few weeks is not unexpected (Rodgers et al., 2012). At the conclusion of behavioral testing, the area of Aβ immunostaining was significantly higher in untreated mice than in dox-treated mice for both cortex and hippocampus (two-way ANOVA, treatment × time interaction, $F_{(1,26)} = 18.49$, $p < 0.05$, Bonferroni *post hoc* test, $p < 0.001$ for cortex at 5 weeks and $F_{(1,26)} = 8.44$, $p < 0.05$, Bonferroni *post hoc* test, $p < 0.01$ for hippocampus at 5 weeks). Thus, our findings suggest that the two groups began behavioral testing with identical amounts of fibrillar and total amyloid. Growth of diffuse plaques in untreated animals lead to an increase in total amyloid during this time, while fibrillar amyloid remained stable throughout behavioral testing in both dox-treated and untreated animals such that they ended the experiments with the same amount as they started.

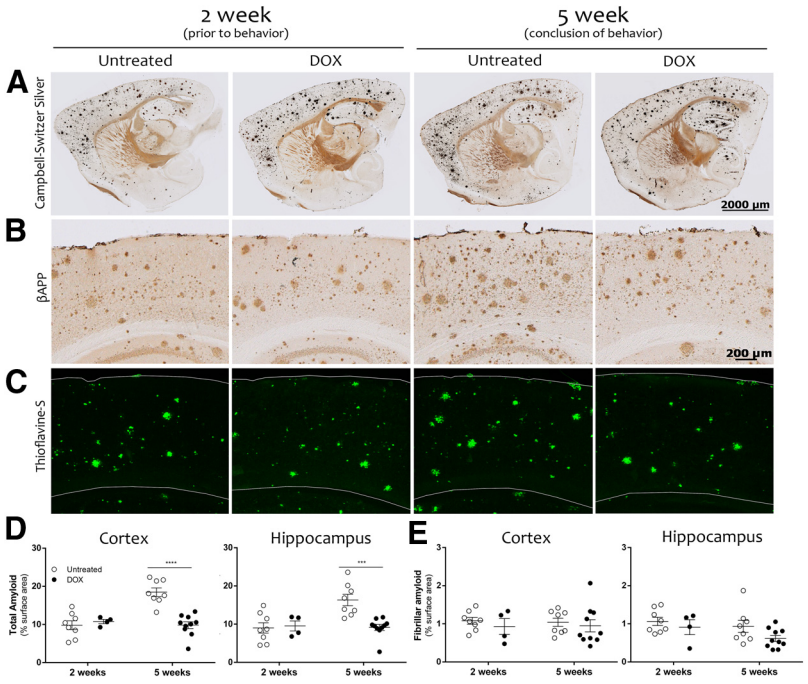

Figure 3. Amyloid load is identical between treatment groups at the start of behavioral testing and remains stable with dox treatment. Silver staining (***A***), anti-Aβ immunohistochemistry (***B***), and thioflavine-S staining (***C***) were used to assess amyloid burden of the cortex and hippocampus of APP/TTA transgenic mice harvested before or after behavioral testing, following 2 weeks (2 week, left; $n = 8$ untreated, $n = 4$ dox) or 5 weeks of differential treatment, respectively (5 week, right; $n = 8$ untreated, $n = 10$ dox). ***D***, Aβ immunostaining was used to measure total amyloid burden as a percentage of surface area in the cortex and hippocampus. In both regions, amyloid load remained steady during behavioral testing in dox-treated mice, but increased in untreated animals. The two treatment groups had similar amyloid loads at the start of testing, but were significantly different by the end (***$p < 0.001$). ***E***, Thioflavine-S staining was used to measure fibrillar amyloid in the cortex and hippocampus. The area of thioflavine-S staining was identical between groups before behavioral testing, and remained unchanged over the 3 weeks of behavioral testing.

Acquisition of spatial reference memory is restored by short-term suppression of transgenic APP

Our initial experiments demonstrated that 2 weeks of dox treatment allowed us to selectively lower ISF Aβ levels while leaving deposited amyloid unchanged. We took advantage of this situation to test whether acute reduction of soluble Aβ was sufficient to normalize behavioral impairments in plaque-bearing animals.

Behavioral analysis began with an assessment of open-field activity to ensure that the APP/TTA mice did not display the locomotor hyperactivity described previously with this line (Rodgers et al., 2012). Open-field activity revealed no difference in total distance traveled ($F_{(5,51)} = 1.025$, $p = 0.413$) or in locomotor speed between genotypes or treatment groups ($F_{(5,51)} = 0.66$, $p = 0.66$), indicating that the APP/TTA mice used for this study were not hyperactive compared with their TTA and nontransgenic (NTG) siblings.

Having established that hyperlocomotion would not confound our behavior testing, we proceeded with a battery of cognitive tests designed to examine acquisition and recall of reference, working, and associative memory through a modified MWM, six-arm RAWM, and CFC, respectively. We modified the standard MWM to both improve our sensitivity for subtle performance differences, and to ensure that we could use the same room for subsequent RAWM training. We used a train-to-criteria version of the MWM, in which short-term memory probes at the end of each day of training were used to assess

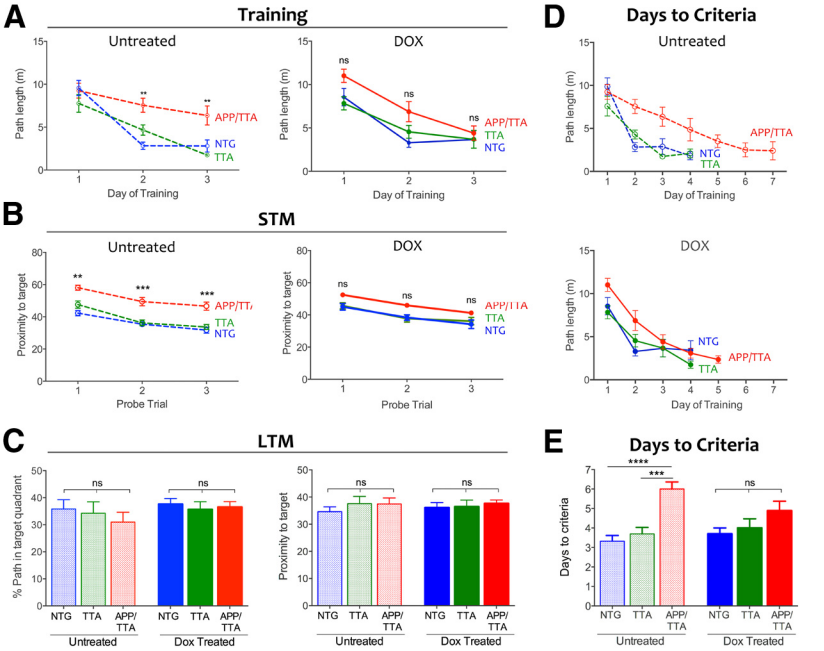

Figure 4. Acute suppression of APP/Aβ results in partial recovery of spatial reference memory. ***A***, Average path length required to reach the hidden platform on the first 3 d of MWM testing. Untreated APP/TTA mice ($n = 10$) perform significantly worse than NTG ($n = 9$; $^{**}p < 0.01$) and TTA controls ($n = 10$; $^{**}p < 0.01$) on days 2 and 3 of training (left). Transgene suppression with dox restored the performance of APP/TTA mice ($n = 9$) to that of NTG ($n = 10$) and TTA controls ($n = 9$; right). ***B***, Short-term memory (STM) probe trials were used to assess immediate recall at the end of each day. STM of untreated APP/TTA mice was worse than controls on the first 3 d of training ($p < 0.01$ for day 1 and $p < 0.001$ for days 2 and 3, left). Acute transgene suppression with dox improved immediate recall in APP/TTA mice to that of controls (right). ***C***, Twenty-four hours after mice reached criteria performance, they were administered one final probe trial to assess long-term memory (LTM). Once all mice reached criterion performance, their long-term recall was identical across groups. Left, Shows percentage path in the trained quadrant; right shows proximity to target. ***D***, Average path length required to reach the hidden platform reflects the number of training days required to reach criteria performance for untreated (top) and dox-treated mice (bottom). ***E***, Untreated APP/TTA mice require more days to reach criterion than NTG ($p < 0.0001$) and TTA controls ($p < 0.001$). Following transgene suppression, all groups reached criteria performance in the same number of days.

spatial learning and decide if mice would proceed to a long-term probe trial or to additional training the following day. As illustrated below, this approach brought all of the mice to the same level of performance before they began RAWM testing. This allowed us to examine long-term memory independent from the rate of acquisition, and yielded days-to-criteria as an added measure of spatial learning.

Untreated APP/TTA mice demonstrated a clear impairment in acquisition of the MWM, swimming farther to locate the hidden platform during days 2 and 3 of training than either NTG or TTA controls ($F_{(2,102)} = 9.98$, $p < 0.001$; *post hoc*, $p < 0.001$ for NTG and $p < 0.01$ for TTA; all F values are from two-way RM-ANOVA including dox-treated groups discussed below; Fig. 4*A*, left). Short-term memory, examined by probe trials at the end of each training day, was also impaired in the untreated APP/TTA mice (Fig. 4*B*, left). APP/TTA mice swam significantly farther from the target zone during probe trials than either control group ($F_{(2,51)} = 39.86$, $p < 0.001$). Analysis of short-term memory by the more common measure of percentage path in the trained quadrant was consistent with proximity: performance of all genotypes improved with training ($F_{(2,102)} = 20.70$, $p < 0.001$) but APP/TTA mice learned more slowly than NTG and TTA controls ($F_{(2,51)} = 13.67$, $p < 0.001$), and by day 3 spent a significantly smaller fraction of their swim path in the correct quadrant than controls (NTG: $p < 0.001$; TTA: $p < 0.01$). Several of the control mice reached criteria performance on day 3 and were removed from further training, therefore comparisons of path length and proximity were limited to days 1–3 when all animals could be evaluated. None of the APP/TTA mice (or 11 of 20 controls) had reached criteria performance by this time, and so continued training and testing until they did (Fig. 4*D*, top). APP/TTA mice required significantly more days of training to reach criteria performance than either TTA or NTG littermates ($F_{(2,51)} = 16.17$, $p < 0.001$, both $p < 0.001$; Fig. 4*E*). As each mouse reached criteria levels, they received one final probe trial 24 h later to assess long-term memory and then were retired from further training until all of the mice completed training (Fig. 4*C*). Although APP/TTA mice required more days to reach criteria, once they acquired the task their long-term memory for the platform location was as precise as their NTG and TTA siblings ($F_{(2,51)} = 1.25$, $p > 0.05$).

Alongside these untreated mice, we examined a replicate cohort of APP/TTA, TTA, and NTG mice that received dox in their drinking water for 2 weeks before testing. During training, the average path length of dox-treated APP/TTA mice was no different from TTA or NTG controls ($p > 0.05$), indicating that transgene suppression restored the performance of APP/TTA mice to that of controls (Fig. 4*A*, right). Additionally, proximity to the trained target during probe trials was similar among genotypes, indicating that dox treatment reversed short-term memory impairment in the APP/TTA mice ($p > 0.05$; Fig. 4*B*, right). Dox-treated APP/TTA mice took the same number of days to reach criteria performance as TTA and NTG controls (both $p > 0.05$; Fig. 4*D*, bottom; *E*). Although transgene suppression brought the performance of APP/TTA mice to the level of similarly treated controls, the effect was not sufficient to distinguish them from untreated APP/TTA mice ($p > 0.05$). Behavioral rescue in this task was thus substantial, but not complete. A final analysis of long-term memory confirmed that all groups recalled the platform location equally well, and were identical to untreated animals (Fig. 4*C*). These findings indicate that transgene suppression partially reversed impairments in spatial reference learning and short-term memory apparent in untreated APP/TTA mice of the same age.

Suppression of transgenic APP rescues working memory deficits in RAWM and associative memory impairment in CFC

Animals next began RAWM training, consisting of eight trials over a single training day. This task allowed us to test working memory errors, which were scored as repeated visits to an incorrect arm. Untreated APP/TTA mice made significantly more errors during RAWM training than either NTG or TTA controls ($F_{(2,52)} = 5.15$, $p < 0.05$, *post hoc*, $p < 0.01$ and $p < 0.05$, respectively; Fig. 5*A*). Dox treatment completely rescued this working memory deficit. Not only did dox-treated APP/TTA mice make fewer errors than untreated APP/TTA mice ($p < 0.01$; Fig.

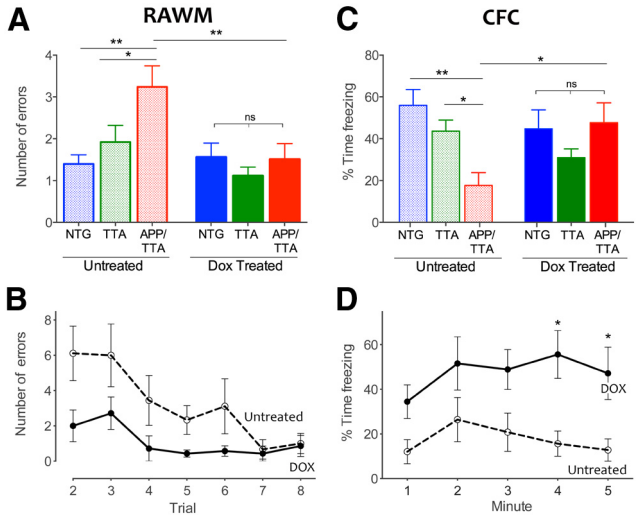

Figure 5. Deficits in working and associative memory are rescued by suppression of transgenic APP/Aβ. ***A***, The average number of errors made by each genotype over trials 2–8 of RAWM provides a measure of overall working memory performance. Untreated APP/TTA mice ($n = 10$) made significantly more repetitive arm entries (errors) than NTG ($n = 9$; $^{**}p < 0.01$) or TTA controls ($n = 10$; $^{*}p < 0.05$). In contrast, APP/TTA mice treated with dox ($n = 9$) perform this task significantly better than untreated APP/TTA mice ($^{**}p < 0.01$) and identically to NTG and TTA controls ($n = 10$ dox NTG; $n = 9$ dox TTA). ***B***, Average RAWM errors plotted by trial for untreated and dox-treated APP/TTA mice. Transgene suppression markedly improved the rate of acquisition in this task. ***C***, Untreated APP/TTA mice ($n = 10$) perform significantly worse in CFC than NTG ($^{**}p < 0.01$) and TTA controls ($^{*}p < 0.05$). Dox treatment rescues this associative memory impairment and returns APP/TTA mice ($n = 9$) to the performance level of control animals. ***D***, Percentage freezing plotted by minute over the 5 min test for untreated and dox-treated APP/TTA mice. Transgene suppression significantly improved associative memory for conditioned fear ($^{*}p < 0.05$).

5*A*,*B*), they performed as well as their dox-treated siblings ($F_{(1,52)} = 5.68$, $p < 0.05$; *post hoc*, $p > 0.05$ for both NTG and TTA).

Two days after completing RAWM, mice were trained in CFC and tested 24 h later in the same setting. Baseline freezing before conditioning was similar between genotypes and treatment groups ($F_{(2,51)} = 0.41$, $p = 0.67$). However, when they were returned to the chamber 1 d after conditioning, untreated APP/TTA mice spent significantly less time freezing than NTG and TTA littermates ($F_{(2,51)} = 3.26$, $p < 0.05$; Fig. 5*C*). In contrast, dox-treated APP/TTA mice showed clear improvement, freezing significantly more than untreated APP/TTA mice ($F_{(2,51)} = 5.69$, $p < 0.01$, *post hoc*, $p < 0.05$; Fig. 5*D*) and similar to controls ($p > 0.05$ for both; Fig. 5*C*). Transgene suppression thus resulted in complete behavioral rescue of working and associative memory in RAWM and CFC alongside partial rescue of spatial reference learning in MWM.

Suppression of Aβ accounts for a portion of behavioral recovery

Because our system regulates Aβ through the expression of transgenic APP, it is impossible to distinguish whether behavioral recovery following dox treatment was due to diminished Aβ, full-length APP, or other processed derivatives. To address this question, we treated a separate cohort of age-matched APP/TTA and TTA animals with the GSI LY41175. Animals were treated for 5 d before behavioral analysis with the same test battery used previously for dox-treated animals (Fig. 6*A*).

Similar to improvements we observed following dox treatment, GSI-treated APP/TTA mice swam the same distance as controls to reach the hidden platform in MWM (Fig. 6*B*). Both GSI-treated groups showed similar short-term memory for the trained location during daily probe trials at the end of each training session ($F_{(1,16)} = 0.99$, $p > 0.05$; Fig. 6*C*). Despite swimming similar distances during training and showing equivalent short-term memory for the platform location, GSI-treated double transgenic mice took slightly longer to reach criteria performance than TTA controls (4.78 ± 0.32 d vs 3.33 ± 0.37 d, $t = 2.25$, df = 16, $p < 0.05$). Nonetheless, the effect of GSI treatment in APP/TTA mice was nearly identical to that of dox: GSI-treated mice required 4.7 ± 0.31 d to reach criterion compared with 4.88 ± 0.48 d for dox-treated mice, and both values were lower than the 6.0 ± 0.36 d required by the untreated APP/TTA group (Fig. 6*D*). Instead, the main difference between GSI and dox was in the TTA controls, where GSI-treated mice required only 3.3 d ± 0.5 d to reach criterion compared with 4.0 ± 0.47 d for dox. Finally, GSI-treated mice of both genotypes performed equally well on long-term memory testing (*t* test, $t = 2.29$, df = 16, $p = 0.29$; Fig. 6*E*).

We were concerned that the side effects of GSI treatment might confound further testing in RAWM and fear conditioning so we conducted a second open-field test following MWM. While we saw no differences between genotypes for distance ($F_{(1,32)} = 0.08$, $p = 0.78$) or center ratio ($t = 0.27$, df = 16, $p = 0.80$), both genotypes were significantly less active during the second open-field test than they had been at the outset of GSI treatment ($F_{(1,32)} = 8.71$, $p < 0.001$). The decline in spontaneous ambulation was accompanied by hair loss and gastrointestinal changes. Although we continued behavioral testing through RAWM and CFC, the mounting side effects of GSI treatment confounded interpretation of these later tests.

Reduction of membrane-associated Aβ oligomers correlates with cognitive improvement

Having demonstrated that transgene suppression restored cognitive function at least in part through its effect on Aβ production, we next examined the possibility that clearance of specific forms of synaptotoxic Aβ may be an important aspect of this response. Using cortical homogenates from behaviorally tested animals, we measured the relative size and abundance of putative Aβ oligomers in the extracellular-enriched and membrane-associated fractions where these Aβ assemblies are predominantly detected (Lesné et al., 2006, 2008 Cheng et al., 2007). Two soluble oligomeric Aβ species, putative hexamers (~27 kDa) and Aβ*56, were present at low levels in the extracellular compartment of untreated APP/TTA mice (Fig. 7*A*). Both oligomers were substantially more concentrated in the membrane-associated extracts, where in addition to hexamers and Aβ*56, we also detected Aβ dimers (Fig. 7*B*). Although identification of Aβ trimers was confounded by a nonspecific band at the same molecular weight in the extracellular extract and by APP C-terminal fragments (β-CTF) in the membrane-enriched fraction, we were able to confirm low levels of apparent Aβ trimers in the extracellular extracts by 6E10 IP, as reported for other APP transgenic lines (Lesné et al., 2006; Larson et al., 2012).

All putative soluble oligomeric Aβ species in both extracellular and membrane-associated extracts were significantly reduced in the dox-treated mice ($F_{(1,36)} = 194.80$, $p < 0.0001$ for the membrane-associated fraction and $F_{(1,24)} = 243.60$, $p < 0.0001$ for extracellular fraction; Fig. 7*A*,*B*). The two most prevalent oligomer species, 6-mer and Aβ*56, were reduced by 79% extracellular ($p < 0.0001$) and 68% at the membrane ($p < 0.0001$) and by 28% extracellular ($p < 0.05$) and 55% at the membrane ($p < 0.0001$), respectively. Although a minor component, Aβ dimers were reduced by 53% in the membrane fraction ($p < 0.001$)

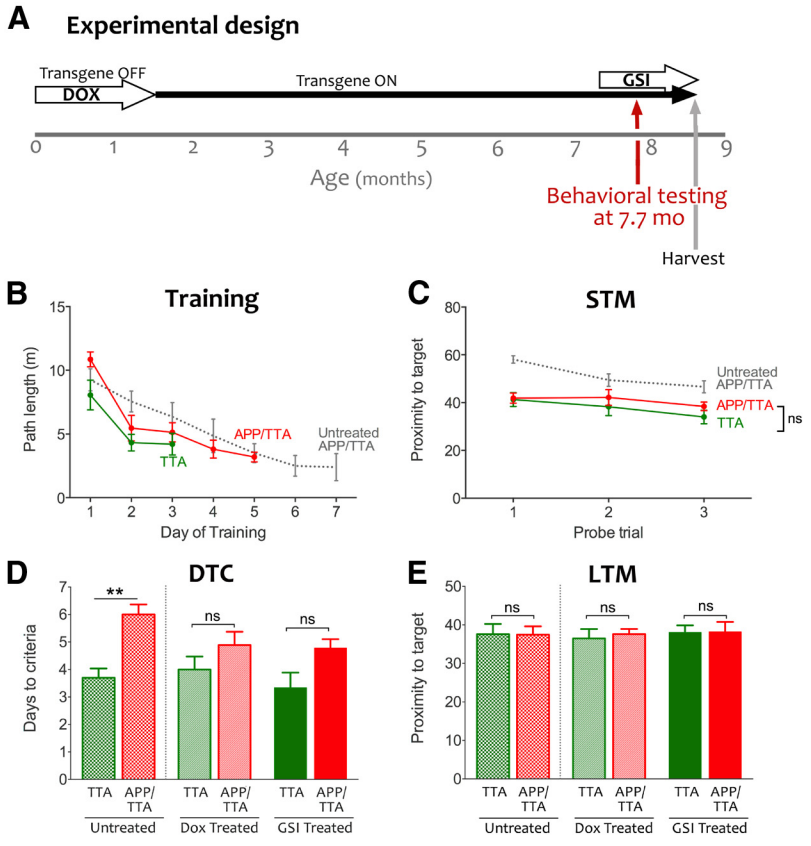

Figure 6. Selective reduction of Aβ with GSI largely phenocopies transgene suppression with dox. ***A***, As in our earlier experiments, dox was used to delay transgene expression until adulthood. Transgenic APP expression was initiated at 6 weeks of age by removing dox from the diet, and remained active for the duration of the experiment. Therapeutic intervention to prevent Aβ release with GSI began at 7.5 months of age, and behavioral testing was started 5 d later. ***B***, Average path length during MWM training for GSI-treated APP/TTA (red) and TTA mice (green). Performance of untreated APP/TTA animals is shown for comparison (gray; reproduced from Fig. 3). GSI-treated APP/TTA mice required fewer training days than untreated APP/TTA mice, but more than GSI-treated TTA controls ($n = 9$ for each genotype). ***C***, GSI treatment improved short-term memory (STM) of APP/TTA mice during daily probe trials to the level of TTA controls. ***D***, Untreated APP/TTA mice required significantly more days of training to reach criteria performance than TTA controls (**$p < 0.01$); however, this impairment was attenuated by both dox and GSI treatment. Data for this graph was analyzed by two-way ANOVA to allow comparison between treatment groups ($F_{(1,50)} = 19.70$, $p < 0.0001$); analyses presented in the text were limited to GSI-treated groups and therefore used *t* test. ***E***, All groups, regardless of genotype or treatment, performed identically during the long-term probe trial conducted 24 h after the final training session. Untreated and dox-treated days to criteria and long-term memory (LTM) values are reproduced from Figure 4.

while the largest aggregates, protofibrils, were decreased by 42% ($p < 0.0001$).

Because 6E10 detects many processed fragments of APP in addition to oligomeric Aβ, we performed nondenaturing analyses using the A11 antibody, which detects soluble nonamyloid oligomers larger than ~20 kDa (Kayed et al., 2003; Lesné et al., 2006). Under these conditions, dot blots probed with A11 confirmed the presence of substantial oligomeric Aβ in both extracellular and membrane extracts from untreated APP/TTA animals. Following transgene suppression, the A11 signal was reduced by 62% in the extracellular fraction (main effect of treatment $F_{(1,12)} = 191.7$, $p < 0.0001$; *post hoc*, $p < 0.0001$) and by 68% in the membrane fraction ($p < 0.01$; Fig. 7*D*). The dot blots were also coincubated with 6E10, which showed a quantitatively larger decrease in signal intensity following dox treatment than in A11 (extracellular, 81%; membrane, 71%), consistent with its ability to detect multiple APP fragments, A11-positive and A11-negative Aβ oligomers, and monomeric Aβ. These findings indicate that soluble oligomeric Aβ species were selectively reduced upon genetic suppression of transgenic APP while the burden of insoluble amyloid remained unchanged. Moreover, the extent this reduction parallels the decrease in ISF Aβ levels observed by microdialysis before and after transgene suppression.

Synaptic recovery despite sustained amyloid

Past work has shown that exposure to oligomeric Aβ is rapidly synaptotoxic *in vitro*, which led us to test whether synaptic markers were also reduced in untreated APP/TTA mice as they are in several other amyloid-bearing AD models (Calon et al., 2004; Almeida et al., 2005; Zhao et al., 2006; D'Amelio et al., 2011). Moreover, we wanted to determine whether synaptic recovery accompanied the decrease in oligomeric Aβ with transgene suppression, which might support their behavioral improvement. We quantified the levels of both postsynaptic PSD95 and presynaptic synapsin Ia/b in cortical extracts from behaviorally tested mice (Fig. 8*A–C*). Western blotting confirmed that untreated APP/TTA mice have less PSD95 than TTA controls ($F_{(1,28)} = 25.80$, $p < 0.01$; Fig. 8*B*) as well as lower levels of synapsin ($F_{(1,27)} = 6.20$, $p = 0.05$; Fig. 8*C*). Dox treatment to suppress transgenic APP increased the amount of both proteins in APP/TTA mice, but did not affect their levels in TTA controls ($F_{(1,28)} = 11.80$, $p = 0.002$ for PSD95 and $F_{(1,27)} = 3.70$, $p = 0.04$ for synapsin).

While these changes in synapsin and PSD95 are consistent with synapse loss throughout the cortex of untreated APP/TTA mice, past work has shown that the greatest decrease in synapse density occurs in the immediate vicinity of amyloid plaques (Spires et al., 2005; Dong et al., 2007; Spires-Jones et al., 2007; Knafo et al., 2009; Koffie et al., 2009). Knowing that dox-treated mice showed behavioral improvements despite the persistence of amyloid plaques, we tested whether plaque-associated synapse loss was rescued by lowering Aβ production. We manually selected thioflavine-positive plaques from the rostral forebrain ranging in size from 2500–11,000 μm^2 so that the distribution of plaque sizes was no different between dox-treated and untreated mice (unpaired Student's *t* test, $p > 0.05$). We then measured the area of synaptophysin immunostaining in a 0.036 mm^2 region surrounding each plaque (one field of view at 40× magnification) to compare the density of synapses in untreated and dox-treated APP/TTA mice (Fig. 8*D*). The area of synaptophysin staining in the vicinity of fibrillar deposits was markedly higher in the dox-treated animals than in their untreated siblings ($t = 3.34$, $p < 0.01$; Fig. 8*E*). This suggests that synaptic loss is reversible, as were cognitive deficits, once APP and Aβ are reduced.

We formally tested the relationship between synaptic protein expression and the concentration of oligomeric Aβ measured in individual APP/TTA mice with or without dox treatment. We focused on the two most prevalent oligomeric Aβ species, Aβ*56

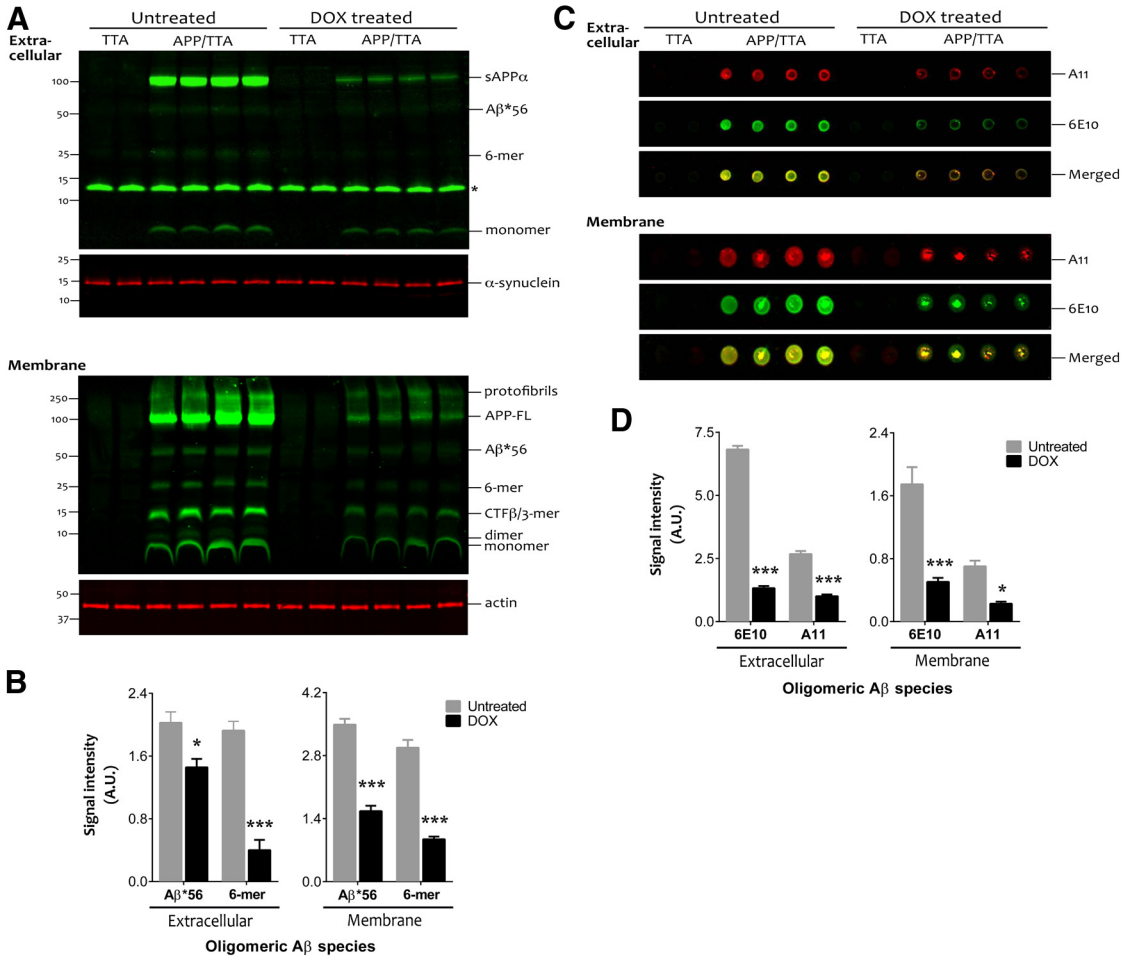

Figure 7. APP suppression reduces soluble synaptotoxic Aβ assemblies. ***A***, A four-step biochemical fractionation was used to enrich for extracellular (top) and membrane-associated proteins (bottom) in cortical samples from behaviorally tested mice ($n = 4$ APP/TTA untreated, $n = 4$ APP/TTA dox; $n = 2$ TTA untreated, $n = 2$ TTA dox). Immunoblotting with anti-Aβ antibody 6E10 revealed multiple oligomeric Aβ species in addition to full-length APP and sAPPα. Putative hexamers (6-mers) and Aβ*56 were especially prevalent in the membrane-associated fraction. The asterisk in the upper blot indicates a band of nonspecific binding present in all samples. Additional gels were prepared with an identical volume of the same samples and probed for α-synuclein (extracellular) or actin (membrane) to demonstrate equal loading across lanes ($p > 0.05$ between treatment conditions for both fractions). ***B***, Densitometry analysis revealed that both Aβ*56 and hexamers were significantly diminished in dox-treated APP/TTA animals compared with untreated controls. ***C***, Dot blots were used to distinguish the signal due to oligomeric Aβ from that caused by other fragments of APP ($n = 4$ APP/TTA untreated, $n = 4$ APP/TTA dox; $n = 2$ TTA untreated, $n = 2$ TTA dox). Blots were coincubated with oligomer-specific A11 and with 6E10, and detected with anti-rabbit IR680 and anti-mouse IR800 secondaries, respectively. ***D***, Signal intensity for both A11 and 6E10 was decreased after transgene suppression compared with untreated controls; $^{*}p < 0.05$, $^{***}p < 0.001$. A.U., arbitrary units.

and hexamers, measured by Western blot of extracellular and membrane extracts (Fig. 7*A*), as well as A11-positive oligomers measured by dot blot (Fig. 7*C*). Levels of these oligomers were tested for correlation against expression of the presynaptic marker synapsin measured by Western blot of intracellular extract from the same animals (Fig. 8*A*). Based on the general trend for each of these proteins before and after transgene suppression, we predicted there would be a strong negative correlation between oligomeric Aβ concentration and synaptic protein expression. Linear regression analyses confirmed this prediction, revealing R^2 of 0.81 (extracellular) and 0.76 (membrane) for hexamers ($p < 0.01$ for both; Fig. 9*A*), R^2 of 0.59 (extracellular) and 0.73 (membrane) for Aβ*56 ($p < 0.05$ and $p < 0.01$, respectively; Fig. 9*B*), and R^2 of 0.69 (extracellular) and 0.68 (membrane) for A11-positive oligomers ($p < 0.05$ for both; Fig. 9*C*). Our data thus supports and extends past *in vitro* studies suggesting a direct relationship between soluble oligomeric Aβ and synaptic integrity.

Synaptic regrowth corresponds with restored cofilin activity

While oligomeric Aβ may initiate synaptic collapse, the intracellular mediator of structural changes at the synapse is the actin cytoskeleton. Opposing actions of Rho- and Rac-GTPases are critical to the balance between synapse maintenance and turnover, and imbalance of these pathways is associated with several neurodegenerative conditions (Antoine-Bertrand et al., 2011; Ma et al., 2012). Both pathways ultimately converge on the actin-binding protein cofilin, which promotes collapse through actin depolymerization, but only in its active, dephosphorylated form. Past work has implicated the Rac-GTPase pathway in amyloid-associated synaptic deficits, showing that exposure to oligomeric Aβ diminishes activity of its downstream effector PAK in primary neurons, and conversely that oligomer-induced loss of synaptic markers can be ameliorated by increasing PAK levels (Zhao et al., 2006).

Western blotting of cortical intracellular homogenates revealed a significant imbalance of cofilin phosphorylation in un-

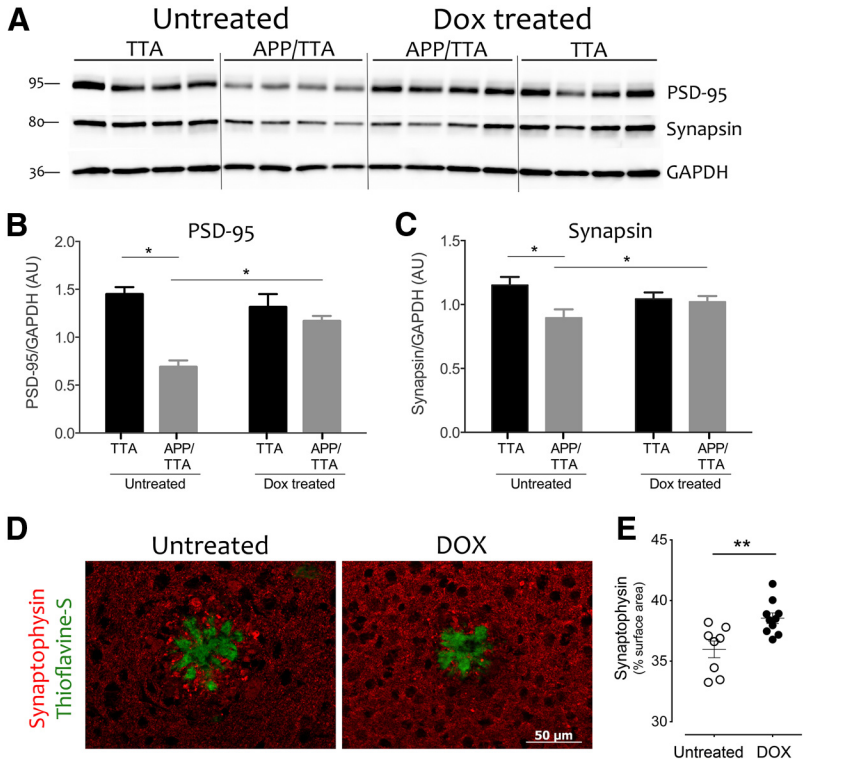

Figure 8. Synaptic protein levels and synaptic area are restored by suppression of transgenic APP/Aβ. ***A***, Immunoblotting was used to measure the levels of presynaptic and postsynaptic proteins synapsin and PSD95 in cortical homogenates from behaviorally tested animals. ***B***, ***C***, The signal intensity revealed significant deficits in both synapsin and PSD95 between untreated APP/TTA mice ($n = 8$) and TTA controls ($n = 8$; $^*p < 0.05$). Levels of both proteins were increased by dox treatment in APP/TTA mice ($n = 8$; $^*p < 0.05$) to levels that were indistinguishable from TTA controls ($n = 8$). ***D***, Synaptophysin immunostaining (red) was used to estimate the area occupied by synaptic terminals in the vicinity of thioflavine-positive fibrillar plaques (green) at the conclusion of behavioral testing. ***E***, Consistent with the recovery of synaptic proteins, the area of synaptophysin immunostaining was significantly greater in dox-treated APP/TTA mice than in untreated controls ($^{**}p < 0.01$; $n = 8$ untreated; $n = 10$ dox).

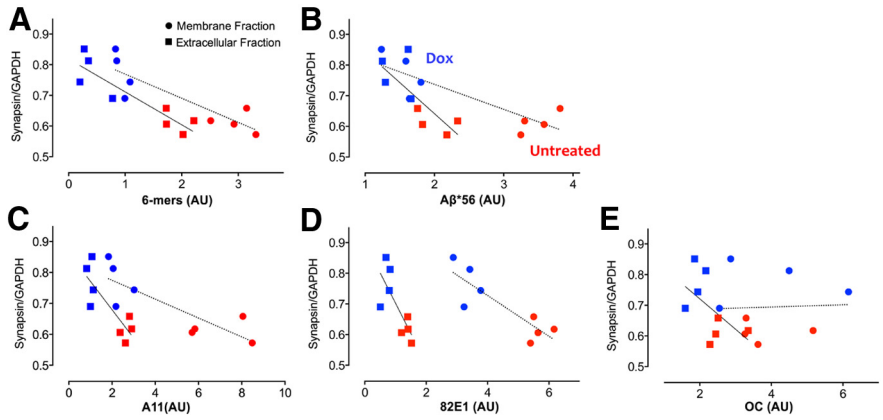

Figure 9. Synaptic protein expression correlates with oligomeric Aβ levels. ***A***, ***B***, Graphs showing the level of synapsin protein measured by Western blot of intracellular tissue extract as a function of the amount of Aβ*56 (***A***) Aβ hexamer (***B***) measured by Western blot of extracellular (squares) or membrane extract (circles) from the same animal. ***C***–***E***, Graph showing synapsin expression as a function of A11-positive (***C***) and 82E1-positive (***D***) oligomeric Aβ or OC-positive fibrils (***E***) measured by dot blot. Values are expressed as arbitrary units (AU). Red, $n = 4$ untreated; blue, $n = 4$ dox.

treated APP/TTA mice, which harbored more protein in the inactive phosphorylated state than controls ($F_{(1,12)} = 8.87$, $p = 0.01$, *post hoc*, $p < 0.05$; Fig. 10*A*). Cofilin phosphorylation was restored to normal by transgene suppression (*post hoc*, $p > 0.05$) without affecting the total amount of cofilin protein (Fig. 10*B*). Our results suggest that aberrant cofilin activation may mediate synaptic loss in our model through a dynamic process that returns to normal once APP/Aβ subsides. Consistent with past work (Zhao et al., 2006; Ma et al., 2008), we observed a significant decrease of Thr423 phosphorylation of PAK1 in double transgenic mice ($F_{(1,12)} = 96.23$, $p < 0.0001$; Fig. 10*C*,*D*). However, pPAK1 levels were not further altered by transgene suppression. These findings suggest that the recovery of cofilin activity after transgene suppression, as well as the rescue of synaptic proteins and cognitive behavior, are all independent of PAK1 activity.

Discussion

One of the uncertainties surrounding new anti-amyloid treatments for AD is whether lowering the concentration of soluble Aβ will be sufficient to achieve substantial and sustained cognitive improvement. Here, we set out to test the extent of behavioral and synaptic recovery that could be achieved by reducing soluble Aβ without macroscopically altering insoluble plaque burden. We describe substantial cognitive deficits while transgene expression persists, but nearly complete behavioral recovery across a wide range of memory tasks following acute reduction of APP and Aβ. Cognitive improvements correlated with restoration of synaptic proteins, increased synaptic density surrounding amyloid plaques, and normalized phosphorylation of actin-binding proteins controlling synaptic stability. Together, these findings argue that high levels of APP and the ensuing supply of soluble Aβ actively dampen synaptic condition and cognitive function, but indicate a striking potential for structural and functional recovery once further production of APP and Aβ are controlled. Remarkably, this recovery occurred despite the continued presence of deposited amyloid and associated pathology, suggesting the possibility for considerable therapeutic benefit by targeting full-length APP and/or soluble Aβ to arrest plaque growth without the need to reduce plaque burden.

To determine whether the cognitive improvements observed following transgene suppression were mediated by the reduction in Aβ, we used chronic GSI treatment to prevent Aβ release while the animals continued to overproduce APP. We found that GSI improved the performance of APP/TTA mice in the MWM, but did not offer complete rescue. This outcome suggests that either our GSI did not lower Aβ enough for full recovery, or that Aβ is only partly responsible for cognitive decline in our mice. Importantly, these behavioral improvements following GSI treatment appear in

sharp contrast to our recent finding that GSI had little effect on other phenotypes such as electroencephalographic sharp-wave discharge that could be attenuated by APP suppression (Born et al., 2014). Thus, Aβ does not contribute to every phenotype observed in APP models, but does appear to play a role in their cognitive dysfunction. Our results join a handful of past studies to separate the effects of APP from Aβ using passive immunization, β-secretase and γ-secretase inhibitors, or γ-secretase modulators. Although they differ in extent of cognitive recovery, starting plaque load, and testing procedures, these studies collectively point to soluble Aβ as an important mediator of cognitive decline in APP transgenic models (Dodart et al., 2002; Comery et al., 2005; Lee et al., 2006; Martone et al., 2009; Fukumoto et al., 2010; Balducci et al., 2011; Chang et al., 2011; Mitani et al., 2012, 2013; Rogers et al., 2012).

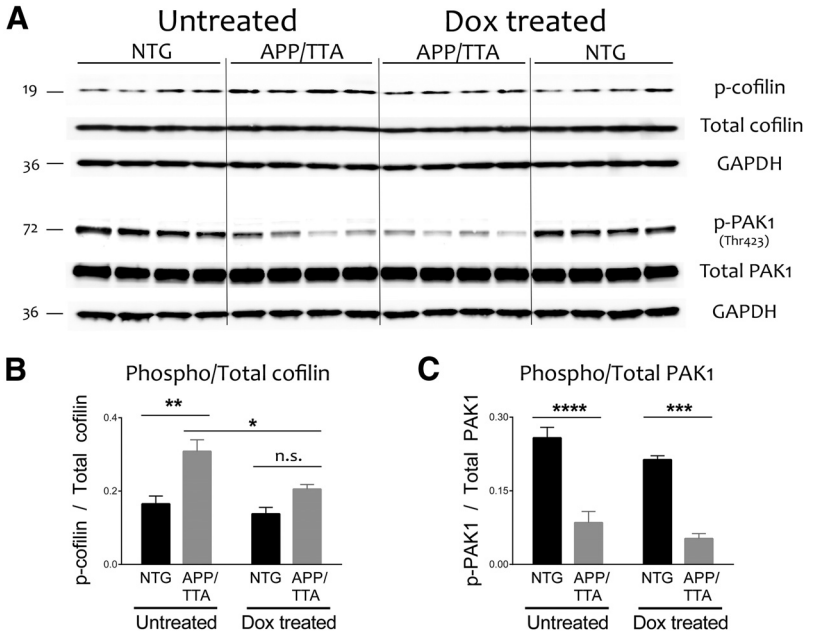

Figure 10. Transgene suppression restores normal cofilin activity independent of PAK1. ***A***, Immunoblotting was used to measure phosphorylation of the actin depolymerizing protein cofilin, and its upstream regulator PAK1, in cortical homogenates from behaviorally tested animals ($n = 4$ per group). ***B***, ***C***, Quantitation of the blots shown in ***A*** revealed that cofilin phosphorylation was significantly increased in untreated APP/TTA mice compared with NTG controls ($^*p < 0.05$), but returned to normal following transgene suppression. In contrast, PAK1 phosphorylation was significantly decreased in untreated APP/TTA mice relative to controls, but remained so even after transgene suppression diminished oligomeric Aβ levels and restored normal expression of synaptic proteins.

Cognitive improvements observed after transgene suppression were associated with structural recovery at the synaptic level. A limited number of studies *in vitro* and *in vivo* have hinted at the possibility of synaptic recovery following treatments to reduce Aβ levels, but never in the context of sustained amyloid load (Buttini et al., 2005; Rozkalne et al., 2009; Spires-Jones et al., 2009; Wei et al., 2010). Consistent with past work showing diminished levels of PSD95 in cultured neurons from Tg2576 mice (Almeida et al., 2005), we observed loss of both the presynaptic and postsynaptic markers in untreated APP/TTA mice. However, this deficit was fully reversible following short-term suppression of transgenic APP. As in other APP transgenic models, we observed diminished synaptic staining surrounding amyloid plaques in untreated APP/TTA mice (Dong et al., 2007; Koffie et al., 2009; Spires-Jones and Knafo, 2012), but demonstrate significant structural recovery following APP/Aβ suppression. Although the thioflavine-positive plaque load remained stable, the concentration of potentially synaptotoxic oligomeric Aβ decreased significantly after APP suppression. The amount of oligomeric Aβ in the brain was inversely correlated with synaptic protein levels and synaptic density. Both markers of synaptic integrity increased significantly when oligomeric Aβ decreased.

Previous work with cultured neurons has suggested a mechanistic link between exposure to oligomeric Aβ and the intracellular signaling pathways that regulate synapse stability. Work has revealed roles for the PAKs and their downstream target cofilin in spine loss following application of soluble Aβ aggregates (Zhao et al., 2006; Shankar et al., 2007; Davis et al., 2011; Mendoza-Naranjo et al., 2012). The activity of both proteins is regulated by phosphorylation, which in the case of cofilin, serves as a way to stabilize synaptic structure by preventing F-actin disassembly (Mizuno, 2013). We find that cofilin phosphorylation was substantially elevated in the cortex of untreated APP/TTA mice, where it may either be a direct result of exposure to soluble forms of Aβ or may serve as a compensatory response to protect against further synapse loss. Consistent with the former idea, cofilin phosphorylation was shown to increase rapidly in primary neurons following application of aggregated Aβ (Heredia et al., 2006). Supporting the latter idea, constitutively inactive cofilin (S3D) protects neurons from spine loss during prolonged exposure to oligomeric Aβ (Shankar et al., 2007). Regardless of whether the response is direct or reactive, cofilin phosphorylation comes at the cost of structural plasticity required for learning-associated changes in synaptic structure and function. Cofilin phosphorylation is dynamically regulated by neuronal stimulation *in vitro* and behavioral learning *in vivo*, where it participates both in modulating synaptic size and in trafficking AMPA receptors to the membrane (Saneyoshi and Hayashi, 2012). Loss of cofilin in the forebrain impairs associative memory, while blocking its activation retards extinction learning (Rust et al., 2010; Wang et al., 2013). Thus, diminished cofilin activity in untreated APP/TTA mice may contribute to their poor cognitive flexibility.

Once the production of transgenic APP and Aβ was suppressed, cofilin activity returned to normal and synapse density around plaques increased. Past work identified p21-associated kinase, PAK1, as a key mediator of oligomeric Aβ-induced synapse loss (Zhao et al., 2006). As shown for the Tg2576 model, we too observed a dramatic reduction of PAK1 phosphorylation in untreated APP/TTA mice. In contrast to the complete rescue of PAK1 activity found by Zhao et al. (2006) following anti-Aβ antibody treatment, we found no further change in PAK1 phosphorylation with APP/Aβ suppression. Although we have not excluded the possibility for cellular redistribution of PAK1 following APP suppression (Ma et al., 2008), our findings suggest that synapse recovery and cognitive improvement in our model are independent of PAK1 signaling.

While past work linking oligomeric Aβ to synapse loss provided a framework for interpreting our data, we cannot exclude the possibility that other fragments of APP may also contribute to

synapse loss and cognitive decline in the APP/TTA mice. Genetically inhibiting the expression of full-length APP not only lowered Aβ production but also reduced APP, soluble extracellular derivatives (sAPP), and APP intracellular domain. Our system thereby provides experimental proof of principle that modulating APP gene expression in the human brain might be therapeutically beneficial. Based on these results, we propose that antisense oligodeoxynucleotides (ASO) targeting APP mRNA could offer a means of lowering Aβ without assuming it is the sole causal agent. ASO therapy has the added advantage of being directly translatable to clinical trials, and is currently in testing for both spinal muscular atrophy and amyotrophic lateral sclerosis (www.Clinicaltrials.gov ID NCT01839656; Miller et al., 2013). Although considerable effort has focused on selectively lowering Aβ, our study shows that targeting full-length APP may offer another means of accomplishing this goal.

Collectively, our results point to transient assemblies of Aβ as the most likely cause of synaptic and cognitive deficits in our APP/TTA mice. We demonstrate substantial structural and functional improvements following short-term suppression of transgenic APP and the subsequent reduction of monomeric and oligomeric Aβ, despite the continued presence of fibrillar amyloid deposits. We further show that aberrant cofilin phosphorylation corresponds with synaptic loss in untreated APP/TTA mice, and that cofilin activity and synaptic integrity are restored to normal following arrest of transgenic APP and Aβ. Future studies will need to address whether this benefit can be maintained long term, and if the same degree of recovery observed here can be achieved at later stages of disease when amyloid load increases exponentially (Kawarabayashi et al., 2001; Rodgers et al., 2012) and cognitive impairment becomes progressively worse (Westerman et al., 2002; Trinchese et al., 2004). Nonetheless, at least at this early stage of disease, our findings support the possibility for considerable functional and structural recovery by genetically targeting transient forms of soluble Aβ.

References

Almeida CG, Tampellini D, Takahashi RH, Greengard P, Lin MT, Snyder EM, Gouras GK (2005) β-amyloid accumulation in APP mutant neurons reduces PSD-95 and GluR1 in synapses. Neurobiol Dis 20:187–198. CrossRef Medline

Antoine-Bertrand J, Villemure JF, Lamarche-Vane N (2011) Implication of rho GTPases in neurodegenerative diseases. Curr Drug Targets 12:1202–1215. CrossRef Medline

Balducci C, Mehdawy B, Mare L, Giuliani A, Lorenzini L, Sivilia S, Giardino L, Calzà L, Lanzillotta A, Sarnico I, Pizzi M, Usiello A, Viscomi AR, Ottonello S, Villetti G, Imbimbo BP, Nisticò G, Forloni G, Nisticò R (2011) The γ-secretase modulator CHF5074 restores memory and hippocampal synaptic plasticity in plaque-free Tg2576 mice. J Alzheimers Dis 24:799–816. CrossRef Medline

Born HA, Kim JY, Savjani RR, Das P, Dabaghian YA, Guo Q, Yoo JW, Schuler DR, Cirrito JR, Zheng H, Golde TE, Noebels JL, Jankowsky JL (2014) Genetic suppression of transgenic APP rescues hypersynchronous network activity in a mouse model of Alzheimer's disease. J Neurosci 34:3826–3840. CrossRef Medline

Busche MA, Eichhoff G, Adelsberger H, Abramowski D, Wiederhold KH, Haass C, Staufenbiel M, Konnerth A, Garaschuk O (2008) Clusters of hyperactive neurons near amyloid plaques in a mouse model of Alzheimer's disease. Science 321:1686–1689. CrossRef Medline

Buttini M, Masliah E, Barbour R, Grajeda H, Motter R, Johnson-Wood K, Khan K, Seubert P, Freedman S, Schenk D, Games D (2005) β-amyloid immunotherapy prevents synaptic degeneration in a mouse model of Alzheimer's disease. J Neurosci 25:9096–9101. CrossRef Medline

Calon F, Lim GP, Yang F, Morihara T, Teter B, Ubeda O, Rostaing P, Triller A, Salem N Jr, Ashe KH, Frautschy SA, Cole GM (2004) Docosahexaenoic acid protects from dendritic pathology in an Alzheimer's disease mouse model. Neuron 43:633–645. CrossRef Medline

Chang WP, Huang X, Downs D, Cirrito JR, Koelsch G, Holtzman DM, Ghosh AK, Tang J (2011) β-secretase inhibitor GRL-8234 rescues age-related cognitive decline in APP transgenic mice. FASEB J 25:775–784. CrossRef Medline

Cheng IH, Scearce-Levie K, Legleiter J, Palop JJ, Gerstein H, Bien-Ly N, Puoliväli J, Lesné S, Ashe KH, Muchowski PJ, Mucke L (2007) Accelerating amyloid-β fibrillization reduces oligomer levels and functional deficits in Alzheimer disease mouse models. J Biol Chem 282:23818–23828. CrossRef Medline

Cirrito JR, May PC, O'Dell MA, Taylor JW, Parsadanian M, Cramer JW, Audia JE, Nissen JS, Bales KR, Paul SM, DeMattos RB, Holtzman DM (2003) *In vivo* assessment of brain interstitial fluid with microdialysis reveals plaque-associated changes in amyloid-β metabolism and half-life. J Neurosci 23:8844–8853. Medline

Cirrito JR, Disabato BM, Restivo JL, Verges DK, Goebel WD, Sathyan A, Hayreh D, D'Angelo G, Benzinger T, Yoon H, Kim J, Morris JC, Mintun MA, Sheline YI (2011) Serotonin signaling is associated with lower amyloid-β levels and plaques in transgenic mice and humans. Proc Natl Acad Sci U S A 108:14968–14973. CrossRef Medline

Comery TA, Martone RL, Aschmies S, Atchison KP, Diamantidis G, Gong X, Zhou H, Kreft AF, Pangalos MN, Sonnenberg-Reines J, Jacobsen JS, Marquis KL (2005) Acute γ-secretase inhibition improves contextual fear conditioning in the Tg2576 mouse model of Alzheimer's disease. J Neurosci 25:8898–8902. CrossRef Medline

D'Amelio M, Cavallucci V, Middei S, Marchetti C, Pacioni S, Ferri A, Diamantini A, De Zio D, Carrara P, Battistini L, Moreno S, Bacci A, Ammassari-Teule M, Marie H, Cecconi F (2011) Caspase-3 triggers early synaptic dysfunction in a mouse model of Alzheimer's disease. Nat Neurosci 14:69–76. CrossRef Medline

D'Amore JD, Kajdasz ST, McLellan ME, Bacskai BJ, Stern EA, Hyman BT (2003) In vivo multiphoton imaging of a transgenic mouse model of Alzheimer disease reveals marked thioflavine-S-associated alterations in neurite trajectories. J Neuropathol Exp Neurol 62:137–145. Medline

Davis RC, Marsden IT, Maloney MT, Minamide LS, Podlisny M, Selkoe DJ, Bamburg JR (2011) Amyloid β dimers/trimers potently induce cofilin-actin rods that are inhibited by maintaining cofilin-phosphorylation. Mol Neurodegener 6:10. CrossRef Medline

Dodart JC, Bales KR, Gannon KS, Greene SJ, DeMattos RB, Mathis C, DeLong CA, Wu S, Wu X, Holtzman DM, Paul SM (2002) Immunization reverses memory deficits without reducing brain Aβ burden in Alzheimer's disease model. Nat Neurosci 5:452–457. Medline

Dong H, Martin MV, Chambers S, Csernansky JG (2007) Spatial relationship between synapse loss and β-amyloid deposition in Tg2576 mice. J Comp Neurol 500:311–321. CrossRef Medline

Fukumoto H, Takahashi H, Tarui N, Matsui J, Tomita T, Hirode M, Sagayama M, Maeda R, Kawamoto M, Hirai K, Terauchi J, Sakura Y, Kakihana M, Kato K, Iwatsubo T, Miyamoto M (2010) A noncompetitive BACE1 inhibitor TAK-070 ameliorates Aβ pathology and behavioral deficits in a mouse model of Alzheimer's disease. J Neurosci 30:11157–11166. CrossRef Medline

Hartman RE, Izumi Y, Bales KR, Paul SM, Wozniak DF, Holtzman DM (2005) Treatment with an amyloid-β antibody ameliorates plaque load, learning deficits, and hippocampal long-term potentiation in a mouse model of Alzheimer's disease. J Neurosci 25:6213–6220. CrossRef Medline

Heredia L, Helguera P, de Olmos S, Kedikian G, Solá Vigo F, LaFerla F, Staufenbiel M, de Olmos J, Busciglio J, Cáceres A, Lorenzo A (2006) Phosphorylation of actin-depolymerizing factor/cofilin by LIM-kinase mediates amyloid β-induced degeneration: a potential mechanism of neuronal dystrophy in Alzheimer's disease. J Neurosci 26:6533–6542. CrossRef Medline

Hong S, Quintero-Monzon O, Ostaszewski BL, Podlisny DR, Cavanaugh WT, Yang T, Holtzman DM, Cirrito JR, Selkoe DJ (2011) Dynamic analysis of amyloid β-protein in behaving mice reveals opposing changes in ISF versus parenchymal Aβa during age-related plaque formation. J Neurosci 31:15861–15869. CrossRef Medline

Jankowsky JL, Slunt HH, Gonzales V, Savonenko AV, Wen JC, Jenkins NA, Copeland NG, Younkin LH, Lester HA, Younkin SG, Borchelt DR (2005) Persistent amyloidosis following suppression of Aβ production in a transgenic model of Alzheimer's disease. PLoS Med 2:e355. CrossRef Medline

Janus C, Pearson J, McLaurin J, Mathews PM, Jiang Y, Schmidt SD, Chishti MA, Horne P, Heslin D, French J, Mount HT, Nixon RA, Mercken M,

Bergeron C, Fraser PE, St George-Hyslop P, Westaway D (2000) Aβ peptide immunization reduces behavioural impairment and plaques in a model of Alzheimer's disease. Nature 408:979–982. CrossRef Medline

Kawarabayashi T, Younkin LH, Saido TC, Shoji M, Ashe KH, Younkin SG (2001) Age-dependent changes in brain, CSF, and plasma amyloid β protein in the Tg2576 transgenic mouse model of Alzheimer's disease. J Neurosci 21:372–381. Medline

Kayed R, Head E, Thompson JL, McIntire TM, Milton SC, Cotman CW, Glabe CG (2003) Common structure of soluble amyloid oligomers implies common mechanism of pathogenesis. Science 300:486–489. CrossRef Medline

Knafo S, Alonso-Nanclares L, Gonzalez-Soriano J, Merino-Serrais P, Fernaud-Espinosa I, Ferrer I, DeFelipe J (2009) Widespread changes in dendritic spines in a model of Alzheimer's disease. Cereb Cortex 19:586–592. CrossRef Medline

Koffie RM, Meyer-Luehmann M, Hashimoto T, Adams KW, Mielke ML, Garcia-Alloza M, Micheva KD, Smith SJ, Kim ML, Lee VM, Hyman BT, Spires-Jones TL (2009) Oligomeric amyloid β associates with postsynaptic densities and correlates with excitatory synapse loss near senile plaques. Proc Natl Acad Sci U S A 106:4012–4017. CrossRef Medline

Kotilinek LA, Bacskai B, Westerman M, Kawarabayashi T, Younkin L, Hyman BT, Younkin S, Ashe KH (2002) Reversible memory loss in a mouse transgenic model of Alzheimer's disease. J Neurosci 22:6331–6335. Medline

Kuchibhotla KV, Goldman ST, Lattarulo CR, Wu HY, Hyman BT, Bacskai BJ (2008) Aβ plaques lead to aberrant regulation of calcium homeostasis in vivo resulting in structural and functional disruption of neuronal networks. Neuron 59:214–225. CrossRef Medline

Kuchibhotla KV, Lattarulo CR, Hyman BT, Bacskai BJ (2009) Synchronous hyperactivity and intercellular calcium waves in astrocytes in Alzheimer mice. Science 323:1211–1215. CrossRef Medline

Larson ME, Lesne SE (2012) Soluble Aβ oligomer production and toxicity. J Neurochem 120 [Suppl 1]:125–139. CrossRef Medline

Larson M, Sherman MA, Amar F, Nuvolone M, Schneider JA, Bennett DA, Aguzzi A, Lesné SE (2012) The complex PrP(c)-Fyn couples human oligomeric Aβ with pathological tau changes in Alzheimer's disease. J Neurosci 32:16857–16871a. CrossRef Medline

Le R, Cruz L, Urbanc B, Knowles RB, Hsiao-Ashe K, Duff K, Irizarry MC, Stanley HE, Hyman BT (2001) Plaque-induced abnormalities in neurite geometry in transgenic models of Alzheimer disease: implications for neural system disruption. J Neuropathol Exp Neurol 60:753–758. Medline

Lee EB, Leng LZ, Zhang B, Kwong L, Trojanowski JQ, Abel T, Lee VM (2006) Targeting amyloid-β peptide (Aβ) oligomers by passive immunization with a conformation-selective monoclonal antibody improves learning and memory in Aβ precursor protein (APP) transgenic mice. J Biol Chem 281:4292–4299. CrossRef Medline

Lesné S, Koh MT, Kotilinek L, Kayed R, Glabe CG, Yang A, Gallagher M, Ashe KH (2006) A specific amyloid-β protein assembly in the brain impairs memory. Nature 440:352–357. CrossRef Medline

Lesné S, Kotilinek L, Ashe KH (2008) Plaque-bearing mice with reduced levels of oligomeric amyloid-β assemblies have intact memory function. Neuroscience 151:745–749. CrossRef Medline

Ma QL, Yang F, Calon F, Ubeda OJ, Hansen JE, Weisbart RH, Beech W, Frautschy SA, Cole GM (2008) p21-activated kinase-aberrant activation and translocation in Alzheimer disease pathogenesis. J Biol Chem 283:14132–14143. CrossRef Medline

Ma QL, Yang F, Frautschy SA, Cole GM (2012) PAK in Alzheimer disease, Huntington disease and X-linked mental retardation. Cell Logist 2:117–125. CrossRef Medline

Martone RL, Zhou H, Atchison K, Comery T, Xu JZ, Huang X, Gong X, Jin M, Kreft A, Harrison B, Mayer SC, Aschmies S, Gonzales C, Zaleska MM, Riddell DR, Wagner E, Lu P, Sun SC, Sonnenberg-Reines J, Oganesian A, et al. (2009) Begacestat (GSI-953): a novel, selective thiophene sulfonamide inhibitor of amyloid precursor protein γ-secretase for the treatment of Alzheimer's disease. J Pharmacol Exp Ther 331:598–608. CrossRef Medline

Mayford M, Bach ME, Huang YY, Wang L, Hawkins RD, Kandel ER (1996) Control of memory formation through regulated expression of a CaMKII transgene. Science 274:1678–1683. CrossRef Medline

Melnikova T, Fromholt S, Kim H, Lee D, Xu G, Price A, Moore BD, Golde TE, Felsenstein KM, Savonenko A, Borchelt DR (2013) Reversible pathologic and cognitive phenotypes in an inducible model of Alzheimer-amyloidosis. J Neurosci 33:3765–3779. CrossRef Medline

Mendoza-Naranjo A, Contreras-Vallejos E, Henriquez DR, Otth C, Bamburg JR, Maccioni RB, Gonzalez-Billault C (2012) Fibrillar amyloid-β 1–42 modifies actin organization affecting the cofilin phosphorylation state: a role for Rac1/cdc42 effector proteins and the slingshot phosphatase. J Alzheimers Dis 29:63–77. CrossRef Medline

Miller TM, Pestronk A, David W, Rothstein J, Simpson E, Appel SH, Andres PL, Mahoney K, Allred P, Alexander K, Ostrow LW, Schoenfeld D, Macklin EA, Norris DA, Manousakis G, Crisp M, Smith R, Bennett CF, Bishop KM, Cudkowicz ME (2013) An antisense oligonucleotide against SOD1 delivered intrathecally for patients with SOD1 familial amyotrophic lateral sclerosis: a phase 1, randomised, first-in-man study. Lancet Neurol 12:435–442. CrossRef Medline

Mitani Y, Yarimizu J, Akashiba H, Shitaka Y, Ni K, Matsuoka N (2013) Amelioration of cognitive deficits in plaque-bearing Alzheimer's disease model mice through selective reduction of nascent soluble Aβ42 without affecting other Aβ pools. J Neurochem 125:465–472. CrossRef Medline

Mitani Y, Yarimizu J, Saita K, Uchino H, Akashiba H, Shitaka Y, Ni K, Matsuoka N (2012) Differential effects between γ-secretase inhibitors and modulators on cognitive function in amyloid precursor protein-transgenic and nontransgenic mice. J Neurosci 32:2037–2050. CrossRef Medline

Mizuno K (2013) Signaling mechanisms and functional roles of cofilin phosphorylation and dephosphorylation. Cell Signal 25:457–469. CrossRef Medline

Morgan D, Diamond DM, Gottschall PE, Ugen KE, Dickey C, Hardy J, Duff K, Jantzen P, DiCarlo G, Wilcock D, Connor K, Hatcher J, Hope C, Gordon M, Arendash GW (2000) Aβ peptide vaccination prevents memory loss in an animal model of Alzheimer's disease. Nature 408:982–985. CrossRef Medline

Rodgers SP, Born HA, Das P, Jankowsky JL (2012) Transgenic APP expression during postnatal development causes persistent locomotor hyperactivity in the adult. Mol Neurodegener 7:28. CrossRef Medline

Rogers K, Felsenstein KM, Hrdlicka L, Tu Z, Albayya F, Lee W, Hopp S, Miller MJ, Spaulding D, Yang Z, Hodgdon H, Nolan S, Wen M, Costa D, Blain JF, Freeman E, De Strooper B, Vulsteke V, Scrocchi L, Zetterberg H, et al. (2012) Modulation of γ-secretase by EVP-0015962 reduces amyloid deposition and behavioral deficits in Tg2576 mice. Mol Neurodegener 7:61. CrossRef Medline

Rozkalne A, Spires-Jones TL, Stern EA, Hyman BT (2009) A single dose of passive immunotherapy has extended benefits on synapses and neurites in an Alzheimer's disease mouse model. Brain Res 1280:178–185. CrossRef Medline

Rust MB, Gurniak CB, Renner M, Vara H, Morando L, Görlich A, Sassoè-Pognetto M, Banchaabouchi MA, Giustetto M, Triller A, Choquet D, Witke W (2010) Learning, AMPA receptor mobility and synaptic plasticity depend on n-cofilin-mediated actin dynamics. EMBO J 29:1889–1902. CrossRef Medline

Saneyoshi T, Hayashi Y (2012) The Ca^{2+} and Rho GTPase signaling pathways underlying activity-dependent actin remodeling at dendritic spines. Cytoskeleton 69:545–554. CrossRef Medline

Shankar GM, Bloodgood BL, Townsend M, Walsh DM, Selkoe DJ, Sabatini BL (2007) Natural oligomers of the Alzheimer amyloid-β protein induce reversible synapse loss by modulating an NMDA-type glutamate receptor-dependent signaling pathway. J Neurosci 27:2866–2875. CrossRef Medline

Sherman MA, Lesné SE (2011) Detecting Aβ*56 oligomers in brain tissues. Methods Mol Biol 670:45–56. CrossRef Medline

Spires TL, Meyer-Luehmann M, Stern EA, McLean PJ, Skoch J, Nguyen PT, Bacskai BJ, Hyman BT (2005) Dendritic spine abnormalities in amyloid precursor protein transgenic mice demonstrated by gene transfer and intravital multiphoton microscopy. J Neurosci 25:7278–7287. CrossRef Medline

Spires-Jones T, Knafo S (2012) Spines, plasticity, and cognition in Alzheimer's model mice. Neural Plast 2012:319836. CrossRef Medline

Spires-Jones TL, Meyer-Luehmann M, Osetek JD, Jones PB, Stern EA, Bacskai BJ, Hyman BT (2007) Impaired spine stability underlies plaque-related spine loss in an Alzheimer's disease mouse model. Am J Pathol 171:1304–1311. CrossRef Medline

Spires-Jones TL, Mielke ML, Rozkalne A, Meyer-Luehmann M, de Calignon A, Bacskai BJ, Schenk D, Hyman BT (2009) Passive immunotherapy

rapidly increases structural plasticity in a mouse model of Alzheimer disease. Neurobiol Dis 33:213–220. CrossRef Medline

Stern EA, Bacskai BJ, Hickey GA, Attenello FJ, Lombardo JA, Hyman BT (2004) Cortical synaptic integration in vivo is disrupted by amyloid-β plaques. J Neurosci 24:4535–4540. CrossRef Medline

Stokin GB, Lillo C, Falzone TL, Brusch RG, Rockenstein E, Mount SL, Raman R, Davies P, Masliah E, Williams DS, Goldstein LS (2005) Axonopathy and transport deficits early in the pathogenesis of Alzheimer's disease. Science 307:1282–1288. CrossRef Medline

Takeda S, Hashimoto T, Roe AD, Hori Y, Spires-Jones TL, Hyman BT (2013) Brain interstitial oligomeric amyloid β increases with age and is resistant to clearance from brain in a mouse model of Alzheimer's disease. FASEB J 27:3239–3248. CrossRef Medline

Trinchese F, Liu S, Battaglia F, Walter S, Mathews PM, Arancio O (2004) Progressive age-related development of Alzheimer-like pathology in APP/PS1 mice. Ann Neurol 55:801–814. CrossRef Medline

Wang A, Das P, Switzer RC 3rd, Golde TE, Jankowsky JL (2011) Robust amyloid clearance in a mouse model of Alzheimer's disease provides novel insights into the mechanism of amyloid-β immunotherapy. J Neurosci 31:4124–4136. CrossRef Medline

Wang Y, Dong Q, Xu XF, Feng X, Xin J, Wang DD, Yu H, Tian T, Chen ZY (2013) Phosphorylation of cofilin regulates extinction of conditioned aversive memory via AMPAR trafficking. J Neurosci 33:6423–6433. CrossRef Medline

Wei W, Nguyen LN, Kessels HW, Hagiwara H, Sisodia S, Malinow R (2010) Amyloid β from axons and dendrites reduces local spine number and plasticity. Nat Neurosci 13:190–196. CrossRef Medline

Westerman MA, Cooper-Blacketer D, Mariash A, Kotilinek L, Kawarabayashi T, Younkin LH, Carlson GA, Younkin SG, Ashe KH (2002) The relationship between Aβ and memory in the Tg2576 mouse model of Alzheimer's disease. J Neurosci 22:1858–1867. Medline

Wilcock DM, Rojiani A, Rosenthal A, Subbarao S, Freeman MJ, Gordon MN, Morgan D (2004) Passive immunotherapy against Aβ in aged APP-transgenic mice reverses cognitive deficits and depletes parenchymal amyloid deposits in spite of increased vascular amyloid and microhemorrhage. J Neuroinflammation 1:24. CrossRef Medline

Wilcock DM, Alamed J, Gottschall PE, Grimm J, Rosenthal A, Pons J, Ronan V, Symmonds K, Gordon MN, Morgan D (2006) Deglycosylated anti-amyloid-β antibodies eliminate cognitive deficits and reduce parenchymal amyloid with minimal vascular consequences in aged amyloid precursor protein transgenic mice. J Neurosci 26:5340–5346. CrossRef Medline

Wilcox KC, Lacor PN, Pitt J, Klein WL (2011) Aβ oligomer-induced synapse degeneration in Alzheimer's disease. Cell Mol Neurobiol 31:939–948. CrossRef Medline

Zago W, Buttini M, Comery TA, Nishioka C, Gardai SJ, Seubert P, Games D, Bard F, Schenk D, Kinney GG (2012) Neutralization of soluble, synaptotoxic amyloid β species by antibodies is epitope specific. J Neurosci 32:2696–2702. CrossRef Medline

Zhao L, Ma QL, Calon F, Harris-White ME, Yang F, Lim GP, Morihara T, Ubeda OJ, Ambegaokar S, Hansen JE, Weisbart RH, Teter B, Frautschy SA, Cole GM (2006) Role of p21-activated kinase pathway defects in the cognitive deficits of Alzheimer disease. Nat Neurosci 9:234–242. CrossRef Medline

Conclusions

Our research showed that this type of tet-off responsive system was able to significantly reduce soluble Aβ burden and halt the further production of Aβ plaques while not increasing plaque clearance. This study also showed that cognition could be recovered, even after Aβ burden was already present. The mice tested here improved both their spatial reference memory and working memory. These cognitive improvements are attributed to a reduction in membrane-associated soluble Aβ oligomers. We also observed synaptic recovery and regrowth despite the sustained presence of Aβ plaques.

Recently, there have been many different pharmacological approaches to increase Aβ clearance through the use of anti-Aβ antibodies that target Aβ plaques for degradation and clearance. So far, none of these clinical trials have been cleared by the FDA due to their inability to show improvements in patients and reach their primary endpoints. This research shows that targeting soluble Aβ or APP production is likely a better path to cognitive improvement in patients.

We also undertook to see if the observed cognitive improvements were mediated by Aβ reduction by blocking Aβ release while APP production continued. We found this method did improve performance, but recovery was not complete. This reduced recovery suggests that Aβ is only part of the AD puzzle and that other mechanisms are involved in producing cognitive decline.

Research into synaptic loss and cognitive deficits in relation to Aβ has been continued by other labs since the publication of this study. Some publications of note include research completed at Brigham and Women's Hospital. Their research expanded on our work by looking at human tissue samples from AD patients to identify the specific Aβ species related to AD-neurodegeneration (Li et al. 2018). They found that soluble Aβ oligomers inhibit hippocampal LTP and induce synaptic and neurite loss, similar to our findings around oligomeric Aβ's critical role in synaptic loss.

Findings around the relationship between soluble Aβ and cognition have also been expanded and have even resulted in drug trials. Crenezumab is a passive immune

therapy drug that was under investigation for the use in AD patients. It targeted oligomeric Aβ to increase cognition (Tariot et al. 2018). Crenezumab was found to significantly lower AB levels in CSF when tested in human trials (Yang et al. 2019). *In vivo* mouse studies have also shown that crenezumab localizes to regions of high Aβ concentration in the brain (Meilandt et al. 2019). Phase III clinical trials of the drug were halted after interim analysis showed it was unlikely to reach its primary efficacy endpoint (Roche 2019).

Chapter 6: Enhancing Astrocytic Lysosome Biogenesis Facilitates Aβ Clearance and Attenuates Amyloid Plaque Pathogenesis

It is well documented that Aβ clearance is decreased in AD. Previous studies have shown that Aβ can be cleared by both neurons and glial cells in the brain via endocytosis, phagocytosis, macropinocytosis, and other pathways. It is hypothesized that the extracellular buildup of Aβ plaques plays a key role in neuronal degradation and subsequent cognitive decline and deficits seen in AD. This buildup may be due to an overproduction of Aβ, a decrease in clearance of the protein, or a combination of both.

Astrocytes have been observed surrounding Aβ plaques and then trafficking them into lysosomes for degradation. It has also been observed that when astrocytes are impaired, plaque load increases. Some studies have suggested that age-related lysosome dysfunction may play a key role in the accumulation of Aβ within astrocytes in elderly individuals.

In our previous work, we showed that Aβ clearance in the cortex is at least partially mediated by LRP1. We also found that the cortex and hippocampus depend on different mechanisms for Aβ clearance. In this study, we attempted to increase Aβ clearance in the hippocampus by increasing the biogenesis of lysosomes in astrocytes. We transfected *in vitro* and *in vivo* murine astrocytes with a viral vector to deliver exogenous transcription factor EB. This transcription factor is known to stimulate lysosome biogenesis.

For this study, I was responsible for the primary astrocyte cultures, the plasmid transfection of the cells, applying the FAM-Aβ42 to the cell cultures, and then washing the wells in order to quantify degradation. I also performed the stereotactic injection of the viral vector into the mice, as well as a second surgery at a later time in order to insert the guide cannula so that *in vivo* microdialysis could be completed. I ensured that all of the samples from the microdialysis were collected and properly stored, and also

administered Compound E. Once the experiments were complete, I harvested the mouse brains for immunostaining and microscopic evaluation. I also performed ELISAs to measure Aβ40 and Aβ42 levels in transfected mice for comparison to the ISF samples.

This paper has been cited in 94 other publications, including publications in high-influence journals such as the Journal of Experimental Medicine (impact factor 10.790), the EMBO Journal (impact factor 9.792), the Journal of Cell Biology (impact factor 8.784), and Trends in Neurosciences (impact factor 17.755).

Neurobiology of Disease

Enhancing Astrocytic Lysosome Biogenesis Facilitates Aβ Clearance and Attenuates Amyloid Plaque Pathogenesis

Qingli Xiao,[1] Ping Yan,[1] Xiucui Ma,[2,3] Haiyan Liu,[2] Ronaldo Perez,[1] Alec Zhu,[1] Ernesto Gonzales,[1] Jack M. Burchett,[1] Dorothy R. Schuler,[1] John R. Cirrito,[1] Abhinav Diwan,[2,3]* and Jin-Moo Lee[1]*

[1]Department of Neurology and the Hope Center for Neurological Disorders and [2]Division of Cardiology and Center for Cardiovascular Research, Washington University School of Medicine, St. Louis, Missouri 63110, and [3]John Cochran VA Medical Center, St. Louis, Missouri 63108

In sporadic Alzheimer's disease (AD), impaired Aβ removal contributes to elevated extracellular Aβ levels that drive amyloid plaque pathogenesis. Extracellular proteolysis, export across the blood–brain barrier, and cellular uptake facilitate physiologic Aβ clearance. Astrocytes can take up and degrade Aβ, but it remains unclear whether this function is insufficient in AD or can be enhanced to accelerate Aβ removal. Additionally, age-related dysfunction of lysosomes, the major degradative organelles wherein Aβ localizes after uptake, has been implicated in amyloid plaque pathogenesis. We tested the hypothesis that enhancing lysosomal function in astrocytes with transcription factor EB (TFEB), a master regulator of lysosome biogenesis, would promote Aβ uptake and catabolism and attenuate plaque pathogenesis. Exogenous TFEB localized to the nucleus with transcriptional induction of lysosomal biogenesis and function *in vitro*. This resulted in significantly accelerated uptake of exogenously applied Aβ42, with increased localization to and degradation within lysosomes in C17.2 cells and primary astrocytes, indicating that TFEB is sufficient to coordinately enhance uptake, trafficking, and degradation of Aβ. Stereotactic injection of adeno-associated viral particles carrying TFEB driven by a glial fibrillary acidic protein promoter was used to achieve astrocyte-specific expression in the hippocampus of APP/PS1 transgenic mice. Exogenous TFEB localized to astrocyte nuclei and enhanced lysosome function, resulting in reduced Aβ levels and shortened half-life in the brain interstitial fluid and reduced amyloid plaque load in the hippocampus compared with control virus-injected mice. Therefore, activation of TFEB in astrocytes is an effective strategy to restore adequate Aβ removal and counter amyloid plaque pathogenesis in AD.

Key words: **Alzheimer's disease; amyloid; astrocytes; lysosomes; TFEB**

Introduction

Astrocytes are the most abundant cell type in the brain and play a critical role in maintaining synaptic transmission and neuronal health in homeostasis (Eroglu and Barres, 2010). Astrocytes are activated in response to injury, with neurodegeneration (Barres, 2008), and in preclinical stages of Alzheimer's disease (AD; Schipper et al., 2006; Owen et al., 2009; Carter et al., 2012). Activated astrocytes surround amyloid plaques and neurofibrillary tangles, which are the neuropathological hallmarks of advanced AD (Funato et al., 1998; Nagele et al., 2003). Interestingly, in these studies, astrocytes demonstrate immunoreactivity for amyloid material, and experimental observations confirm that astrocytes can take up amyloid plaques and precursor Aβ peptides in animal models of AD (Wyss-Coray et al., 2003; Koistinaho et al., 2004). Despite these intriguing observations, the role of astrocytes in AD pathogenesis is under studied.

In AD, an imbalance between the production and degradation of Aβ peptides drives increased extracellular levels in the interstitial fluid (ISF; Hardy and Selkoe, 2002) resulting in their concentration-dependent oligomerization and deposition as amyloid plaques (Lomakin et al., 1997). Recent studies implicate impaired Aβ removal as the dominant underlying mechanism in individuals with the more common sporadic forms of AD (Mawuenyega et al., 2010). Insights from animal models indicate that in addition to extracellular proteolysis and transport across the blood–brain barrier, Aβ can be taken up by astrocytes (Wyss-Coray et al., 2003; Koistinaho et al., 2004) and microglia (Mandrekar et al., 2009). We have observed that impairing astrocyte activation by ablation of intermediate filament proteins, glial fibrillary acidic protein (GFAP) and vimentin, results in increased plaque load (Kraft et al., 2013) pointing to a prominent role for activated astrocytes in countering amyloid pathogenesis. However, whether astrocyte function is inadequate (Wyss-Coray et al., 2003), and therefore needs to be stimulated to accelerate amyloid removal, remains unknown.

Aβ is taken up and trafficked to the lysosomes for degradation in astrocytes (Basak et al., 2012). Impairment of lysosome func-

Received Sept. 3, 2013; revised May 29, 2014; accepted June 6, 2014.

Author contributions: Q.X., J.R.C., A.D., and J.-M.L. designed research; Q.X., P.Y., X.M., H.L., R.P., A.Z., E.G., J.M.B., D.R.S., J.R.C., and A.D. performed research; Q.X., P.Y., X.M., H.L., J.M.B., J.R.C., A.D., and J.-M.L. analyzed data; Q.X., J.R.C., A.D., and J.-M.L. wrote the paper.

This study was supported by grants from Alzheimer's Association (NIRG 12-242588 to A.D.), Brightfocus Foundation (A2012151 to J.R.C.), and from the National Institutes of Health (R21 NS082529 to J.-M.L. and R01 AG042513 to J.R.C.). The authors thank Dr. Katherine Ponder, Washington University, for assistance with Cathepsin assays.

*A.D. and J.-M.L. contributed equally to this work.

The authors declare no competing financial interests.

Correspondence should be addressed to either of the following: Dr. Jin-Moo Lee, Professor of Neurology; 660 South Euclid Avenue, CB 8111, St. Louis, MO 63110, E-mail: leejm@wustl.edu; or Dr. Abhinav Diwan, Assistant Professor of Medicine, 4940 Parkview Place, CSRB 827, St. Louis, MO 63110, E-mail: adiwan@dom.wustl.edu.

DOI:10.1523/JNEUROSCI.3788-13.2014

 0270-6474/14/349607-14$15.00/0

tion with aging (Kato et al., 1998; Cuervo and Dice, 2000; Wolfe et al., 2013), or with loss of presenilin, as observed in familial AD, (Lee et al., 2010; Coen et al., 2012) has been implicated in AD pathogenesis. It is suspected to be the underlying mechanism for accumulation of Aβ and phagocytosed amyloid material within astrocytes (Funato et al., 1998; Wyss-Coray et al., 2003), which may paradoxically promote amyloid plaque progression (Nagele et al., 2003). Recent studies demonstrate that activation of ubiquitously expressed transcription factor EB (TFEB) coordinately stimulates lysosome biogenesis and cellular trafficking pathways to promote breakdown of lipids and proteins to generate nutrients (Sardiello et al., 2009; Settembre et al., 2011, 2013b) and remove abnormal aggregates in lysosome storage disorders (Settembre et al., 2013a). In this study, we evaluated whether targeted expression of TFEB in astrocytes stimulates uptake and lysosomal degradation of Aβ to reduce ISF Aβ levels and attenuate amyloid plaque pathogenesis, in a mouse model of AD.

Materials and Methods

Reagents. Aβ1–42 was purchased from American Peptide; FAM-Aβ42 from AnaSpec; LysoTracker Red DND-99 from Invitrogen; and trifluoroacetic acid, 1,1,1,3,3,3-hexafluoro-2-propanol, bafilomycin A1, heparin, biotin-labeled transferrin, and Dynasore from Sigma.

Aβ preparation. Aβ42 was prepared as described previously (Hu et al., 2009). Briefly, dried peptide was pretreated with neat trifluoroacetic acid, distilled under nitrogen, washed with 1,1,1,3,3,3-hexafluoro-2-propanol, distilled under nitrogen, and stored at −20°C. The peptide was diluted in DMSO to a final concentration of 200 μM. In this form, Aβ is in its monomeric form, but aggregates in culture medium (Gong et al., 2003) into oligomeric Aβ species.

Primary astrocyte cultures. Murine cortical primary astrocytes were cultured from postnatal day 2 pups. Cortices were dissected from the brain, washed with HBSS, and treated with 0.25% trypsin/EDTA for 15 min at 37°C. Following trypsin digestion, the tissue was resuspended and triturated in DMEM with 10% FBS and 100 U/ml penicillin/streptomycin. The cell suspension was then plated into T-75 flasks coated with poly-D-lysine. The medium of the mixed glial cultures was changed every 3 d. Once the cells reached confluence, they were shaken at 180 rpm for 30 min to remove the microglial cells. The adherent cells were shaken at 240 rpm for an additional 6 h to remove the oligodendrocyte precursor cells. The astrocyte-enriched cultures were then passed into 12-well plates for experiments.

Plasmid construction, cell transfection, and lentivirus transduction. Mouse TFEB cDNA containing an N-terminal-linked FLAG or Cerulean fluorophore was cloned into a pAAV vector containing the CMV promoter (pAAV-CMV-FLAG-TFEB). For specific expression of TFEB in astrocytes, a GFAP promoter (gfa2; Brenner et al., 1994) was used to drive TFEB expression in AAV vector (pAAV-GFAP-FLAG-TFEB) or lentiviral vector (LV-GFAP-FLAG-TFEB). C17.2 neural progenitor cells were transfected with pAAV-CMV-FLAG-TFEB or the control vectors using Lipofectamine 2000 (Invitrogen) for 48 h and harvested for further analysis. For transduction of lentiviral vectors in astrocytes, the virus was added to the cells (multiplicity of infection of 5) and incubated at 37°C for 48 h. Fresh medium was then added and the cells were cultured for 8–10 d before performing experimental assays, changing the medium every 3 d. We observed >90% efficiency for transfection or transduction of exogenous TFEB (or GFP as control) in these *in vitro* studies.

Flow cytometry. C17.2 cells were incubated with LysoTracker Red (1 μM) for 15 min and subjected to flow cytometry on FACScan instrument (Becton-Dickinson). Cyflogic software (CyFlo) was used to analyze 20,000 events per run.

Aβ uptake and degradation. C17.2 cells were plated in 8-well chamber slides, and 500 nM FAM-Aβ42 was added for 1–4 h. The cells were stained with LysoTracker Red (100 nM) before confocal imaging. To quantify uptake, synthetic Aβ42 (500 nM) was applied to C17.2 cells and astrocytes for varying times. The cells were washed with PBS three times, trypsinized, and lysed in RIPA buffer. To quantify degradation, media containing Aβ42 was removed and cells were thoroughly washed after 4 h incubation. At varying times after washing, the cells were trypsinized and lysed for ELISA. Bafilomycin A1 (100 nM) was added to the cells 30 min before harvest to inhibit lysosome acidification.

Transferrin internalization. Transferrin uptake assay was performed as described previously (Xiao et al., 2012). Briefly, primary astrocytes were cultured in serum-free medium for 2 h, and then incubated with biotinylated transferrin (20 μg/ml) in serum-free medium for 5 min at 37°C. Cells were placed on ice, washed with ice-cold PBS, and then subsequently incubated three times for 10 min on ice in 25 mM MesNa, pH 5.0, containing 150 mM NaCl and 50 μM deferoxamine mesylate to remove surface bound transferrin. Cell lysate was immunoblotted with anti-biotin antibody (Cell Signaling Technology) to detect internalized transferrin.

Dextran uptake assay. Primary astrocytes were incubated with 70 kDa dextran-TMR conjugate (10 μM) for the indicated duration. Thereafter, cells were washed thoroughly and trypsinized, followed by flow cytometric analysis with analysis of 20,000 events per run.

Animal model studies. B6C3-Tg (APPswe/PS1ΔE9)85Dbo/Mmjax (also known as APP/PS1) transgenic mice, obtained from The Jackson Laboratory (Jankowsky et al., 2004), were injected with AAV8 viral particles (generated by the Hope Center Viral Core at Washington University), as described previously (Xiao et al., 2012). For plaque load studies, APP/PS1 mice were injected with 2 μl of AAV8-GFAP-FLAG-TFEB or AAV8-GFAP-eGFP (1.5×10^{12} viral particles/ml) into bilateral hippocampi at 6 months of age. Mice were killed 4 months later. One hemisphere was fixed and coronal sections (50 μm) were cut for histological analysis (X-34 staining and HJ3.4 immunostaining). The other hemisphere was immediately dissected, snap frozen on dry ice, and stored at −80°C for biochemical analysis (ELISA and Western blot). To detect the Aβ level in predepositing mice, the abovementioned AAV viral vectors were injected into the hippocampi of APP/PS1 mice at 3 months of age, and the animals were killed 2 months later. All animal care and surgical procedures were approved by the Animal Studies Committee of Washington University School of Medicine in accordance with guidelines of the U.S. National Institutes of Health.

In vivo *microdialysis.* Two-month-old AAP/PS1 transgenic mice were transduced in the hippocampus with AAV8-GFAP-FLAG-TFEB and AAV8-GFAP-GFP particles, as above, and studied 4 weeks later by *in vivo* microdialysis, as previously described (Cirrito et al., 2003, 2011). Briefly, a guide cannula (BR-style; Bioanalytical Systems) was implanted and cemented with the tip at coordinates: bregma –3.1 mm, midline −2.5 mm, 1.2 mm below dura at a 12° angle. A 2 mm microdialysis probe was then inserted into the hippocampus that contained a 38 kDa MWCO semipermeable membrane (Bioanalytical Systems) allowing molecules smaller than this cutoff to diffuse into the probe. Aβ capable of entering the probe is dubbed "exchangeable Aβ" (Cirrito et al., 2003). The probe was flushed with 0.15% bovine serum albumin (Fisher Scientific) in an artificial CSF perfusion buffer at a constant rate (1.0 μl/min). The effluent was collected into a refrigerated fraction collector and assayed by sandwich ELISA for Aβx-40 and Aβx-42 peptides at the end of each experiment. All studies were initiated at the identical time of the day. During microdialysis, animals were housed in specially designed cages to permit free movement and *ad libitum* food and water while ISF Aβ was being sampled. Baseline levels of ISF Aβ were sampled every 90 min between hours 9 and 16 (after the microdialysis probe is inserted) and averaged to determine the "baseline ISF Aβ level" in each mouse. Absolute *in vivo* concentration of ISF eAβ for each mouse was determined by correcting for the 20.8% recovery (1.0 μl/min) as obtained by the interpolated zero flow method as described previously (Menacherry et al., 1992; Cirrito et al., 2003). At hour 16 ($t = 0$), a γ-secretase inhibitor Compound E (200 nM reverse microdialysis; synthesized by AsisChem), was administered directly to the hippocampus by adding the drug to the microdialysis perfusion buffer. ISF Aβ was then sampled every 60 min for an additional 6 h. This enabled measurement of the elimination half-life of endogenous ISF Aβ *in vivo* similar to (Cirrito et al., 2003).

Immunohistochemistry. Sections were incubated in 0.3% H_2O_2 in Tris-buffered saline (TBS) for 10 min, washed with TBS, blocked with 3% dry milk in TBS-X (0.25% Triton X-100 in TBS) for 1 h, and incubated with HJ3.4 antibody (anti-Aβ-1–13; Roh et al., 2012) overnight. A solution

from Vectastain ABC kit (1:400) was applied to brain slices for 1 h, followed by 0.025% 3–3′ diaminobenzidine tetrachloride in 0.25% NiCl and 0.05% H_2O_2 for 10–15 min. The slices were placed on glass slides, dried overnight, dehydrated, and mounted. Images were obtained with confocal microscope (Zeiss LSM).

X-34 plaque staining. Brain slices were mounted on SuperFrost Plus slides, permeabilized with 0.25% Triton X-100 for 30 min, and stained with X-34 (a generous gift from Robert Mach, Washington University) dissolved in 40% ethanol and 60% water, pH 10, for 20 min. Tissue was then thoroughly rinsed in PBS and mounted with Fluoromount mounting media.

Plaque quantification. Brain sections (50 μm) were collected every 300 μm from rostral anterior commissure to caudal hippocampus. Sections were stained with X-34 or immunostained with HJ3.4 antibodies ($n = 10$ per group, 5 male and 5 female). Four slices per animal were used. NanoZoomer Digital Scanner (Hamamatsu Photonics) was used to create high-resolution digital images of the stained brain slices. The total area of plaque coverage in the hippocampus or piriform cortex (devoid of viral transduction) was measured using NIH ImageJ software and expressed as percentage total area for each slice. Results from $n = 4$ sections were averaged to represent each animal.

Immunofluorescence. Fixed cells or paraffin-embedded brain sections were washed with PBS, permeabilized with 0.3% Triton X-100 in PBS for 20 min, and blocked. For double labeling, a mixture of the following antibodies was used: rabbit anti-FLAG (Sigma; 1:500), rat anti-LAMP1 (Santa Cruz Biotechnology; 1:50), mouse anti-TFEB (MyBioSource; 1:50), rabbit anti-TFEB (Bethyl Laboratories; 1:100), rabbit anti-GFAP (Sigma; 1:100), rabbit anti- Iba1 (Wako Chemicals; 1:1000),and mouse anti-NeuN (Sigma; 1:1000). A secondary antibody mixture of Alexa Fluor 488-conjugated goat anti-rabbit IgG and Alexa Fluor 594-conjugated goat anti-rat IgG (Invitrogen), or Cy3-conjugated donkey anti-rabbit IgG (Jackson ImmunoResearch) and Alexa Fluor 488-conjugated donkey anti-mouse IgG (Invitrogen) was applied. Cells or sections were examined by confocal microscope (Zeiss LSM).

Stereological analysis. The sections were stained with 0.05% cresyl violet solution. The total neuron number in CA1 stratum pyramidale (sp) and CA3 sp in the dorsal hippocampus was assessed using a computer-based stereology system (Stereo Investigator; MicroBrightField). Neuron numbers were estimated with the optical fractionator (West et al., 1991). Cresyl violet-stained cells were counted in four equally spaced 50 μm sections in the dorsal hippocampus of CA1 sp and CA3 sp, respectively. Cresyl violet stained cells with nuclei imaged within the inclusive zone of each dissector frame were counted. Results were reported in units of density (cells per mm^3).

Aβ ELISA. Aβ in cell lysates from transfected C17.2 cells and transduced astrocytes were detected by sandwich ELISA, as previously described (Verges et al., 2011). To detect total Aβ in the hippocampus in 5-month-old mice, dissected tissue was sequentially homogenized in PBS followed by RIPA buffer (50 mM Tris-HCl, 150 mM NaCl, 1% Triton X-100, 0.5% deoxycholate, 0.1% SDS, and 1× protease inhibitor cocktail, to obtain detergent soluble Aβ at an age when plaques are not observed; Yan et al., 2009), and samples were pooled for analysis. In aged mice (10 months old, when plaques are abundant), hippocampal tissues were sequentially homogenized in PBS followed by 5 M guanidine in TBS, pH 8.0 (to extract fibrillar and membrane bound Aβ). For ELISA assays, Aβx-40 and Aβx-42 peptides were captured with mouse monoclonal-coating antibodies HJ2 (anti-Aβ35–40) and HJ7.4 (anti-Aβ37–42) or HJ5.1 (anti-Aβ13–28), respectively (Kim et al., 2009). HJ5.1 (anti-Aβ13–28), a biotinylated antibody targeting the central domain, and HJ3.5 (anti-Aβ1–13, provided by Dr. David Holtzman, Washington University School of Medicine, St. Louis, MO), which targets the N-terminal amino acids, were used as the detecting antibody, followed by streptavidin-poly-HRP-40 (Fitzgerald Industries). All ELISA assays were developed using Super Slow ELISA TMB (Sigma) and absorbance read on a Bio-Tek Epoch plate reader at 650 nm. Standard curves were generated from synthetic human Aβ1–40 or Aβ1–42 peptides (American Peptide).

Quantitative PCR. Real-time PCR was performed as described previously (Ma et al., 2012). Briefly, total RNA was prepared from transfected C17.2 cells or AAV-transduced hippocampus using an RNA-easy mini kit (Qiagen), and cDNA was synthesized with 1 μg of total RNA using SuperScript III first-strand synthesis system (Invitrogen). One microliter of cDNA template was mixed with 12.5 μl of 2 × SYBR Green PCR Master Mix (Invitrogen) and subjected to quantitative PCR in triplicate under the following conditions: 50°C, 2 min; 95°C, 10 min; followed by 40 cycles of 95°C, 15 s; 60°C, 1 min in the ABI7500 Fast RealTime PCR system. The housekeeping gene *GAPDH* was also amplified in parallel as a reference for the quantification of transcripts. Primer sequences used are shown in Table 1).

Table 1. Primer sequences employed for quantitative PCR analysis for indicated murine genes

Gene	Forward (5′–3′)	Reverse (5′–3′)
LAMP1	ACATCAGCCCAAATGACACA	GGCTAGAGCTGGCATTCATC
CATHB	AAATCAGGAGTATACAAGCATGA	GCCCAGGGATGCGGATGG
CATHD	CTGAGTGGCTTCATGGGAAT	CCTGACAGTGGAGAAGGAGC
ADAM17	AGGACGTAATTGAGCGATTTTGG	TGTTATCTGCCAGAAACTTCCC
ADAM10	GTGCCAAACGAGCAGTCTCA	ATTCGTAGGTTGAACTGTCTTCC
BACE1	CAGTGGGACCACCAACCTTC	GCTGCCTTGATGGACTTGAC
PSEN1	TGCACCTTTGTCCTACTTCCA	GCTCAGGGTTGTCAAGTCTCTG
PEN2	ATCTTGGTGGATTTGCGTTCC	GCGCCAAACATAGCCTTTGATTT
LDLR	CGCGGATCTGATGCGTCGCT	CGGCCCTGGCAGTTCTGTGG
LRP1	AACCCCTGCAGTGTCAACAA	GGAGCGAGTCGTCTCTGATG
APOE	CTGACAGGATGCCTAGCCG	CGCAGGTAATCCCAGAAGC
APOJ	GCCAGTGTGAAAAGTGCCAG	GTTAGCCTGGGCAGGATTGT
MMP2	CCTGGACCCTGAAACCGTG	TCCCCATCATGGATTCGAGAA
MMP9	GGACCCGAAGCGGACATTG	GAAGGGATACCCGTCTCCGT
IDE	TAATCCGGCCATCCAGAGAAT	CCAGCTCTAGTCCACGGTATT
NEP	GGCCTCCCTTCCAGAGACTA	ACGAATCAGTCTGGCCACAG
GAPDH	ACTCCCACTCTTCCACCTTC	TCTTGCTCAGTGTCCTTGC

Cathepsin assay. Cathepsin activity was measured as described previously (Baldo et al., 2011) with slight modifications. Cell pellets or brain tissues were homogenized in 100 mM sodium acetate, pH 5.5, with 2.5 mM EDTA, 0.01% Triton X-100, and 2.5 mM DTT. For the Cathepsin B assay, the supernatant was incubated with 100 μM Z-Arg-Arg-AMC (Bachem) at pH 6.0. The fluorescent intensity of the cleavage product was determined by excitation at 355 nm and emission at 460 nm using kinetic readings in a TECAN Infinite M200 Pro microplate reader (Tecan), and comparison was performed with a standard (7-amino-4-methylcoumarin, AMC; AnaSpec). The Cathepsin D assay was performed at pH 4.0 by incubating the supernatant with 10 μM substrate 7-methoxycoumarin-4-acetyl (Mca)-Gly-Lys-Pro-Ile-Leu-Phe-Phe-Arg-Leu-Lys-2,4 nitrophenyl (Dnp)-D-Arg-NH_2, with Mca-Pro-Leu-OH (Enzo Life Sciences) as the standard; fluorescent intensity was determined with 320 nm excitation at 420 nm emission using the microplate reader.

Immunoblotting. Protein samples were run on 4–12% Bis-Tris gels. Blots were probed with the following antibodies: FLAG (1:1000), TFEB (1:500), LAMP1 (1:500), Cathepsin B (Abcam; 1:500), Cathepsin D (Santa Cruz Biotechnology; 1:200), low-density lipoprotein receptor (LDLR; Novus; 1:500), LDL-receptor related peptide-1 (LRP1; Abcam; 1:500), and Actin (Sigma; 1:2000). Normalized band intensity was quantified using ImageJ software.

Statistical analysis. All data are shown as mean ± SEM. Data were analyzed by two-tailed Student's *t* test for detecting significant differences between two groups. Differences among groups were analyzed by one-way ANOVA followed by *post hoc* Tukey's test. Differences were deemed statistically significant at $^*p < 0.05$ and $^{**}p < 0.01$.

Results

Exogenous TFEB expression stimulates lysosome biogenesis in neural cells, *in vitro*

Astrocytes take up Aβ and amyloid material for lysosomal degradation (Wyss-Coray et al., 2003; Koistinaho et al., 2004; Basak et al., 2012), but age-related lysosome dysfunction is suspected to underlie Aβ accumulation within astrocytes in elderly individuals (Funato et al., 1998) and in patients with AD (Nagele et al.,

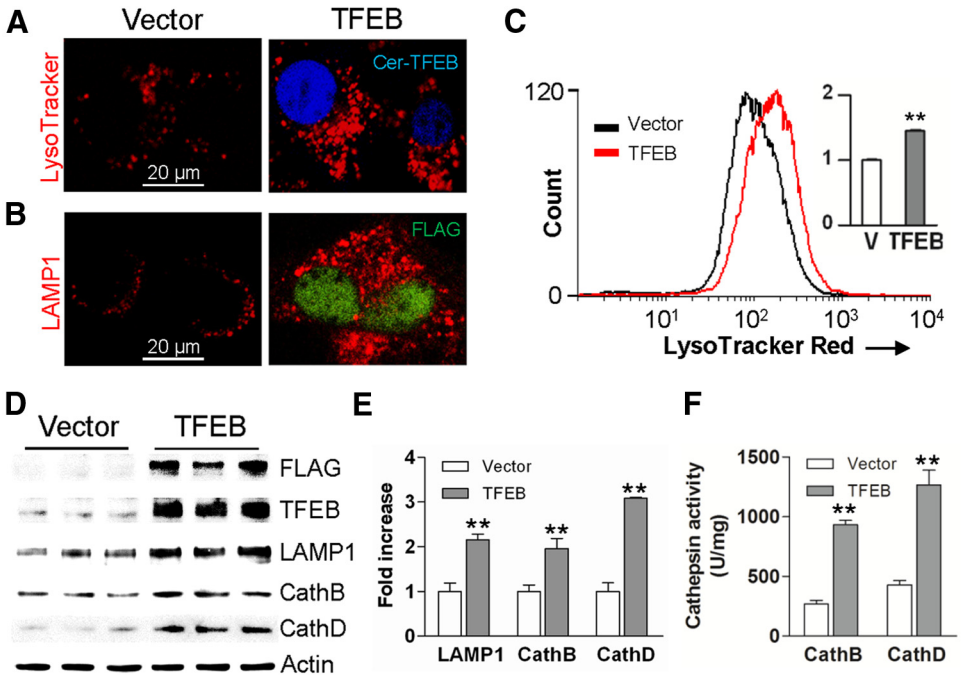

Figure 1. TFEB stimulates lysosome biogenesis and function. ***A***, Representative confocal images demonstrating LysoTracker Red expression in Cerulean-tagged TFEB-transfected (Cer-TFEB) C17.2 cells versus empty vector transfected controls. Representative of $n = 4$ independent experiments. ***B***, Representative confocal images demonstrating LAMP1 expression in C17.2 cells transfected with FLAG-tagged TFEB versus empty vector transfected controls. Representative of $n = 4$ experiments. ***C***, Flow cytometric analysis of LysoTracker Red staining in cells transfected with FLAG-tagged TFEB or empty vector (V; as control), with quantification of mean fluorescence expressed as fold over control (inset). $N = 3$/group. ***D***, ***E***, Immunoblots (***D***) and quantification (***E***) of LAMP1 and Cathepsin B and D expression in cells transfected as in ***C***. ***F***, Cathepsin B and D activity in cells transfected as in ***C***. $N = 4$/group; $^{**}p < 0.01$.

2003). TFEB, a recently described basic helix-loop-helix transcriptional activator, stimulates lysosome biogenesis with activation of lysosomal degradative pathways (Sardiello et al., 2009; Settembre et al., 2011, 2013b; Roczniak-Ferguson et al., 2012), and cellular trafficking pathways (Medina et al., 2011; Peña-Llopis et al., 2011). Accordingly, we tested the hypothesis that enhancing lysosomal degradative pathways in astrocytes by exogenous expression of TFEB will counter amyloid pathogenesis. To confirm that TFEB stimulates lysosome biogenesis and function in neural cells, we exogenously expressed murine TFEB in a mouse neural progenitor C17.2 cell line (which can transdifferentiate into astrocytes; Zang et al., 2008), and examined lysosome abundance, and expression and function of Cathepsin B and D, which are two lysosomal enzymes implicated in Aβ catabolism and AD pathogenesis (Sun et al., 2008; Butler et al., 2011; Schuur et al., 2011; Yang et al., 2011; Avrahami et al., 2013). Exogenously expressed Cerulean-tagged (Fig. 1*A*) or FLAG-tagged TFEB (Fig. 1*B*) localized to the nucleus indicating that it was transcriptionally active (Sardiello et al., 2009; Settembre et al., 2012) with an increase in abundance of acidic organelles stained with LysoTracker Red (Fig. 1*A*,*C*) or lysosome membrane protein, LAMP1 (Fig. 1*B*), indicating stimulation of lysosome biogenesis compared with the nontransfected cells. Exogenous expression of TFEB also resulted in transcriptional upregulation of lysosomal genes, LAMP1 and Cathepsin B and D (by 21, 26, and 34%, respectively, over vector control; $n = 4$/group, $p < 0.05$). This was associated with >6-fold increase in TFEB protein expression ($p < 0.01$, $n = 3$/group), and a 2- to 3-fold increase in expression of LAMP1, Cathepsin B, and Cathepsin D proteins (Fig. 1*D*,*E*). An ~3-fold increase in Cathepsin B and D activity was observed in TFEB transfected cells compared with controls (Fig. 1*F*). Collectively, these results confirm that exogenous TFEB transcriptionally upregulates lysosome abundance and stimulates activity of lysosomal enzymes, *in vitro*.

Exogenous TFEB expression enhances Aβ uptake and degradation

To determine the effect of TFEB on the kinetics of Aβ uptake and its subcellular localization, C17.2 cells were transfected with TFEB or empty vector and incubated with 500 nM FAM-labeled Aβ42 for increasing periods of time (1, 2, and 4 h) at 37°C. At these time points, cells were imaged using confocal microscopy with colabeling for LysoTracker Red, which is selectively taken up in acidic vesicles, i.e., late endosomes and lysosomes (Sardiello et al., 2009). Punctate intracellular Aβ was first apparent within 1 h, and progressively increased thereafter (Fig. 2*A*), indicating that FAM-Aβ42 uptake was time dependent. Importantly, all intracellular FAM-Aβ42 eventually localized to LysoTracker-stained vesicles, suggesting that Aβ is taken up and trafficked into lysosomes. Notably, TFEB enhanced Aβ uptake with increased colocalization of Aβ with LysoTracker-stained organelles at all the time points examined. To confirm these observations, we measured intracellular Aβ levels in C17.2 cells transfected with TFEB or empty vector for 48 h, after application of Aβ42 (500 nM) for increasing periods of time (1, 2, 4, and 8 h). The cells were thoroughly washed and trypsinized to digest surface-bound Aβ, followed by lysis, and intracellular Aβ42 was quantified with ELISA. Immunodetectable levels of intracellular Aβ levels progressively increased in control transfected cells (Fig. 2*B*), as imaged above (Fig. 2*A*). TFEB-transfected cells demonstrated significantly higher levels of intracellular Aβ42 compared with controls (Fig. 2*B*), suggesting faster rates of Aβ internalization. We next determined whether TFEB affects intracellular Aβ degradation. The cells were incubated with Aβ42 for 4 h and then thoroughly

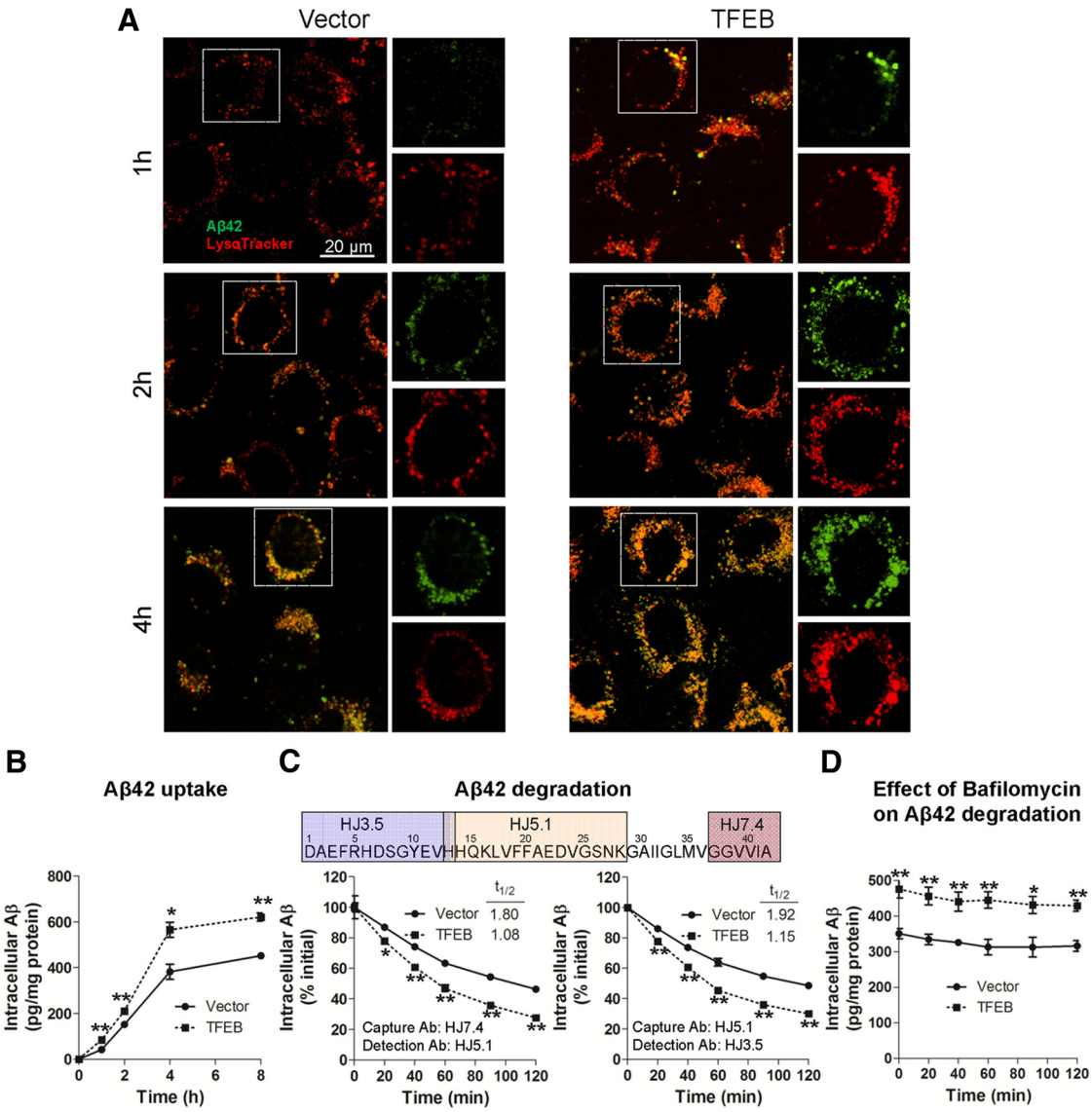

Figure 2. TFEB enhances Aβ uptake and degradation in C17.2 cells. ***A***, Representative confocal images of C17.2 cells transfected with TFEB or empty vector, and incubated with 500 nM FAM-Aβ42 at varying times, as indicated and imaged with LysoTracker Red colabeling. Representative of $n = 3$ independent experiments. ***B***, C17.2 cells were transfected with TFEB or empty vector for 48 h, and subsequently incubated with Aβ42 (500 nM) for an additional 1–8 h, and intracellular Aβ42 was analyzed by ELISA at the time points indicated. $N = 3$/group per time point. ***C***, C17.2 cells were transfected with TFEB or empty vector for 48 h and Aβ42 (500 nM) was applied for 4 h, followed by its removal. Cells were then thoroughly washed. At varying times after washing (as indicated), the cells were trypsinized, lysed, and intracellular Aβ42 was quantified by ELISA using two separate strategies. Specific antibodies used (refer to schematic, top) are noted (bottom). $N = 3$/group per time point. ***D***, Cells treated as in ***C*** with the addition of Bafilomycin A1 (100 nM) for 30 min before washing out the Aβ and cultured in its presence until the cells were collected for assay. $N = 4$/group; $^{*}p < 0.05$, $^{**}p < 0.01$.

washed. At varying times thereafter, the cells were trypsinized (to digest surface-bound Aβ) and lysed for assessment of intracellular Aβ levels. Our results demonstrate that the rate of decline of intracellular Aβ levels was significantly enhanced by TFEB expression compared with controls (Fig. 2*C*). This was reflected in the shortened half-life ($t_{(1/2)}$) in TFEB-transfected cells, and confirmed with an alternate Aβ peptide capture and detection strategy using distinct epitopes. These data suggest that TFEB enhances both the uptake and complete degradation of Aβ. To determine whether TFEB-mediated elimination of Aβ proceeded via lysosomal degradation, we cultured cells in the presence of Bafilomycin A1, a proton pump inhibitor that blocks lysosome acidification and impairs function (Yamamoto et al., 1998; Mousavi et al., 2001), beginning 30 min before removal of Aβ42 from the medium. Bafilomycin A1 treatment largely prevented the decline in intracellular Aβ42 levels (Fig. 2*D*), to the same extent in both TFEB-transfected and control cells. These data indicate that clearance of intracellular Aβ requires normal lysosome function, and TFEB enhances Aβ removal via stimulating lysosomal function.

Recent studies have ascribed a prominent role for receptor-mediated uptake of Aβ via LDLR (Basak et al., 2012) and LRP1 (Kanekiyo et al., 2011; Verghese et al., 2013), as well as via macropinocytosis, a heparan sulfate proteoglycan-mediated process (Kanekiyo et al., 2011). Therefore, to confirm whether TFEB accelerates Aβ uptake and degradation in astrocytes and to examine the mechanisms involved, we lentivirally transduced primary murine astrocytes with TFEB or GFP (as control) and examined intracellular Aβ after incubation with Aβ42 for 4 h in the presence of Dynasore (a dynamin-specific inhibitor of endocytosis),

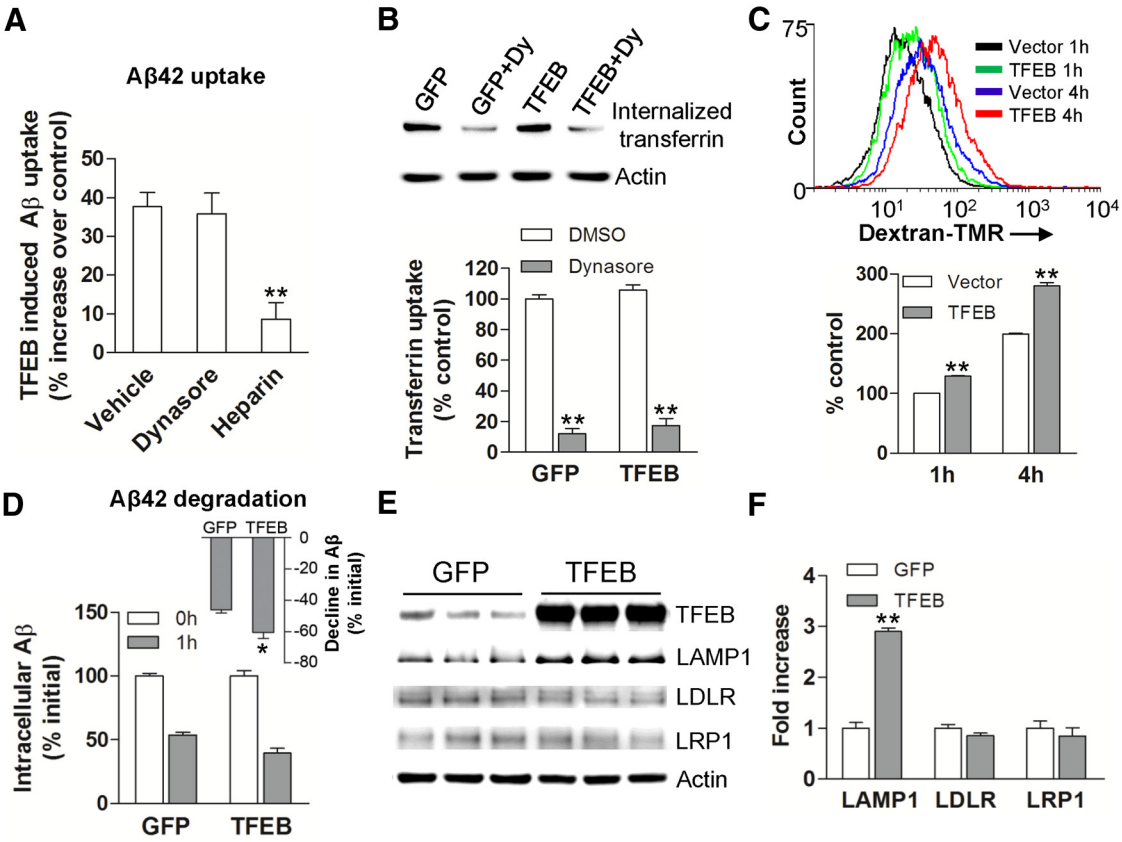

Figure 3. TFEB stimulates Aβ uptake and degradation in primary astrocytes. ***A***, Percentage increase in Aβ uptake over a duration of 4 h in primary astrocytes transduced with TFEB over those transduced with GFP (as control), in the presence of Dynasore (100 μM), heparin (100 μg/ml; ~18 U/ml), and vehicle (as control). $N = 3$ experiments. ***B***, Transferrin uptake in primary astrocytes transduced with TFEB or GFP (as control). $N = 3$/group. Dy, Dynasore. ***C***, Flow cytometric analysis with representative tracings (top) and quantitation of mean fluorescence (bottom) for 70 kDa dextran-TMR uptake in primary astrocytes transduced with TFEB or empty vector (as control) for the indicated duration. $N = 4$/group. ***D***, Primary astrocytes were transduced with TFEB or GFP (as control) and incubated with Aβ for 4 h, followed by washing and trypsinization. Intracellular Aβ levels were measured thereafter at T (time) = 0 and 1 h. Inset shows percentage reduction in Aβ levels over this duration. $N = 3$ experiments. ***E***, ***F***, Immunoblot and quantitation of LAMP1, LRP1, and LDLR expression in TFEB- transduced versus GFP-transduced primary astrocytes. $N = 3$/group; $^*p < 0.05$, $^{**}p < 0.01$.

heparin (to antagonize heparan sulfate proteoglycans), or diluent as control. As shown in Figure 3*A*, TFEB expression (~9-fold over control; Fig. 3*E*) resulted in significantly increased intracellular Aβ levels compared with control transduced cells. This increase was not affected by Dynasore treatment, but was significantly attenuated by heparin. Consistent with this observation, we found that TFEB transduction did not upregulate transferrin-receptor endocytosis (which was inhibited by Dynasore treatment; Fig. 3*B*), but significantly upregulated the internalization of 70 kDa dextran (Fig. 3*C*), which is known to occur via fluid-phase macropinocytosis (Fan et al., 2007). Additionally, as observed with C17.2 cells (Fig. 2*B*), TFEB transduction accelerated the decline in intracellular Aβ in primary astrocytes (Fig. 3*D*). Consistent with the observation of a lack of effect of TFEB on endocytosis of Aβ, we did not detect TFEB-binding CLEAR sites (Palmieri et al., 2011) in the promoters of murine LDLR and LRP1, and TFEB did not affect their transcript levels (data not shown) or protein abundance (Fig. 3*E*,*F*). Importantly, TFEB induced upregulation of lysosomal protein, LAMP1, in astrocytes indicating increased lysosomal biogenesis, as observed in C17.2 cells (see above).These data suggest that TFEB may accelerate Aβ uptake via heparan sulfate proteoglycan binding and macropinocytosis (Mandrekar et al., 2009; Holmes et al., 2013).

AAV-mediated TFEB transduction in astrocytes induces lysosome biogenesis and upregulates Cathepsin activity, *in vivo*

Given the *in vitro* demonstration of TFEB-mediated enhancement of Aβ uptake and lysosomal degradation, we examined whether enhancing the cellular degradative capacity of astrocytes, *in vivo*, may be an effective strategy to reduce ISF Aβ levels and attenuate plaque pathogenesis in AD. Indeed, astrocytes demonstrate intracellular accumulation of Aβ-immunoreactive material in mouse models of AD, which may reflect a failure of catabolism (Wyss-Coray et al., 2003). Enhancement of lysosomal degradative capacity by exogenous TFEB expression may correct this underlying defect, as was observed with diverse conditions of lysosome dysfunction (Settembre et al., 2013a). To test this premise, we used a viral gene transfer approach to target TFEB expression to astrocytes in the hippocampus of 6-month-old APP/PS1 mice, at a stage of early plaque deposition and growth (Yan et al., 2009). N-terminal FLAG- tagged murine TFEB was packaged in an AAV8 vector driven by a human GFAP promoter, which was highly efficacious and specific in targeting astrocytes in our previous studies (Kraft et al., 2013). AAV8 carrying a GFAP promoter driving eGFP served as control. The viral particles were stereotactically injected into bilateral hippocampi of 6-month-old APP/PS1 mice. The hippocampus was chosen for viral target-

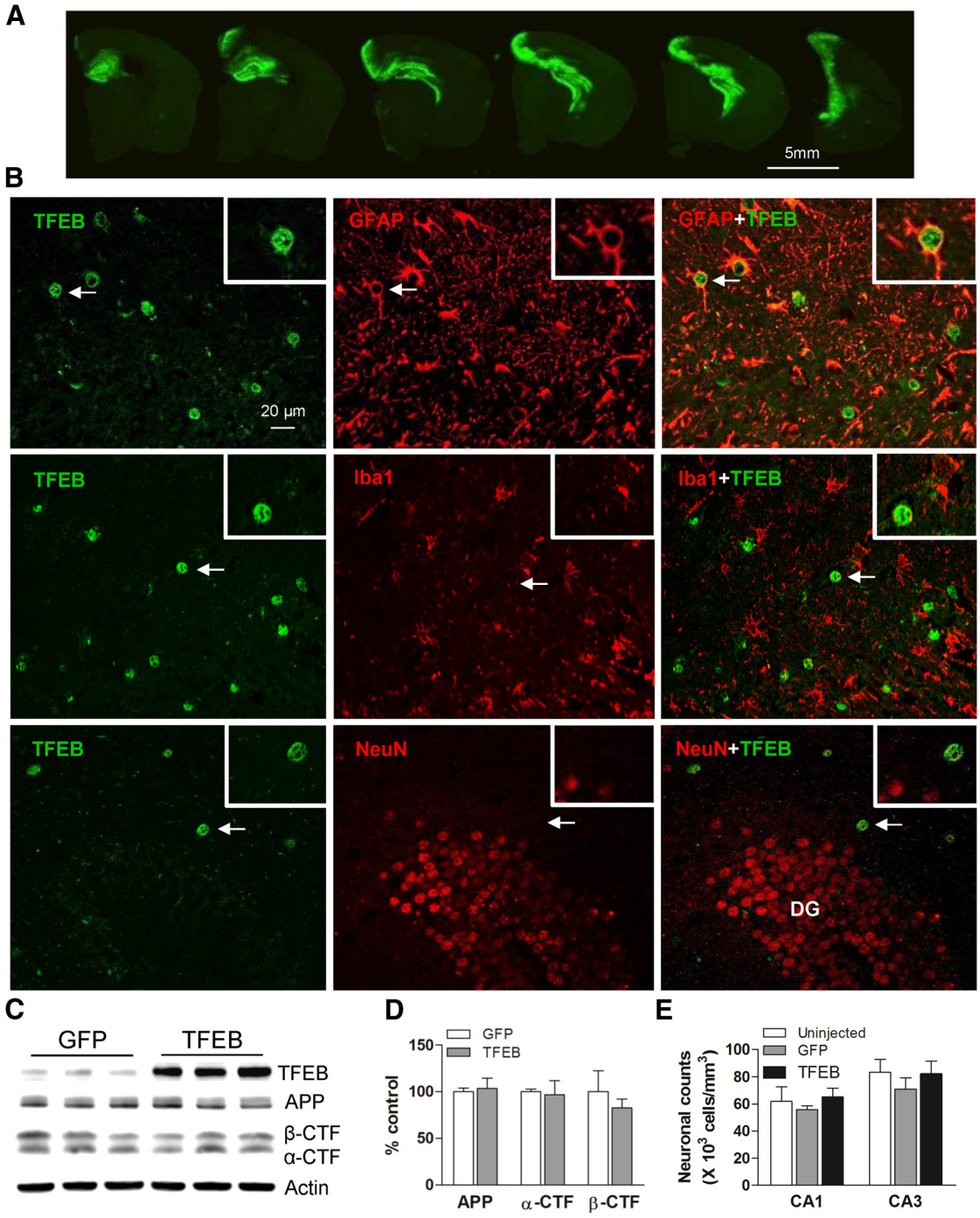

Figure 4. AAV8-mediated gene transfer of GFAP-promoter driven TFEB targets expression specifically to astrocytes. ***A***, Representative fluorescence images of GFP expression in the hippocampus of APP/PS1 mice injected with AAV8-GFAP-eGFP viral particles. Sequential images of brain sections confirm high transduction efficiency throughout the anterior hippocampus. ***B***, Representative confocal images demonstrating expression of TFEB (green) with GFAP (red, top), Iba-1 (red, middle), and NeuN (red, bottom) in the hippocampus of APP/PS1 mice injected with AAV8-GFAP-FLAG-TFEB particles, demonstrating astrocyte-specific expression of TFEB. The boxed inserts (upper right corner) demonstrate magnified images of individual TFEB-labeled cells (arrows). DG, dentate gyrus. ***C***, ***D***, Immunoblot and quantitation of APP, α-CTF, and β-CTF in AAV8-GFAP-FLAG-TFEB and AAV8-GFAP-eGFP transduced hippocampi. $N = 3$/group. ***E***, Neuronal counts in the CA1 and CA3 layers of the hippocampi from AAV8-GFAP-FLAG-TFEB and AAV8-GFAP-eGFP transduced APP/PS1 mice and uninjected age- and sex-matched APP/PS1 mice as controls. $N = 4$/group.

ing because of its easily accessible location and its characteristic and representative deposition of amyloid plaques (Yan et al., 2009). Four months after injection (at 10 months of age), mice were killed and assessed for efficacy of viral gene transfer. In control brains, GFP was observed throughout the anterior hippocampus, spanning 3–4 mm in the AP direction (Fig. 4*A*). The FLAG-TFEB construct was selectively transduced to astrocytes in the hippocampus, as assessed by colocalization of TFEB and GFAP within cells demonstrating characteristic astrocytic morphology (Fig. 4*B*). Exogenous TFEB did not colocalize with Iba-1 (a microglial protein) or NeuN (a neuronal marker) demonstrating specificity of the targeting strategy (Fig. 4*B*). Consistent with the lack of neuronal transduction, we did not observe alterations in abundance of APP, its α-C-terminal fragment (α-CTF), or the β-C-terminal fragment (β-CTF), and no changes in transcript levels coding for Aβ processing enzymes (ADAM17, ADAM10,

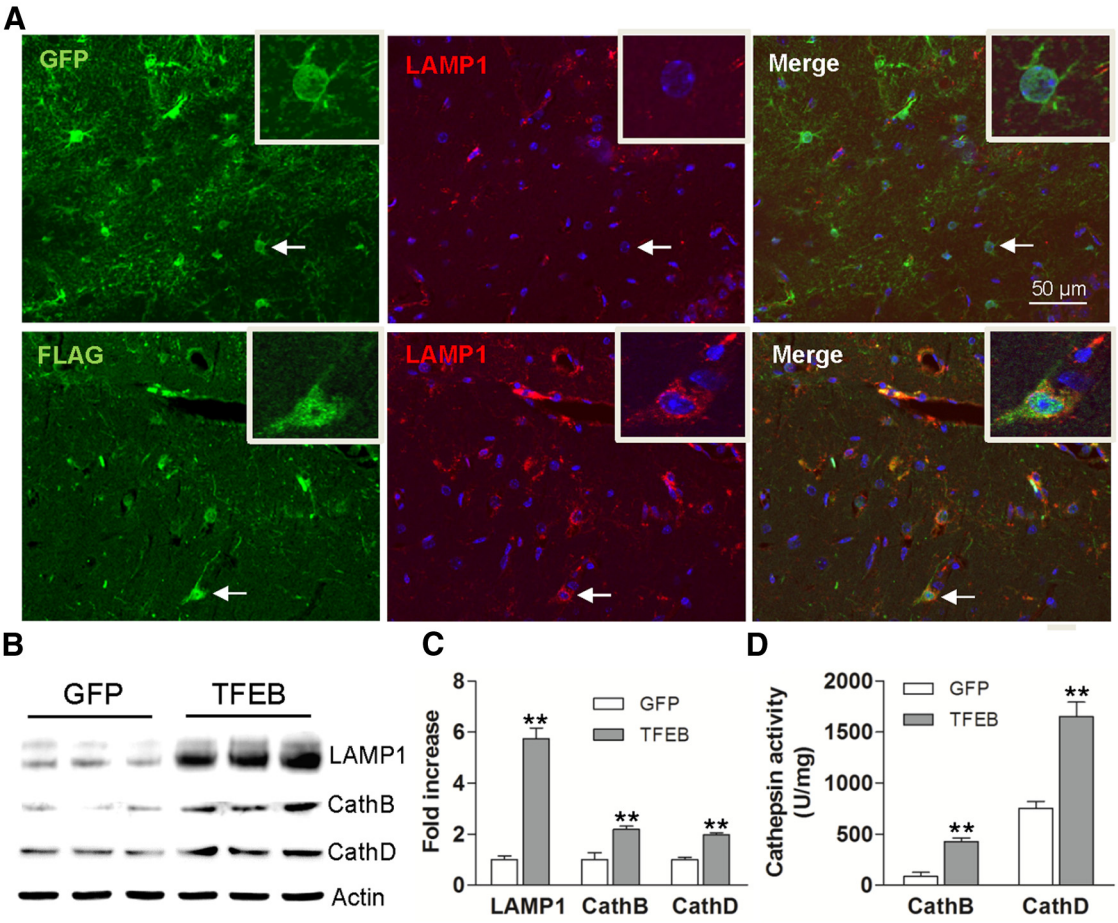

Figure 5. AAV8-mediated astrocytic gene transfer of TFEB in astrocytes promotes lysosome biogenesis in APP/PS1 mice. ***A***, Representative confocal images demonstrating expression of FLAG (green) and LAMP1 (red) in hippocampal tissues transduced with AAV8-GFAP-FLAG-TFEB (bottom) and AAV8-GFAP-eGFP (top) viral particles. Arrow indicates individual double-labeled cell shown under high magnification (insert, right upper corner). ***B***, ***C***, Immunoblots (***B***) with quantification (***C***) of lysosomal proteins in extracts from hippocampi transduced with AAV8-GFAP-FLAG-TFEB or AAV8-GFAP-eGFP. $N = 3$/group. ***D***, Cathepsin B and D activity in extracts from hippocampi transduced with AAV8-GFAP-FLAG-TFEB or AAV8-GFAP-eGFP. $N = 4$/group; $^{**}p < 0.01$.

BACE, PSEN1, and PEN2; data not shown) in AAV8-GFAP-FLAG-TFEB transduced mice, compared with control. This indicates a lack of effect of TFEB expression on APP processing (Fig. 4*C*,*D*). Additionally, we did not observe a difference in neuronal counts in the hippocampus between TFEB-transduced, GFP-transduced, and uninjected APP/PS1 mice (Fig. 4*E*). These data demonstrate a lack of toxicity with AAV-mediated TFEB or GFP transduction strategy and the lack of neuronal pathology in this mouse model of AD (APP/PS1 mice) at 10 months of age.

Exogenous TFEB localized to the nucleus of transduced astrocytes (Fig. 5*A*), indicating that it was transcriptionally "active" (Settembre et al., 2011; Roczniak-Ferguson et al., 2012). AAV-mediated transduction of TFEB resulted in a sixfold increase in TFEB expression compared with controls ($p < 0.01$, $n = 3$/group; Fig. 5*B*), and increased LAMP1 expression (Fig. 5*A–C*), consistent with stimulation of lysosome biogenesis, as observed *in vitro* (Figs. 1*A–E*; 3*C*,*D*). Immunoblotting of hippocampal extracts confirmed a sixfold increase in LAMP1 and a twofold increase in Cathepsin B and D compared with controls (Fig. 5*B*,*C*). TFEB expression resulted in a dramatic increase of Cathepsin B and D activity (Fig. 5*D*), indicating that exogenous TFEB stimulates lysosome function, *in vivo*.

Astrocytic TFEB expression reduces brain ISF Aβ half-life and ISF Aβ concentration *in vivo*

The concentration of soluble Aβ in the extracellular space (ISF) reflects a steady state determined by the rates of Aβ generation and elimination (Cirrito et al., 2003). Given that Aβ peptides are primarily generated within neurons then secreted into the ISF (Hartmann et al., 1997; Kamenetz et al., 2003), and AAV-transduced TFEB was expressed selectively in astrocytes by design, we postulated that enhanced astrocytic TFEB expression will stimulate uptake and degradation of Aβ, *in vivo*, similar to that observed *in vitro* (Fig. 2). Accordingly, we transduced 2-month-old APP/PS1 mice with AAV8-GFAP-FLAG-TFEB and control AAV8-GFAP-eGFP viral particles to determine whether astrocytic TFEB expression impacts ISF Aβ. These studies were performed before the deposition of plaques (Yan et al., 2009) to determine the role of astrocytic TFEB in normal Aβ metabolism without the complicating factor of deposited Aβ. We performed *in vivo* microdialysis to ascertain Aβ levels in the ISF 1 month after viral injection (Fig. 6*A*). TFEB-expressing mice had significantly lower steady-state concentration of ISF Aβ (by 39%) compared with control mice (Fig. 6*A*,*C*). After steady-state measures of ISF Aβ were obtained, mice were administered the potent γ-secretase inhibitor, Compound E (Cirrito et al., 2011), and ISF

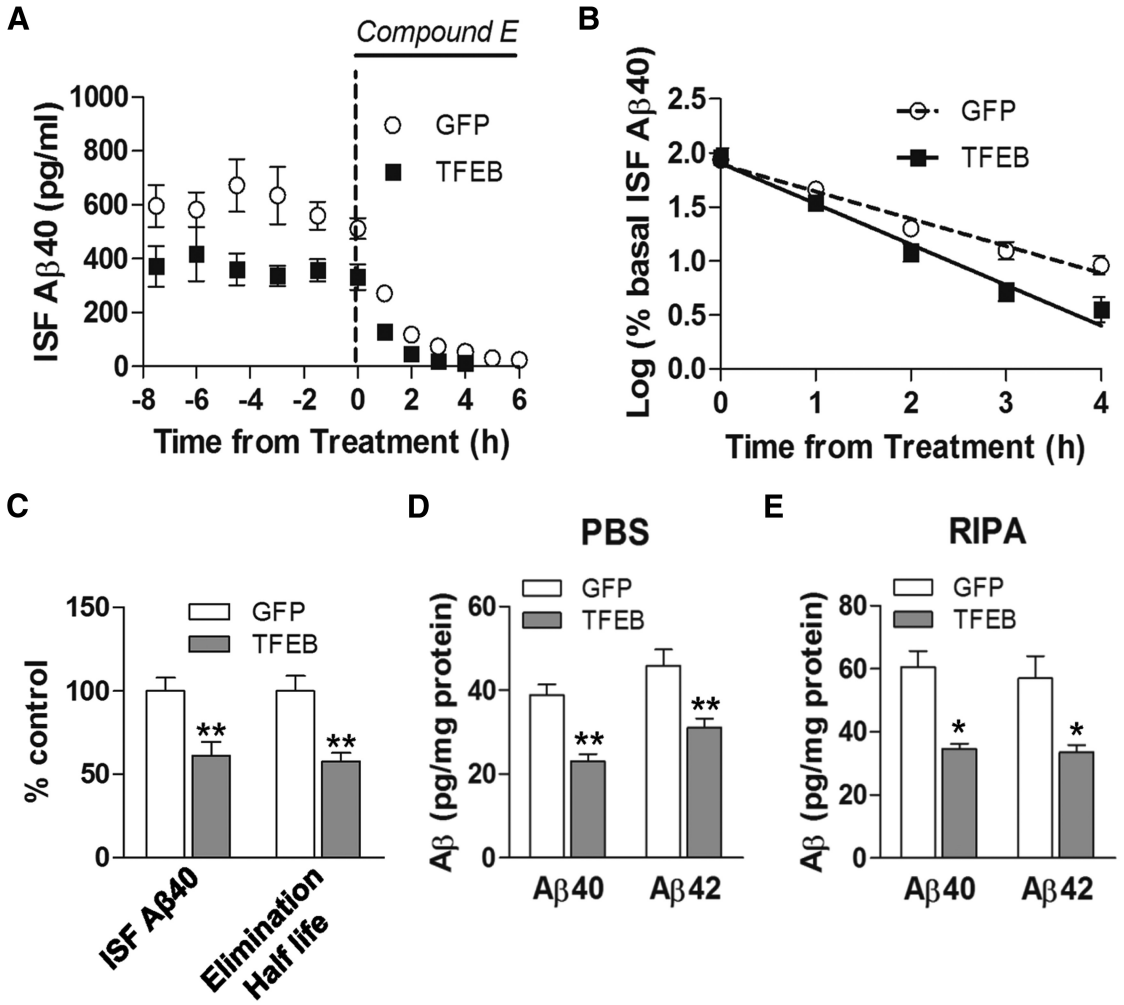

Figure 6. AAV8-mediated astrocytic gene transfer of TFEB reduces brain ISF Aβ levels and reduces *in vivo* Aβ half-life. ***A***, Assessment of Aβ levels by *in vivo* microdialysis in 3-month-old APP/PS1 mice transduced with AAV8-GFAP-FLAG-TFEB (TFEB) and AAV8-GFAP-eGFP (GFP) with serial hourly measurements. $N = 5$ mice/group. At $t = 0$, mice were continually administered Compound E directly to the hippocampus (200 nM, reverse microdialysis) followed by hourly sampling for Aβ. Mean absolute *in vivo* "exchangeable" Aβ (eAβx-40) concentration was averaged over a 9 h period before drug administration, and assessed to be 362.4 ± 49.0 pg/ml in TFEB-transduced mice versus 592.5 ± 46.9 pg/ml in controls. ***B***, Semi-log plot of decline in percentage basal ISF Aβ levels during administration of Compound E, in animals in ***A***. Half-life in control mice was 1.26 ± 0.11 h and 0.76 ± 0.06 h in TFEB-expressing mice. ***C***, Quantification of averaged concentration and elimination half-life of ISF Aβ as calculated in ***A*** and ***B***; $^{**}p < 0.01$. ***D***, ***E***, Aβ40 and Aβ42 levels in dissected hippocampal tissues from AAV8-GFAP-FLAG-TFEB (TFEB) and AAV8-GFAP-eGFP (GFP) transduced APP/PS1 mice (5 months of age). Tissue was homogenized first in PBS (***D***) and then in RIPA (***E***) quantified with ELISA assay. HJ2 and HJ7.4 antibodies were used for capture Aβ40 and Aβ42, respectively, and HJ5.1 antibody was used for detection. $N = 5$ mice/group; $^{*}p < 0.05$, $^{**}p < 0.01$.

was sampled for an additional 6 h to determine the elimination rate (half-life) of pre-existing Aβ (Fig. 6*A*). As shown, the elimination of ISF Aβ followed first-order kinetics in both control and TFEB-expressing mice (Fig. 6*B*). Astrocytic expression of TFEB significantly reduced the *in vivo* elimination half-life of ISF Aβ by 40%, compared with controls (Fig. 6*B*,*C*), mirroring the magnitude of half-life reduction in *in vitro* studies (Fig. 2*C*). To confirm that the reduction in ISF Aβ levels with astrocytic TFEB expression resulted in increased Aβ elimination, and not merely increased cellular uptake, we assessed total Aβ abundance in hippocampal tissue and observed a significant reduction in total immunodetectable Aβ levels in TFEB-transduced hippocampi (by ~40% vs control, at this time point; Fig. 6*D*,*E*). This directly demonstrates that exogenous TFEB expression in astrocytes enhances Aβ degradation, *in vivo*.

We did not observe any significant difference in transcript levels for Aβ-binding receptors (LRP1, LDLR), chaperones (ApoE, Apo J), or Aβ metabolizing enzymes (MMP2, MMP9, IDE, or Neprilysin) in the AAV-TFEB transduced hippocampi compared with controls (data not shown), suggesting that astrocytic TFEB expression does not alter the extracellular degradation or transport of Aβ peptides. These observations are consistent with enhanced cellular uptake and degradation of Aβ by TFEB-transduced astrocytes, *in vivo*, as observed *in vitro* (Figs. 2, 3).

Astrocytic TFEB expression reduces total Aβ levels and amyloid plaque load in APP/PS1 mice

To evaluate the effect of astrocytic TFEB expression on Aβ levels and amyloid accumulation in aging mice, hippocampal tissue from the 10-month-old mice was sequentially homogenized in PBS followed by guanidine to extract PBS-soluble and -insoluble fractions (Yan et al., 2009). Each fraction was quantified using ELISAs to measure both Aβ40 and Aβ42. Exogenous TFEB expression resulted in a decrease in both PBS-soluble and insoluble fractions of Aβ40 and Aβ42 (Fig. 7*A*,*B*), to a comparable extent as observed in the ISF (Fig. 6*A*,*C*) and in the hippocampi from TFEB-transduced predepositing APP/PS1 mice (Fig. 6*D*,*E*). Importantly, expression of GFAP promoter-driven GFP used as

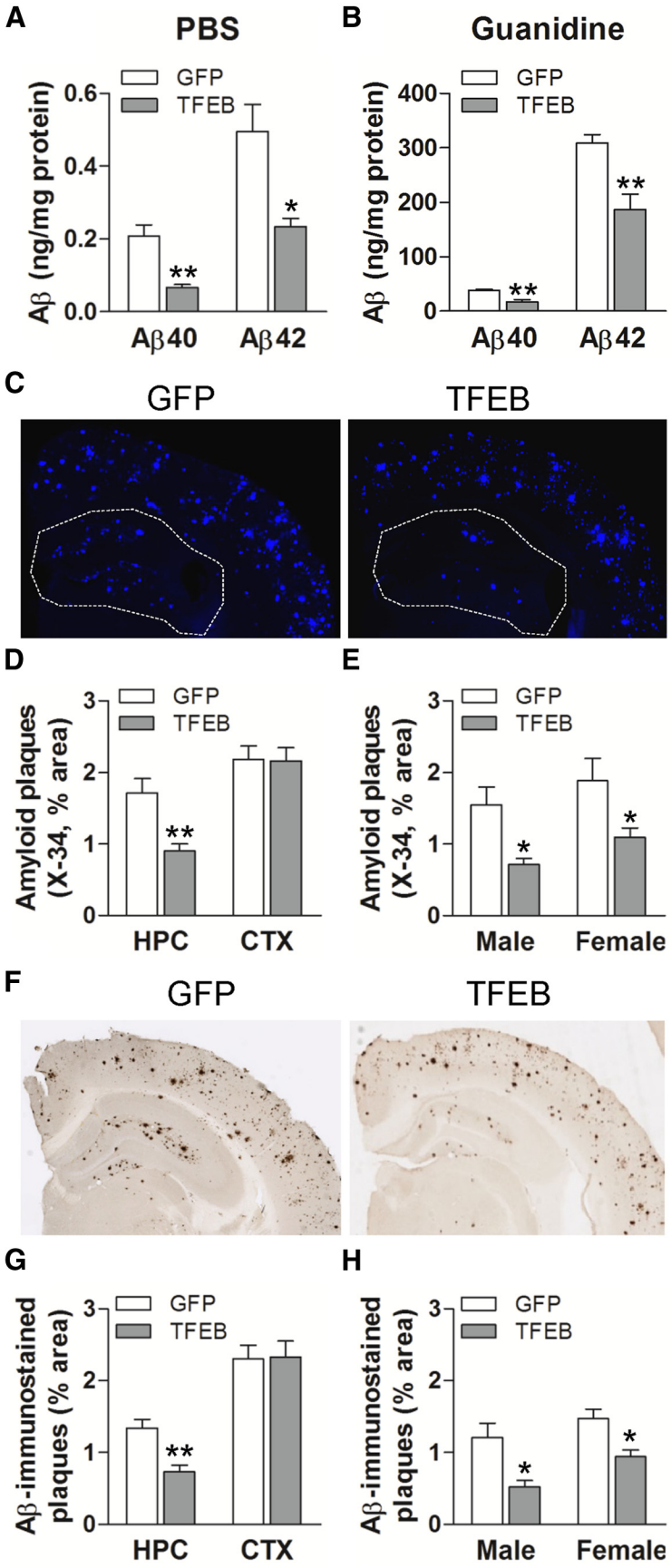

Figure 7. Astrocytic TFEB overexpression decreases amyloid plaque load in hippocampus of APP/PS1 mice. ***A***, ***B***, Aβ40 and Aβ42 levels in dissected hippocampal tissues from AAV8-GFAP-FLAG-TFEB (TFEB) and AAV8-GFAP-eGFP (GFP) transduced mice (10 months of age). Tissue was homogenized first in PBS (soluble levels, ***A***), then in 5 mM guanidine (insoluble levels, ***B***) quantified with ELISA assay. HJ2 and HJ7.4 antibodies were used for capture Aβ40 and Aβ42, respectively, and HJ5.1 antibody was used for detection. $N = 8$ mice/group; $^{**}p < 0.01$. ***C***, Representative X-34-stained images from APP/PS1 mice treated as in ***A***. The area of the hippocampus is outlined with a dotted line. ***D***, ***E***, Quantification of X-34-stained plaque burden in the hippocampus in mice treated as in ***A*** (***D***) and plaque burden stratified by sex (***E***). $N = 10$ (5 male and 5 female) mice/group. ***F***, Representative Aβ-immunostained images from mice treated as in ***A***. ***G***, ***H***, Quantification of Aβ-stained plaque burden in the hippocampus in mice treated as in ***A*** (***G***) and plaque burden stratified by sex (***H***). $N = 10$ (5 male and 5 female) mice/group; $^{*}p < 0.05$, $^{**}p < 0.01$.

control for these studies did not result in altered Aβ levels compared with uninjected age- and sex-matched mice (data not shown). These data indicate that exogenous TFEB enhanced both uptake and degradation of Aβ within astrocytes, *in vivo*.

To determine whether TFEB-mediated decline in ISF Aβ influences amyloid plaque pathogenesis, we stained brain slices with X-34 to assess compact amyloid plaques and immunostained with anti-Aβ antibodies to assess Aβ plaque load. Quantitative analysis of X-34 staining (Fig. 7*C*) demonstrated that amyloid plaque load in TFEB-transduced hippocampus was significantly decreased (Fig. 7*D*,*E*) compared with control. This reduction was anatomically localized to the hippocampus (see area enclosed within dotted line), which was the site of experimental TFEB transduction, without an effect on cortical plaque load (Fig. 7*D*), consistent with a local effect of enhanced astrocyte Aβ uptake and degradation. In addition, TFEB-stimulated reduction in plaque load was similar in magnitude in both sexes (Fig. 7*E*; $n = 5$ mice/sex/group), despite a higher plaque load observed in female mice, as previously described (Callahan et al., 2001). Similarly, TFEB-transduced hippocampi (but not the cortex) demonstrated significantly reduced Aβ-immunostained plaque load (Fig. 7*F–H*) compared with control. The reduction in amyloid plaque load with TFEB expression (by ~45%) is consistent with the magnitude of decline in ISF Aβ levels (by 40%), mirroring previous observations, suggesting a robust effect of increased Aβ removal from the extracellular space on reducing amyloid plaque load (Yan et al., 2009). Collectively, these results indicate that astrocytic TFEB expression attenuates amyloid plaque accumulation, likely via enhancing Aβ uptake from the ISF and facilitating clearance via lysosomal degradation, in the brain.

Discussion

We have demonstrated that targeted gene delivery of TFEB to astrocytes is effective in countering amyloid plaque pathogenesis. Specifically, astrocytic TFEB expression in the hippocampus (6- to 9-fold above basal level) resulted in TFEB activation (localization to the nucleus) and induction of the lysosomal machinery, including enhanced Cathepsin B and D activity (Figs. 1, 4, 5). TFEB also stimulated Aβ uptake and degradation via lysosomes (Figs. 2, 3), resulting in significantly lower Aβ levels (Figs. 6, 7) and shortened Aβ half-life, both intracellularly as observed *in vitro* (Fig. 2) and extracellularly in the ISF (Fig. 6). This resulted in a substantial attenuation in amyloid plaque load (Fig. 7) in the hippocampus of APP/PS1 mice. These observations point to a direct effect of TFEB on stimulating Aβ degradation by astrocytes to attenuate amyloid plaque pathogenesis.

Astrocytes play a critical role in maintaining neuronal homeostasis by providing energy, eliminating waste, regulating transport across the blood–brain barrier, clearing neurotransmitters at the synapse, regulating cellular ionic fluxes, and mediating repair in response to injury (Eroglu and Barres, 2010). Moreover, astrocytes provide complete coverage of brain parenchyma by virtue of their territorial relationships, forming a mosaic with adjacent astrocytes (Bushong et al., 2002). Thus, astrocytes are well positioned both metabolically and anatomically to play an important homeostatic role under basal conditions and during disease pathogenesis. A prominent role for astrocytes in AD pathogenesis is evidenced by astrocyte activation early in the disease process (Schipper et al., 2006; Owen et al., 2009; Carter et al., 2012) together with their ability to take up and degrade Aβ (Wyss-Coray et al., 2003; Koistinaho et al., 2004; Nielsen et al., 2009). These observations suggest that while astrocytes may participate in physiologic clearance of Aβ peptides to maintain their steady-state levels in the extracellular fluids in normal individuals (Bateman et al., 2006), their role in the removal of extracellular Aβ and amyloid material may be insufficient in the setting of AD (Wyss-Coray et al., 2003; Nielsen et al., 2009). Our results indicate that the ability of astrocytes to eliminate amyloid material may be enhanced or restored by stimulating TFEB-mediated trafficking and degradative pathways, as a therapeutic and/or preventive strategy in individuals predisposed to developing AD.

Astrocytes take up Aβ bound to membrane receptors such as LDLR (Basak et al., 2012) or LRP1 (Verghese et al., 2013) via endocytosis. Multiple studies have demonstrated the efficacy of enhancing cellular uptake and degradation by overexpressing these receptors (Kim et al., 2009; Basak et al., 2012; Castellano et al., 2012). Glial cells may also take up Aβ bound to heparan sulfate proteoglycans by macropinocytosis (Mandrekar et al., 2009), involving invagination of the cell membrane to engulf extracellular material. In addition, activated astrocytes with hypertrophied processes exist in close contact with amyloid plaques, and have been postulated to phagocytose amyloid material (Funato et al., 1998; Wyss-Coray et al., 2003). Our data indicate that TFEB stimulates uptake of Aβ via heparan sulfate proteoglycans and macropinocytosis without affecting the Aβ-binding receptors and endocytosis. The underlying molecular mechanisms for this observation warrant further exploration.

We and others have observed that Aβ is rapidly trafficked to the lysosomes after uptake (Kanekiyo et al., 2011; Basak et al., 2012) and exogenous TFEB accelerates this process. Degradation of Aβ requires intact lysosome function. Indeed, normal lysosome function in astrocytes is essential to prevent neurodegeneration, as targeted astrocytic ablation of sulfatase-modifying factor 1 (loss of function causing multiple sulfatase deficiencies), provokes degeneration of cortical neurons (Di Malta et al., 2012). Emerging evidence has fostered suspicion that aging-induced impairment in lysosome function facilitates pathogenesis in AD (Nixon and Cataldo, 2006; Wolfe et al., 2013). While it remains to be determined whether a specific impairment in astrocytic lysosome function causes or contributes to amyloid plaque deposition, our data indicate that upregulation of lysosomal numbers and enhanced lysosome function with TFEB-induced lysosome biogenesis (Settembre et al., 2011) is highly efficacious in facilitating Aβ and amyloid plaque elimination by astrocytes.

We have also found that exogenous TFEB expression results in increased abundance and activity of Cathepsin B and D, both *in vitro* and *in vivo*, which is likely involved in Aβ degradation. Evidence suggests that Cathepsin activity is essential for maintaining normal levels of Aβ in the extracellular space, as germline ablation of Cathepsin B increases Aβ levels and worsens plaque deposition (Mueller-Steiner et al., 2006). Lentiviral transduction of Cathepsin B (Mueller-Steiner et al., 2006) or germline ablation of endogenous protease inhibitors such as cystatin C (Sun et al., 2008) and B (Yang et al., 2011) increases Cathepsin activity, reduces Aβ levels, and attenuates plaque deposition. Polymorphisms in the gene coding for Cathepsin D have been implicated in conferring increased risk for developing AD (Schuur et al., 2011), and Cathepsin D activity, reduced in AD mouse models (Avrahami et al., 2013), may be pharmacologically stimulated with inhibition of glycogen synthase kinase-3β (GSK3β) to attenuate amyloid plaque pathogenesis. Aside from the specific induction of Cathepsin B and D, it is likely that other Cathepsins are induced (Palmieri et al., 2011) and mediate a general increase in lysosomal degradation.

Among other plausible subcellular mechanisms that may underlie TFEB-induced reduction in Aβ levels, enhanced lysosomal acidification by transcription of the lysosomal proton pump machinery (Settembre et al., 2011; Roczniak-Ferguson et al., 2012) may be highly relevant. Indeed, TFEB expression may rectify the impaired acidification of lysosomes with aging (Wolfe et al., 2013), or with loss of presenilin, as observed in familial AD (Lee et al., 2010). TFEB also stimulates lysosomal calcium release (Medina et al., 2011) and promotes autophagosome–lysosome fusion (Settembre et al., 2011), which may be other mechanisms whereby TFEB may correct the lysosomal calcium storage and release defects observed with presenilin deficiency (Coen et al., 2012). The synergistic effect of these multiple TFEB-stimulated mechanisms may be to promote complete proteolysis of Aβ and prevent aggregation into fibrils in an acidic environment (Hu et al., 2009), in the setting of underlying impairment in lysosome function.

Astrocytes are "activated" (displaying hypertrophied processes and increased GFAP expression) surrounding amyloid plaques in humans with AD (Schipper et al., 2006; Owen et al., 2009; Carter et al., 2012) and in APP transgenic mouse models (Nagele et al., 2003; Wyss-Coray et al., 2003; Nielsen et al., 2009). Activated astrocytes are observed in virtually all neurodegenerative diseases. In some, it has been suggested that astrocyte activation may be protective, as impairment in astrocyte activation with targeted ablation of intermediate filament proteins, GFAP and vimentin, worsens the pathology in neuronal ceroid lipofuscinosis, a lysosomal storage disease (Macauley et al., 2011). Importantly, we have observed that activated astrocytes play a critical role in attenuating plaque pathogenesis (Kraft et al., 2013). TFEB may stimulate astrocyte activation and phagocytosis of amyloid material via its upregulation of the phagocytotic ma-

chinery (Palmieri et al., 2011), an activity that warrants further investigation.

Reduced TFEB activation may underlie aging-related impairment in lysosomal function in AD (Nixon and Cataldo, 2006; Wolfe et al., 2013), a premise that needs further exploration. Indeed, insufficient TFEB activity has been implicated in causing lysosomal dysfunction in models of Parkinson's disease and AAV-mediated transduction of TFEB accelerated clearance of α-synuclein and protection against cytotoxicity (Decressac et al., 2013). Activation of mTOR, which provokes phosphorylation and cytoplasmic retention of TFEB in diverse cell types (Zoncu et al., 2011; Settembre et al., 2012; Martina and Puertollano, 2013), is observed in AD mouse models (Lafay-Chebassier et al., 2005). Various studies have demonstrated attenuation of plaque pathology with pharmacological inhibition of mTOR and GSK3β (Cai et al., 2012; Avrahami et al., 2013) or administration of lysosomal modulator Z-Phe-Ala-diazomethylketone (Butler et al., 2011). Activation of TFEB with GSK3β inhibition in neural tissue indicates the need to examine the therapeutic efficacy of TFEB targeting to various cell types in countering AD pathogenesis. Although small molecules that enhance TFEB expression have not been extensively explored, a recent study suggests that identification of such agents may be feasible (Song et al., 2014). Further studies are also needed to examine possible adverse effects of targeting TFEB activity, but current studies do not reveal obvious adverse effects (Tsunemi et al., 2012; Decressac et al., 2013).

A major strength of our viral gene transfer approach is the rapid assessment of cellular and molecular mechanisms involved in amyloid plaque pathogenesis, exploiting regional differences (targeting hippocampus) in cell-autonomous effects to establish specificity of targeting TFEB in astrocytes. However, focal targeting of TFEB expression to the hippocampus precludes an evaluation of its effects on cognitive parameters or neuronal pathology, which is not observed in the APP/PS1 model. Notwithstanding these limitations, our data demonstrate that TFEB activation enhances Aβ uptake and degradation in astrocytes, thereby lowering ISF Aβ concentrations and resulting in decreased plaque load. This study lays the foundation for exploring therapeutic strategies targeting TFEB activation, either pharmacologically or via gene therapy, both globally and in specific cell types, to counter AD pathogenesis.

References

Avrahami L, Farfara D, Shaham-Kol M, Vassar R, Frenkel D, Eldar-Finkelman H (2013) Inhibition of glycogen synthase kinase-3 ameliorates beta-amyloid pathology and restores lysosomal acidification and mammalian target of rapamycin activity in the Alzheimer disease mouse model: in vivo and in vitro studies. J Biol Chem 288:1295–1306. CrossRef Medline

Baldo G, Wu S, Howe RA, Ramamoothy M, Knutsen RH, Fang J, Mecham RP, Liu Y, Wu X, Atkinson JP, Ponder KP (2011) Pathogenesis of aortic dilatation in mucopolysaccharidosis VII mice may involve complement activation. Mol Genet Metab 104:608–619. CrossRef Medline

Barres BA (2008) The mystery and magic of glia: a perspective on their roles in health and disease. Neuron 60:430–440. CrossRef Medline

Basak JM, Verghese PB, Yoon H, Kim J, Holtzman DM (2012) Low-density lipoprotein receptor represents an apolipoprotein E-independent pathway of Abeta uptake and degradation by astrocytes. J Biol Chem 287:13959–13971. CrossRef Medline

Bateman RJ, Munsell LY, Morris JC, Swarm R, Yarasheski KE, Holtzman DM (2006) Human amyloid-beta synthesis and clearance rates as measured in CSF in vivo. Nat Med 12:856–861. CrossRef Medline

Brenner M, Kisseberth WC, Su Y, Besnard F, Messing A (1994) GFAP promoter directs astrocyte-specific expression in transgenic mice. J Neurosci 14:1030–1037. Medline

Bushong EA, Martone ME, Jones YZ, Ellisman MH (2002) Protoplasmic astrocytes in CA1 stratum radiatum occupy separate anatomical domains. J Neurosci 22:183–192. Medline

Butler D, Hwang J, Estick C, Nishiyama A, Kumar SS, Baveghems C, Young-Oxendine HB, Wisniewski ML, Charalambides A, Bahr BA (2011) Protective effects of positive lysosomal modulation in Alzheimer's disease transgenic mouse models. PLoS One 6:e20501. CrossRef Medline

Cai Z, Zhao B, Li K, Zhang L, Li C, Quazi SH, Tan Y (2012) Mammalian target of rapamycin: a valid therapeutic target through the autophagy pathway for Alzheimer's disease? J Neurosci Res 90:1105–1118. CrossRef Medline

Callahan MJ, Lipinski WJ, Bian F, Durham RA, Pack A, Walker LC (2001) Augmented senile plaque load in aged female beta-amyloid precursor protein-transgenic mice. Am J Pathol 158:1173–1177. CrossRef Medline

Carter SF, Schöll M, Almkvist O, Wall A, Engler H, Långström B, Nordberg A (2012) Evidence for astrocytosis in prodromal Alzheimer disease provided by 11C-deuterium-L-deprenyl: a multitracer PET paradigm combining 11C-Pittsburgh compound B and 18F-FDG. J Nucl Med 53:37–46. CrossRef Medline

Castellano JM, Deane R, Gottesdiener AJ, Verghese PB, Stewart FR, West T, Paoletti AC, Kasper TR, DeMattos RB, Zlokovic BV, Holtzman DM (2012) Low-density lipoprotein receptor overexpression enhances the rate of brain-to-blood Abeta clearance in a mouse model of beta-amyloidosis. Proc Natl Acad Sci U S A 109:15502–15507. CrossRef Medline

Cirrito JR, May PC, O'Dell MA, Taylor JW, Parsadanian M, Cramer JW, Audia JE, Nissen JS, Bales KR, Paul SM, DeMattos RB, Holtzman DM (2003) In vivo assessment of brain interstitial fluid with microdialysis reveals plaque-associated changes in amyloid-beta metabolism and half-life. J Neurosci 23:8844–8853. Medline

Cirrito JR, Disabato BM, Restivo JL, Verges DK, Goebel WD, Sathyan A, Hayreh D, D'Angelo G, Benzinger T, Yoon H, Kim J, Morris JC, Mintun MA, Sheline YI (2011) Serotonin signaling is associated with lower amyloid-beta levels and plaques in transgenic mice and humans. Proc Natl Acad Sci U S A 108:14968–14973. CrossRef Medline

Coen K, Flannagan RS, Baron S, Carraro-Lacroix LR, Wang D, Vermeire W, Michiels C, Munck S, Baert V, Sugita S, Wuytack F, Hiesinger PR, Grinstein S, Annaert W (2012) Lysosomal calcium homeostasis defects, not proton pump defects, cause endo-lysosomal dysfunction in PSEN-deficient cells. J Cell Biol 198:23–35. CrossRef Medline

Cuervo AM, Dice JF (2000) When lysosomes get old. Exp Gerontol 35:119–131. CrossRef Medline

Decressac M, Mattsson B, Weikop P, Lundblad M, Jakobsson J, Björklund A (2013) TFEB-mediated autophagy rescues midbrain dopamine neurons from alpha-synuclein toxicity. Proc Natl Acad Sci U S A 110:E1817–E1826. CrossRef Medline

Di Malta C, Fryer JD, Settembre C, Ballabio A (2012) Astrocyte dysfunction triggers neurodegeneration in a lysosomal storage disorder. Proc Natl Acad Sci U S A 109:E2334–E2342. CrossRef Medline

Eroglu C, Barres BA (2010) Regulation of synaptic connectivity by glia. Nature 468:223–231. CrossRef Medline

Fan TC, Chang HT, Chen IW, Wang HY, Chang MD (2007) A heparan sulfate-facilitated and raft-dependent macropinocytosis of eosinophil cationic protein. Traffic 8:1778–1795. CrossRef Medline

Funato H, Yoshimura M, Yamazaki T, Saido TC, Ito Y, Yokofujita J, Okeda R, Ihara Y (1998) Astrocytes containing amyloid beta-protein (Abeta)-positive granules are associated with Abeta40-positive diffuse plaques in the aged human brain. Am J Pathol 152:983–992. Medline

Gong Y, Chang L, Viola KL, Lacor PN, Lambert MP, Finch CE, Krafft GA, Klein WL (2003) Alzheimer's disease-affected brain: presence of oligomeric A beta ligands (ADDLs) suggests a molecular basis for reversible memory loss. Proc Natl Acad Sci U S A 100:10417–10422. CrossRef Medline

Hardy J, Selkoe DJ (2002) The amyloid hypothesis of Alzheimer's disease: progress and problems on the road to therapeutics. Science 297:353–356. CrossRef Medline

Hartmann T, Bieger SC, Brühl B, Tienari PJ, Ida N, Allsop D, Roberts GW, Masters CL, Dotti CG, Unsicker K, Beyreuther K (1997) Distinct sites of intracellular production for Alzheimer's disease A beta40/42 amyloid peptides. Nat Med 3:1016–1020. CrossRef Medline

Holmes BB, DeVos SL, Kfoury N, Li M, Jacks R, Yanamandra K, Ouidja MO, Brodsky FM, Marasa J, Bagchi DP, Kotzbauer PT, Miller TM, Papy-Garcia D, Diamond MI (2013) Heparan sulfate proteoglycans mediate

internalization and propagation of specific proteopathic seeds. Proc Natl Acad Sci U S A 110:E3138–E3147. CrossRef Medline

Hu X, Crick SL, Bu G, Frieden C, Pappu RV, Lee JM (2009) Amyloid seeds formed by cellular uptake, concentration, and aggregation of the amyloid-beta peptide. Proc Natl Acad Sci U S A 106:20324–20329. CrossRef Medline

Jankowsky JL, Fadale DJ, Anderson J, Xu GM, Gonzales V, Jenkins NA, Copeland NG, Lee MK, Younkin LH, Wagner SL, Younkin SG, Borchelt DR (2004) Mutant presenilins specifically elevate the levels of the 42 residue beta-amyloid peptide in vivo: evidence for augmentation of a 42-specific gamma secretase. Hum Mol Genet 13:159–170. Medline

Kamenetz F, Tomita T, Hsieh H, Seabrook G, Borchelt D, Iwatsubo T, Sisodia S, Malinow R (2003) APP processing and synaptic function. Neuron 37:925–937. CrossRef Medline

Kanekiyo T, Zhang J, Liu Q, Liu CC, Zhang L, Bu G (2011) Heparan sulphate proteoglycan and the low-density lipoprotein receptor-related protein 1 constitute major pathways for neuronal amyloid-beta uptake. J Neurosci 31:1644–1651. CrossRef Medline

Kato Y, Maruyama W, Naoi M, Hashizume Y, Osawa T (1998) Immunohistochemical detection of dityrosine in lipofuscin pigments in the aged human brain. FEBS Lett 439:231–234. CrossRef Medline

Kim J, Castellano JM, Jiang H, Basak JM, Parsadanian M, Pham V, Mason SM, Paul SM, Holtzman DM (2009) Overexpression of low-density lipoprotein receptor in the brain markedly inhibits amyloid deposition and increases extracellular A beta clearance. Neuron 64:632–644. CrossRef Medline

Koistinaho M, Lin S, Wu X, Esterman M, Koger D, Hanson J, Higgs R, Liu F, Malkani S, Bales KR, Paul SM (2004) Apolipoprotein E promotes astrocyte colocalization and degradation of deposited amyloid-beta peptides. Nat Med 10:719–726. CrossRef Medline

Kraft AW, Hu X, Yoon H, Yan P, Xiao Q, Wang Y, Gil SC, Brown J, Wilhelmsson U, Restivo JL, Cirrito JR, Holtzman DM, Kim J, Pekny M, Lee JM (2013) Attenuating astrocyte activation accelerates plaque pathogenesis in APP/PS1 mice. FASEB J 27:187–198. CrossRef Medline

Lafay-Chebassier C, Paccalin M, Page G, Barc-Pain S, Perault-Pochat MC, Gil R, Pradier L, Hugon J (2005) mTOR/p70S6k signalling alteration by Abeta exposure as well as in APP-PS1 transgenic models and in patients with Alzheimer's disease. J Neurochem 94:215–225. CrossRef Medline

Lee JH, Yu WH, Kumar A, Lee S, Mohan PS, Peterhoff CM, Wolfe DM, Martinez-Vicente M, Massey AC, Sovak G, Uchiyama Y, Westaway D, Cuervo AM, Nixon RA (2010) Lysosomal proteolysis and autophagy require presenilin 1 and are disrupted by Alzheimer-related PS1 mutations. Cell 141:1146–1158. CrossRef Medline

Lomakin A, Teplow DB, Kirschner DA, Benedek GB (1997) Kinetic theory of fibrillogenesis of amyloid beta-protein. Proc Natl Acad Sci U S A 94:7942–7947. CrossRef Medline

Ma X, Liu H, Foyil SR, Godar RJ, Weinheimer CJ, Hill JA, Diwan A (2012) Impaired autophagosome clearance contributes to cardiomyocyte death in ischemia/reperfusion injury. Circulation 125:3170–3181. CrossRef Medline

Macauley SL, Pekny M, Sands MS (2011) The role of attenuated astrocyte activation in infantile neuronal ceroid lipofuscinosis. J Neurosci 31:15575–15585. CrossRef Medline

Mandrekar S, Jiang Q, Lee CY, Koenigsknecht-Talboo J, Holtzman DM, Landreth GE (2009) Microglia mediate the clearance of soluble Abeta through fluid phase macropinocytosis. J Neurosci 29:4252–4262. CrossRef Medline

Martina JA, Puertollano R (2013) Rag GTPases mediate amino acid-dependent recruitment of TFEB and MITF to lysosomes. J Cell Biol 200:475–491. CrossRef Medline

Mawuenyega KG, Sigurdson W, Ovod V, Munsell L, Kasten T, Morris JC, Yarasheski KE, Bateman RJ (2010) Decreased clearance of CNS beta-amyloid in Alzheimer's disease. Science 330:1774. CrossRef Medline

Medina DL, Fraldi A, Bouche V, Annunziata F, Mansueto G, Spampanato C, Puri C, Pignata A, Martina JA, Sardiello M, Palmieri M, Polishchuk R, Puertollano R, Ballabio A (2011) Transcriptional activation of lysosomal exocytosis promotes cellular clearance. Dev Cell 21:421–430. CrossRef Medline

Menacherry S, Hubert W, Justice JB Jr (1992) In vivo calibration of microdialysis probes for exogenous compounds. Anal Chem 64:577–583. CrossRef Medline

Mousavi SA, Kjeken R, Berg TO, Seglen PO, Berg T, Brech A (2001) Effects of inhibitors of the vacuolar proton pump on hepatic heterophagy and autophagy. Biochim Biophys Acta 1510:243–257. CrossRef Medline

Mueller-Steiner S, Zhou Y, Arai H, Roberson ED, Sun B, Chen J, Wang X, Yu G, Esposito L, Mucke L, Gan L (2006) Antiamyloidogenic and neuroprotective functions of cathepsin B: implications for Alzheimer's disease. Neuron 51:703–714. CrossRef Medline

Nagele RG, D'Andrea MR, Lee H, Venkataraman V, Wang HY (2003) Astrocytes accumulate A beta 42 and give rise to astrocytic amyloid plaques in Alzheimer disease brains. Brain Res 971:197–209. CrossRef Medline

Nielsen HM, Veerhuis R, Holmqvist B, Janciauskiene S (2009) Binding and uptake of A beta1–42 by primary human astrocytes in vitro. Glia 57:978–988. CrossRef Medline

Nixon RA, Cataldo AM (2006) Lysosomal system pathways: genes to neurodegeneration in Alzheimer's disease. J Alzheimers Dis 9:277–289. Medline

Owen JB, Di Domenico F, Sultana R, Perluigi M, Cini C, Pierce WM, Butterfield DA (2009) Proteomics-determined differences in the concanavalin-A-fractionated proteome of hippocampus and inferior parietal lobule in subjects with Alzheimer's disease and mild cognitive impairment: implications for progression of AD. J Proteome Res 8:471–482. CrossRef Medline

Palmieri M, Impey S, Kang H, di Ronza A, Pelz C, Sardiello M, Ballabio A (2011) Characterization of the CLEAR network reveals an integrated control of cellular clearance pathways. Hum Mol Genet 20:3852–3866. CrossRef Medline

Peña-Llopis S, Vega-Rubin-de-Celis S, Schwartz JC, Wolff NC, Tran TA, Zou L, Xie XJ, Corey DR, Brugarolas J (2011) Regulation of TFEB and V-ATPases by mTORC1. EMBO J 30:3242–3258. CrossRef Medline

Roczniak-Ferguson A, Petit CS, Froehlich F, Qian S, Ky J, Angarola B, Walther TC, Ferguson SM (2012) The transcription factor TFEB links mTORC1 signaling to transcriptional control of lysosome homeostasis. Sci Signal 5:ra42. CrossRef Medline

Roh JH, Huang Y, Bero AW, Kasten T, Stewart FR, Bateman RJ, Holtzman DM (2012) Disruption of the sleep-wake cycle and diurnal fluctuation of beta-amyloid in mice with Alzheimer's disease pathology. Sci Transl Med 4:150ra122. CrossRef Medline

Sardiello M, Palmieri M, di Ronza A, Medina DL, Valenza M, Gennarino VA, Di Malta C, Donaudy F, Embrione V, Polishchuk RS, Banfi S, Parenti G, Cattaneo E, Ballabio A (2009) A gene network regulating lysosomal biogenesis and function. Science 325:473–477. CrossRef Medline

Schipper HM, Bennett DA, Liberman A, Bienias JL, Schneider JA, Kelly J, Arvanitakis Z (2006) Glial heme oxygenase-1 expression in Alzheimer disease and mild cognitive impairment. Neurobiol Aging 27:252–261. CrossRef Medline

Schuur M, Ikram MA, van Swieten JC, Isaacs A, Vergeer-Drop JM, Hofman A, Oostra BA, Breteler MM, van Duijn CM (2011) Cathepsin D gene and the risk of Alzheimer's disease: a population-based study and meta-analysis. Neurobiol Aging 32:1607–1614. CrossRef Medline

Settembre C, Di Malta C, Polito VA, Garcia Arencibia M, Vetrini F, Erdin S, Erdin SU, Huynh T, Medina D, Colella P, Sardiello M, Rubinsztein DC, Ballabio A (2011) TFEB links autophagy to lysosomal biogenesis. Science 332:1429–1433. CrossRef Medline

Settembre C, Zoncu R, Medina DL, Vetrini F, Erdin S, Huynh T, Ferron M, Karsenty G, Vellard MC, Facchinetti V, Sabatini DM, Ballabio A (2012) A lysosome-to-nucleus signalling mechanism senses and regulates the lysosome via mTOR and TFEB. EMBO J 31:1095–1108. CrossRef Medline

Settembre C, Fraldi A, Medina DL, Ballabio A (2013a) Signals from the lysosome: a control centre for cellular clearance and energy metabolism. Nat Rev Mol Cell Biol 14:283–296. CrossRef Medline

Settembre C, De Cegli R, Mansueto G, Saha PK, Vetrini F, Visvikis O, Huynh T, Carissimo A, Palmer D, Klisch TJ, Wollenberg AC, Di Bernardo D, Chan L, Irazoqui JE, Ballabio A (2013b) TFEB controls cellular lipid metabolism through a starvation-induced autoregulatory loop. Nat Cell Biol 15:647–658. CrossRef Medline

Song W, Wang F, Lotfi P, Sardiello M, Segatori L (2014) 2-Hydroxypropyl-beta-cyclodextrin promotes transcription factor EB-mediated activation of autophagy: implications for therapy. J Biol Chem 289:10211–10222. CrossRef Medline

Sun B, Zhou Y, Halabisky B, Lo I, Cho SH, Mueller-Steiner S, Devidze N, Wang X, Grubb A, Gan L (2008) Cystatin C-cathepsin B axis regulates amyloid beta levels and associated neuronal deficits in an animal model of Alzheimer's disease. Neuron 60:247–257. CrossRef Medline

Tsunemi T, Ashe TD, Morrison BE, Soriano KR, Au J, Roque RA, Lazarowski ER, Damian VA, Masliah E, La Spada AR (2012) PGC-1alpha rescues Huntington's disease proteotoxicity by preventing oxidative stress and promoting TFEB function. Sci Transl Med 4:142ra97. CrossRef Medline

Verges DK, Restivo JL, Goebel WD, Holtzman DM, Cirrito JR (2011) Opposing synaptic regulation of amyloid-beta metabolism by NMDA receptors *in vivo*. J Neurosci 31:11328–11337. CrossRef Medline

Verghese PB, Castellano JM, Garai K, Wang Y, Jiang H, Shah A, Bu G, Frieden C, Holtzman DM (2013) ApoE influences amyloid-beta (Abeta) clearance despite minimal apoE/Abeta association in physiological conditions. Proc Natl Acad Sci U S A 110:E1807–1816. CrossRef Medline

West MJ, Slomianka L, Gundersen HJ (1991) Unbiased stereological estimation of the total number of neurons in the subdivisions of the rat hippocampus using the optical fractionator. Anat Rec 231:482–497. CrossRef Medline

Wolfe DM, Lee JH, Kumar A, Lee S, Orenstein SJ, Nixon RA (2013) Autophagy failure in Alzheimer's disease and the role of defective lysosomal acidification. Eur J Neurosci 37:1949–1961. CrossRef Medline

Wyss-Coray T, Loike JD, Brionne TC, Lu E, Anankov R, Yan F, Silverstein SC, Husemann J (2003) Adult mouse astrocytes degrade amyloid-beta in vitro and in situ. Nat Med 9:453–457. CrossRef Medline

Xiao Q, Gil SC, Yan P, Wang Y, Han S, Gonzales E, Perez R, Cirrito JR, Lee JM (2012) Role of phosphatidylinositol clathrin assembly lymphoid-myeloid leukemia (PICALM) in intracellular amyloid precursor protein (APP) processing and amyloid plaque pathogenesis. J Biol Chem 287:21279–21289. CrossRef Medline

Yamamoto A, Tagawa Y, Yoshimori T, Moriyama Y, Masaki R, Tashiro Y (1998) Bafilomycin A1 prevents maturation of autophagic vacuoles by inhibiting fusion between autophagosomes and lysosomes in rat hepatoma cell line, H-4-II-E cells. Cell Struct Funct 23:33–42. CrossRef Medline

Yan P, Bero AW, Cirrito JR, Xiao Q, Hu X, Wang Y, Gonzales E, Holtzman DM, Lee JM (2009) Characterizing the appearance and growth of amyloid plaques in APP/PS1 mice. J Neurosci 29:10706–10714. CrossRef Medline

Yang DS, Stavrides P, Mohan PS, Kaushik S, Kumar A, Ohno M, Schmidt SD, Wesson D, Bandyopadhyay U, Jiang Y, Pawlik M, Peterhoff CM, Yang AJ, Wilson DA, St George-Hyslop P, Westaway D, Mathews PM, Levy E, Cuervo AM, Nixon RA (2011) Reversal of autophagy dysfunction in the TgCRND8 mouse model of Alzheimer's disease ameliorates amyloid pathologies and memory deficits. Brain 134:258–277. CrossRef Medline

Zang Y, Yu LF, Pang T, Fang LP, Feng X, Wen TQ, Nan FJ, Feng LY, Li J (2008) AICAR induces astroglial differentiation of neural stem cells via activating the JAK/STAT3 pathway independently of AMP-activated protein kinase. J Biol Chem 283:6201–6208. CrossRef Medline

Zoncu R, Bar-Peled L, Efeyan A, Wang S, Sancak Y, Sabatini DM (2011) mTORC1 senses lysosomal amino acids through an inside-out mechanism that requires the vacuolar H(+)-ATPase. Science 334:678–683. CrossRef Medline

Conclusions

In this study, we demonstrated that exogenous TFEB delivered via a viral vector was effective at increasing Aβ degradation in astrocytes. This method reduced both the soluble and insoluble levels of Aβ in the hippocampus of treated mice. Our previous research showed that LRP1 plays a critical role in neuronal uptake of Aβ and that by blocking LRP1 we could increase extracellular Aβ levels. This did not have any effect in the hippocampus though. Here, we showed that astrocytes have a critical role in the uptake and degradation of extracellular Aβ in the hippocampus.

By genetically targeting an increase in lysosome biogenesis, we were able to decrease Aβ levels and Aβ degradation. Increasingly, evidence is pointing to the conclusion that as we age our lysosomes decrease in function. It has not yet been proven that astrocytic lysosome impairment is responsible for the increased plaques found in AD, but our data shows that increasing the number of astrocytic lysosomes is very effective at eliminating plaque burden in the hippocampus.

These findings suggest that a reduction in TFEB activation may also play an important role in lysosome function and AD. Reduced TFEB activation has also been implicated by other studies as well and should be further explored to see if genetic manipulation of TFEB may be a helpful treatment for patients with AD. Low TFEB activity has also been found in other neurodegenerative diseases, such as Parkinson’s, suggesting that this research could have wide-reaching implications for multiple disease states.

New research into TFEB activation has led to the identification of the small molecule curcumin analog C1 that activates TFEB and can easily pass through the BBB (Song et al. 2016). After verifying that C1 specifically binds to TFEB and promotes its nuclear translocation (Song et al. 2016), the researchers tested C1 in four different transgenic mouse models of AD: APP, 5FAD, tau, and APP/Tau crossed mice (Song et al. 2020). Oral administration of C1 promoted the nuclear translocation of TFEB and increased TFEB levels. They also found that administration of C1 promoted lysosome biogenesis, degraded APP and tau aggregates, reduced levels of Aβ, reversed synaptic dysfunction, and improved cognitive deficits in these mouse models (Song et al. 2020).

Research has even expanded into other neurodegenerative disorders. Zhuang et al. (2020) found that TFEB-mediated autophagy is protective in a mouse model of Parkinson's disease. These protective effects were blocked by knocking down TFEB and by using autophagy inhibitors such as chloroquine (Zhuang et al. 2020).

Chapter 7: Development, Application, and Results from a Precision-Medicine Platform That Personalizes Multi-modal Care Plans for Mild Alzheimer's Disease and At-risk Individuals

AD is the most common form of dementia, and yet no disease-modifying drug has been found to help treat it. It is now accepted that finding a monotherapeutic approach to AD is unlikely, given the complexity of the disease. There are numerous different systems and risk factors involved in the process of the disease, and many if not all must be addressed in order to see measurable progress. It is also likely that addressing the disease in its prodromal stage may be best as the disease processes are estimated to begin up to 20 years before clinical diagnosis.

The research presented here is a multidomain, personalized treatment plan for AD patients. The treatment plans are created with the use of an AI CDSS platform to better decipher each patient’s drivers of AD, and recommend treatments to address them individually and systemically.

In the US, the FDA has regulated medical devices to assure reasonable safety and effectiveness since 1976 (Food and Drug Administration 2019). The advent of new digital health products created an entirely new category of medical product though. For many years, CDSS fell into a gray area of regulation.

The 21st Century Cures Act passed in 2016 amended the Food, Drug, and Cosmetics Act (FEDERAL FOOD, DRUG, AND COSMETIC ACT) to exclude specific software functions from the definition of a medical device. As previously stated, CDSS is not considered to be a medical device if a software platform meets four requirements: 1) not intended to acquire, process, or analyze a medical image or a signal from an *in vitro* diagnostic device or a pattern or signal from a signal acquisition system, 2) intended for the purpose of displaying, analyzing, or printing medical information about a patient or

other medical information (such as peer-reviewed clinical studies and clinical practice guidelines), 3) intended for the purpose of supporting or providing recommendations to a health care professional about prevention, diagnosis, or treatment of a disease or condition, and 4) intended for the purpose of enabling such health care professional to independently review the basis for such recommendations that such software presents so that it is not the intent that such health care professionals rely primarily on any of such recommendations to make a clinical diagnosis or treatment decision regarding an individual patient (114th Congress 2016).

In addition to the 21st Century Cures Act, the FDA issued draft guidance for CDSS regulations in September 2019 (Food and Drug Administration 2019). This guidance provides further clarification on the specific functions of CDSS that will bring it under FDA regulation. Here, the FDA cites specific examples of CDSS functions that would and would not be regulated, and those that would not fall under the definition of a medical device.Non-device CDSS includes software that 1) is used to diagnose common illnesses, 2) identifies drug-drug interactions, and 3) provides healthcare professionals with prescription recommendations that are consistent with FDA-required labeling (Food and Drug Administration 2019). There are some cases where CDSS would be considered a medical device, but the FDA does not intend to enforce compliance. These cases include CDSS that is intended for healthcare providers or patients to inform clinical management for non-serious situations or conditions.

The guidance also provides further clarification for CDSS that is intended to inform the clinical management of patients with serious or critical situations or conditions. In these cases, the CDSS would be considered a medical device and thus fall under FDA regulations unless it provides information so that the healthcare provider can independently “evaluate the basis for the software’s recommendations” (Food and Drug Administration 2019). The data inputs and the logic behind the output recommendations must be made available to the provider (Food and Drug Administration 2019).

The CDSS presented in the following publications does not fall under the FDA’s regulation because it 1) follows current medical guidelines, 2) provides healthcare professionals with prescription recommendations that are consistent with FDA-required

labeling, 3) shares all collected data and data inputs with providers, and 4) informs providers of the reasoning and logic behind the therapy recommendations.

My role in the research and creation of this publication ranged widely from analyzing new publications to investigate what should be incorporated into the treatment algorithm, to setting up the inclusion criteria. I performed literature searches to find relevant information to AD and the known mechanisms and risk factors for the disease to help create the rules-based algorithm. I was also responsible for designing what the final product would look like to patients and physicians, including what types of information each version would or specifically would not contain.

I was also responsible for creating the medical forms each participant completed to gather the necessary medical data to create their personalized treatment. Working with a consultant neurologist, I defined the inclusion and exclusion criteria based on the research used to create our algorithm and existing clinical guidelines.

As this was a new approach, a large part of my focus was on clinical training and education for physicians and staff so they knew how this program would fit in their clinic, which patients should be considered for the program, and how to enroll a patient.

I also defined the tests that were needed to analytically and objectively assess if the treatment was working. These tests included a battery of cognitive tests, psychological screens to establish overall wellbeing and depression rates, as well as blood biomarkers that were completed at baseline before treatment, and each time before the treatment plan was updated. This allowed us to track each patient's progress and see if the treatment was resulting in improvements.

After the data was collected, I was responsible for all data analysis and manuscript creation for this publication.

As of writing this, this publication has been available for less than six months and has not yet been cited.

Current Aging Science, 2018, *11*, 173-181

RESEARCH ARTICLE

Development, Application, and Results from a Precision-medicine Platform that Personalizes Multi-modal Treatment Plans for Mild Alzheimer's Disease and At-risk Individuals

Dorothy Keine[1,*], John Q. Walker[1], Brian K. Kennedy[2,3,4,5] and Marwan N. Sabbagh[6]

[1]*uMETHOD Health, Raleigh, North Carolina, USA;* [2]*AFFIRMATIVhealth, PLLC, Sonoma, California, USA;* [3]*Departments of Biochemistry and Physiology, National University of Singapore, Singapore;* [4]*Centre for Healthy Ageing, National University Health System, Singapore;* [5]*Buck Institute For Research on Aging, Novato, California, USA;* [6]*Cleveland Clinic Lou Ruvo Center for Brain Health, Las Vegas, NV, USA*

ARTICLE HISTORY

Received: March 31, 2018
Revised: October 04, 2018
Accepted: October 05, 2018

DOI:
10.2174/1874609811666181019101430

Abstract: ***Introduction*:** Alzheimer's Disease (AD) is a progressive neurodegenerative condition in which individuals exhibit memory loss, dementia, and impaired metabolism. Nearly all previous single-treatment studies to treat AD have failed, likely because it is a complex disease with multiple underlying drivers contributing to risk, onset, and progression. Here, we explored the efficacy of a multi-therapy approach based on the disease risk factor status specific to individuals with AD diagnosis or concern.

***Methods*:** Novel software from uMETHOD Health was designed to execute a precision-medicine-based approach to develop personalized treatment recommendations with the goal of slowing or reversing biologic drivers of AD. AD-associated inputs encompassed genomic data, bio-specimen measurements, imaging data (such as MRIs or PET scans), medical histories, medications, allergies, co-morbidities, relevant lifestyle factors, and results of neuropsychological testing. Algorithms were then employed to prioritize physiologic and lifestyle states with the highest probability of contributing to disease status, and these priorities were incorporated into a personalized care plan, which was delivered to physicians and supported by health coaches to increase adherence. The sample included 40 subjects with Subjective Cognitive Decline patients (SCD), and Mild Cognitive Impairment Patients (MCI).

***Results*:** Software analysis was completed for 40 individuals. They remained on their treatment plan for an average of 8.4 months, equal to 2.8 iterations of care plans. 80% of individuals overall showed improved memory function scores or held steady, as measured by standardized cognitive evaluations. Cognitive assessments showed significant improvement in the SCD group (Composite *P value* .002, Executive *P value* .01), and the CNS-VS Executive domain showed significant results in the combined group as well (*P value* .01). There was also biomarker improvement over time observed from the blood panels. 8 out of 12 selected biomarkers showed slight, though statistically non-significant, improvement overall for symptomatic individuals, and 6 out of 12 for the overall population. Only one biomarker, homocysteine, showed significant improvement, though (*P values* .03, .04, .002).

***Conclusions*:** Our analysis of these individuals lead to several interesting observations together suggesting that AD risk factors comprise a network of interlocking feedback loops that may be modifiable. Our findings indicate previously unidentified connectivity between AD risk factors, suggesting that treatment regimens should be tailored to the individual and multi-modal to simultaneously return several risk factors to a normative state. If successfully performed, the possibility to slow progression of AD and possibly reverse aspects of cognitive decline may become achievable.

Keywords: Alzheimer's disease, mild cognitive impairment, precision medicine, combination therapy, software, treatment.

1. INTRODUCTION

Alzheimer's Disease (AD) is a progressive neurodegenerative condition in which individuals exhibit memory loss, dementia, and impaired metabolism. It is commonly a late-onset disease, with symptoms developing around the age of 65. AD is one of the most common forms of dementia, accounting for 50 to 80 percent of all dementia cases [1] and is a growing economic and social burden [2-4]. Early symptoms include difficulty in recalling recent events, personality changes, trouble with problem-solving, and confusion. As

Address correspondence to this author at the uMETHOD Health, Raleigh, North Carolina, USA; Tel: 984-232-6705; Fax: 984-232-7522; E-mails: dorothykeine@umethod.com, dorothykeine@gmail.com

the disease progresses, symptoms include mood swings, irritability, aggression, trouble with language, and long-term memory loss. In the late stages of AD, bodily functions are lost, leading to death. Life expectancy after diagnosis is seven years [1].

Nearly all previous single-domain studies to treat AD have failed, likely because it is a complex disease with multiple underlying drivers contributing to risk, onset, and progression. Often potential pathologic drivers of AD (*e.g.*, high homocysteine, genetic biases, insulin resistance, poor diet, poor sleep, lack of exercise, chronic inflammation, toxicity) are active simultaneously and need to be addressed accordingly [5]. It is now recognized that many of these underlying drivers are modifiable, allowing persons to reduce their risk and potentially delay disease onset. Even without any personal optimization, as many of one-third of cases could be attributed to modifiable risk factors [6, 7].

It is also increasingly being recognized that early intervention is key to developing an effective therapy. The neuropathological changes of AD evolve many years before clinical onset of the disease. If the diagnosis and treatment are left until a patient has progressed to dementia, their "cerebral compensatory reserves have been exhausted because of extensive neurodegeneration" [8]. Therefore, it is believed that targeting patients who present with Mild Cognitive Impairment (MCI) due to AD and Subjective Cognitive Decline (SCD) are good targets for early treatment. MCI due to AD, also known as amnestic MCI, is when a patient's cognitive capacity is below the level appropriate to their age, gender, and education level, but the cognitive decline has not reached dementia level. SCD is a cognitively-normal individual with self-reported cognitive impairment, suggestive of a prodromal AD phase [8, 9].

Clinical informatics platforms can improve the treatment of those with chronic, complex diseases such as AD (and its early phases) by optimizing a personalized multifactorial approach. With a multitude of underlying drivers of AD, genetic factors, comorbidities, medications, and optimizations for each person, the amount of data used in generating a care plan quickly accumulates, making a repeatable and reliable process beyond the scope of what a physician can do by hand, or do well quickly. But where manual methods fail, clinical informatics platforms excel. These platforms can provide a personalized treatment method for each individual in a repeatable, predictable, and timely manner.

2. MATERIALS AND METHODS

uMETHOD Health has developed a precision-medicine platform that follows the multi-modal principles of the FINGER trial [7], the Weill-Cornell Alzheimer's Prevention Clinic [10], the AHRQ Report [11], and others [12-16]. Large datasets about each person are analyzed to generate personalized treatment plans for those at risk (SCD) or in early stages (MCI). The platform identifies and addresses active issues, and creates repeatable and practical treatment plans for use in doctors' practices. The algorithms identify more than 50 drivers of AD [17-41].

2.1. Overview of Population

All individuals presented here self-selected to follow the care plan. The program was recommended by their local physician or they found uMH's website through their own searches and chose to purchase the evaluation and follow the care plan under the guidance of their physician. As this was not a controlled trial and the care plan was available to all patients through the physician, only those who wanted to continue for multiple iterations did so. Some did not continue due to cost, others due to complexity, and others were not yet due to renew for a second care plan at the time of this publication.

Patients often had a family history of AD and, out of concern for their own health, sought out our program. Others were recommended for the program by their physician, based on the physician's office analysis of the patient's cognitive state. uMH was not involved in these initial analyses, but physicians were expected to have followed standard of care for these initial assessments.

In order to enroll a patient in the program, physicians were instructed to follow a set of inclusion and exclusion criteria for interested patients before enrolling them (see Table **1**). All participants were initially assessed with the Self-Administered Gerocognitive Examination (SAGE) to deter-

Table 1. Acceptance and exclusion criteria.

Acceptance Criteria
Diagnosis of mild cognitive impairment or subjective cognitive impairment
Progressive memory loss
SAGE score of 12 or higher
Exclusion Criteria
Alcoholic (patient must be sober for at least 3 months)
Diagnosed with any other neurological disease outside of MCI or Alzheimer's disease
BMI above 35
Cancer, both current and recurring
Current Lyme disease
Currently in an Alzheimer's trial
History of major stroke, repeated strokes, recurring TIA's, or speech impediment due to stroke
Smoking
Stage 4 or 5 of chronic kidney disease (using K/DOQI guidelines)
Uncontrolled blood pressure greater than 140/90 (must be medically controlled to enroll)
Uncontrolled seizures or on multiple medications to treat seizures
Major depression; as defined by 3 or more medications needed to treat, counseling more than once a month, currently having suicidal thoughts/ideas

mine their cognitive status and the amount of cognitive impairment present. SCD *vs*. MCI was defined following the University of Ohio's validity and normality data [42], with SCD patients scoring 19 or higher, and MCI patients scoring from 12-18. Participants who scored below 12 on SAGE were excluded, as the care plan is best suited for those with mild symptoms, and not those who are have progressed into the dementia stages.

Of the 40 individuals who continued for multiple iterations of their care plan, it was observed that they were of an appropriate age to be registering cognitive concerns due to AD. The MCI individuals (n = 20) were an average of 5 years older than SCD (n = 20) ones. These self-selected individuals have a higher percentage of *APOE ε4*, a lower occurrence of diabetes, metabolic syndrome, and obesity, and are well-educated when compared to the general public (Table **2**). In other words, this population is not representative of the general public.

2.2. Input: Diverse Medical Data

Data collected from multiple health domains contribute to individuals' risk profile, helps identify underlying drivers of decline, and leads to their treatment recommendations.

Raw data files of genomic information are collected from consumer-focused companies such as 23andMe or Ancestry.com. Alternatively, a full-exome VCF file of genomic data can be read. More than 2,000 Single Nucleotide Polymorphism (SNPs) were analyzed per individual.

Personal medical history is gathered from forms completed by the individual or their caretaker. This information includes current medications, nutraceuticals, over the counter drugs, along with comorbidities, past procedures and surgeries, allergies, imaging such as MRI, EEG, or PET scans, immunization history, and family history of dementia or cardiovascular conditions.

Lifestyle data, vitals, and biometrics are also supplied. Information on sleep, diet, stress, educational attainment, physical activity, quality of life, and activities of daily living are all collected for input into the precision-medicine engine.

All forms were completed by the participants and/or their caregiver *via* an online portal, or using printed forms depending on computer skills and access. See Table **3** for a full list of questions provided to the patient.

A panel of more than 100 blood tests was requested. These include complete blood count, comprehensive metabolic panel, homocysteine level, lipid panel, endocrine panel, essential and toxic metals, and vitamin levels. Other biospecimen results, such as metabolomics, urine, saliva, and cerebrospinal fluid, are also incorporated if available.

Cognitive testing is performed before each care plan generation. Care plans are updated every 3 months. The battery includes the Montreal Cognitive Assessment (MoCA) [43], the Self-Administered Gerocognitive Exam (SAGE) [44], and CNS Vital Signs (CNS-VS) [45]. CNS-VS employs a normative dataset comprising the scores from 1,069 cognitively-normal people. Each test-taker's results are organized by age-group and compared to the appropriate normative data set for percentile scoring [45]. Alternate forms of all

Table 2. Overview of baseline: Population and cognitive testing results.

-	MCI n = 20 mean (SD)	SCD n = 20 mean (SD)
Demographic Characteristics		
Age	67.20 (9.45)	61.09 (9.47)
ApoE4	80.00%	65.00%
Education (yrs.)	16.85 (2.58)	18.89 (2.40)
Number of medications	15.75 (11.84)	12.50 (9.32)
BMI	24.07 (3.36)	23.01 (3.46)
Depression	35.00%	10.00%
Gender: Male Female	7 13	6 14
Cognitive tests		
SAGE (best = 22)	16.77 (3.02)	21.35 (1.34)
CNS-VS Composite Memory (%tile)	6.83 (8.45)	51.61 (28.78)
CNS-VS Executive Function (%tile)	5.17 (6.68)	44.50 (25.80)
SF-36 mental health	63.56 (31.33)	72.32 (17.89)
SF-36 physical health	80.44 (15.93)	79.00 (19.63)

Unless otherwise indicated, data reported as mean (±SD).

SAGE = Self-Administered Gerocognitive Exam, CNS-VS = CNS Vital Signs. *APOE4* = Apolipoprotein E ε4 allele.

Table 3. Participant forms and questions.

Medications
Current medications
Current supplements
Dosage
When started
Who prescribed
Allergies
Food
Medication
Environmental
Past Surgeries and Procedures
Date
Reason
Successful or not
Family History
Cognitive impairment
Cardiovascular conditions
Lifestyle
Alcohol intake per week
Average exercise intensity (1-10)
Average time spent exercising
Caffeine intake per day
Daily stress level (1-10)
Days of exercise per week
Hours of sleep per night
SF-36
Tobacco use
Female Only
Have you entered menopause? When?
Have you had a hysterectomy?
Medical History
Past head trauma
Past medical conditions

General list of questions asked to each participant. Answers are used in creating their care plan.

cognitive tests were used at subsequent administrations to prevent learning curves.

The blood labs panel, a subset of the lifestyle and diet information, and cognitive tests are updated with each iteration of the care plan.

All granular data that is received is retained not only for the purpose of the algorithm processing, but also so that it is available to the physicians to help them in their decision process when reviewing the recommended treatment plan.

2.3. Output: Recommended Interventions

Each participant's information is analyzed by the informatics platform and compared to standardized databases, peer-reviewed publications, and reference tables to generate treatment recommendations. Databases and reference tables used were sourced from the Centers for Disease Control, Food and Drug Administration, National Institutes of Health, DrugBank, and OMIM. The information in these databases and tables relates to SNPs, drug-drug interactions, drug-gene interactions, drug indications, and diagnostics.

The care plan recommendations consist of prescription medications, nutraceuticals, lifestyle changes, as well as specific additional diagnostics to be pursued. Lifestyle changes focus on nutrition, beginning with the MIND diet (17), exercise, sleep, autophagy, stress reduction, and brain stimulation. Each recommendation is listed by priority from highest to lowest, so the care plan may be more easily tailored to the person's capabilities. Every recommendation is personalized to the individual, including the prioritization and dosage components. Medication recommendations may involve dosage changes, changes in formulation, or deprescribing.

Each care plan is updated after three months of implementation, allowing individual's blood levels and medication response to be closely monitored and recommendations adjusted accordingly.

Separate care plan reports generated by the software are optimized for the physician, the person under treatment, and their coaching team – with the goal of suggesting what can best be achieved in a clinical setting in the long term, taken in three-month segments.

Coaches meet with individuals once a week for about one hour. They focus on explaining which areas of lifestyle changes to make in the coming week, so that improvements may be readily observable (an encouragement factor). They design personalized goals around what's achievable over a week or month and are a resource for the individual and caregiver for 1) Scheduling, 2) Explaining the complexities of terminology, 3) Understanding what others have observed, and 4) interfacing with the medical team.

2.4. Informatics Platform

This informatics platform reads medical data about a person and generates reports that describe recommended therapeutics given their current state. Internal software is written in the Python language. Interfaces to an external portal, used by the medical, care, and coaching teams to gather input and return reports, is written in PHP and Java. External medical databases support internal rules-processing algorithms. These are sourced from bodies such as the NIH, FDA, pharmaceutical trade groups, and consortia focused on topics such as genetics or allergies.

The initial input for a person is often on the order of one million data points. This count can vary (generally upwards),

depending on several input categories: 1) The completeness of the genetic exome data, 2) The resolution and number of images and image files, 3) The number of historical biospecimen lab results and cognitive assessments, 4) The granularity and history of wearable data samples, and 5) Any attached photos, scans, and faxes. Some of this input data is well-structured, such as genome data files or raw image data; other data is less well-structured, such as personal medical histories, medication lists, and image processing summaries. Natural language processing (NLP) techniques are used throughout the input steps, particularly for precise identification of lab tests, medications, drug indications, and comorbidities. A range of NLP techniques is employed to normalize input data.

The algorithms that implement this information platform go through a consistent set of steps each time they load a person's input to generate a new set of reports. These steps are rules-based, so the logic and evidence sources can be tracked (and evaluated). First, the person's current medical issues are identified, based on their available input data. There are frequently dozens of issues, so decision theory techniques are used to assign weights, priorities, and strategies to the issues. This prioritization is drawn from a wide array of medical knowledge and is done in such a way that they are self-consistent for a person's current state. Exceptional conditions can be encountered, where data values are far out of range or the need to address an issue is urgent. Examples include untreated kidney or liver disease, or a serum value, such as creatine kinase, that is at an alarm level. When exceptional issues are determined, the generation of a regular care plan is stopped, the issues are described in detail, and the physician and care team are alerted: these exceptional issues are beyond the scope of recommending a protocol for addressing cognitive decline in the next few months.

Next, interventions are selected to address the issues prioritized high enough to be the focus for the care plan period of three months. For each issue, interventions may range from those that work slowly and have few side effects to those that work quickly but may have undesirable effects for the person in their current state. Interventions also have a wide range of costs, including financial costs, pain, an effort by the person being treated, and so on. Currently, no invasive interventions are recommended in the generated care plans. The selected interventions are fitted together as a group, in an iterative manner. Many interactions may be observed, such as drug-to-drug, drug-to-genome, drug-to-diet, and diet-to-existing-comorbidity. Algorithms determine an appropriate path forward, given the many potential conflicts.

Finally, a recommended dosage or amount for each intervention is calculated, and again, the interactions among their current medications (and their dosages) and the recommended interventions are compared (Fig. **1**). The generated care plan contains recommendations for prescription and supplemental medications to be added, increased, decreased, changed, or discontinued. Specific changes to lifestyle and diet are recommended. Additional diagnostics, such as lab tests and imaging, may be recommended.

Every word in every report is generated by the informatics algorithms. Natural Language Generation (NLG) techniques assure all text, tables, and images are human-readable, in high-quality natural language (such as American English). Multiple versions of the reports are generated suited to the presumed education (*e.g.*, physician), reading ability (*e.g.*, those under treatment and their caregivers), and vocabulary (*e.g.*, dietitian, coach, physical therapist) of the readers.

3. STATISTICAL ANALYSIS

The rate of change between data values was established by calculating the delta of the final and baseline visit and controlling for the baseline score $(x_2 - x_1)/x_1$ for each biomarker reported, SAGE, and two CNS-VS subdomains.

To test for significance, normal distribution was established with the Anderson-Darling test. Samples that were found to be normally distributed were further analyzed with a paired t-test to assess if results were significant. Welch's t-test was used for any non-normally distributed samples.

Power calculations for the paired t-test were done using the following:

$$n_A = Kn_B \; and \; n_B = \left(1 + \frac{1}{K}\right)\left(\sigma \frac{Z_{1-\frac{\alpha}{2}} + Z_{1-\beta}}{\square_A - \square_B}\right)^2$$

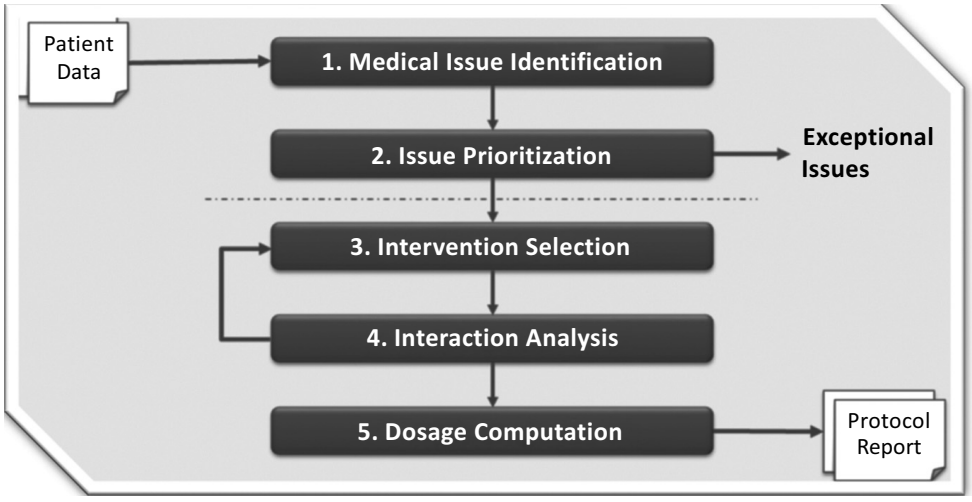

Fig. (1). Informatics platform process.

Table 4. Percent of individuals with steady or improved cognitive status.

Cognitive Tests	MCI n=20	SCD n=20	Combined n=40
SAGE	71%	78%	76%
CNS-VS Composite Memory	57%	88%	80%
CNS-VS Executive Function	43%	94%	76%

SAGE = Self-Administered Gerocognitive Exam, CNS-VS = CNS Vital Signs.

4. RESULTS

4.1. Memory Function & Biomarkers Improved

Of the 40 individuals who followed the care plan for an average of 8.4 months, 80% of the overall population (SCD + MCI) improved or held steady on their CNS-VS composite memory scores (Table **4**), with overall percentile scores improving from 40.4 (below average), to 55.87 (slightly above average) (Fig. **2**). For the MCI subset of that population, 57% showed improvement or held steady in their CNS-VS composite memory percentile scores (Table **4**). This data is promising since the improvement in memory scores is rarely observed, especially in the context of MCI, and suggests that adherence to the treatment regime may have long-lasting benefits.

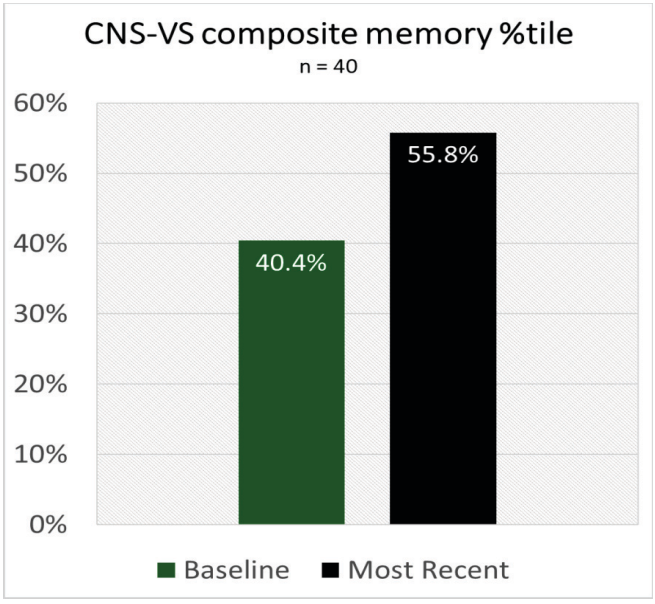

Fig. (2). Overall Memory Improvement.

76% of all individuals also showed improvement or held steady in their SAGE scores, with 71% of the MCI portion of that population showing improvement or no decline (Table **4**), indicating the consistency of program results across multiple testing measures.

Of the cognitive assessments given, both CNS-VS domains showed significant improvement in the SCD group (Composite *P value* .002, Executive *P value* .01), and the CNS-VS Executive domain showed significant results in the overall population (SCD+MCI) as well (*P value* .01) (Table **5**).

Although trends were noted, no other cognitive test showed significant improvement or decline in scores. Longer adherence to the program and/or more enrolled subjects is likely necessary to determine whether these cognitive outcomes are significantly impacted.

There was also biomarker improvement over time observed from the blood panels. Eight out of 12 selected biomarkers showed slight improvement overall for symptomatic individuals and six out of 12 for the overall sample population (Table **5**). Only one biomarker, homocysteine, showed significant improvement though (*P values* .03, .04, .002). Although not currently feasible due to the limited number of subjects, it will be interesting to compare the behavior of different variables relative to each other. For instance, cognitive performance may be more impacted by improvements in some biomarkers relative to others. This analysis may provide further prioritization and simplification as to the key parameters that treated and identify those subjects most likely to respond to the program.

5. DISCUSSION

The results of this work show that not only are individuals able to follow a multi-modal treatment, but this approach also produced measurable improvements in both cognitive testing and biomarkers (Tables **4** and **5**). Longer-term studies are needed to show that addressing multiple disease drivers simultaneously can be an effective path to improve cognitive function and to delay or prevent AD for patients in the preclinical and prodromal stages.

Precision medicine is quickly becoming more realistic with advances in genetics, proteomics, lipidomics, metabolomics, and many other fields of scientific and medical study. But implementing it in the clinic by hand is not simple. Algorithmic platforms are necessary to combine and analyze the wide range of information necessary to create individualized, detailed reports. The need for these platforms is increasingly being recognized in peer-reviewed publications as well as in industry settings [46, 47]. The United States government has recognized the need for precision medicine with the 2015 Precision Medicine Initiative [48, 49].

As Galvin points out, a well-balanced diet and healthy lifestyle may be paramount to continued overall and brain health, but every disease risk factor has the potential to act both independently and to augment the effect of other risk factors [46]. Alzheimer's, and potentially other complex

Table 5. Changes for Individuals with Multiple Care Plans.

Biomarkers	MCI n=20				SCD n=20				Combined n=40			
	x̄Start	x̄End	P(T<=t) two-tail	Cohen's D	x̄Start	x̄End	P(T<=t) two-tail	Cohen's D	x̄Start	x̄End	P(T<=t) two-tail	Cohen's D
Homocysteine	9.65 (2.45)	8.36 (1.64)	0.03	-0.63	8.85 (2.27)	7.49 (1.62)	0.04	-0.70	9.25 (2.37)	7.925 (1.67)	0.002	-0.66
Fasting insulin	7.63 (8.14)	6.945 (8.1)	0.79	-0.08	6.53 (6.29)	6.28 (7.16)	0.91	-0.04	7.11 (7.25)	6.63 (7.57)	0.80	-0.06
Glucose	90.75 (11.99)	93.2 (9.51)	0.47	0.23	89.75 (8.19)	88.3 (11)	0.63	-0.15	90.25 (10.15)	90.75 (10.44)	0.79	0.05
Total cholesterol	212.21 (40.19)	190.26 (43.22)	0.12	-0.53	202.74 (32.52)	205.79 (28.13	0.80	0.09	207.47 (38.36)	198.03 (36.81)	0.30	-0.25
TSH	2.05 (1.16)	1.28 (1.2)	0.05	-0.65	1.91 (1.29)	1.73 (1.17)	0.61	-0.15	1.98 (1.21)	1.5 (1.2)	0.09	-0.40
rT3	5.39 (5.89)	17.24 (7.57)	0.39	0.27	15.93 (3.92)	15.96 (4.66)	0.99	0.01	15.63 (5.05)	16.67 (6.39)	0.45	0.18
AM cortisol	16.62 (4.82)	16.94 (4.49)	0.83	0.07	14.24 (4.98)	14.29 (4.8)	0.99	0.01	15.46 (4.98)	15.65 (4.77)	0.84	0.04
hs-CRP	1.05 (1.13)	1.07 (1.55)	0.96	0.02	0.73 (1.03)	0.75 (1.07)	0.96	0.01	0.89 (1.08)	0.91 (1.33)	0.96	0.02
A/G ratio	2.03 (0.2)	2.03 (0.27)	0.95	0.02	1.87 (0.37)	1.83 (0.4)	0.79	-0.11	1.96 (0.3)	1.94 (0.35)	0.84	-0.05
Zinc	92.1 (17.72)	92.39 (13.87)	0.96	0.02	96.31 (26.05)	92.06 (20.11)	0.60	-0.18	94.12 (21.9)	92.23 (16.9)	0.70	-0.10
25(OH)D	45.55 (18.54)	54.28 (27.92)	0.25	0.38	51.26 (24.25)	48.17 (13.7)	0.71	-0.13	48.4 (27.67)	51.22 (21.93)	0.61	0.11
Creatinine clearance	68.17 (17.1)	68.8 (16.73)	0.91	0.04	74.6 (17.4)	79.16 (19.53)	0.47	0.25	71.38 (17.33)	73.98 (18.7)	0.54	0.14
Cognitive tests												
SAGE (best =22)	17.07 (3.83)	16.29 (5.31)	0.43	-0.17	21.5 (1.14)	21.27 (2.39)	0.69	-0.13	19.78 (3.32)	19.33 (4.47)	0.63	-0.11
CNS-VS Composite Memory (%tile)	6.83 (8.02)	3.67 (3.07)	0.42	-0.55	51.6 (27.93)	73.28 (20.71)	0.002	0.89	40.42 (31.71)	55.87 (35.6)	0.15	0.46
CNS-VS Executive Function (%tile)	5.17 (6.68)	32 (32.27)	0.10	1.38	44.5 (25.17)	64.33 (19.77)	0.01	0.88	34.67 (27.94)	56.25 (26.83)	0.01	0.79

Unless otherwise indicated, data reported as mean (±SD).
*One outlier with an unexplained high hs-CRP of 37.5 was removed from mean and SD.
Improvements are highlighted in green.
TSH = Thyroid-stimulating hormone, rT3= reverse triiodothyronine, hs-CRP = high-sensitivity C-reactive protein, A/G ratio = albumin to globulin ratio, 25(OH)D = 25-hydroxy vitamin D, SAGE = Self-Administered Gerocognitive Exam, CNS-VS = CNS Vital Signs.

diseases, must be approached as a disease that results from a system of risk factors with a multi-modal care plan that targets the system as a whole.

A precision-medicine platform enables an actionable combination therapy for AD. Well-established, big-data analytics techniques are utilized, including prioritizing, weightings, probabilities, partial differential equations, and tools from artificial intelligence. Diagnosis, treatment recommendations and ongoing tracking is extensible. Health coaches are considered essential to adherence, providing guidance and influencing individuals' compliance. Individuals comply with the recommendations and can achieve goals leading to measurable cognitive improvements sustained over an average of 8.4 months.

80% of the population, and, of those, 57% of the MCI individuals, improved or held steady in their cognitive status as measured by CNS-VS composite memory. Even though MCI SAGE scores decreased by 0.6 points over 8.4 months (Table **5**), this is still less than the average decrease of 1.91

points per year observed in previous studies for the untreated AD [50].

No cognitive test score showed a significant change for MCI individuals. This finding does show that while individuals did not improve their scores, they also did not decline.

The individuals here have a high rate of *APOE ε4*, are well-educated, average in their 60s, and can sense their cognitive decline. We saw a range of natural biological variability in the population data, although the population was not representative of the general public.

CONCLUSION

As such, further research on a larger population is warranted to conclude if these results remain consistent, and perhaps show more significant trends for a larger and more generalized population.

Additionally, future research could focus on finding ways to bring the cost of care down even further for this type of multi-modal approach. Every recommendation is given a priority and weight, as well as a monetary cost. The current algorithm has the ability to filter on those requirements for each person and setting.

This multi-modal approach also has the potential for use with other dementias and disease states. uMH's software platform was developed to specifically address the issues and contributors to AD, but parts such as improved diet, exercise, and sleep can be applied to large populations. Software-enabled, personalized combination treatment plans could be developed for many other disease states backed by similar research. Our research has shown that patients are able to follow these more complex treatment plans, and applying them to a broader audience through the development of other disease state-specific algorithms could increase the quality of life for many in the aging population, and subsequently reduce costs associated with many aging-related disease states.

ETHICS APPROVAL AND CONSENT TO PARTICIPATE

Not applicable.

HUMAN AND ANIMAL RIGHTS

No animals were used in this study. All humans research procedures followed were in accordance with the guidelines from National Institutes of Health approved by the Human Research Protections.

CONSENT FOR PUBLICATION

Informed consent was obtained from all participants starting the care plan.

CONFLICT OF INTEREST

Please note the following authors are employed by and/or hold stock in uMETHOD Health: Dorothy Keine, MS, John Q. Walker, PhD, Marwan N. Sabbagh, MD, FAAN. The following author is employed by AFFIRMATIVhealth which has a financial relationship with uMETHOD Health: Brian K. Kennedy, PhD.

ACKNOWLEDGEMENTS

Partial funding for this work and article processing charges were funded by uMETHOD Health located in Raleigh, NC, USA.

All authors had full access to all of the data in this work and take complete responsibility for the integrity of the data and accuracy of the data analysis.

All named authors meet the International Committee of Medical Journal Editors (ICMJE) criteria for authorship for this manuscript, take responsibility for the integrity of the work as a whole, and have given final approval to the version to be published.

REFERENCES

[1] Alzheimer's Association. [Online]. [cited 2017]. Available from: http://www.alz.org/.

[2] WHO and Alzheimer's Disease International. Geneva: World Health Organization. [Online]. Geneva: World Health Organization; 2012 [cited 2017]. Available from: http://www.who.int/mental_health/publications/dementia_ report_2012/en/.

[3] World Health Organization. First WHO ministerial conference on global action against dementia: Meeting report. WHO Headquarters Geneva, Switzerland; 2015.

[4] Winblad B, Amouyel P, Andrieu S, *et al*. Defeating alzheimer's disease and other dementias: A priority for European science and society. Lancet Neurol 2016; 15(5): 455-532.

[5] Doraiswamy PM, Steffens DC. Combination therapy for early Alzheimer's disease: What are we waiting for? J Am Geriatr Soc 1998; 46(10):1322-4.

[6] Livingston G, Sommerlad A, Orgeta V, *et al*. Dementia prevention, intervention, and care. Lancet 2017; 390(10113): 2673-734.

[7] Ngandu T, Lehtisalo J, Solomon A, *et al*. A 2 year multidomain intervention of diet, exercise, cognitive training, and vascular risk monitoring *versus* control to prevent cognitive decline in at-risk elderly people (FINGER): A randomized controlled trial. Lancet 2015; 385(9984): 2255-63.

[8] Bachurin S, Gavrilova S, Samsonova A, *et al*. Mild cognitive impairment due to alzheimer disease: Contemporary approaches to diagnostics and pharmacological intervention. Pharmocol Res 2017; 129: 216-26.

[9] Moreno-Grau S, Rodriguez-Gomez O, Sanabria A, *et al*. Exploring APOE genotype effects on Alzheimer's disease risk and amyloid β burden in individuals with subjective cognitive decline: The FundacioACE Healthy Brain Initiative (FACEHBI) study baseline results. Alzheimers Dementia J Alzheimers Assoc 2017; 14(5): 634-43.

[10] Seifan A, Isaacson R. The alzheimer's prevention clinic at Weill Cornell medical college/ New-York Presbyterian hospital: Risk stratification and personalized early intervention. J Prev Alzheimers Dis 2015; 2(4): 254-66.

[11] Kane RL, Butler M, Fink HA, *et al*. Interventions to Prevent Age-Related Cognitive Decline, Mild Cognitive Impairment, and Clinical Alzheimer's-Type Dementia Rockville, MD: Agency for Healthcare Research and Quality (US); 2017.

[12] Cummings JL, Isaacson RS, Schmitt FA, *et al*. A practical algorithm for managing Alzheimer's disease: What, when, and why? Ann Clin Transl Neurol 2015; 2(3): 307-23.

[13] Østergaard SD, Mukherjee S, Sharp SJ, *et al*. Associations between potentially modifiable risk factors and Alzheimer disease: A Mendelian randomization study. PLoS Med 2015; 12(6): e1001841.

[14] Stephenson D, Perry D, Bens C, *et al*. Charting a path toward combination therapy for Alzheimer's disease. Expert Rev Neurother 2015; 15(1): 107-13.

[15] Xu W, Tan L, Wang HF, *et al*. Meta-analysis of modifiable risk factors for Alzheimer's disease. J Neurol Neurosurg Psychiat 2015; 86: 1284-5.

[16] Norton S, Matthews FE, Barnes DE, *et al*. Potential for primary prevention of Alzheimer's disease: An analysis of population-based data. Lancet Neurol 2014; 13(8): 788-94.

[17] Morris MC, Tangney CC, Wang Y, *et al*. MIND diet associated with reduced incidence of Alzheimer's disease. J Alzheimers Dement 2015; 11(9): 1007-14.

[18] Paddock CP. Concussion linked to brain changes in people at genetic risk for Alzheimer's. Medical News Today. 2017.

[19] Joubert LM, Manore M. Exercise, nutrition, and homocysteine. Int J Sport Nutr Exerc Metab 2006; 16(4): 341-61.

[20] Rodrigue KM, Rieck JR, Kennedy KM, *et al*. Risk factors for β-Amyloid deposition in healthy aging: Vascular and genetic effects. JAMA Neurol 2013; 70(5): 600-6.

[21] Hong H, Kim BS, Im H. Pathophysiological role of neuroinflammation in neurodegenerative diseases and psychiatric disorders. Int Neurol J 2016; 20(Suppl 1): p. S2-7.

[22] Chaker L, Wolters F, Korevaar TI, *et al*. Thyroid function and the risk of dementia: The rotterdam study. Neurology 2016; 87(16): 1688-95.

[23] Rosales-Corral S, Tan DX, Manchester L, *et al*. Diabetes and alzheimer's disease, two overlapping pathologies with the same background: Oxidative stress. Oxid Med Cell Longev 2015; http://dx.doi.org/10.1155/2015/985845.

[24] Chatterjee S, Peters SAE, Woodward M, *et al*. Type 2 Diabetes as a risk factor for dementia in women compared with men: A pooled analysis of 2.3 million people comprising more than 100,000 cases of dementia. Diabetes Care 2016; 39(2): 300-7.

[25] Bucossi S, Ventriglia M, Panetta V, *et al*. Copper in alzheimer's disease: A Meta-analysis of serum, plasma, and cerebrospinal fluid studies. J Alzheimers Dis 2011; 24(1): 175-85.

[26] Singh I, Sagare AP, Coma M, *et al*. Low levels of copper disrupt brain amyloid-β homeostasis by altering its production and clearance. PNAS 2013; https://doi.org/10.1073/pnas.1302212110.

[27] Lövheim H, Gilthorpe J, Adolfsson R, *et al*. Reactivated herpes simplex infection increases the risk of Alzheimer's disease. Alzheimers Dement 2015; 11(6): 593-9.

[28] Lovheim H, Gilthorpe J, Johansson A, *et al*. Herpes simplex infection and the risk of Alzheimer's disease- A nested case-control study. Alzheimers Dement 2015; 11(6): 587-92.

[29] Itzhaki RF, Lathe R, Balin BJ, *et al*. Microbes and Alzheimer's disease. J Alzheimers Dis 2016; 51(4): 979-84.

[30] Bezprozvanny I, Mattson MP. Neuronal calcium mishandling and the pathogenesis of Alzheimer's disease. Trends Neurosci 2008; 31(19): 454-63.

[31] Campbell N, Boustani M, Limbil T, *et al*. The cognitive impact of anticholinergics: A clinical review. Clin Interv Aging 2009; 4: 225-33.

[32] Han L, Agostini JV, Allore HG. Cumulative anticholinergic exposure is associated with poor memory and executive function in older men. J Am Geriatr Soc 2008; 56(12): 2203-10.

[33] Hirai K, Aliev G, Ninomura A, *et al*. Mitochondrial abnormalities in alzheimer's disease. J Neurosci 2001; 21(9): 3017-23.

[34] García-Escudero V, Martín-Maestro P, Perry G, *et al*. Deconstructing mitochondrial dysfunction in alzheimer disease. Oxid Med Cell Longev 2013; 2013: http://dx.doi.org/10.1155/2013/162152.

[35] Xu W, Tan L, Wang H, *et al*. Meta-analysis of modifiable risk factors for Alzheimer's disease. Cognitive Neurol 2015; 86(12): 1299-306.

[36] Chakrabarti S, Khemka V, Banerjee A, *et al*. Metabolic risk factors of sporadic alzheimer's disease: Implications in the Pathology, Pathogenesis and Treatment. Aging Dis 2015; 6(4): 282-99.

[37] Cerutti-Kopplin D, Feine J, Padilha DM, *et al*. Tooth Loss Increases the Risk of Diminished Cognitive Function: A Systematic Review and Meta-analysis. JDR Clin Trans Res 2016; 10-9.

[38] Last W. Health Science. [Online]. 2016 [cited 2017]. Available from: www.health¬science-spirit.com\pyroluria.htm.

[39] Xie L, Kang H, Xu Q, *et al*. Sleep drives metabolite clearance from the adult brain. Science 2013; 342(6156): 373-37.

[40] Ferreira LK, Tamashiro-Duran JH, Squarzoni P, *et al*. The link between cardiovascular risk, Alzheimer's disease, and mild cognitive impairment: Support from recent functional neuroimaging studies. Braz J Psychiatry 2014; 36(4): 344-57.

[41] Kim HA, Miller AA, Drummond GR, *et al*. Vascular cognitive impairment and Alzheimer's disease: Role of cerebral hypoperfusion and oxidative stress. Naunyn Schmiedebergs Arch Pharmacol 2012; 385(10): 953-9.

[42] Ohio State University. Wexner Medical Center. [Online]. 2017. Available from: https://wexnermedical.osu.edu/brain-spine-neuro/memory-disorders/sage.

[43] Nasreddine ZS, Phillips NA, Bédirian V, *et al*. The Montreal Cognitive Assessment, MoCA: a brief screening tool for mild cognitive impairment. J Am Geriatr Soc 2015; 53(4): 695-9.

[44] Scharre DW, Chang SI, Murden RA, *et al*. Self-administered Gerocognitive Examination (SAGE): A brief cognitive assessment Instrument for Mild Cognitive Impairment (MCI) and early dementia. Alzheimer Dis Assoc Disorders 2010; 24(1): 64-71.

[45] Gualtieri CT, Johnson LG. Reliability and validity of a computerized neurocognitive test battery, CNS Vital Signs. Arch Clin Neuropsychol 2006; 21(7): 623-43.

[46] Galvin J. The prevention of alzheimer's disease: Lessons learned and applied. J Am Geriatr Soc 2017; 65(10): 2128-33.

[47] Isaacson R. Is alzheimer's prevention possible? J Am Geriatr Soc 2017; 65(10): 2153-4.

[48] Obama white house archives. [Online].; 2015 [cited 2017]. Available from: https://obamawhitehouse.archives.gov/node/333101.

[49] National Institutes of Health: All of Us Research Program. [Online]. 2017 [cited 2017]. Available from: https://allofus.nih.gov/.

[50] Scharre D, Chang S, Nagaraja H, *et al*. Longitudinal Changes in Self-Administered Gerocognitive Examination (SAGE) and Mini-Mental State Exam (MMSE) Score for Subjective Cognitive Impairment (SCI), Mild Cognitive Impairment (MCI), Dementia Converters, and Alzheimer's Disease (AD) Patients. Alzheimers Dement J Alzheimers Assoc 2015; 11(7): 570.

Conclusions

To the authors' knowledge, this was the first time that a treatment for AD has been created using CDSS, or any algorithm platform. Our research showed that patients were willing to take the extra steps needed to provide all of the information to create a personalized treatment plan, and that they were motivated to learn and follow their plan for an extended period of time.

The results showed promise for this CDSS platform in treating and potentially delaying AD in patients. As mentioned in the discussion, further research is needed on a larger population, as well as controlled trials to truly test its effectiveness against the standard of care. The authors did recognize the need for a larger study and applied for future grant money in order to fund a larger, controlled clinical trial.

Further research is also needed to identify the core data needed to create an effective treatment protocol. At this time, the algorithm can run with any amount of data input. There is likely a minimum set of required data to make recommendations that are informed enough to positively influence patient outcomes in the personalized manner that the software was designed to achieve.

Without knowledge of this minimum information set, the algorithm's recommendations could be very general in nature and apply to lifestyle changes only. While these types of changes have been proven to be effective in some cases (Ngandu et al. 2015), and many experts agree that generalized lifestyle changes could have a major impact on delaying disease onset (Lista et al. 2015; Cummings et al. 2015; Otaegui-Arrazola et al. 2014; Reiner et al. 2013; Shinto et al. 2014; Douaud et al. 2013; Farina et al. 2017; Norton et al. 2014), a personalized combination therapy is likely to be the most effective approach (Doraiswamy & Steffens 1998; Cummings et al. 2015; Cummings et al. 2019; Stephenson et al. 2015; Hampel et al. 2017; Isaacson 2017; Galvin 2017).

The risks from following the recommendations generated by the software platform are minimal because they are based on current medical guidelines and not experimental medications. Additionally, every treatment plan is evaluated by a

physician before being given to or implemented by a patient. This allows an additional layer of protection for all patients as the physician is able to evaluate the appropriateness and safety of all recommendations and make changes to the treatment plan as they see fit.

In the process of working with these patients and analyzing their data and results, we noticed that patients were frequently on an extensive list of medications. Some of which interacted, counteracted, or should have been discontinued after a set amount of time. This led us to further examine the prevalence of polypharmacy in the AD population and to examine what, if any, adverse effects it was causing.

Chapter 8: Polypharmacy in an elderly population: Enhancing medication management through the use of clinical decision support software platforms

Elderly populations are prone to comorbidities, and AD patients even more so. Because of this, they are often prescribed many different medications. The implications of this polypharmacy are not being fully considered by prescribing physicians though. Each drug has its own potential side effects, and when medications are taken together, there is also a potential for those medications to interact. The risk grows with each added medication.

While a physician on their own may not be able to parse all of the possible complications for a patient's medication regime, CDSS is capable of alerting them to all of these interactions and side effects.

The next publication addresses the growing use of polypharmacy and the increased risk for those with AD. Medication management has become increasingly complex, surpassing physicians' ability to know all the possible interactions and adverse events patients might face. CDSS can be used to identify potential issues with a patient's medication regime, including drug-drug interactions (DDIs), drug-genome interactions (DGIs), depression-inducing medication (DIDs), and anticholinergic burden (ACB). The output from these algorithms can help physicians better prescribe for their patients and remove patients from medications that are interacting or causing adverse events. Machine learning also has the capability to suggest formulary alternatives that have fewer interactions and adverse events. This would help AD patient populations as they are often unable to identify or articulate when they are having issues due to medications and would also help to reduce the cognitive and psychological burden that certain medications can cause for patients.

Our research showed that algorithms could be used to identify DDIs, DGIs, DIDs, and ACB in a manner that would alert physicians and help them to better manage their patient's medication regime. We added these new algorithm additions to our existing AD-treatment platform.

Because of the large amount of data that was collected on every patient, I was able to analyze the cohort's information in many different ways, resulting in new additions to our algorithm that further enhanced patients' treatment and safety. My work on this research project included gathering the patient population from our existing database to be analyzed, completing all statistical analyses, and identifying the different drugs the patients were taking that fit into each medication class that we were analyzing for potential issues. I was then responsible for compiling the completed data and pulling together the results in cohesive manner. Finally, I was responsible for writing and completing the manuscript.

This publication has only recently been published and has been cited by one other researcher.

Neurol Ther
https://doi.org/10.1007/s40120-019-0131-6

ORIGINAL RESEARCH

Polypharmacy in an Elderly Population: Enhancing Medication Management Through the Use of Clinical Decision Support Software Platforms

Dorothy Keine · Mark Zelek · John Q. Walker · Marwan N. Sabbagh

Received: November 26, 2018

ABSTRACT

Introduction: Polypharmacy is a growing problem in the United States. The use of multiple medications increases the likelihood that a patient will experience potential drug interactions and adverse drug reactions (ADRs). Those individuals with dementia or Alzheimer's disease (AD) are at greater risk, due to age, comorbidities, and an increased likelihood of being on a greater number of neuroactive medications.

Methods: uMETHOD Health (uMH) has developed a precision medicine platform to address dementia and mild AD through the creation of personalized, multidomain treatment plans. Many interactions and ADRs may be observed, such as drug–drug interactions (DDIs), drug–gene interactions (DGIs), anticholinergic cognitive burden (ACB), and depression-inducing drugs (DIDs). uMH's algorithms can parse these interactions, rate them based on input from open-source databases, and then record all these interactions in a generated treatment plan. A total of 295 individuals aged 65 and older were included in this analysis.

Results: Of 295 individuals, 97.59% were on at least one medication, with an overall mean of 11.5 medications per person; 83.66% were on five or more medications. A total of 102 DGIs, 3642 DDIs, and one high-priority DDI were found in this population. There was a significant increase in the number of DDIs as medications per person increased (P value < 0.0001). Of the population, 65.86% were on one or more anticholinergic drugs. There was a significant difference in the ACB score between individuals with cognitive decline and those without. In total, 60.98% of the overall population were on DIDs, with a mean of 1.19 medications per person.

Conclusions: The results of this work show that older populations have a high medication burden. With the growing elderly and AD populations, medication management for polypharmacy is a need that grows direr every year. uMH's platform was able to identify a multitude of polypharmacy problems that individuals are currently facing.

Funding: uMETHOD Health.

Keywords: Anticholinergic drugs; Drug–drug interactions; Drug–genome interactions; Depression-inducing drugs; Machine learning; Polypharmacy

Enhanced digital features To view enhanced digital features for this article, go to https://doi.org/10.6084/m9.figshare.7739627.

D. Keine (✉) · M. Zelek · J. Q. Walker
uMETHOD Health, Raleigh, NC, USA
e-mail: dorothykeine@gmail.com

M. N. Sabbagh
Cleveland Clinic Lou Ruvo Center for Brain Health, Las Vegas, NV, USA

Published online: 21 March 2019

INTRODUCTION

Polypharmacy, defined as the use of five or more medications [1], is a growing problem in the United States [2]. Medication regimes comprised of multiple medications increase the likelihood that a patient will experience potential drug interactions and adverse drug reactions (ADRs) [3]. ADRs place many patients in the hospital every year and can have life-threatening consequences. They are among the top ten leading causes of death [2, 4].

These risks are even higher for the elderly, due to age-related changes of pharmacokinetics (PK) and pharmacodynamics (PD) of many drugs. Changes in PK and PD are related to an overall decrease in total body water which decreases the spread of hydrophilic drugs, increasing body fat that in turn increases the distribution of lipophilic drugs, and a breakdown in the blood–brain barrier that results in a higher distribution of drugs that affect the central nervous system [3]. Moreover, age-related diseases can further change patients' PK and PD by increasing sensitivity to drug effects and thus increasing their susceptibility to ADRs.

Among those taking any prescription medication, half are exposed to two or more drugs with 5% exposed to eight or more [2]. This high rate of multiple medications is driven in large part by people who have multiple chronic conditions. Approximately half of the US population has at least one chronic condition, and one in four have multiple [5]. Those individuals with dementia or Alzheimer's disease (AD) are also at greater risk due to age, an increased number of comorbidities, and an increased likelihood of being on a greater number of neuroactive medications. In one study, only 8.7% of AD patients did not have a physical condition, compared to 15.9% of controls [6].

AD is a progressive neurodegenerative condition in which individuals exhibit memory loss, dementia, and impaired metabolism. It is commonly a late-onset disease, with symptoms developing around the age of 65. AD is one of the most common forms of dementia, accounting for 50–80% of all dementia cases [7] and is a growing economic and social burden [8, 9]. Early symptoms include difficulty in recalling recent events, personality changes, trouble with problem-solving, and confusion. As the disease progresses, symptoms include mood swings, irritability, aggression, trouble with language, and long-term memory loss. In the late stages of AD, bodily functions are lost, leading to death. Life expectancy after diagnosis is 7 years [7]. Comorbidity and polypharmacy are both associated with worsening cognition, functional ability, and survival for patients with dementia [6].

AD patients may be at greater risk for ADRs when it comes to neuroactive drugs compared to a normal elderly population, due to the neurological damage that is characteristic of the disease. According to Dr. Pasqualetti at the University of Pisa, "the impaired neurotransmission in AD patients represents the major pharmacological target (especially cholinergic system) for disease treatment, it might also represent a point of weakness for AD patients" [3].

Both chronic diseases and medication numbers increase when considering a population that is 65 and older. Polypharmacy has been shown to be a statistically significant predictor of hospitalization, nursing home placement, death, hypoglycemia, fractures, impaired mobility, pneumonia, and malnutrition for older populations [10]. In the United States, 30% of adults over 65 take 5 or more medications [2].

Each drug has the potential to cause side effects and adverse events, but drugs also interact. These interactions can be so minor as to be recommended to ignore, or they can be very serious, with the potential for death with concurrent use [11]. Interactions and adverse events can arise from multiple factors, including drug–drug interaction (DDI), drug–genome interaction (DGI), anticholinergic burden (ACB), and depression-inducing drugs (DIDs), creating new risks for the patient with each additional medication. Indeed, the inability of patients and providers alike to distinguish drug-induced symptoms from new disease symptoms often results in the addition of more medications to treat drug-induced symptoms, further increasing the risk of DDIs and ADRs [3].

DDIs occur when individuals are exposed to medications that interact to produce an undesirable result. They fall into two categories: PK and PD interactions [12]. Exposure to potential DDIs does not always result in a direct adverse drug event or measurable clinical effect, but they can have an additive effect [12, 13]. As Katie Quinn of Stanford University states in "A dataset quantifying polypharmacy in the United States," "exposure to multiple drugs puts patients at additive risk of each single drug's potential adverse outcomes" [2].

Genetic factors also affect the PK and PD of drugs, altering patients' response [14–16]. In recent years, databases have been created to track and aid in the study of DGIs. This has become known as the "druggable genome," and is defined as "genes or gene products that are known or predicted to interact with drugs, ideally with a therapeutic benefit to patients" [14].

Anticholinergic drugs block the neurotransmitter acetylcholine in the central and peripheral nervous systems. They are indicated for use in many different disease states, including depression, gastrointestinal disorders, Parkinson's disease, urinary incontinence, epilepsy, and seasonal allergies [17]. In fact, many commonly used drugs have anticholinergic properties, including over-the-counter-medications. These drugs are widely available and include antihistamines, drugs to reduce frequency of urination, and medications for sleep disturbances. The availability and number of non-prescription drugs with anticholinergic properties is increasing in recent years [18]. The cumulative effect of taking multiple medications with anticholinergic properties is referred to as ACB [19].

Many studies have shown that anticholinergic drugs can adversely impact cognition, physical function, cause dizziness, delirium, confusion, falls, and increase the risk of mortality in elderly populations [19, 20]. ACB has also been shown to be a risk factor for developing mild cognitive impairment (MCI) and dementia [17, 21–23]. Each definite anticholinergic drug has the potential to increase the risk of cognitive impairment by 46% over 6 years [21]. In addition, the odds ratio for a diagnosis of MCI was 2.73 for adults exposed to at least 3 anticholinergics for a minimum of 90 days. The odds ratio for dementia was 0.43 [22].

Many cognitively impaired and AD patients are simultaneously taking cholinesterase inhibitors along with anticholinergic drugs. Cholinesterase inhibitors are one of the most prescribed drugs types for dementia and AD patients [24]. One study showed that 35.4% of patients received these two drug types in combination [25]. The use of these medications in combination is likely to decrease their pharmacological benefit as they counteract each other [26], making their simultaneous use seldomly appropriate due to the drugs' invalidating pharmacological effect [25].

Guidelines such as Beers and the Screening Tool of Older Persons' potentially inappropriate Prescriptions (STOPP) both state that the use of anticholinergic drugs should be avoided in older populations [17, 23]. Even with these accepted guidelines, physicians often prescribe these medications for their anticipated therapeutic outcomes, overlooking the possible risks [19].

Anticholinergic drugs are also one of the most commonly prescribed DIDs. Numerous medications and medication classes have been classified as depression-inducing. Other common DIDs include sedative-hypnotics and analgesics [27, 28]. Drug-induced depression is more likely to occur in individuals who have a higher risk factor for depressive disorder [29], as may be the case for individuals with the APOE ε4 allele and AD patients.

An increase in drug-induced depression is another result of the increasing occurrence of polypharmacy [30]. Many studies that identify potential DIDs are observational in nature, and results have been contradictory. Nevertheless, DIDs should be considered as a potential cause when new symptoms of depression occur [31].

The elderly are less likely to recognize ADRs for what they are and can even be more likely to have their concerns dismissed by medical providers. Elderly people often have lower expectations for what their health should be, and are therefore less likely to let their physician know when they are experiencing new issues. Those with cognitive impairment may also be unable to recognize new symptoms or may have

difficulty communicating them. In some cases, ADRs are mistaken for the consequences of old age [18].

The aging population along with the number of people diagnosed with AD are quickly growing in the United States. It is estimated that by 2030, more than 20% of all US residents will be 65 or older, compared with just 13% in 2010 [32].

With the quick growth of these populations and the ever-increasing number of drugs available on the market, medication management is necessary, but too complex to be handled by a single physician. We propose that clinical decision support software (CDSS) with machine-learning algorithms should be employed in this complicated space to increase physician effectiveness and patient safety.

CDSS is software created to provide treatment decision support to medical professionals. CDSS can process large amounts of information in a quick and effective manner, creating actionable recommendations to improve clinical decision-making [33, 34]. Because of this ability, the guidance provided is patient-specific instead of generalized [34]. The output of CDSS contains guidance on the diagnosis, treatment, prevention, cure, or mitigation of disease [35].

Machine learning enables the CDSS platforms to make successful predictions based on past experiences [36, 37]. There may be dozens of issues identified for one patient, so decision-theory techniques can be used to assign weights, priorities, and strategies to the issues. Next, interventions are selected. These interventions have a wide range of costs, including financial costs, pain, and effort by the person being treated which should be taken into account by the CDSS platform. Many interactions may be observed, such as DDIs, DGIs, and drug-to-diet interactions. Algorithms determine an appropriate path forward, given the many potential conflicts.

This method would enable physicians to have access to an automated, repeatable, and reliable analysis that can be applied to every patient, is based on the latest clinical guidelines, and is personalized to the individual. It can process copious amounts of information quickly, making it useful in a clinical setting.

METHODS

Population Overview

A total of 295 individuals were included in this analysis. All of the data presented here was previously collected for the purposes of creating treatment plans for patients with a family history of AD, with mild cognitive decline, or mild AD.

Following the guidelines put forth in the 21st Century Cures Act [35], CDSS is not regulated by the US Food and Drug Administration (FDA), and uMETHOD Health's (uMH) treatment protocol does not include any investigational drugs. Because of this, uMH's precision medicine platform was taken straight to market and did not need an approval by an ethics committee or board.

When participants were enrolled for the treatment plan, uMH obtained permission from every individual to use their data for future research purposes, in compliance with ethics guidelines. uMH's Terms and Conditions for the commercially available treatment plan outlined that data would be saved and used only in a de-identified manner.

Each participant receiving a treatment plan accessed an online consent form or was given a printed version if access was an issue, outlining uMH's Terms and Conditions for the commercially available treatment plan. Individuals who presented with cognitive decline were encouraged by uMH and their physician to have a caretaker or family member review all documents and consent forms before signing.

Before initial enrollment, all individuals were first evaluated by a physician to ensure they were a good fit for the program. Cognitive testing was done at baseline and these results were used to classify the individuals as either cognitively normal or demented. Cut-off scores for dementia classification followed the University of Ohio's validity and normality data for the Self-administered Gerocognitive Examination (SAGE) with a score of 17–22 considered normal cognition [38, 39].

uMH's algorithm platform automatically assigns every participant a random eight-character ID when they are first entered into the

system to de-identify their information. All data was collected under their randomly assigned ID, and the investigators here only had access to this de-identified information.

Following the guidelines set out by "Coded Private Information or Specimens Use in Research" by the Office for Human Research Protection [40], since the data presented here was not collected for the currently proposed polypharmacy research project and no investigator could ascertain the identity of the individuals, the data presented here is not classified as involving human subjects.

Institutional review board approval was not required as data are recorded in such a manner that subjects cannot be identified, directly or through identifiers linked to the subjects. Meeting these conditions makes this research exempt from the requirements of 45 CFR 46 under the Department of Health and Human Services (HHS): Research, involving the collection or study of existing data, documents, records, pathological specimens, if these sources are publicly available or if the information is recorded by the investigator in such a manner that subjects cannot be identified, directly or through identifiers linked to the subjects.

For the purposes of this analysis, only individuals who were aged 65 and older were included. Our population was 55.25% female (n = 163). See Tables 1 and 2 for a full analysis of the research cohort.

Table 2 Cognitive status

Cohort	Cognitive state	Frequency	% of population
All	Normal	109	49.1
	MCI	91	41
	AD	22	9.91
Female	Normal	52	43.3
	MCI	56	46.7
	AD	12	10
Male	Normal	57	55.9
	MCI	35	34.3
	AD	10	9.8

MCI mild cognitive impairment, *AD* Alzheimer's disease

Bioinformatics Platform

uMH has developed a precision medicine platform to address dementia and mild AD through the creation of personalized, multidomain treatment plans [41]. Large data sets are collected and analyzed for each patient to generate a treatment plan. Each treatment plan is reviewed by a trained physician before being delivered to the patient. uMH's platform identifies and addresses active issues, and creates repeatable and practical treatment plans for use in doctors' practice.

Many interactions and ADRs may be observed, such as DDIs, DGIs, ACB, as well as DIDs. uMH's algorithms can parse these interactions, rate them based on input from open-source databases, and then record all these interactions in the person's generated treatment plan. This allows a physician to easily review and amend a patient's medication regime.

The internal software of the bioinformatics platform is written in the Python language. It interfaces to an external portal, used by the medical, care, and coaching teams to gather

Table 1 Population overview

Variable	Mean	Standard deviation	Minimum	Maximum
Age (years)	75.51	7.31	64.92	102.46
Education (years)	16.11	3.48	5	24
BMI	26.45	5.17	17.4	45.9
Total medications	11.53	8.83	0	67
SAGE score	16.23	4.60	0	22

BMI body mass index, *SAGE* Self-administered Gerocognitive Examination

input and return reports written in PHP and Java. External medical databases support the internal rules-processing algorithms. These are sourced from bodies such as the National Institutes of Health (NIH), FDA, pharmaceutical trade groups, and consortia focused on topics such as genetics or allergies.

The initial data input for a person is often about one million data points. This count can vary (generally upwards), depending on several input categories: (1) the completeness of the genetic exome data, (2) the resolution and number of images and image files, (3) the number of historical biospecimen lab results and cognitive assessments, (4) the granularity and history of wearable data samples, and (5) any attached photos, scans, and faxes. Natural language processing (NLP) techniques are used throughout the input steps, particularly for precise identification of lab tests, medications, drug indications, and comorbidities. A range of NLP techniques are employed to normalize input data.

The algorithms that implement this information platform go through a consistent set of steps each time they load a person's input to generate a new set of reports. These steps are rules-based, so the logic and evidence sources can be tracked (and evaluated). When ADRs are determined, the issues are described in detail, and the physician and care team are alerted.

Every word in every report is generated by the bioinformatics algorithms. Natural language generation (NLG) techniques assure all text, tables, and images are human-readable, in high-quality natural language (such as American English). Multiple versions of the reports are generated suited to the presumed education (e.g., physician), reading ability (e.g., those under treatment and their caregivers), and vocabulary (e.g., dietitian, coach, physical therapist) of the readers.

Input

Data was collected using either paper forms or uMH's online portal depending on the individual's computer skills and access.

Personal medical histories were gathered from forms completed by the individual or their caregiver. This information includes current medications, nutraceuticals, over-the-counter drugs, comorbidities, past procedures and surgeries, allergies, imaging such as MRI, EEG, or PET scans, immunization history, and family history of dementia or cardiovascular conditions.

Lifestyle data, information on sleep, diet, stress, educational attainment, physical activity, quality of life, activities of daily vitals, and biometrics were also supplied by the individual, their caregiver, and/or the physician.

Measures

All medications, including prescriptions, vitamins, and over-the-counter drugs, reported were counted toward each person's total medication number. Three medication categories were chosen for statistical analysis due to their large prevalence, and in some cases accepted guidelines for avoidance, in older and AD populations: neuroactive medications, anticholinergics, and DIDs.

Drug–Drug Interactions

Information on each person's current medication regimes was collected through uMH's patient questionnaires or supplied by physicians.

uMH's CDSS platform utilized existing national databases to determine interactions. DDIs were determined using the NIH RxNorm database, including the "ONC High" subset (ONC is the Office of the National Coordinator for Health Information Technology). The RxNorm database is a normalized naming system for generic and brand-name drugs produced by the National Library of Medicine [42]. The RxNorm system is used by hospitals, pharmacies, and other organizations nationwide to record and process drug information through computer systems. The goal of RxNorm "is to allow computer systems to communicate drug-related information efficiently and unambiguously." The RxNorm database covers clinical drugs and drug packs. Each drug in the RxNorm database receives a RxNorm concept unique identifier (RxCUI). The RxCUI is normalized to a numeric code that computers are able to parse [42].

DDIs are determined pairwise, using the RxNorm RxCUI code for each of the two drugs.

The RxCUIs identify the specific brand of medication (if supplied by the participant), or their generic form (if no brand name was supplied). uMH's bioinformatics platform has a Representational State Transfer (REST) open application-programming interface (API) to the RxNorm database. Results are cached to speed processing.

DDI priority was derived from the Lexicomp rating system [11]. Lexicomp's DDI risk-rating scale stratifies risk to provide medical professionals with relevant information about the potential urgency associated with each interaction. The informatics platform examines all DDIs. Those that have a rating of C or above are identified to physicians in uMH's reports as clinically significant. Those with a rating of D or X are considered high-priority DDIs, as these drug combinations are contraindicated.

Drug–Genome Interactions

uMH's platform mines publicly available databases to check for DGIs in each individual. Individuals' raw data files of genomic information were collected from consumer-focused companies such as 23andMe or Ancestry.com. Alternatively, a full-exome VCF file of genomic data can be read. The platform analyzes more than 2000 single nucleotide polymorphisms (SNPs) per individual, some of which pertain to DGIs, and others are used to quantify the genetic risk of AD as well as other genetic diseases.

DGI information was drawn from three sources of pharmacogenomic information: the Clinical Pharmacogenetics Implementation Consortium (CPIC) effort [43], DrugBank [13, 44], and SNPedia's SNP and genoset compilations [45, 46]. DGIs are looked at in two categories: genetics that influence how enzymes metabolize each drug, and relationships between specific genes and drugs. Each medication a person is currently taking is compared against a table of genes that affect it, and these genes are, in turn, compared to those in the person's genome. CPIC rates each DGI on a scale from A to D, where prescribing action is recommended for levels A or B, but not necessarily for levels C or D. No DGI priorities are assigned in the DrugBank or SNPedia databases.

Anticholinergic Burden

ACB is measured using the ACB scale. This scale was created by expert consensus to rank each medication with known anticholinergic activity from high to low. Each drug that has anticholinergic properties is assigned a score of 1–3 depending on the severity. The list is currently comprised of 195 different medications [19, 21].

Drugs with possible ACB are assigned a value of 1, and those with definite anticholinergics are given a value of 2 or 3. To get the total ACB score for a patient, the value attributed to each medication is summed. Each point a patient has on the ACB scale has been correlated to a decline in mini-mental state examination (MMSE) score of 0.33 over 2 years [21].

The use of the ACB scale in clinical practice is burdensome and challenging, which limits its use in physicians' offices. Although some electronic health systems do flag drugs with ACB, most physicians would have to look up the drugs and their ratings. Hospitals and care homes are most likely to use the scale. The scale is often used for research purposes as well [47–51].

uMH's platform examined each medication being taken by a person, and determined the ACB score for each. A score (0 through 3) is assigned to each current medication. The cumulative score was calculated, and an estimate was made of how much these drugs might be lowering someone's MMSE score. Definite ACBs (those with a score of 2 or 3) are tabulated, as those can directly contribute to cognitive decline. A meta-review of ACB medications, which are implemented in this informatics system, can be found in "Anticholinergic burden quantified by anticholinergic risk scales and adverse outcomes in older people: a systematic review" [19].

Depression-Inducing Drugs

DIDs were identified using "Prevalence of Prescription Medications with Depression as a Potential Adverse Effect Among Adults in the United States" [30]. The DIDs listed here were coded into uMH's informatics platform so that each person's medication list could be checked against this published list by the algorithms.

Output

Each person's information was analyzed by the informatics platform and compared to standardized databases, peer-reviewed publications, and reference tables to generate treatment recommendations. Databases and reference tables used were sourced from the Centers for Disease Control, FDA, NIH, DrugBank, and the Online Mendelian Inheritance in Man (OMIM) catalogue. The information in these databases and tables relates to SNPs, DDIs, DGIs, drug indications, and diagnostics.

Along with treatment recommendations, the informatics platform also looks for any and all drug interactions or potential ADRs (see Fig. 1).

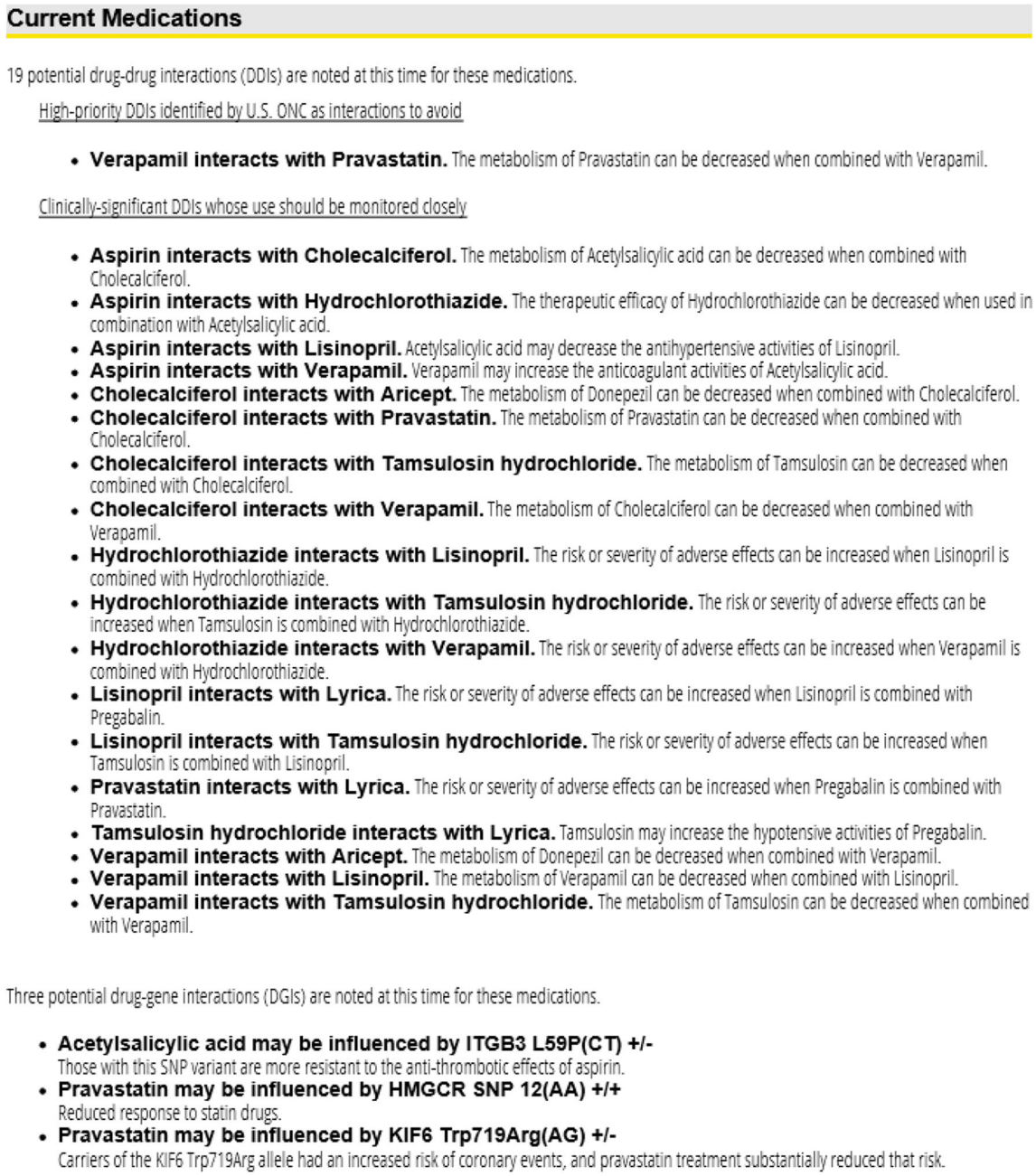

Current Medications

19 potential drug-drug interactions (DDIs) are noted at this time for these medications.

High-priority DDIs identified by U.S. ONC as interactions to avoid

- **Verapamil interacts with Pravastatin.** The metabolism of Pravastatin can be decreased when combined with Verapamil.

Clinically-significant DDIs whose use should be monitored closely

- **Aspirin interacts with Cholecalciferol.** The metabolism of Acetylsalicylic acid can be decreased when combined with Cholecalciferol.
- **Aspirin interacts with Hydrochlorothiazide.** The therapeutic efficacy of Hydrochlorothiazide can be decreased when used in combination with Acetylsalicylic acid.
- **Aspirin interacts with Lisinopril.** Acetylsalicylic acid may decrease the antihypertensive activities of Lisinopril.
- **Aspirin interacts with Verapamil.** Verapamil may increase the anticoagulant activities of Acetylsalicylic acid.
- **Cholecalciferol interacts with Aricept.** The metabolism of Donepezil can be decreased when combined with Cholecalciferol.
- **Cholecalciferol interacts with Pravastatin.** The metabolism of Pravastatin can be decreased when combined with Cholecalciferol.
- **Cholecalciferol interacts with Tamsulosin hydrochloride.** The metabolism of Tamsulosin can be decreased when combined with Cholecalciferol.
- **Cholecalciferol interacts with Verapamil.** The metabolism of Cholecalciferol can be decreased when combined with Verapamil.
- **Hydrochlorothiazide interacts with Lisinopril.** The risk or severity of adverse effects can be increased when Lisinopril is combined with Hydrochlorothiazide.
- **Hydrochlorothiazide interacts with Tamsulosin hydrochloride.** The risk or severity of adverse effects can be increased when Tamsulosin is combined with Hydrochlorothiazide.
- **Hydrochlorothiazide interacts with Verapamil.** The risk or severity of adverse effects can be increased when Verapamil is combined with Hydrochlorothiazide.
- **Lisinopril interacts with Lyrica.** The risk or severity of adverse effects can be increased when Lisinopril is combined with Pregabalin.
- **Lisinopril interacts with Tamsulosin hydrochloride.** The risk or severity of adverse effects can be increased when Tamsulosin is combined with Lisinopril.
- **Pravastatin interacts with Lyrica.** The risk or severity of adverse effects can be increased when Pregabalin is combined with Pravastatin.
- **Tamsulosin hydrochloride interacts with Lyrica.** Tamsulosin may increase the hypotensive activities of Pregabalin.
- **Verapamil interacts with Aricept.** The metabolism of Donepezil can be decreased when combined with Verapamil.
- **Verapamil interacts with Lisinopril.** The metabolism of Verapamil can be decreased when combined with Lisinopril.
- **Verapamil interacts with Tamsulosin hydrochloride.** The metabolism of Tamsulosin can be decreased when combined with Verapamil.

Three potential drug-gene interactions (DGIs) are noted at this time for these medications.

- **Acetylsalicylic acid may be influenced by ITGB3 L59P(CT) +/-**
  Those with this SNP variant are more resistant to the anti-thrombotic effects of aspirin.
- **Pravastatin may be influenced by HMGCR SNP 12(AA) +/+**
  Reduced response to statin drugs.
- **Pravastatin may be influenced by KIF6 Trp719Arg(AG) +/-**
  Carriers of the KIF6 Trp719Arg allele had an increased risk of coronary events, and pravastatin treatment substantially reduced that risk.

Fig. 1 Example report: medication interactions

Separate care plan reports generated by the software are optimized for the physician, the person under treatment, and their coaching team—with the goal of suggesting what can best be achieved in a clinical setting in the long-term, taken in three-month segments.

Statistical Analysis

All statistical analyses were performed using SAS University Edition. Significance was determined using a 95% confidence interval.

Power calculations for independent, two-sided *t* tests were completed to compare population means. Either pooled or Satterthwaite *P* values were used based on equality of variance testing.

Means, standard deviations, and frequencies were established using SAS. One-way analysis of variance (ANOVA) testing was completed to compare mean values between independent groups with categorical and continuous analysis variables. Linear and multiple linear regression models were completed for continuous response variables and singular or multiple continuous explanatory variables.

RESULTS

Of the 295 people analyzed in this group, 97.59% of them were on at least one medication, with an overall mean of 11.5 medications per person; 83.66% were on 5 or more medications (see Tables 3, 4). No significant differences were found between the total number of medications for people with normal cognitive status versus those with cognitive decline.

A higher percentage of people with cognitive decline were taking medications in all the drug categories reviewed: neuroactive medications, anticholinergic drugs, and DIDs. Those with cognitive decline also took more medications for these drug classes compared to those with no cognitive decline (see Tables 5, 6, 7).

A total of 102 DGIs, 3642 DDIs, and one high-priority DDI were found in this population. Only ten people on medications did not have any observed DDIs or DGIs. There was a significant increase in the number of DDIs as the number of medications per person increased (P value < 0.0001; see Fig. 2).

Table 3 Medication totals

Cohort	Mean (SD)	Min.	Max.	*N*	% of population
All	11.52 (8.77)	0	67	294	97.59
Cognitively normal	12.88 (10.26)	0	66	108	95.41
Demented	11.30 (9.19)	0	67	109	97.22

Table 4 Number of patients on medication

Cohort	Medications	*N*	% of population
All	Total	287	97.59
	5 +	240	83.66
Cognitively normal	Total	103	95.41
	5 +	82	75.97
Demented	Total	106	97.22
	5 +	93	85.3

Table 5 Medication categories

Cohort	Variable	Mean (SD)	Min.	Max.	% of population
All	Neuroactive	2.82 (2.02)	0	11	97.23
	ACBs (count)	1.43 (1.48)	0	7	65.86
	ACBs (score)	2.15 (2.47)	0	12	NA
	DIDs	1.19 (1.31)	0	7	60.98
Female	Neuroactive	3.03 (2.15)	0	11	98.75
	ACBs (count)	1.67 (1.55)	0	7	74.22
	ACBs (score)	2.50 (2.62)	0	12	NA
	DIDs	1.35 (1.39)	0	7	66.04
Male	Neuroactive	2.55 (1.83)	0	9	95.31
	ACBs (count)	1.13 (1.34)	0	6	55.47
	ACBs (score)	1.71 (2.20)	0	10	NA
	DIDs	0.99 (1.19)	0	5	54.68
Cognitively normal	Neuroactive	2.16 (1.56)	0	7	95.47
	ACBs (count)	0.85 (1.06)	0	4	54.55
	ACBs (score)	1.28 (1.66)	0	6	NA
	DIDs	0.88 (1.11)	0	5	54.55
Cognitive decline	Neuroactive	3.00 (2.07)	0	10	97.25
	ACBs (count)	1.67 (1.58)	0	7	73.39
	ACBs (score)	2.39 (2.61)	0	12	NA
	DIDs	1.31 (1.46)	0	7	63.3

ACB anticholinergic burden, *DIDs* depression-inducing drugs

Neuroactive Medications

A total of 97.23% of people were on at least one neuroactive medication, with a mean of 2.82 medications per person. Females were on a significantly higher amount of neuroactive medications than males (3.03 vs. 2.55, *P* value 0.02; see Table 5). Those with cognitive decline were also on more neuroactive medications than individuals with normal cognition (3.00 vs. 2.16, *P* value 0.0004; see Table 5).

Anticholinergics

Of the population, 65.86% were on one or more anticholinergic drug. There was a significant difference in the ACB score between individuals with cognitive decline than those without (2.39 vs. 1.28, *P* value 0.01). Females were also placed on more anticholinergic drugs than males (1.67 vs. 1.13, *P* value 0.002), and had a higher ACB score (2.50 vs. 1.71, *P* value 0.006; see Table 5).

Depression-Inducing Drugs

Females were on a significantly higher number of DIDs than males (1.34 vs. 0.99, *P* value 0.01). In total, 60.98% of the overall population were on DIDs, with a mean of 1.19 medications per person (see Table 5).

Table 6 Drug interactions

Cohort	Variable	Mean (SD)	Min.	Max.	% of population
All	DGIs	0.63 (1.11)	0	6	34.82
	DDIs	10.70 (10.73)	0	72	93.08
	High-priority DDIs	0.004 (0.06)	0	1	0.36
Female	DGIs	0.59 (1.05)	0	5	32.81
	DDIs	10.90 (11.21)	0	72	90.58
	High-priority DDIs	0.00 (0.00)	0	0	0
Male	DGIs	0.66 (1.17)	0	6	36.63
	DDIs	10.45 (10.11)	0	51	95.14
	High-priority DDIs	0.01 (0.09)	0	1	0.83
Cognitively normal	DGIs	0.66 (1.20)	0	6	34.44
	DDIs	8.13 (7.77)	0	33	81.53
	High-priority DDIs	0.01 (0.10)	0	1	0.97
Cognitive decline	DGIs	0.47 (0.98)	0	6	34.82
	DDIs	12.13 (12.46)	0	72	93.21
	High-priority DDIs	0.00 (0.00)	0	0	0

DGIs drug–genome interactions, *DDIs* drug–drug interactions

Table 7 Drug interactions for patients taking 5 + medications

Variable	Mean (SD)	Min.	Max.
DGIs	0.61 (1.14)	0	6
DDIs	12.19 (10.89)	0	72
High-priority DDIs	0.00 (0.06)	0	1

DGIs drug–genome interactions, *DDIs* drug–drug interactions

DISCUSSION

The results of this work show that older populations have a high medication burden. Patients had an average of ten DDIs alone. The mean duration of a physician visit in the United States is 21.07 min. [52], most of which is spent discussing a person's current health and not their medication regime. The numbers presented here as well as in other publications show that physicians and patients need more support to ensure medication regimes are safe.

Those with cognitive impairment face an even higher burden than the average elderly patient, taking more medications that can adversely impair their cognitive abilities and mood.

Females in this population were placed on a higher number of neuroactive and mood-altering drugs. Females are already at a higher risk of developing AD [53–55], nearly two thirds of AD patients are women [56]. While our research cannot say if a higher risk of cognitive decline results in more medications or a more complex medication regime, it is apparent that females are at greater risk of drug interactions and ADRs.

With the growing elderly and AD populations, medication management for polypharmacy is a need that grows direr every year. Studies have shown that adding a medical professional with the sole job of medication review to reduce the use of ineffective medications increases patient safety [1], but this remains

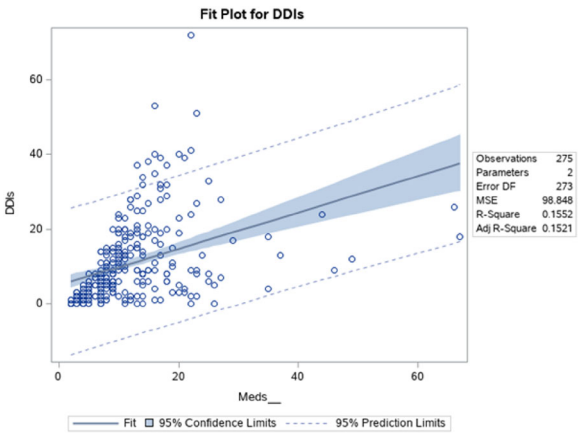

DDIs: Drug-drug interactions

Fig. 2 Comparing number of medications to number of DDIs

unrealistic in the real world due to cost and personnel constraints. CDSS does not face the same concerns though.

uMH's CDSS was able to identify a multitude of polypharmacy problems that individuals are currently facing. With the added knowledge that this type of algorithmic analysis can provide, physicians will have the tools and information needed to amend a person's medications to avoid interactions and ADRs, and to more closely monitor patients for expected reactions.

While the use of electronic medical records (EMRs) is becoming more prevalent in large hospitals and even private practices, it does not mean that physicians are taking more actions to prevent drug interactions in their patients. Studies have shown that between 33% and 96% of medication-related EMR alerts are overridden and ignored [57]. This is referred to as "alert fatigue." Even clinically significant alerts are being ignored [57, 58].

The reports generated by uMH's informatics platform do not allow physicians to dismiss alerts, as it is provided in an un-editable PDF format as opposed to a dismissible alert in an EMR. uMH's report format allows for review of the recommendations and findings before a patient visit, and presents alerts and recommendations in a consistent format, allowing physicians to focus on whatever piece of the review is relevant at the time and return to others later.

The population presented here was compared to the National Alzheimer's Coordinating Center's (NACC) database to check how closely they resemble a more generalized population. Only those aged 65 and older in the NACC database were used to match the age range for the population presented here. We found that our population was comparable in both education, BMI, and age at visit. uMH's population was on more total medications than those in the NACC's database (see Table 8).

CONCLUSIONS

This informatics platform has immense potential for use in clinical practice and helps fulfill the need of increasing patient medication regime safety. It could be further improved by the addition of actionable recommendations for how physicians can safely reduce the medications causing interactions and ADRs. These recommendations could include stopping medications (with information on how to safely wean patients off specific drugs), dosage changes based on precision medicine, and formulary

Table 8 Comparative normative data

Variable	uMH data, mean (SD)	NACC data, mean (SD)
Education (years)	16.11 (3.48)	15.01 (3.54)
Total medications	11.53 (8.83)	5.77 (3.76)
BMI	26.45 (5.17)	26.62 (5.08)
Age (years)	75.51 (7.31)	75.72 (6.88)

BMI body mass index

alternatives that would provide the same pharmaceutical benefit without the potential for interactions.

ACKNOWLEDGMENTS

The authors thank the participants in this study. The NACC database is funded by NIA/NIH grant U01 AG016976. NACC data are contributed by the NIA-funded ADCs: P30 AG019610 (PI Eric Reiman, MD), P30 AG013846 (PI Neil Kowall, MD), P50 AG008702 (PI Scott Small, MD), P50 AG025688 (PI Allan Levey, MD, PhD), P50 AG047266 (PI Todd Golde, MD, PhD), P30 AG010133 (PI Andrew Saykin, PsyD), P50 AG005146 (PI Marilyn Albert, PhD), P50 AG005134 (PI Bradley Hyman, MD, PhD), P50 AG016574 (PI Ronald Petersen, MD, PhD), P50 AG005138 (PI Mary Sano, PhD), P30 AG008051 (PI Thomas Wisniewski, MD), P30 AG013854 (PI M. Marsel Mesulam, MD), P30 AG008017 (PI Jeffrey Kaye, MD), P30 AG010161 (PI David Bennett, MD), P50 AG047366 (PI Victor Henderson, MD, MS), P30 AG010129 (PI Charles DeCarli, MD), P50 AG016573 (PI Frank LaFerla, PhD), P50 AG005131 (PI James Brewer, MD, PhD), P50 AG023501 (PI Bruce Miller, MD), P30 AG035982 (PI Russell Swerdlow, MD), P30 AG028383 (PI Linda Van Eldik, PhD), P30 AG053760 (PI Henry Paulson, MD, PhD), P30 AG010124 (PI John Trojanowski, MD, PhD), P50 AG005133 (PI Oscar Lopez, MD), P50 AG005142 (PI Helena Chui, MD), P30 AG012300 (PI Roger Rosenberg, MD), P30 AG049638 (PI Suzanne Craft, PhD), P50 AG005136 (PI Thomas Grabowski, MD), P50 AG033514 (PI Sanjay Asthana, MD, FRCP), P50 AG005681 (PI John Morris, MD), P50 AG047270 (PI Stephen Strittmatter, MD, PhD).

Funding. All funding for this study was provided by uMETHOD Health. No funding or sponsorship was received for the publication of this article. All authors had full access to all of the data in this study and take complete responsibility for the integrity of the data and accuracy of the data analysis.

Authorship. All named authors meet the International Committee of Medical Journal Editors (ICMJE) criteria for authorship for this article, take responsibility for the integrity of the work as a whole, and have given their approval for this version to be published.

Disclosures. Dorothy Keine is employed by, had a previous financial relationship with, and/or holds stock in uMETHOD Health. Mark Zelek is employed by, had a previous financial relationship with, and/or holds stock in uMETHOD Health. John Q. Walker is employed by, had a previous financial relationship with, and/or holds stock in uMETHOD Health. Marwan Sabbagh is employed by, had a previous financial relationship with, and/or holds stock in uMETHOD Health; he is also Editor in Chief of the journal.

Compliance with Ethics Guidelines. Following the guidelines set out by "Coded Private Information or Specimens Use in Research" by the Office for Human Research Protection, the work presented here does not qualify as human research. The investigators utilized existing, de-identified data from patients who gave previous informed consent to have their data used in future research, but did not involve the patients in any therapy or intervention. Institutional review board approval was not required as data are recorded in such a manner that subjects cannot be identified, directly or through identifiers linked to the subjects. Meeting these conditions makes this research exempt from the requirements of 45 CFR 46 under the Department of Health and Human Services (HHS): Research, involving the collection or study of existing data, documents, records, pathological specimens, if these sources are publicly available or if the information is recorded by the investigator in such a manner that subjects cannot be identified, directly or through identifiers linked to the subjects.

Data Availability. The data that support the findings of this study are available from uMETHOD Health, but restrictions apply to the availability of these data, which are proprietary company information, and so are not publicly

available. Data are however available from the authors upon reasonable request and with permission of uMETHOD Health.

REFERENCES

1. Maher RL, Hanlon J, Hajjar ER. Clinical consequences of polypharmacy in elderly. Expert Opin Drug Saf. 2014;13(1):57–65.

2. Quinn KJ, Shah NH. A dataset quantifying polypharmacy in the United States. Sci Data. 2017;31(4):170167.

3. Pasqualetti G, Tognini S, Calsolaro V, Polini A, Monzani F. Potential drug–drug interactions in Alzheimer patients with behavioral symptoms. Clin Interv Aging. 2015;8(10):1457–66.

4. Lazarou J, Pomeranz BH, Corey PN. Incidence of adverse drug reactions in hospitalized patients: a meta-analysis of prospective studies. JAMA. 1998;279(15):1200–5.

5. Ward BW, Schiller JS, Goodman RA. Multiple chronic conditions among US adults: a 2012 update. Prev Chronic Dis. 2014;17(11):E62.

6. Clague F, Mercer SW, McLean G, Reynish E, Guthrie B. Comorbidity and polypharmacy in people with dementia: insights from a large, population-based cross-sectional analysis of primary care data. Age Ageing. 2017;46(1):33–9.

7. What is Alzheimer's|Alzheimer's Association (Internet). https://www.alz.org/alzheimers-dementia/what-is-alzheimers. Accessed 22 Oct 2018.

8. World Health Organization. First WHO ministerial conference on global action against dementia. Geneva: World Health Organization; 2015.

9. Winblad B, Amouyel P, Andrieu S, Ballard C, Brayne C, Brodaty H, et al. Defeating Alzheimer's disease and other dementias: a priority for European science and society. Lancet Neurol. 2016;15(5):455–532.

10. Frazier SC. Health outcomes and polypharmacy in elderly individuals: an integrated literature review. J Gerontol Nurs. 2005;31(9):4–11.

11. Interactions|Clinical Drug Information (Internet). https://www.wolterskluwercdi.com/lexicomp-online/user-guide/tools-interactions/. Accessed 26 Oct 2018.

12. Wiese K, Ellingrod V. Avoiding common drug–drug interactions. Curr Psychiatr. 2015;14(7):21–3.

13. Ayvaz S, Horn J, Hassanzadeh O, Zhu Q, Stan J, Tatonetti NP, et al. Toward a complete dataset of drug–drug interaction information from publicly available sources. J Biomed Inform. 2015;55:206–17.

14. Griffith M, Griffith OL, Coffman AC, Weible JV, McMichael JF, Spies NC, et al. DGIdb: mining the druggable genome. Nat Methods. 2013;10(12):1209–10.

15. Cotto KC, Wagner AH, Feng Y-Y, Kiwala S, Coffman AC, Spies G, et al. DGIdb 3.0: a redesign and expansion of the drug-gene interaction database. Nucleic Acids Res. 2018;46(D1):D1068–D1073.

16. Pirmohamed M. Personalized pharmacogenomics: predicting efficacy and adverse drug reactions. Annu Rev Genomics Hum Genet. 2014;29(15):349–70.

17. Richardson K, Fox C, Maidment I, Steel N, Loke YK, Arthur A, et al. Anticholinergic drugs and risk of dementia: case–control study. BMJ. 2018;25(361):k1315.

18. Mintzer J, Burns A. Anticholinergic side-effects of drugs in elderly people. J R Soc Med. 2000;93:457–62.

19. Salahudeen MS, Duffull SB, Nishtala PS. Anticholinergic burden quantified by anticholinergic risk scales and adverse outcomes in older people: a systematic review. BMC Geriatr. 2015;25(15):31.

20. Gorup E, Rifel J, Petek Šter M. Anticholinergic burden and most common anticholinergic-acting medicines in older general practice patients. Zdr Varst. 2018;57(3):140–7.

21. Anticholinergic cognitive burden (ACB) scale 2012 update. Indianapolis: Regenstrief Institute, Inc.; 2012.

22. Cai X, Campbell N, Khan B, Callahan C, Boustani M. Long-term anticholinergic use and the aging brain. Alzheimers Dement. 2013;9(4):377–85.

23. Pfistermeister B, Tümena T, Gaßmann K-G, Maas R, Fromm MF. Anticholinergic burden and cognitive function in a large German cohort of hospitalized geriatric patients. PLoS ONE. 2017;12(2):e0171353.

24. Orhan IE, Orhan G, Gurkas E. An overview on natural cholinesterase inhibitors—a multi-targeted drug class—and their mass production. Mini Rev Med Chem. 2011;11(10):836–42.

25. Carnahan RM, Lund BC, Perry PJ, Chrischilles EA. The concurrent use of anticholinergics and cholinesterase inhibitors: rare event or common practice? J Am Geriatr Soc. 2004;52(12):2082–7.

26. Schultz BR, Takeshita J, Goebert D, Takeshita S, Lu BY, Guilloux A, et al. Simultaneous usage of dementia medications and anticholinergics among Asians and Pacific Islanders. Psychogeriatrics. 2017;17(6):423–9.

27. Alagiakrishnan K, Wiens CA. An approach to drug induced delirium in the elderly. Postgrad Med J. 2004;80(945):388–93.

28. Rogers D, Pies R. General medical drugs associated with depression. Psychiatry (Edgmont). 2008;5(12):28–41.

29. Substance-induced mood disorder: overview, substances linked to depression or mania, etiology (Internet). https://emedicine.medscape.com/article/286885-overview. Accessed 7 Nov 2018.

30. Qato DM, Ozenberger K, Olfson M. Prevalence of prescription medications with depression as a potential adverse effect among adults in the United States. JAMA. 2018;319(22):2289–98.

31. Kotlyar M, Dysken M, Adson DE. Update on drug-induced depression in the elderly. Am J Geriatr Pharmacother. 2005;3(4):288–300.

32. Population estimates and projections. An aging nation: the older population in the United States.

33. Hunt DL, Haynes RB, Hanna SE, Smith K. Effects of computer-based clinical decision support systems on physician performance and patient outcomes: a systematic review. JAMA. 1998;280(15):1339–46.

34. Kawamoto K, Houlihan CA, Balas EA, Lobach DF. Improving clinical practice using clinical decision support systems: a systematic review of trials to identify features critical to success. BMJ. 2005;330(7494):765.

35. H.R.34—114th congress (2015–2016): 21st century cures act |congress.gov| library of congress (Internet). https://www.congress.gov/bill/114th-congress/house-bill/34. Accessed 28 Nov 2018.

36. Deo RC. Machine learning in medicine. Circulation. 2015;132(20):1920–30.

37. Başţanlar Y, Ozuysal M. Introduction to machine learning. Methods Mol Biol. 2014;1107:105–28.

38. Scharre DW, Chang S-I, Murden RA, Lamb J, Beversdorf DQ, Kataki M, et al. Self-administered gerocognitive examination (SAGE): a brief cognitive assessment instrument for mild cognitive impairment (MCI) and early dementia. Alzheimer Dis Assoc Disord. 2010;24(1):64–71.

39. SAGE—memory disorders|Ohio State Medical Center (Internet). https://wexnermedical.osu.edu/brain-spine-neuro/memory-disorders/sage. Accessed 5 Oct 2018.

40. Coded private information or specimens use in research, guidance (2008)|HHS.gov (Internet). https://www.hhs.gov/ohrp/regulations-and-policy/guidance/research-involving-coded-private-information/index.html. Accessed 20 Jan 2019.

41. Keine D, Walker JQ, Kennedy BK, Sabbagh MN. Development, application, and results from a precision-medicine platform that personalizes multimodal treatment plans for mild Alzheimer's disease and at-risk individuals. Curr Aging Sci. 2018;18(11):1–1.

42. RxNorm overview (Internet). https://www.nlm.nih.gov/research/umls/rxnorm/overview.html. Accessed 14 Nov 2018.

43. Prioritization—CPIC (Internet). https://cpicpgx.org/prioritization/#flowchart. Accessed 14 Nov 2018.

44. DrugBank (Internet). Pharmaco-transcriptomics. https://www.drugbank.ca/pharmaco/transcriptomics. Accessed 14 Nov 2018.

45. Pharmacogenomics—SNPedia (Internet). https://www.snpedia.com/index.php/Pharmacogenomics. Accessed 14 Nov 2018.

46. Genoset—SNPedia (Internet). https://www.snpedia.com/index.php/Genoset. Accessed 14 Nov 2018.

47. Welsh TJ, van der Wardt V, Ojo G, Gordon AL, Gladman JRF. Anticholinergic drug burden tools/scales and adverse outcomes in different clinical settings: a systematic review of reviews. Drugs Aging. 2018;35(6):523–38.

48. Campbell NL, Perkins AJ, Bradt P, Perk S, Wielage RC, Boustani MA, et al. Association of anticholinergic burden with cognitive impairment and health care utilization among a diverse ambulatory older adult population. Pharmacotherapy. 2016;36(11):1123–31.

49. Campbell N, Boustani M, Limbil T, Ott C, Fox C, Maidment I, et al. The cognitive impact of anticholinergics: a clinical review. Clin Interv Aging. 2009;9(4):225–33.

50. Campbell NL, Boustani MA, Lane KA, Gao S, Hendrie H, Khan BA, et al. Use of anticholinergics and the risk of cognitive impairment in an African American population. Neurology. 2010;75(2):152–9.

51. Myint PK, Fox C, Kwok CS, Luben RN, Wareham NJ, Khaw K-T. Total anticholinergic burden and risk of mortality and cardiovascular disease over 10 years in 21,636 middle-aged and older men and women of EPIC-Norfolk prospective population study. Age Ageing. 2015;44(2):219–25.

52. Irving G, Neves AL, Dambha-Miller H, Oishi A, Tagashira H, Verho A, et al. International variations in primary care physician consultation time: a systematic review of 67 countries. BMJ Open. 2017;7(10):e017902.

53. Podcasy JL, Epperson CN. Considering sex and gender in Alzheimer disease and other dementias. Dialogues Clin Neurosci. 2016;18(4):437–46.

54. Altmann A, Tian L, Henderson VW, Greicius MD, Alzheimer's Disease Neuroimaging Initiative Investigators. Sex modifies the APOE-related risk of developing Alzheimer disease. Ann Neurol. 2014;75(4):563–73.

55. Zhao L, Mao Z, Woody SK, Brinton RD. Sex differences in metabolic aging of the brain: insights into female susceptibility to Alzheimer's disease. Neurobiol Aging. 2016;18(42):69–79.

56. Snyder HM, Asthana S, Bain L, Brinton R, Craft S, Dubal DB, et al. Sex biology contributions to vulnerability to Alzheimer's disease: a think tank convened by the Women's Alzheimer's Research Initiative. Alzheimers Dement. 2016;12(11):1186–96.

57. Phansalkar S, Desai AA, Bell D, Yoshida E, Doole J, Czochanski M, et al. High-priority drug-drug interactions for use in electronic health records. J Am Med Inform Assoc. 2012;19(5):735–43.

58. Paterno MD, Maviglia SM, Gorman PN, Seger DL, Yoshida E, Seger AC, et al. Tiering drug–drug interaction alerts by severity increases compliance rates. J Am Med Inform Assoc. 2009;16(1):40–6.

Conclusions

There is no other paper in the current scientific literature that has a similar approach to the problem of polypharmacy. Our manuscript and machine learning approach is novel and will hopefully lead to further research in this field.

The extensive list of medications that this population was on led to a multitude of different interactions and harmful side effects. Our research showed that CDSS has potential to fill this gap in patient care. Because these platforms are built to process large amounts of data, they can quickly review a patient's medication regime to check for safety issues and interactions that a physician may not have the time to do. Our population had an average of 10 DDIs per person, showing that there is a great need for better prescription oversight, especially in elderly populations.

Not only can these platforms better detect and flag these medication issues, the code can also be expanded to provide actionable recommendations based on current guidelines. This would provide further benefit to patients and physicians because it would present not only the problem, but also potential solutions for the physician to consider.

In doing this research, it came to our attention that many AD patients are taking DIDs. Depression has long been associated with AD, and while it is yet to be determined if it is causal or symptomatic, putting AD patients on DIDs could be detrimental to their health.

Chapter 9: Depression-inducing drugs and the frequency of depression in MCI and Alzheimer's disease

Depression and AD are often seen together in patients. What many physicians and patients do not realize is that some of these symptoms of depression may be due to medication instead of an actual mental disorder. This lack of knowledge can lead not only to an incorrect diagnosis, but may also have detrimental neurological and cognitive effects on patients if depression does indeed increase the risk of AD.

Presented here is the first research completed that looks at the frequency of depressogenic drug use in a cognitively impaired population. CDSS was used to create alerts for these medications with the hope of changing physician behavior to decrease the use of these medications in at-risk populations.

I was responsible for first identifying this issue in our population. I wanted to investigate to see if depressogenic drugs were having a larger impact on our population, especially with the strong link that exists between depression and AD. For this research, I compiled all of the data from our database and national medical databases to determine all of the depression-inducing medications the population was on.

After noticing that this AD population had a higher than average depressogenic drug burden, I further evaluated to see if there was any difference between those with and without APOE ε4. I then compared the population to see if there were any correlations between antidepressant medications, depression, and depressogenic drugs.

In order to better qualify our data set, I found a normative AD data set to compare it to. This allowed me to better inspect if our population was comparable to the general public. I also performed the literature review, compiled all of the data into a presentable format, and was the sole author in the creation of the manuscript.

This publication has only recently been published and has not yet been cited by other researchers.

RESEARCH ARTICLE

Depression-inducing drugs and the frequency of depression in Alzheimer's disease and APOE ε4 carriers [version 1; peer review: awaiting peer review]

Dorothy Keine

3Prime Medical Writing, Durham, NC, 27703, USA

First published: 22 Oct 2019, **8**:1782 (https://doi.org/10.12688/f1000research.20857.1)

Latest published: 22 Oct 2019, **8**:1782 (https://doi.org/10.12688/f1000research.20857.1)

Abstract

Background: Depression is associated with a greater risk of Alzheimer's disease (AD). Drug-induced depression is a well-known side effect of many medications and is more likely to occur in those who have a higher risk of depressive disorder.

Methods: A total of 292 individuals ages 65 and older were included in this dataset. Depressive symptoms were determined through self-reporting, the Short Form Geriatric Depression Scale (SF-GDS), prior diagnosis, or use of antidepressant medication. Depression-inducing drugs (DIDs) were identified using published references.

Results: Individuals took 11.51 (SD 8.86) medications and 1.16 (SD 1.27) DIDs per person. Depressed patients were more likely to be taking at least one DID (71.15% vs 28.85%, P value 0.005). Of the total population, 60.56% were taking at least one DID. Those with APOE ε4 had a significantly higher rate of depression than those without (69.12% vs 30.88%, P value 0.03).

Conclusions: DIDs are a substantial clinical, medical, and public health problem in older populations. DID consideration is important in populations with an increased risk or diagnosis of AD. Clinical decision support software (CDSS) provides a reliable method to help with DIDs.

Keywords

Depression, Alzheimer's, drug-induced depression, APOE, clinical decision support software

Introduction

Alzheimer's disease (AD) is the most common form of dementia[1]. It is a degenerative brain disease that eventually leads to death. Characteristic symptoms of the disease include difficulties with memory, language problems, agitation, and cognitive deficits that affect a person's ability to perform everyday tasks. As the disease progresses, the burden increases and the individual will need help with even basic activities of daily living[1].

An estimated 5.7 million people in the United States have AD, and over 35.6 million people are affected worldwide[2]. This number is projected to grow as the population aged 65 and older in the USA is anticipated to increase from its current level of 53 million to 88 million by 2050. Today, the total US spending on AD is estimated to be $277 billion[1].

Research now suggests that the brain changes associated with AD begin as much as 20 years before initial symptoms[3]. Individuals often begin to show early signs of cognitive decline when they develop mild cognitive impairment (MCI). A systemic review of 32 studies found that 32% of people with MCI will go on to develop AD within five years[1].

Like many chronic diseases, AD is not caused by one factor but instead develops because of multiple factors. Contributing factors include age, family history, the APOE ε4 gene[4,5], as well as modifiable lifestyle factors[1].

One factor often associated with AD is depression, both late-life (depression occurring after the age of 60 or 65) and recurring earlier-life cases. One in five individuals experience at least one depressive episode in their lifespan[6], and it occurs more often in older populations[2,7]. In 2009–2012, depression was estimated to affect more than 5% of all US adults[8]. Depression has also been found to be more common among women[9]. Many people with depression go undiagnosed and untreated[8].

Evidence suggests that depression is preventable and treatable, and may be a modifiable risk factor for preventing or delaying dementia in later life[7]. Depression can lead to cognitive deficits in some individuals, sometimes referred to as "pseudodementia"[2,10]. Older adults are at an even greater risk of developing pseudodementia[9,11].

It is currently unknown if depression is a risk factor for developing AD, or a prodromal sign of the disease[2,5,9,12–14]. The weight of the evidence suggests that depression is likely a risk factor, though[2,10,15]. This question remains partly due to the timing of studies that have been conducted in late-life, the variability in follow-up time, and also the fact that depression frequency and duration times are often not recorded[2].

Research has established that depression is associated with a greater risk for AD. Many studies have concluded that depression doubles an individual's risk of developing dementia, particularly AD[7,9,10,16,17]. Other studies on depression and AD have shown that those who develop depression are 1.5 times more likely to develop AD compared to those who are not depressed[9]. The evidence is not yet conclusive as to if early or late-onset depression might be a greater risk factor, but the severity of late-life depression has been found to be an important risk factor for dementia[2,7]. Some studies have shown that depression in earlier life is more closely associated with vascular dementia, and depression in later life is a greater risk for developing AD[18].

APOE ε4 status has been linked to higher rates of depression and is a definitive risk factor for AD[5,19]. A study completed in India found that those with APOE ε4 had a 4.7 times higher risk of developing depression in old age[20]. Populations in Sweden with the APOE ε4 gene also had a higher risk of developing depression. Furthermore, APOE ε4 is associated with more severe depressive symptoms[4]. Post-mortem studies have reported greater hippocampal amyloid plaque and neurofibrillary tangle pathology in AD patients with a history of depression than those without[21].

While the specific pathway, or pathways, linking depression and AD have not been defined yet, many mechanisms have been hypothesized. Depression may lead to an increase in amyloid plaques through the depression-associated stress response. This response ultimately results in an increase in β amyloid production[22]. Chronic inflammation also plays a significant role in the pathophysiology of AD[23] and is seen in both depression and AD[24]. It is hypothesized that stress leads to chronic inflammation in depressed persons. Neuroendocrine changes comparable to those found in chronic stress have also been found in depression and AD models[10]. Additionally, pro-inflammatory cytokines have been shown to interfere with serotonin metabolism, leading to a reduction in synaptic plasticity and hippocampal neurogenesis[22,23]. Increased cortisol production can also lead to atrophy in the hippocampus and cognitive deficit[25]. Interleukin-6 (IL-6), C-reactive protein, and tumor necrosis factor are all increased in depression and may be risk factors for dementia[26]. Brain-derived neurotrophic factor (BDNF), often associated with synaptic plasticity, is decreased in depression and AD[27]. Furthermore, MRI studies have found that hippocampal atrophy occurs in cases of depression, suggestive of AD pathology[28]. Lastly, many lifestyle factors associated with depression are also known risk factors for AD, including poor diet, lack of physical activity, and low social engagement[1,9].

Of the studies conducted on depression and AD, this author could not find one that examined the link between depression, AD, APOE, and depression-inducing-drugs (DIDs). Drug-induced depression, also referred to as substance-induced mood disorder in the literature, is a well-known side effect of many medications. The first notion of a "depressogenic" drug was documented in 1954, referring to long periods of treatment with the antihypertensive drug reserpine[29].

Older populations have a greater risk of exposure to DIDs, as they are more likely to be on multiple medications[8,30–32]. It has been found that the use of multiple medications increases the risk of simultaneous depression and that older age is significantly associated with the use of DIDs[8].

The most common DIDs include narcotics, benzodiazepines, anticholinergic medications, antidepressants, sedatives, beta-blockers, calcium channel blockers, and oral contraceptives[8,30,33]. The mechanisms for a few depressogenic drugs have been studied, and their additive risk factor for AD cannot be ruled out. In one longitudinal study, seven out of 15 individuals who developed AD had been taking antidepressants[5].

Possible mechanisms for DIDs have been proposed[34]. These mechanisms include inhibiting calcium-dependent neurotransmitter release by blocking the inflow of calcium into cells[35], decreased serotonin[36], reduction in G-protein-coupled catecholaminergic or cholinergic receptors[37], decreased levels of dopamine[38], and displacing nicotine from acetylcholine receptors[38]. Because of the wide range of drugs that can cause this side effect, there is "no known reason to presume that all drugs produce depression via a common pathophysiological mechanism"[34].

Drug-induced depression is more likely to occur in those who have a higher risk factor for depressive disorder, as may be the case for individuals with the APOE ε4 allele. For those already predisposed to depression, such as carriers of APOE ε4, DIDs might have an amplified effect, leading to more frequent occurrences of depression.

Here, the author examined the prevalence of DIDs in elderly non-symptomatic and symptomatic AD patients to find how many DIDs the population was taking, the prevalence of depression, and whether APOE ε4 status has any effect on depression levels with concurrent DIDs.

Methods

Bioinformatics platform

The data presented here is from uMETHOD Health's (uMH) database of patients. uMH has created a precision-medicine platform to create personalized treatment plans for patients with and at risk of dementia and AD[39]. All individuals self-selected to follow their treatment plan. The treatment program was recommended to them by their physician, or they found uMH online and chose to purchase the personalized evaluation and treatment.

uMH's platform identifies and addresses active issues and creates repeatable and practical treatment plans for use in doctors' practices.

The bioinformatics platform's internal software is written in the Python language. It interfaces to an external portal, used by the medical and coaching teams to gather input, and returns reports written in PHP and Java. External medical databases support internal rules-processing algorithms. These are sourced from bodies such as the National Institutes of Health (NIH), Food and Drug Administration (FDA), pharmaceutical trade groups, and consortia focused on topics such as genetics or allergies.

Natural language processing (NLP) techniques are used throughout the input steps, particularly for precise identification of lab tests, medications, drug indications, and comorbidities. A range of NLP techniques are employed to normalize input data. The algorithms that implement this information platform go through a consistent set of steps each time they load a person's input to generate a new set of reports. These steps are rules-based, so the logic and evidence sources can be tracked (and evaluated).

The platform was used as a source of data only and was not used for data analysis in this study.

Dataset

The data set consists of all the patients in uMH's database who were 65 or older.

The inputs to uMH's data-analytics engine comprise genomics, bio-specimen measurements, medical histories, medications, allergies, comorbidities, lifestyle data, and cognitive evaluations. Data was collected from physicians, patients, and caregivers from annual wellness visits and through uMH's patient forms. Forms were completed online via uMH's secure portal or in paper format, depending on the individual's computer skills and access. Physicians were instructed to follow a set of inclusion and exclusion criteria from Keine *et al.* 2018[39] before enrolling patients.

Each patient was evaluated by a physician to determine if they were symptomatic for AD following standard of care guidelines[40]. This evaluation included administering a baseline cognitive test to determine patients' cognitive status at the time of enrollment. The physician chose to administer either the Self-Administered Gerocognitive Exam (SAGE) or the Montreal Cognitive Assessment. Cognitive impairment was determined following each tests' specific guidelines[41,42]. Tests were scored at the physician's office by trained personnel, and completed tests were either uploaded to uMH's secure portal or were sent to uMH by the physician's office to be entered into the database. The physician then used the findings to qualify the patient as symptomatic or non-symptomatic in uMH's database.

Genomic data was obtained through consumer-focused companies such as 23andMe or Ancestry.com. Interested patients purchased a genomic kit through the company of their choice and followed the procedures outlined by the genomic testing company. Raw datasets were accessed by the patient directly from the genomic company's website and uploaded to uMH's secure portal. As this was an optional step, many people chose to complete their analysis without genomic information. Therefore, APOE ε4 status is only known for a subset of the population presented here.

Depressive symptoms were determined through patients' self-reporting, the Short Form Geriatric Depression Scale (SF-GDS)

at the physician's office[43], prior physician diagnosis as indicated by the patient's medical history, or a prescription for antidepressant medication.

DIDs were identified from Qato *et al.* Table 2[8]. The DIDs listed here were coded into uMH's bioinformatics platform so that each patients' medication list from uMH's database was checked against this published list by the platform's algorithms.

Study design

The data was analyzed using statistical methods to examine the prevalence of DIDs and depression in an elderly population currently at risk of or diagnosed with AD. The frequency of DIDs, antidepressant medications, and depression was analyzed against gender, cognitive impairment levels, depression symptoms, and current medications. This information was then subsequently compared to APOE status to investigate if a possible relationship exists between the APOE ε4 allele and depression levels, with or without DIDs.

Statistical analysis

All statistical analyses were performed using SAS University Edition. Power calculations for independent, two-sided t-tests were completed to compare population means. Either pooled or Satterthwaite P values were used based on equality of variance testing. Chi-square tests were completed for categorical data. Means, standard deviations, and frequencies were established using SAS. Significance was determined using a 95% confidence interval.

Ethical statement

Following the guidelines put forth in the 21st Century Cures Act[44], Clinical Decision Support Software (CDSS) is not regulated by the FDA, and uMH's treatment protocol does not include any investigational drugs. Because of this, the platform was taken straight to market and did not need approval by an ethics committee or board.

uMH's algorithm platform automatically assigns every participant a random eight-character ID when they are first entered into the system to de-identify their information. All data was collected under their randomly assigned ID, and the investigators here only had access to this de-identified information.

The data presented here is an analysis of data already gathered from patients; no experiments were performed on humans. Each participant self-selected to participate under the guidance of their individual physician. No patients were recruited by uMETHOD Health. All patients gave consent upon initial data collection and were informed that their de-identified information would be used for future research purposes. For patients who presented with cognitive decline, their caregiver or power of attorney was also informed of all data collection and gave consent to use de-identified data for future research.

Results

Utilizing uMH's data set, 292 individuals were analyzed for this paper (Table 1). A total of 189 people chose to provide genomic data. Of these 189, 111 have at least one copy of the APOE ε4 allele (Table 1). Those with the APOE ε4 allele are referred to as ε4 and those without are referred to as nε4. This population took an average of 11.51 (SD 8.86) medications per person, and 1.16 (SD 1.27) DIDs per person. The maximum number of DIDs seen for one person was five (Table 1).

Depression

36.21% of the population had depressive symptoms (Table 1). Individuals with depression were significantly more likely to be taking at least one DID (71.15% vs 28.85%, P value 0.005) (Table 2 and Figure 1). Those with ε4 had a significantly higher rate of depression than nε4s (69.12% vs 30.88%, P value 0.03) (Table 2). Females were also more likely to be depressed than males (65.71% vs 34.29%, P value 0.005) (Figure 2). The same held true when APOE ε4 status was

Table 1. Population overview.

Variable	Mean	Std Dev	Minimum	Maximum	N	% Population
Age (years)	75.62	7.27	65.18	102.46	292	100
Education (years)	16.13	3.48	5	24	194	-
BMI	26.34	5.03	17.4	45.9	263	-
Medications	11.51	8.86	0	67	284	97.48
DIDs	1.16	1.27	0	5	172	60.56
Antidepressants	0.43	0.76	0	4	84	29.58
Male	-	-	-	-	132	45.21
Female	-	-	-	-	160	54.79
Depressed	-	-	-	-	105	36.21
Cognitive impairment	-	-	-	-	171	75.33
APOE ε4 Male	-	-	-	-	55	56.12
APOE ε4 Female	-	-	-	-	56	61.54

BMI, body mass index; DIDs, depression-inducing drugs.

Table 2. Depression, gender, APOE, cognition, and drug comparison.

	Gender				APOE status			DIDs			Cognitive status		
	Female	Male	χ2 P value	T-test P value	ε4	χ2 P value	T-test P value	Taking DID	χ2 P value	T-test P value	Cognitively impaired	χ2 P value	T-test P value
Depression	65.71%	34.29%	0.005	-	69.12%	0.031	-	71.15%	0.005	-	78.48%	0.421	-
Depression and ε4	68.09%	31.91%	0.002	-	-	-	-	51.06%	0.721	-	74.42%	0.718	-
Antidepressants	67.86%	32.14%	0.005	0.029	70.00%	0.084	0.613	77.38%	0.0002	<.0001	80.00%	0.316	0.036
DIDs	59.30%	40.70%	0.067	0.045	55.10%	0.167	0.147	-	-	-	57.49%	0.394	0.136
ε4	50.45%	49.55%	0.450	-	-	-	-	49.09%	0.167	-	72.55%	0.038	-
Cognitive impairment	54.39%	45.61%	0.301	-	68.52%	0.038	-	57.49%	0.394	0.136	-	-	-

DIDs, depression-inducing drugs.

Figure 1. Depressed on DID vs no DID. Proportion of depressed patients taking a DID versus depressed patients not on DID. DID, depression-inducing drug,

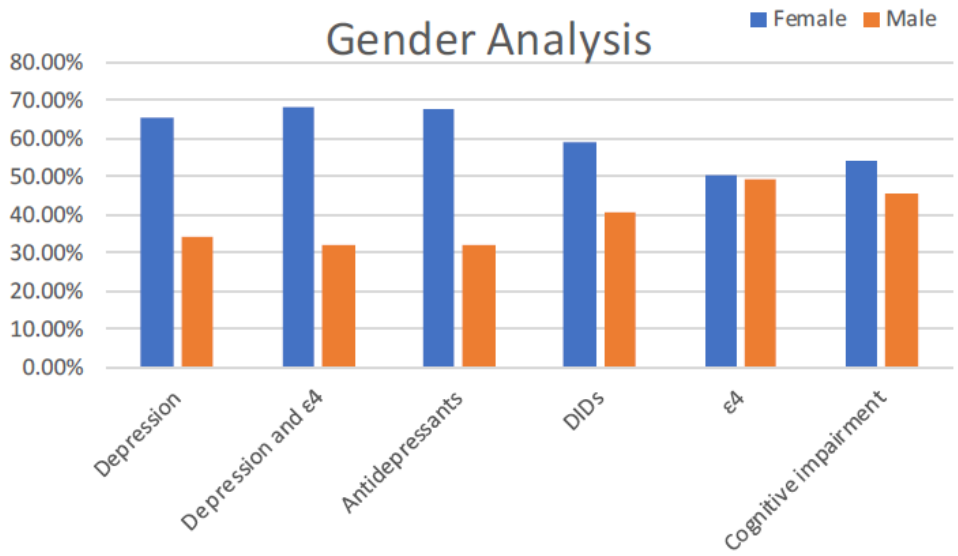

Figure 2. Gender analysis. Analysis of the percentage of each gender with depression, depression and APOE ε4, taking antidepressant medication, taking a depression-inducing drug (DID), possessing the APOE ε4 allele, and measurable cognitive impairment.

considered with gender (68.09% vs 31.91%, P value 0.002) (Table 2).

DIDs

60.56% of the total population was taking at least one DID (Table 1). Females were more likely to be taking a greater number of concurrent DIDs than males (1.29 [SD 1.32] vs 0.99 [SD 1.19], P value 0.045) (Table 2 and Table 3 and Figure 2). Those taking a DID were more likely to be taking a higher number of antidepressants (0.58 [SD 0.88] vs 0.2 [SD 0.46], P value <0.0001) (Table 2 and Table 3).

Antidepressants

29.58% of the overall population was taking at least one antidepressant medication (Table 1). Those taking an antidepressant were more likely to be taking concurrent DIDs (77.38% vs 22.62%, P value 0.0002) (Table 2). Gender was also a significant factor for antidepressants. Females were more likely to be on at least one antidepressant (67.86% vs 32.14%, P value 0.005) (Figure 2), as well as taking a greater number of concurrent antidepressants (0.52 [SD 0.80] vs 0.32 [SD 0.71], P value 0.029) (Table 2 and Table 3).

A higher, though not statistically significant, number of people taking antidepressants were more likely to have ε4 (70% vs 30%, P value 0.084) (Table 2).

Cognitive impairment

75.33% of this population had measurable cognitive impairment (Table 1). Those who were impaired took a higher number of concurrent antidepressant medications (0.46 [SD 0.83] vs 0.25 [SD 0.52], P value 0.036) (Table 2 and Table 3). There was also a higher percentage of cognitively impaired individuals taking antidepressants, but the number did not reach significance (80% vs 20%, P value 0.316). A higher percentage of people with cognitive impairment were also taking DIDs (57.49% vs 42.51%, P value 0.394), but again the number did not reach significance (Table 2).

Discussion

DIDs are a substantial clinical, medical, and public health problem[34] that has yet to be addressed in older populations. DID consideration is especially important in populations with an increased risk or a current diagnosis of AD. Prescriptions for elderly patients, especially those with a family history of AD or who currently have symptoms of cognitive decline, should be closely monitored and should avoid taking DIDs whenever possible.

The results of this work support that ε4 populations are at a greater risk of depression. Whether depression is a prodromal symptom or a risk factor for AD cannot be concluded from this data, but many other studies provide compelling evidence that depression may contribute to a person's risk of developing AD. If depression is a precursor to AD, then DIDs may accelerate the clinical presentation of AD. It is worth further study to see if those who possess the ε4 allele should avoid drugs likely to cause depression symptoms, as they may be predisposed to develop depression. Further research into the possible mechanisms of DIDs is also warranted and

Table 3. Drug analysis.

Drug		Mean	Std Dev	Minimum	Maximum	Count on medication	% Population
Antidepressants	Female	0.52	0.80	0	4	57	67.86
	Male	0.32	0.71	0	3	27	32.14
Antidepressant	No cognitive impairment	0.25	0.52	0	2	12	20.00
	Cognitive impairment	0.46	0.83	0	4	48	80.00
Antidepressant	nE4	0.35	0.82	0	4	15	30.00
	E4	0.41	0.65	0	2	35	70.00
Antidepressant	No DID	0.20	0.46	0	2	19	22.62
	DID	0.58	0.88	0	4	65	77.38
DIDs	Female	1.29	1.32	0	5	102	59.30
	Male	0.99	1.19	0	5	70	40.70
DID	No cognitive impairment	0.82	1.09	0	5	28	22.58
	Cognitive impairment	1.11	1.29	0	5	96	77.42
DID	nE4	1.01	1.08	0	5	44	44.90
	E4	0.78	1.04	0	5	54	55.10
DID	Not depressed	0.97	1.14	0	5	97	56.73
	Depressed	1.49	1.42	0	5	74	43.27

DIDs, depression-inducing drugs.

could possibly help further elucidate the correlation between depression and the development of AD.

This work also showed that DIDs are abundant in elderly individuals' medication regimes. Re-evaluation of medications that have been documented to cause depression could potentially lead to better cognitive function for many patients. This may be especially beneficial to the ε4 population. Further research may improve guidelines for prescribing DIDs to elderly patients, and additional specifications may be needed for those with the ε4 allele.

Females appear to be at an even greater risk for DIDs as this study found they may already be pre-disposed to depression, with the risk increasing with the ε4 gene, and are more likely to be taking DIDs and taking a higher number.

Further research is warranted to see if patients with different levels of cognitive impairment respond differently to DIDs, or if there are other contributors to developing depression as a side effect. Other factors such as age, body mass index, and comorbidities could also be explored to see if they impact patients' risk of developing DID.

With the rising numbers of elderly in the US, along with concurrent use of multiple prescription drugs, DID burden on cognitive health continues to grow. 30% of older adults in the United States take five or more medications daily[45], known as polypharmacy. Each additional drug increases a patient's risk of experiencing adverse effects, including depression and cognitive impairment.

CDSS provides a reliable and reproducible method to help with polypharmacy and DIDs. CDSS is software that is created to provide decision support for the diagnosis, treatment, prevention, cure, or mitigation of diseases or other conditions[44]. The goal of CDSS is to provide clinicians with actionable recommendations to improve clinical decision making[46,47]. One considerable advantage of CDSS is its inherent ability to process immense amounts of data quickly. This makes CDSS ideal for dealing with complicated medication regimes.

Machine-learning algorithms, one element of CDSS, can be equipped to help physicians and patients better curate their medications to prevent adverse events, unwanted side effects, and even duplicated prescriptions. It's estimated that 25% of people aged 65–69 take at least five prescriptions, and it is not uncommon for people to take 20 or more drugs[48]. One individual in this dataset was on a total of 67 medications. The considerable number of patients with polypharmacy and an average of 32 new drugs approved by the FDA each year make this an insurmountable task for a physician to take on by themselves[49].

CDSS can quickly review a patient's medication list, no matter how large, matching it to current guidelines to provide physicians with reproducible guidance. This guidance could include recommendations for deprescribing medications that are therapeutically repetitive, medications that interact with other drugs, and medications that interact or have diminished therapeutic benefit due to an individual's genetics. CDSS can also alert physicians to medications such as DIDs and anticholinergic drugs that have been shown to cause cognitive burden for elderly patients. CDSS also has the ability to suggest formulary alternatives to reduce the amount of DIDs in a medication list.

CDSS has the potential to support pharmacogenomics. Pharmacogenomics is the study of identifying genomic variants that affect drug efficacy and pharmacokinetics (PK) or pharmacodynamics (PD)[50]. There are many examples of medications that are effective or ineffective for patients based on their genome, including antidepressants. As of 2015, 20 genetic variations have been found that can affect around 80 medications[50]. In fact, one gene can affect multiple medications. Many of uMH's clients choose to get their genome sequenced to find out more about their genetic risk and protection against AD. This same data can also be used to help select the most beneficial medications for each person.

uMH's bioinformatics platform currently mines publicly available databases to check for drug-gene interactions (DGIs). The platform analyzes more than 2,000 single nucleotide polymorphism (SNPs) per individual, some of which pertain to DGIs, others are used to quantify the genetic risk of AD as well as other genetic diseases.

DGI information is drawn from three sources of pharmacogenomic information: the Clinical Pharmacogenetics Implementation Consortium (CPIC) effort[51], DrugBank[52,53], and SNPedia's SNP and genoset compilations[54,55]. DGIs are looked at in two categories: genetics that influence how enzymes metabolize each drug, and relationships between specific genes and drugs. Each medication a person is currently taking is compared against a table of genes that affect it, and these genes are, in turn, compared to those in the person's genome.

Approximately half of the people placed on an antidepressant medication do not show signs of improvement and over half will experience an adverse side effect. This is partly due to each person's genetic makeup and its impact on the PK and PD of the medication[56]. Many pharmacogenomic studies have been conducted on antidepressant medications and found that their efficacy is highly correlated with SNP variations. Metabolizing enzymes such as P450 and the *CYP2D6* polymorphism have both been found to have an effect on the drug plasma levels of antidepressant medications[57].

Precision-medicine platforms, like uMH's CDSS, offer the opportunity to improve the fitting of a drug to a patient with less trial and error, based on their genetics. This would allow for patients to be placed on the most effective medication as soon as possible, potentially speeding up recovery time from depressive symptoms.

CDSS could also be made more effective if linked to systems pharmacology models. These models have been developed to help predict *in vivo* drug effects in biological networks[58,59]. This

approach seeks to look at the whole, instead of the more traditional single transduction pathway of drug administration and response. Drugs often have off-target or secondary effects that can be hard to predict as multiple systems can be involved and must be accounted for. Patients' responses to drugs are also inherently variable due to their unique genome, environment, disease state, and the high prevalence of polypharmacy[32,58].

A systems biology analysis could be useful in further defining the mechanisms behind DIDs. This information could then further inform future research into potentially lessening the depressive effects of these drugs, and also inform research into whether depression is a true risk factor for AD or a prodromal symptom.

Many older adults who experience late-life depression never fully recover from their depression-induced cognitive impairment, even after successful treatment of the depression. All these observations magnify the urgent need to provide better vigilance when prescribing medications for the elderly.

A more technology-friendly view is needed when it comes to managing complex medication regimes, especially when medications that can affect patients' cognitive abilities are involved (as evidenced by the lack of publications on DIDs and the AD population).

The findings presented here support numerous previous publications indicating a relationship between depression and cognitive decline. While our observational data can only provide conjecture and find correlations, it is clearly worth closely monitoring DIDs in elderly populations. It is of even more importance when a patient may already be at increased risk of AD. There is a better path forward for patients with precision medicine and CDSS.

Data availability

The data that support the findings of this study are available from uMETHOD Health but restrictions apply to the availability of these data, which are proprietary company information, and so are not publicly available. Data are, however, available with permission of uMETHOD Health. Requests will be granted on a case-by-case basis to researchers affiliated with an accredited institution following the submission of an ethically approved and relevant research proposal. Readers and reviewers can request access to the dataset used in this manuscript by sending a request to info@umethod.com. The National Alzheimer's Coordinating Center (NACC) database is a publicly available dataset that is representative of the dataset analyzed in this study and can be used to apply the methodology described in this manuscript.

Acknowledgments

Authors had full access to all of the data in this study and take complete responsibility for the integrity of the data and accuracy of the data analysis.

Thanks to Dr. John Q Walker and Mark Zelek for their support.

Dr. John R. Cirrito confirms that the author has an appropriate level of expertise to conduct this research and confirms that the submission is of an acceptable scientific standard. Dr. John R. Cirrito declares they have no competing interests. Affiliation: Department of Neurology, Washington University, St. Louis, USA.

References

1. Alzheimer's Association: 2018 Alzheimer's disease facts and figures. *Alzheimers Dement.* 2018; **14**(3): 367–429.
Publisher Full Text

2. Byers AL, Yaffe K: **Depression and risk of developing dementia.** *Nat Rev Neurol.* 2011; **7**(6): 323–331.
PubMed Abstract | Publisher Full Text | Free Full Text

3. Price JL, Morris JC: **Tangles and plaques in nondemented aging and "preclinical" Alzheimer's disease.** *Ann Neurol.* 1999; **45**(3): 358–368.
PubMed Abstract

4. Skoog I, Waern M, Duberstein P, *et al.*: **A 9-year prospective population-based study on the association between the APOE*E4 allele and late-life depression in Sweden.** *Biol Psychiatry.* 2015; **78**(10): 730–736.
PubMed Abstract | Publisher Full Text

5. Qiu WQ, Zhu H, Dean M, *et al.*: **Amyloid-associated depression and ApoE4 allele: longitudinal follow-up for the development of Alzheimer's disease.** *Int J Geriatr Psychiatry.* 2016; **31**(3): 316–322.
PubMed Abstract | Publisher Full Text | Free Full Text

6. Kessler RC, Berglund P, Demler O, *et al.*: **Lifetime prevalence and age-of-onset distributions of DSM-IV disorders in the National Comorbidity Survey Replication.** *Arch Gen Psychiatry.* 2005; **62**(6): 593–602.
PubMed Abstract | Publisher Full Text

7. Diniz BS, Butters MA, Albert SM, *et al.*: **Late-life depression and risk of vascular dementia and Alzheimer's disease: systematic review and meta-analysis of community-based cohort studies.** *Br J Psychiatry.* 2013; **202**(5): 329–335.
PubMed Abstract | Publisher Full Text | Free Full Text

8. Qato DM, Ozenberger K, Olfson M: **Prevalence of Prescription Medications With Depression as a Potential Adverse Effect Among Adults in the United States.** *JAMA.* 2018; **319**(22): 2289–2298.
PubMed Abstract | Publisher Full Text | Free Full Text

9. Saczynski JS, Beiser A, Seshadri S, *et al.*: **Depressive symptoms and risk of dementia: the Framingham Heart Study.** *Neurology.* 2010; **75**(1): 35–41.
PubMed Abstract | Publisher Full Text | Free Full Text

10. Butters MA, Young JB, Lopez O, *et al.*: **Pathways linking late-life depression to persistent cognitive impairment and dementia.** *Dialogues Clin Neurosci.* 2008; **10**(3): 345–357.
PubMed Abstract | Free Full Text

11. Barnes DE, Alexopoulos GS, Lopez OL, *et al.*: **Depressive symptoms, vascular disease, and mild cognitive impairment: findings from the Cardiovascular Health Study.** *Arch Gen Psychiatry.* 2006; **63**(3): 273–279 .
PubMed Abstract | Publisher Full Text

12. Berger AK, Fratiglioni L, Forsell Y, *et al.*: **The occurrence of depressive symptoms in the preclinical phase of AD: a population-based study.** *Neurology.* 1999; **53**(9): 1998–2002.
PubMed Abstract | Publisher Full Text

13. Chen P, Ganguli M, Mulsant BH, *et al.*: **The temporal relationship between depressive symptoms and dementia: a community-based prospective study.** *Arch Gen Psychiatry.* 1999; **56**(3): 261–266.
PubMed Abstract | Publisher Full Text

14. Geerlings MI, Schoevers RA, Beekman AT, *et al.*: **Depression and risk of cognitive decline and Alzheimer's disease. Results of two prospective community-based studies in The Netherlands.** *Br J Psychiatry.* 2000; **176**: 568–575.
PubMed Abstract | Publisher Full Text

15. Kessing LV, Søndergård L, Forman JL, *et al.*: **Antidepressants and dementia.** *J Affect Disord.* 2009; **117**(1-2): 24–29.
PubMed Abstract | Publisher Full Text

16. Jorm AF: **History of depression as a risk factor for dementia: an updated review.** *Aust N Z J Psychiatry.* 2001; **35**(6): 776–781.
PubMed Abstract | Publisher Full Text

17. Ownby RL, Crocco E, Acevedo A, *et al.*: **Depression and risk for Alzheimer disease: systematic review, meta-analysis, and metaregression analysis.** *Arch Gen Psychiatry.* 2006; **63**(5): 530–538.
PubMed Abstract | Publisher Full Text | Free Full Text

18. Barnes DE, Yaffe K, Byers AL, *et al.*: **Midlife vs late-life depressive symptoms and risk of dementia: differential effects for Alzheimer disease and vascular dementia.** *Arch Gen Psychiatry.* 2012; **69**(5): 493–498 .
PubMed Abstract | Publisher Full Text | Free Full Text

19. Namekawa Y, Baba H, Maeshima H, *et al.*: **Heterogeneity of elderly depression: increased risk of Alzheimer's disease and Aβ protein metabolism.** *Prog Neuropsychopharmacol Biol Psychiatry.* 2013; **43**: 203–208 .
PubMed Abstract | Publisher Full Text

20. Sureshkumar R, Bharath S, Jain S, *et al.*: **ApoE4 and late onset depression in Indian population.** *J Affect Disord.* 2012; **136**(3): 244–248.
PubMed Abstract | Publisher Full Text

21. Rapp MA, Schnaider-Beeri M, Grossman HT, *et al.*: **Increased hippocampal plaques and tangles in patients with Alzheimer disease with a lifetime history of major depression.** *Arch Gen Psychiatry.* 2006; **63**(2): 161–167.
PubMed Abstract | Publisher Full Text

22. Caraci F, Copani A, Nicoletti F, *et al.*: **Depression and Alzheimer's disease: neurobiological links and common pharmacological targets.** *Eur J Pharmacol.* 2010; **626**(1): 64–71.
PubMed Abstract | Publisher Full Text

23. Maes M, Yirmyia R, Noraberg J, *et al.*: **The inflammatory & neurodegenerative (I&ND) hypothesis of depression: leads for future research and new drug developments in depression.** *Metab Brain Dis.* 2009; **24**(1): 27–53.
PubMed Abstract | Publisher Full Text

24. Leonard BE: **Inflammation, depression and dementia: are they connected?** *Neurochem Res.* 2007; **32**(10): 1749–1756.
PubMed Abstract | Publisher Full Text

25. Sierksma ASR, van den Hove DL, Steinbusch HW, *et al.*: **Major depression, cognitive dysfunction and Alzheimer's disease: is there a link?** *Eur J Pharmacol.* 2010; **626**(1): 72–82.
PubMed Abstract | Publisher Full Text

26. Engelhart MJ, Geerlings MI, Meijer J, *et al.*: **Inflammatory proteins in plasma and the risk of dementia: the rotterdam study.** *Arch Neurol.* 2004; **61**(5): 668–672.
PubMed Abstract | Publisher Full Text

27. Zuccato C, Cattaneo E: **Brain-derived neurotrophic factor in neurodegenerative diseases.** *Nat Rev Neurol.* 2009; **5**(6): 311–322.
PubMed Abstract | Publisher Full Text

28. Steffens DC, Byrum CE, McQuoid DR, *et al.*: **Hippocampal volume in geriatric depression.** *Biol Psychiatry.* 2000; **48**(4): 301–309.
PubMed Abstract | Publisher Full Text

29. Freis ED: **Mental depression in hypertensive patients treated for long periods with large doses of reserpine.** *N Engl J Med.* 1954; **251**(25): 1006–1008.
PubMed Abstract | Publisher Full Text

30. Chandragiri SS: **Substance-Induced Mood Disorder: Overview, Substances Linked to Depression or Mania, Etiology.** *Medscape.* 2016.
Reference Source

31. Ganzini L, Walsh JR, Millar SB: **Drug-induced depression in the aged. What can be done?** *Drugs Aging.* 1993; **3**(2): 147–158.
PubMed Abstract | Publisher Full Text

32. Keine D, Zelek M, Walker JQ, *et al.*: **Polypharmacy in an Elderly Population: Enhancing Medication Management Through the Use of Clinical Decision Support Software Platforms.** *Neurol Ther.* 2019; **8**(1): 79–94.
PubMed Abstract | Publisher Full Text | Free Full Text

33. Alagiakrishnan K, Wiens CA: **An approach to drug induced delirium in the elderly.** *Postgrad Med J.* 2004; **80**(945): 388–393.
PubMed Abstract | Publisher Full Text | Free Full Text

34. Rogers D, Pies R: **General medical with depression drugs associated.** *Psychiatry (Edgmont).* 2008; **5**(12): 28–41.
PubMed Abstract | Free Full Text

35. Dhondt TDF, Beekman ATF, Deeg DJH, *et al.*: **Iatrogenic depression in the elderly. Results from a community-based study in the Netherlands.** *Soc Psychiatry Psychiatr Epidemiol.* 2002; **37**(8): 393–398.
PubMed Abstract | Publisher Full Text

36. Broderick PA: **Alprazolam, diazepam, yohimbine, clonidine: *in vivo* CA_1 hippocampal norepinephrine and serotonin release profiles under chloral hydrate anesthesia.** *Prog Neuropsychopharmacol Biol Psychiatry.* 1997; **21**(7): 1117–1140.
PubMed Abstract | Publisher Full Text

37. Kreider ML, Tate CA, Cousins MM, *et al.*: **Lasting effects of developmental dexamethasone treatment on neural cell number and size, synaptic activity, and cell signaling: critical periods of vulnerability, dose-effect relationships, regional targets, and sex selectivity.** *Neuropsychopharmacology.* 2006; **31**(1): 12–35.
PubMed Abstract | Publisher Full Text

38. Pumariega AJ, Nelson R, Rotenberg L: **Varenicline-induced mixed mood and psychotic episode in a patient with a past history of depression.** *CNS Spectr.* 2008; **13**(6): 511–514.
PubMed Abstract | Publisher Full Text

39. Keine D, Walker JQ, Kennedy BK, *et al.*: **Development, Application, and Results from a Precision-medicine Platform that Personalizes Multi-modal Treatment Plans for Mild Alzheimer's Disease and At-risk Individuals.** *Curr Aging Sci.* 2018; **11**(3): 173–181.
PubMed Abstract | Publisher Full Text | Free Full Text

40. McKhann GM, Knopman DS, Chertkow H, *et al.*: **The diagnosis of dementia due to Alzheimer's disease: recommendations from the National Institute on Aging-Alzheimer's Association workgroups on diagnostic guidelines for Alzheimer's disease.** *Alzheimers Dement.* 2011; **7**(3): 263–269.
PubMed Abstract | Publisher Full Text | Free Full Text

41. Scharre DW, Chang S, Murden RA, *et al.*: **Self-administered Gerocognitive Examination (SAGE): a brief cognitive assessment Instrument for mild cognitive impairment (MCI) and early dementia.** *Alzheimer Dis Assoc Disord.* 2010; **24**(1): 64–71.
PubMed Abstract | Publisher Full Text

42. Nasreddine ZS, Phillips NA, Bédirian V, *et al.*: **The Montreal Cognitive Assessment, MoCA: a brief screening tool for mild cognitive impairment.** *J Am Geriatr Soc.* 2005; **53**(4): 695–699.
PubMed Abstract | Publisher Full Text

43. Yesavage JA, Brink TL, Rose TL, *et al.*: **Development and validation of a geriatric depression screening scale: a preliminary report.** *J Psychiatr Res.* 1982–1983; **17**(1): 37–49.
PubMed Abstract | Publisher Full Text

44. 114th Congress: **H.R.34 - 114th Congress (2015-2016): 21st Century Cures Act.** *Congress gov.* 2016.
Reference Source

45. Quinn KJ, Shah NH: **A dataset quantifying polypharmacy in the United States.** *Sci Data.* 2017; **4**: 170167.
PubMed Abstract | Publisher Full Text | Free Full Text

46. Hunt DL, Haynes RB, Hanna SE, *et al.*: **Effects of computer-based clinical decision support systems on physician performance and patient outcomes: a systematic review.** *JAMA.* 1998; **280**(15): 1339–1346.
PubMed Abstract | Publisher Full Text

47. Kawamoto K, Houlihan CA, Balas EA, *et al.*: **Improving clinical practice using clinical decision support systems: a systematic review of trials to identify features critical to success.** *BMJ.* 2005; **330**(7494): 765.
PubMed Abstract | Publisher Full Text | Free Full Text

48. Charlesworth CJ, Smit E, Lee DSH, *et al.*: **Polypharmacy Among Adults Aged 65 Years and Older in the United States: 1988-2010.** *J Gerontol A Biol Sci Med Sci.* 2015; **70**(8): 989–995.
PubMed Abstract | Publisher Full Text | Free Full Text

49. Engagemen I: **Advancing Health Through Innovation: 2017 New Drug Therapy Approvals Report (PDF - 2.8MB)**. 2017.

50. Relling MV, Evans WE: **Pharmacogenomics in the clinic.** *Nature.* 2015; **526**(7573): 343–350.
PubMed Abstract | Publisher Full Text | Free Full Text

51. Clinical Pharmacogenetics Implementation Consortium: **Prioritization.** *Clinical Pharmacogenetics Implementation Consortium.*
Reference Source

52. Ayvaz S, Horn J, Hassanzadeh O, *et al.*: **Toward a complete dataset of drug-drug interaction information from publicly available sources.** *J Biomed Inform.* 2015; **55**: 206–217.
PubMed Abstract | Publisher Full Text | Free Full Text

53. Drug Bank: **Pharmaco-transcriptomics: Up/down regulation of genes due to the metabolism of pharmaceutical compounds.** *DrugBank.*
Reference Source

54. Lu M, Lewis CM, Traylor M: **Pharmacogenetic testing through the direct-to-consumer genetic testing company 23andMe.** *BMC Med Genomics.* 2017; **10**(1): 47.
PubMed Abstract | Publisher Full Text | Free Full Text

55. SNPedia: **Genoset.** *SNPedia.* 2013.
Reference Source

56. Bousman CA, Forbes M, Jayaram M, *et al.*: **Antidepressant prescribing in the precision medicine era: a prescriber's primer on pharmacogenetic tools.** *BMC Psychiatry.* 2017; **17**(1): 60.
PubMed Abstract | Publisher Full Text | Free Full Text

57. Binder EB, Holsboer F: **Pharmacogenomics and antidepressant drugs.** *Ann Med.* 2006; **38**(2): 82–94.
PubMed Abstract | Publisher Full Text

58. Danhof M: **Systems pharmacology - Towards the modeling of network interactions.** *Eur J Pharm Sci.* 2016; **94**: 4–14.
PubMed Abstract | Publisher Full Text

59. van Hasselt JGC, Iyengar R: **Systems Pharmacology: Defining the Interactions of Drug Combinations.** *Annu Rev Pharmacol Toxicol.* 2019; **59**: 21–40.
PubMed Abstract | Publisher Full Text

Conclusions

More than half of the population examined here was on at least one DID. This research shows that in this population, DIDs correlate with a higher rate of depression. Since these drugs have been previously been shown to have depression as a side effect, it is likely they are causing some of the depression symptoms in this population.

This was the first paper to examine an at-risk or AD population and the number of DIDs that they were taking. The research is ongoing as to if depression is a risk factor for AD, but until proven otherwise, patients at risk of AD or experiencing cognitive decline should avoid taking DIDs. Especially patients who have ε4 as they are already at an increased risk of depression.

While the CDSS platform here was only used to analyze existing medications, CDSS platforms could be coded to alert physicians when they are prescribing a DID to a patient that has an increased risk of AD, or to alert physicians when these patients are already taking one or more DIDs. As presented in the earlier discussion, CDSS also has the potential to assist physicians in prescribing the best medications based on a patient's genetics and their likely response to the drug. Using this method could help reduce the trial-and-error that is the current standard when placing patients on new medications. If a physician knows ahead of time that a patient has a predisposition to respond or not respond to a certain drug, then they can make better prescribing decisions.

Chapter 10: Discussion

As has been shown by this research, AD is a complex disease for which it is unlikely that one therapeutic target will be enough to attenuate the disease. The cellular and mouse model research presented here has helped to further the understanding of AD mechanisms and highlighted possible pharmacological therapeutic targets.

This new information was made possible by the use of *in vivo* microdialysis techniques, and adaptations of those surgical techniques for EEG measurement. Microdialysis allows for the real-time collection of ISF in awake and freely moving mice. Sample collection can be as short as 24 hours, or it can continue for weeks, providing a unique method of analyte collection that can provide information about kinetics and how levels are changing over time and in response to different manipulations.

The microdialysis techniques used in this research are a novel technique that was developed by the head of the lab to measure ISF Aβ. By using this technique in combination with behavioral, cellular, and chemical assays, this research has helped to further the understanding of the pathways that control Aβ levels. That knowledge, in turn, leads to further experiments to better understand the risk factors of AD and well as new therapeutic targets.

Experiments presented here further advanced the microdialysis technique by proving that apoE could also be collected this way. Previously, only small molecules were measurable with microdialysis.

New findings about Aβ clearance were also discovered using microdialysis. Aβ appears to be taken up differently in various parts of the brain. Lysosomes mediate the degradation of the protein, but the cells mediating the update, the receptors facilitating the endocytosis, and the mechanisms that are affected by AD differ. The research showed that neuronal clearance of Aβ in the cortex is dependent on LRP1. But this same protein does not seem to have any effect on Aβ clearance in the hippocampus. In the hippocampus, Aβ clearance is more dependent on astrocytes

and on those astrocytes having healthy and abundant lysosomes. This suggests that just targeting LRP1 or lysosome biogenesis might not be enough to make a measurable impact on patients. A combination approach would likely be more efficacious as it would allow for the targeting of many different brain areas instead of just one.

In recent years, there has been an increasing number of Aβ antibodies being tested as a therapeutic option for AD (Ferrero et al. 2016). These molecules target the Aβ plaque deposits, breaking them up into smaller pieces. They do not, however, target soluble forms of Aβ.

In early 2019, both Roche and Biogen announced that they would be discontinuing all trials of their therapeutic antibodies (Lowe n.d.; Fagan 2019) for failure to meet their endpoints. By only targeting the plaque form of Aβ, these antibody therapies may have inadvertently been making the issues related to Aβ worse. The research presented here, and in other publications, offers an explanation for this failure.

By selectively targeting and halting the production of APP, levels of soluble Aβ can be reduced without affecting existing plaque levels. The research here shows that this was enough to regain some aspects of cognitive function and memory in mice and points to soluble Aβ as the real, or at least first-line, target for pharmaceutical AD therapies. In fact, by breaking up Aβ plaques, these antibody treatments may have been increasing the levels of soluble Aβ, and thereby also increasing toxicity.

An often overlooked aspect of AD is that it is associated with an increase in seizures and aberrant electrical activity in the brain. Both of which can induce excitotoxicity, leading to cognitive deficits. Many publications in this area of AD research have focused on trying to better understand Aβ's role in seizure activity. The research presented here broadens that view by exploring tau's role and attempting to separate APP's contributions from Aβ's.

The results showed that tau is a promising target for reducing seizure severity and susceptibility. It has already been documented that tau$^{-/-}$ mice have significantly

reduced seizure activity after chemically-induced seizures compared to nontransgenic mice. The findings presented here showed that this protective effect is not due to some developmental compensation mechanism, but is, in fact, a consequence of tau reduction. This finding provides another potential therapeutic target to protect against cognitive decline in AD.

Further research is needed to find a good way to target tau reduction in humans, but the *in vivo* experiments here show that ASOs could potentially be used. ASOs have already been used in other human clinical trials and have been proven well-tolerated and safe (Miller et al. 2013). It is not known how much of a reduction in tau would be needed to provide this protective effect in humans. Further research is needed to find not only the optimal dose but also how often the ASO would need to be given. A recent trial in Huntington's disease showed that their huntingtin-targeting ASO is effective with less frequent dosing. Initially, the trial was designed to administer the drug monthly, but after an open-label study, they found that bi-monthly dosing is just as effective. This led them to amend their future phase II trial to be bi-monthly and quarterly dosing instead of monthly (Ionis Pharmaceuticals 2019).

Another point of exploration would be to look at how early in the disease to start this type of tau-reduction intervention. The animal models used here were young, and the experiment does not provide comparative information for an older population that would be farther along in the disease process.

While the research here used nontransgenic mouse models, other studies of tau reduction in Aβ-producing mice have been completed. These studies found that tau reduction is protective against many Aβ-induced insults. Our research adds to these findings to show that preventing excitotoxicity from aberrant electrical activity is one of the ways in which reducing tau is protective in AD.

The research into APP and Aβ's roles in seizures provided another therapeutic target as well as mechanistic information as to what is potentially leading to the increase in seizures seen in AD. As discussed, the findings of the experiments were not wholly expected, but they did provide interesting information for future study.

The results showed that APP may be much more involved than Aβ when it comes to seizure activity in AD. When transgenic APP mice stopped producing APP through the administration of DOX, a subsequent normalization of EEG measurements was found. This finding was not replicated when Aβ production was stopped.

Suppression of APP did not have the same protective effects as tau reduction for chemically-induced seizures though. Mice that had previously overexpressed APP and had APP production halted before inducing seizures still showed the same high response and susceptibility to convulsants. This finding suggests that overproduction of APP may permanently alter the CNS in some manner. The experiments here were not able to conclude why some changes in relation to APP production and seizures are permanent while others are not.

It has been shown that EOAD and LOAD have very different risk profiles when it comes to seizures. The research presented here shows that there are likely different mechanisms involved in this risk. EOAD patients often have mutations in the APP gene. The mouse models that expressed APP from an early age were predisposed to increased seizures. Taking this information together, it can be hypothesized that mutations in the APP gene may be an important factor in this increased seizure risk. LOAD patients, on the other hand, are less likely to develop seizures than EOAD patients. When mouse models were prevented from expressing APP until they were fully grown, they were less likely to have a strong response to chemically-induced seizures. This suggests that development without APP mutations allows a more normal neurological development, making them more resistant to seizures and aberrant electrical activity. But as patients age, this protective effect likely declines due to normal aging and AD mechanisms that result in neurodegeneration.

The laboratory research presented here follows in a long line of research that highlights AD's complexity. This disease has been studied for over 100 years, but an effective drug still eludes us. These attempts will continue to fail as they do not address the disease systemically.

Cognitively impaired and AD patients face many hurdles when it comes to treatment

options, but these barriers can be overcome with the help of CDSS. The current drug treatments for AD are only symptomatic agents and do not address the underlying mechanisms of disease. The multidomain CDSS platform described here is different from the current standard of care. It is designed to find and recommend treatments for each person's specific drivers of AD.

This results of the study corroborate other current research into multidomain treatments. When patients' lifestyle, genomics, and medical histories are taken into account, each person has a unique mix of risk factors contributing to their decline. Because of this, it is necessary to decipher these unique drivers to create an effective treatment plan for each patient. This mix and multitude of drivers also means that addressing one driver of the disease is not enough to make a meaningful therapeutic difference. The patient's drivers must be addressed systemically.

Multidomain treatment plans are inherently harder to follow than simply taking a pill. This research shows that patients, even those with current cognitive decline, are capable of following a complex treatment plan though. For those patients already experiencing decline, it is important to have a supportive caretaker working with them. Trained health coaches also played an important role in this research. They were able to help patients incorporate this multidomain treatment plan in a stepwise manner so as to make it achievable and a sustainable part of their everyday lives.

Utilizing the CDSS platform, the patients studied here showed measurable improvements in both neurocognitive testing as well as blood biomarkers. The improvements in cognitive testing scores exceeded what has been seen in the past when patients are only on the standard of care, demonstrating that this personalized multidomain treatment outperforms the current published data for standard of care.

It is also well established in the literature that elderly patients' medication regimes consist of multiple medications, often reaching the threshold of polypharmacy. In the US 30% of adults over the age of 65 take five or more medications (Quinn & Shah 2017). With each added medication, the risk of interactions, adverse events, and side effects increases. AD patients in particular may be at even greater risk due to

the neurological damage already inflicted by the course of the disease (Pasqualetti et al. 2015). Furthermore, AD patients are often prescribed competing medications. The current medications for AD are mainly ChEIs and patients are simultaneously prescribed anticholinergic drugs, which cancels out any beneficial effects of the ChEIs. As many as 35.4% of AD patients are taking these competing drugs concurrently (Carnahan et al. 2004).

The population studied here was on an average of 11.52 medications per person, with 83.66% of the population taking five or more medications. This polypharmacy regime resulted in 93.08% of the population experiencing at least one DDI, with an average of 10.7 DDIs per person. All of the DDIs identified have a rating of C or higher, making them all clinically significant. The specific ADRs experienced by this population were not documented in this study, but ADRs are among the top ten leading causes of death (Lazarou et al. 1998; Quinn & Shah 2017), making the 10.7 DDIs per person an extremely worrisome number.

Anticholinergic drugs also present a medication burden on their own. This medication class has been shown to adversely impact cognition, cause confusion, delirium, and even increase the risk of mortality in elderly populations (Salahudeen et al. 2015; Gorup et al. 2018). ACB has also been shown to be a risk factor for developing MCI and dementia (Aging Brain Program of the Indiana University Center for Aging Research 2012; Cai et al. 2013; Richardson et al. 2018; Pfistermeister et al. 2017). The study population in this research was taking an average of 1.43 anticholinergic drugs per person, resulting in an average ACB score of 2.15 (SD 2.47). Each point on the ACB scale has been correlated to a decline in MMSE score of 0.33 over two years (Aging Brain Program of the Indiana University Center for Aging Research 2012). With an average score over 2, this population faces a very real drug-induced cognitive burden.

These results show that current checks on medications, including EMRs, are not enough. Many patients are experiencing numerous DDIs, DGIs, and side effects that put them at increased risk for adverse health events, including cognitive decline and

death. CDSS can improve the current system of prescribing because it is able to process more information, is programmed to follow evidence-based clinical guidelines, and can review patients' information against these guidelines in a quick and more efficient manner than any one physician.

By employing the CDSS platform, we were able to identify many risks imposed by patients' medication regimes. Currently, the platform only identifies the problems, but even with its current limitations, it still confirms that CDSS can be a useful clinical tool to help improve patient safety. In the future, the algorithm could be enhanced to also provide actionable steps to physicians to help them reduce these issues. While this addition would need substantial validation, it does demonstrate the further capabilities of CDSS.

The research presented here is also the first to look at DIDs and AD patients specifically. As discussed, it is not yet known if depression is a risk factor or a prodromal sign of AD. But it is known that the two are closely related. Furthermore, those with the APOE $\boldsymbol{\varepsilon}4$ gene are more likely to experience depression. The mechanisms behind DIDs have not been fully elucidated, but because it has not been proven that depression is not causal to AD, there exists the possibility that DIDs increase patients' risk of cognitive decline and AD. Making them important to flag and potentially avoid for patients at risk of AD.

Aside from this issue, DIDs can also result in patients being misdiagnosed as having a disease when in reality the symptoms are a side effect to a medication. This misdiagnosis can lead to the addition of yet more medications, when in fact a reduction of medications would resolve the symptoms.

In the population studied here, 60.56% of them were taking at least one DID, with a mean of 1.16 DIDs per person. 36.21% had depression, and those with depression were significantly more likely to be taking at least one DID (*P value* 0.005). While the research here can only find correlations and cannot prove cause, it does highlight the need for more research in this area. And also the potential risk that is being placed on AD patients and those at risk of developing the disease.

CDSS was successfully used to identify these DIDs in the population. The use of this platform in a clinic could help physician identify this under-investigated medication issue. Making a physician aware of DIDs would hopefully influence how they prescribe, and decrease the number of DIDs per patient. Further advances to the platform could be made to not only identify these issues, but also help physicians wean patients off of unnecessary DIDs and to pick pharmacological alternatives that are not depression-inducing.

Research into multimodal treatment plans for AD could be further improved by a larger study population, as well as placebo controlled trials. This would allow conclusions to be drawn as to if this treatment approach is indeed better than the standard of care. The current results suggest that this will be the case. Further studies should also focus on standardizing the population so that the results can be applied more generally. The population placed on the multimodal treatment in this study was not representative of a larger generalized population, having more education, a lower body mass index, and a higher rate of APO $\boldsymbol{\varepsilon}4$.

It may also be enlightening to research if presymptomatic, MCI, or mild AD patients see better results from this multimodal treatment. Based on current research, the prevailing theory is that the earlier the intervention the more effective it will be at preventing cognitive decline. Once a patient is already symptomatic, it may be too late to intervene and ameliorate the decline. Studies on how APO $\boldsymbol{\varepsilon}4$ positive versus negative patients respond to the multimodal treatment could also provide more information on how much influence modifiable risk factors have to delay disease onset or slow decline compared to negative genetic factors.

More research could also be done to see how physicians respond to a more robust CDSS that makes suggestions for alternative medications. Conclusions cannot be drawn from the research presented here as to if physicians will react positively to such a platform making recommendations in a domain that has traditionally been theirs alone. It would also be worthwhile to see if these types of recommendations result in patients taking fewer medications, and experiencing fewer DDI, DGIs, and a

lower ACB.

CDSS platforms have many applications and can be used to solve current and dire medication issues in an elderly and AD population. We are only beginning to scratch the surface on the possible uses for CDSS. It has great potential to not only personalize treatments for patients, but also to improve patient safety through better analysis of their medications, and better recommendations. While many of the current CDSS platforms in use today are of a more simplified or moderate complexity level, technology and our medical knowledge are both advancing and those advancements can only be made better by synchronous use of medical and technological knowledge.

This research has shown that it is possible to create a personalized, multimodal treatment plan for patients to address their unique drivers of AD, and to expand that treatment to include enhancement of their current medication regimes as well. Personalized treatment is possible today. This same systematic approach can be applied to other complex diseases as well. Systems biology does not only apply to AD, there are many complex diseases that a single-therapy approach has failed for. As proven to cancer, tuberculosis, HIV and autoimmune disorders (Stephenson et al. 2015). And CDSS is to key to help realize those new multimodal treatments. It is only limited by medical knowledge, and clinical acceptance of its use. CDSS has great potential to advance patient care by equipping physicians to make better care choices for individuals.

Bibliography

114th Congress, 2016. H.R.34 - 114th Congress (2015-2016): 21st Century Cures Act . *Congress.gov*. Available at: https://www.congress.gov/bill/114th-congress/house-bill/34 [Accessed November 28, 2018].

Aging Brain Program of the Indiana University Center for Aging Research, 2012. *Anticholinergic Cognitive Burden (ACB) Scale 2012 Update*, Regenstrief Institute, Inc.

Albert, M. et al., 2019. The Use of MRI and PET for Clinical Diagnosis of Dementia and Investigation of Cognitive Impairment: A Consensus Report Prepared by Neuroimaging Work Group(1) Of The Alzheimer's Association.

Albert, M.S. et al., 2011. The diagnosis of mild cognitive impairment due to Alzheimer's disease: recommendations from the National Institute on Aging-Alzheimer's Association workgroups on diagnostic guidelines for Alzheimer's disease. *Alzheimer's & Dementia*, 7(3), pp.270–279.

Aldosari, B., Alanazi, A. & Househ, M., 2017. Pitfalls of ontology in medicine. *Studies in Health Technology and Informatics*, 238, pp.15–18.

Alexopoulos, G.S., 2003. Vascular disease, depression, and dementia. *Journal of the American Geriatrics Society*, 51(8), pp.1178–1180.

Alldred, D.P. et al., 2013. Interventions to optimise prescribing for older people in care homes. *Cochrane Database of Systematic Reviews*, (2), p.CD009095.

Alzheimer's Association, 2018. 2018 Alzheimer's disease facts and figures. *Alzheimer's & Dementia*, 14(3), pp.367–429.

Alzheimer's Disease Neuroimaging Initiative, ADNI | Data Types. Available at: http://adni.loni.usc.edu/data-samples/data-types/ [Accessed February 21, 2019].

Alzheimer's Society, Dementia tax. *Alzheimer's Society*. Available at: https://www.alzheimers.org.uk/about-us/policy-and-influencing/what-we-think/dementia-tax [Accessed March 6, 2019].

Amatniek, J.C. et al., 2006. Incidence and predictors of seizures in patients with Alzheimer's disease. *Epilepsia*, 47(5), pp.867–872.

American Geriatrics Society 2015 Beers Criteria Update Expert Panel, 2015.

American geriatrics society 2015 updated beers criteria for potentially inappropriate medication use in older adults. *Journal of the American Geriatrics Society*, 63(11), pp.2227–2246.

Anand, P. & Singh, B., 2013. A review on cholinesterase inhibitors for Alzheimer's disease. *Archives of Pharmacal Research*, 36(4), pp.375–399.

Andel, R. et al., 2008. Physical exercise at midlife and risk of dementia three decades later: a population-based study of Swedish twins. *The Journals of Gerontology. Series A, Biological Sciences and Medical Sciences*, 63(1), pp.62–66.

Andersen, C.K. et al., 2004. Ability to perform activities of daily living is the main factor affecting quality of life in patients with dementia. *Health and Quality of Life Outcomes*, 2, p.52.

Ard, M.D. et al., 1996. Scavenging of Alzheimer's amyloid beta-protein by microglia in culture. *Journal of Neuroscience Research*, 43(2), pp.190–202.

Arrowsmith, J. & Miller, P., 2013. Trial watch: phase II and phase III attrition rates 2011-2012. *Nature Reviews. Drug Discovery*, 12(8), p.569.

Atri, A., 2019. The alzheimer's disease clinical spectrum: diagnosis and management. *The Medical Clinics of North America*, 103(2), pp.263–293.

Attems, J. et al., 2011. Review: sporadic cerebral amyloid angiopathy. *Neuropathology and Applied Neurobiology*, 37(1), pp.75–93.

Baglioni, S. et al., 2006. Prefibrillar amyloid aggregates could be generic toxins in higher organisms. *The Journal of Neuroscience*, 26(31), pp.8160–8167.

Barghorn, S. et al., 2005. Globular amyloid beta-peptide oligomer - a homogenous and stable neuropathological protein in Alzheimer's disease. *Journal of Neurochemistry*, 95(3), pp.834–847.

Bateman, R.J. et al., 2006. Human amyloid-beta synthesis and clearance rates as measured in cerebrospinal fluid in vivo. *Nature Medicine*, 12(7), pp.856–861.

Bates, D.W. & Gawande, A.A., 2003. Improving safety with information technology. *The New England Journal of Medicine*, 348(25), pp.2526–2534.

Bayoumi, I. et al., 2014. The effectiveness of computerized drug-lab alerts: a systematic review and meta-analysis. *International Journal of Medical*

Informatics, 83(6), pp.406–415.

Belichenko, P.V. et al., 2009. Excitatory-inhibitory relationship in the fascia dentata in the Ts65Dn mouse model of Down syndrome. *The Journal of Comparative Neurology*, 512(4), pp.453–466.

Benilova, I., Karran, E. & De Strooper, B., 2012. The toxic Aβ oligomer and Alzheimer's disease: an emperor in need of clothes. *Nature Neuroscience*, 15(3), pp.349–357.

Bennett, C.F., 2018. Effects of IONIS-HTTRx in Patients with Early Huntington's Disease, Results of the First HTT-Lowering Drug Trial (CT.002). *Neurology*, 90(15 Supplement).

Berner, E.S., 2009. *Clinical decision support systems: State of the Art*,

Bezprozvanny, I. & Mattson, M.P., 2008. Neuronal calcium mishandling and the pathogenesis of Alzheimer's disease. *Trends in Neurosciences*, 31(9), pp.454–463.

Biessels, G.J. et al., 2006. Risk of dementia in diabetes mellitus: a systematic review. *Lancet Neurology*, 5(1), pp.64–74.

Bikowski, R.M., Ripsin, C.M. & Lorraine, V.L., 2001. Physician-patient congruence regarding medication regimens. *Journal of the American Geriatrics Society*, 49(10), pp.1353–1357.

Birks, J.S. & Harvey, R.J., 2018. Donepezil for dementia due to Alzheimer's disease. *Cochrane Database of Systematic Reviews*, 6, p.CD001190.

Blenkinsop, A. et al., 2020. Non-memory cognitive symptom development in Alzheimer's disease. *European Journal of Neurology*.

Bond, M. et al., 2012. The effectiveness and cost-effectiveness of donepezil, galantamine, rivastigmine and memantine for the treatment of Alzheimer's disease (review of Technology Appraisal No. 111): a systematic review and economic model. *Health Technology Assessment*, 16(21), pp.1–470.

Born, H.A., 2015. Seizures in Alzheimer's disease. *Neuroscience*, 286, pp.251–263.

Broersen, K., Rousseau, F. & Schymkowitz, J., 2010. The culprit behind amyloid beta peptide related neurotoxicity in Alzheimer's disease: oligomer size or conformation? *Alzheimer's research & therapy*, 2(4), p.12.

Busche, M.A. et al., 2008. Clusters of hyperactive neurons near amyloid plaques in a mouse model of Alzheimer's disease. *Science*, 321(5896), pp.1686–1689.

Busche, M.A. et al., 2012. Critical role of soluble amyloid-β for early hippocampal hyperactivity in a mouse model of Alzheimer's disease. *Proceedings of the National Academy of Sciences of the United States of America*, 109(22), pp.8740–8745.

Butters, M.A. et al., 2008. Pathways linking late-life depression to persistent cognitive impairment and dementia. *Dialogues in Clinical Neuroscience*, 10(3), pp.345–357.

Byers, A.L. & Yaffe, K., 2011. Depression and risk of developing dementia. *Nature Reviews. Neurology*, 7(6), pp.323–331.

Cai, X. et al., 2013. Long-term anticholinergic use and the aging brain. *Alzheimer's & Dementia*, 9(4), pp.377–385.

Campioni, S. et al., 2010. A causative link between the structure of aberrant protein oligomers and their toxicity. *Nature Chemical Biology*, 6(2), pp.140–147.

Carnahan, R.M. et al., 2004. The concurrent use of anticholinergics and cholinesterase inhibitors: rare event or common practice? *Journal of the American Geriatrics Society*, 52(12), pp.2082–2087.

Casserly, I. & Topol, E., 2004. Convergence of atherosclerosis and Alzheimer's disease: inflammation, cholesterol, and misfolded proteins. *The Lancet*, 363(9415), pp.1139–1146.

Chandragiri, S.S., 2016. Substance-Induced Mood Disorder: Overview, Substances Linked to Depression or Mania, Etiology. *Medscape*. Available at: https://emedicine.medscape.com/article/286885-overview [Accessed November 7, 2018].

Cheng, I.H. et al., 2007. Accelerating amyloid-beta fibrillization reduces oligomer levels and functional deficits in Alzheimer disease mouse models. *The Journal of Biological Chemistry*, 282(33), pp.23818–23828.

Chiang, J.-C. et al., 2018. Trisomy silencing by XIST normalizes Down syndrome cell pathogenesis demonstrated for hematopoietic defects in vitro. *Nature Communications*, 9(1), p.5180.

Cholerton, B. et al., 2016. Precision medicine: clarity for the complexity of dementia. *The American Journal of Pathology*, 186(3), pp.500–506.

Choong, X.Y. et al., 2015. Dissecting Alzheimer disease in Down syndrome using mouse models. *Frontiers in Behavioral Neuroscience*, 9, p.268.

Chu, L.W., 2012. Alzheimer's disease: early diagnosis and treatment. *Hong Kong Medical Journal*, 18(3), pp.228–237.

Cirrito, J.R. et al., 2003. In vivo assessment of brain interstitial fluid with microdialysis reveals plaque-associated changes in amyloid-beta metabolism and half-life. *The Journal of Neuroscience*, 23(26), pp.8844–8853.

Cleary, J.P. et al., 2005. Natural oligomers of the amyloid-beta protein specifically disrupt cognitive function. *Nature Neuroscience*, 8(1), pp.79–84.

ClinicalTrials.gov, 2014. A Study to Evaluate Safety, Tolerability, and Efficacy of BAN2401 in Subjects With Early Alzheimer's Disease. Available at: https://clinicaltrials.gov/ct2/show/NCT01767311?term=BAN2401+for+Early+Alzheimer%27s+Disease&rank=1 [Accessed March 5, 2019].

Committee on Diagnostic Error in Health Care et al., 2015. *Improving diagnosis in health care* E. P. Balogh, B. T. Miller, & J. R. Ball, eds., Washington (DC): National Academies Press (US).

Consumer Reports, 2012. Evaluating Drugs to Treat Alzheimer's Disease. *Consumer Reports*. Available at: https://www.consumerreports.org/cro/2012/07/evaluating-drugs-to-treat-alzheimer-s-disease/index.htm [Accessed March 6, 2019].

Corder, E.H. et al., 1994. Protective effect of apolipoprotein E type 2 allele for late onset Alzheimer disease. *Nature Genetics*, 7(2), pp.180–184.

Cummings, J. et al., 2017. Alzheimer's disease drug development pipeline: 2017. *Alzheimer's & dementia : translational research & clinical interventions*, 3(3), pp.367–384.

Cummings, J. et al., 2016. Drug development in Alzheimer's disease: the path to 2025. *Alzheimer's research & therapy*, 8, p.39.

Cummings, J.L. et al., 2015. A practical algorithm for managing Alzheimer's disease: what, when, and why? *Annals of clinical and translational neurology*, 2(3),

pp.307–323.

Cummings, J.L., 2004. Alzheimer's disease. *The New England Journal of Medicine*, 351(1), pp.56–67.

Cummings, J.L. et al., 2016. Double-blind, placebo-controlled, proof-of-concept trial of bexarotene in moderate Alzheimer's disease. *Alzheimer's research & therapy*, 8, p.4.

Cummings, J.L., Morstorf, T. & Zhong, K., 2014. Alzheimer's disease drug-development pipeline: few candidates, frequent failures. *Alzheimer's research & therapy*, 6(4), p.37.

Cummings, J.L., Tong, G. & Ballard, C., 2019. Treatment combinations for alzheimer's disease: current and future pharmacotherapy options. *Journal of Alzheimer's Disease*.

Cuyvers, E. & Sleegers, K., 2016. Genetic variations underlying Alzheimer's disease: evidence from genome-wide association studies and beyond. *Lancet Neurology*, 15(8), pp.857–868.

Danysz, W. & Parsons, C.G., 2003. The NMDA receptor antagonist memantine as a symptomatological and neuroprotective treatment for Alzheimer's disease: preclinical evidence. *International Journal of Geriatric Psychiatry*, 18(Suppl 1), pp.S23–32.

DeVita, V.T. & Chu, E., 2008. A history of cancer chemotherapy. *Cancer Research*, 68(21), pp.8643–8653.

DeVos, S.L. et al., 2017. Tau reduction prevents neuronal loss and reverses pathological tau deposition and seeding in mice with tauopathy. *Science Translational Medicine*, 9(374).

Dodart, J.-C. et al., 2002. Immunization reverses memory deficits without reducing brain Abeta burden in Alzheimer's disease model. *Nature Neuroscience*, 5(5), pp.452–457.

Doody, R.S. et al., 2013. A phase 3 trial of semagacestat for treatment of Alzheimer's disease. *The New England Journal of Medicine*, 369(4), pp.341–350.

Doody, R.S. et al., 2001. Open-label, multicenter, phase 3 extension study of the

safety and efficacy of donepezil in patients with Alzheimer disease. *Archives of Neurology*, 58(3), pp.427–433.

Doody, R.S. et al., 2014. Phase 3 trials of solanezumab for mild-to-moderate Alzheimer's disease. *The New England Journal of Medicine*, 370(4), pp.311–321.

Doraiswamy, P.M. & Steffens, D.C., 1998. Combination therapy for early Alzheimer's disease: what are we waiting for? *Journal of the American Geriatrics Society*, 46(10), pp.1322–1324.

Douaud, G. et al., 2013. Preventing Alzheimer's disease-related gray matter atrophy by B-vitamin treatment. *Proceedings of the National Academy of Sciences of the United States of America*, 110(23), pp.9523–9528.

Duffy, A.M. et al., 2015. Entorhinal cortical defects in Tg2576 mice are present as early as 2-4 months of age. *Neurobiology of Aging*, 36(1), pp.134–148.

Dunn, N. et al., 2005. Association between dementia and infectious disease: evidence from a case-control study. *Alzheimer Disease and Associated Disorders*, 19(2), pp.91–94.

Ek, M. et al., 2001. Inflammatory response: pathway across the blood-brain barrier. *Nature*, 410(6827), pp.430–431.

Engelhart, M.J. et al., 2002. Dietary intake of antioxidants and risk of Alzheimer disease. *The Journal of the American Medical Association*, 287(24), pp.3223–3229.

Engelhart, M.J. et al., 2004. Inflammatory proteins in plasma and the risk of dementia: the rotterdam study. *Archives of Neurology*, 61(5), pp.668–672.

Fagan, T., 2019. Biogen/Eisai Halt Phase 3 Aducanumab Trials. *ALZFORUM*. Available at: https://www.alzforum.org/news/research-news/biogeneisai-halt-phase-3-aducanumab-trials [Accessed March 25, 2019].

Farina, N. et al., 2017. Vitamin E for Alzheimer's dementia and mild cognitive impairment. *Cochrane Database of Systematic Reviews*, 4, p.CD002854.

Farlow, M.R. & Cummings, J.L., 2007. Effective pharmacologic management of Alzheimer's disease. *The American Journal of Medicine*, 120(5), pp.388–397.

FEDERAL FOOD, DRUG, AND COSMETIC ACT (1938) *Congress.gov*. Available at:

https://www.congress.gov/congressional-record/congressional-record-index/114th-congress/1st-session/federal-food-drug-and-cosmetic-act/8594 [Accessed March 14, 2020b].

De Felice, F.G., Lourenco, M.V. & Ferreira, S.T., 2014. How does brain insulin resistance develop in Alzheimer's disease? *Alzheimer's & Dementia*, 10(1 Suppl), pp.S26–32.

Ferrari, C. et al., 2014. Imaging and cognitive reserve studies predict dementia in presymptomatic Alzheimer's disease subjects. *Neuro-Degenerative Diseases*, 13(2-3), pp.157–159.

Ferreira-Vieira, T.H. et al., 2016. Alzheimer's disease: Targeting the Cholinergic System. *Current neuropharmacology*, 14(1), pp.101–115.

Ferrero, J. et al., 2016. First-in-human, double-blind, placebo-controlled, single-dose escalation study of aducanumab (BIIB037) in mild-to-moderate Alzheimer's disease. *Alzheimer's & dementia : translational research & clinical interventions*, 2(3), pp.169–176.

Fessel, W.J., 2017. Concordance of several subcellular interactions initiates alzheimer's dementia: their reversal requires combination treatment. *American Journal of Alzheimer's Disease and Other Dementias*, 32(3), pp.166–181.

Fjell, A.M. et al., 2009. One-year brain atrophy evident in healthy aging. *The Journal of Neuroscience*, 29(48), pp.15223–15231.

Food and Drug Administration, A History of Medical Device Regulation & Oversight in the United States | FDA. Available at: https://www.fda.gov/medical-devices/overview-device-regulation/history-medical-device-regulation-oversight-united-states [Accessed March 14, 2020a].

Food and Drug Administration, 2019. Clinical Decision Support Software: Draft Guidance for Industry and Food and Drug Administration Staff' ' .

Förstl, H. & Kurz, A., 1999. Clinical features of Alzheimer's disease. *European Archives of Psychiatry and Clinical Neuroscience*, 249(6), pp.288–290.

Frisoni, G.B. et al., 2010. The clinical use of structural MRI in Alzheimer disease. *Nature Reviews. Neurology*, 6(2), pp.67–77.

Frölich, L. et al., 1998. Brain insulin and insulin receptors in aging and sporadic Alzheimer's disease. *Journal of Neural Transmission*, 105(4-5), pp.423–438.

Gali, C.C. et al., 2019. Amyloid-beta impairs insulin signaling by accelerating autophagy-lysosomal degradation of LRP-1 and IR-β in blood-brain barrier endothelial cells in vitro and in 3XTg-AD mice. *Molecular and Cellular Neurosciences*, 99, p.103390.

Galvin, J.E., 2017. Prevention of alzheimer's disease: lessons learned and applied. *Journal of the American Geriatrics Society*, 65(10), pp.2128–2133.

Garcia, R.M., 2006. Five ways you can reduce inappropriate prescribing in the elderly: a systematic review. *The Journal of Family Practice*, 55(4), pp.305–312.

García-Escudero, V. et al., 2013. Deconstructing mitochondrial dysfunction in Alzheimer disease. *Oxidative medicine and cellular longevity*, 2013, p.162152.

Gates, G.A. et al., 2002. Central auditory dysfunction may precede the onset of clinical dementia in people with probable Alzheimer's disease. *Journal of the American Geriatrics Society*, 50(3), pp.482–488.

Gates, G.A., 2012. Central presbycusis: an emerging view. *Otolaryngology--Head and Neck Surgery*, 147(1), pp.1–2.

Giacobini, E., 2000. Cholinesterase inhibitors stabilize Alzheimer's disease. *Annals of the New York Academy of Sciences*, 920, pp.321–327.

Gillaizeau, F. et al., 2013. Computerized advice on drug dosage to improve prescribing practice. *Cochrane Database of Systematic Reviews*, (11), p.CD002894.

Goedert, M. & Spillantini, M.G., 2006. A century of Alzheimer's disease. *Science*, 314(5800), pp.777–781.

Gong, Y. et al., 2003. Alzheimer's disease-affected brain: presence of oligomeric A beta ligands (ADDLs) suggests a molecular basis for reversible memory loss. *Proceedings of the National Academy of Sciences of the United States of America*, 100(18), pp.10417–10422.

Gopinath, B. et al., 2009. Depressive symptoms in older adults with hearing impairments: the Blue Mountains Study. *Journal of the American Geriatrics*

Society, 57(7), pp.1306–1308.

Gorup, E., Rifel, J. & Petek Šter, M., 2018. Anticholinergic Burden and Most Common Anticholinergic-acting Medicines in Older General Practice Patients. *Zdravstveno varstvo*, 57(3), pp.140–147.

Goure, W.F. et al., 2014. Targeting the proper amyloid-beta neuronal toxins: a path forward for Alzheimer's disease immunotherapeutics. *Alzheimer's research & therapy*, 6(4), p.42.

Gray, S.L. et al., 2008. Antioxidant vitamin supplement use and risk of dementia or Alzheimer's disease in older adults. *Journal of the American Geriatrics Society*, 56(2), pp.291–295.

Greenes, R.A. ed., 2006. *Clinical Decision Support: The Road Ahead* 1st ed., Academic Press.

Gu, H. et al., 2014. The role of choroid plexus in IVIG-induced beta-amyloid clearance. *Neuroscience*, 270, pp.168–176.

Haass, C. & Selkoe, D.J., 2007. Soluble protein oligomers in neurodegeneration: lessons from the Alzheimer's amyloid beta-peptide. *Nature Reviews. Molecular Cell Biology*, 8(2), pp.101–112.

Hampel, H. et al., 2017. A Precision Medicine Initiative for Alzheimer's disease: the road ahead to biomarker-guided integrative disease modeling. *Climacteric*, 20(2), pp.107–118.

Hampel, H. et al., 2008. Core candidate neurochemical and imaging biomarkers of Alzheimer's disease. *Alzheimer's & Dementia*, 4(1), pp.38–48.

Hampel, H. et al., 2018. The cholinergic system in the pathophysiology and treatment of Alzheimer's disease. *Brain: A Journal of Neurology*, 141(7), pp.1917–1933.

Hampel, H., Lista, S. & Khachaturian, Z.S., 2012. Development of biomarkers to chart all Alzheimer's disease stages: the royal road to cutting the therapeutic Gordian Knot. *Alzheimer's & Dementia*, 8(4), pp.312–336.

Hardy, J. & Selkoe, D.J., 2002. The amyloid hypothesis of Alzheimer's disease: progress and problems on the road to therapeutics. *Science*, 297(5580), pp.353–356.

Harvey, A.L., 1995. The pharmacology of galanthamine and its analogues. *Pharmacology & Therapeutics*, 68(1), pp.113–128.

Haynes, R.B., Wilczynski, N.L. & Computerized Clinical Decision Support System (CCDSS) Systematic Review Team, 2010. Effects of computerized clinical decision support systems on practitioner performance and patient outcomes: methods of a decision-maker-researcher partnership systematic review. *Implementation Science*, 5, p.12.

Hébert-Croteau, N. et al., 2004. Compliance with consensus recommendations for systemic therapy is associated with improved survival of women with node-negative breast cancer. *Journal of Clinical Oncology*, 22(18), pp.3685–3693.

Heinsinger, N.M., Gachechiladze, M.A. & Rebeck, G.W., 2016. Apolipoprotein E genotype affects size of apoe complexes in cerebrospinal fluid. *Journal of Neuropathology and Experimental Neurology*, 75(10), pp.918–924.

Hemens, B.J. et al., 2011. Computerized clinical decision support systems for drug prescribing and management: a decision-maker-researcher partnership systematic review. *Implementation Science*, 6, p.89.

Hemingway, H. & Marmot, M., 1999. Evidence based cardiology: psychosocial factors in the aetiology and prognosis of coronary heart disease. Systematic review of prospective cohort studies. *BMJ (Clinical Research Ed.)*, 318(7196), pp.1460–1467.

Hirai, K. et al., 2001. Mitochondrial abnormalities in Alzheimer's disease. *The Journal of Neuroscience*, 21(9), pp.3017–3023.

Holmes, C. & Butchart, J., 2011. Systemic inflammation and Alzheimer's disease. *Biochemical Society Transactions*, 39(4), pp.898–901.

Hong, S. et al., 2014. Soluble Aβ oligomers are rapidly sequestered from brain ISF in vivo and bind GM1 ganglioside on cellular membranes. *Neuron*, 82(2), pp.308–319.

Howard, R. et al., 2012. Donepezil and memantine for moderate-to-severe Alzheimer's disease. *The New England Journal of Medicine*, 366(10), pp.893–903.

Huang, C.-Q. et al., 2010. Chronic diseases and risk for depression in old age: a

meta-analysis of published literature. *Ageing Research Reviews*, 9(2), pp.131–141.

Hyman, B.T. et al., 2012. National Institute on Aging-Alzheimer's Association guidelines for the neuropathologic assessment of Alzheimer's disease. *Alzheimer's & Dementia*, 8(1), pp.1–13.

Ingusci, S. et al., 2019. Gene therapy tools for brain diseases. *Frontiers in pharmacology*, 10, p.724.

Institute of Medicine (US) Committee on Standards for Developing Trustworthy Clinical Practice Guidelines, 2011. *Clinical practice guidelines we can trust* R. Graham et al., eds., Washington (DC): National Academies Press (US).

Ionis Pharmaceuticals, 2019. Huntington's Disease Pivotal Program Modified to Less Frequent Dosing Easing Burden on Sites and Patients. *Ionis Pharmaceuticals*. Available at: https://www.ionispharma.com/update-roche-huntingtons-disease-pivotal-program/ [Accessed March 25, 2019].

Ionis Pharmaceuticals, Inc., 2017. Safety, Tolerability, Pharmacokinetics, and Pharmacodynamics of IONIS-MAPTRx in Patients With Mild Alzheimer's Disease. *ClinicalTrials.gov*. Available at: https://clinicaltrials.gov/ct2/show/NCT03186989?term=IONIS-MAPTRx&draw=2&rank=1 [Accessed March 25, 2020].

Isaacson, R., 2017. Is alzheimer's prevention possible today? *Journal of the American Geriatrics Society*, 65(10), pp.2153–2154.

Ishida, K. et al., 2020. 5-Caffeoylquinic Acid Ameliorates Cognitive Decline and Reduces Aβ Deposition by Modulating Aβ Clearance Pathways in APP/PS2 Transgenic Mice. *Nutrients*, 12(2).

Jaspers, M.W.M. et al., 2011. Effects of clinical decision-support systems on practitioner performance and patient outcomes: a synthesis of high-quality systematic review findings. *Journal of the American Medical Informatics Association*, 18(3), pp.327–334.

Jellinger, K.A. & Bancher, C., 1998. Neuropathology of Alzheimer's disease: a critical update. *Journal of Neural Transmission. Supplementum*, 54, pp.77–95.

Jia, P. et al., 2016. The effects of clinical decision support systems on medication

safety: an overview. *Plos One*, 11(12), p.e0167683.

Jiang, S. et al., 2014. M1 muscarinic acetylcholine receptor in Alzheimer's disease. *Neuroscience Bulletin*, 30(2), pp.295–307.

Johnson, K.A. et al., 2012. Brain imaging in Alzheimer disease. *Cold Spring Harbor perspectives in medicine*, 2(4), p.a006213.

Jutkowitz, E. et al., 2017. Societal and family lifetime cost of dementia: implications for policy. *Journal of the American Geriatrics Society*, 65(10), pp.2169–2175.

Kaczmarczyk, R. et al., 2017. Microglia modulation through external vagus nerve stimulation in a murine model of Alzheimer's disease. *Journal of Neurochemistry*.

Kang, D.E. et al., 2000. Modulation of amyloid beta-protein clearance and Alzheimer's disease susceptibility by the LDL receptor-related protein pathway. *The Journal of Clinical Investigation*, 106(9), pp.1159–1166.

Kaushal, R., Shojania, K.G. & Bates, D.W., 2003. Effects of computerized physician order entry and clinical decision support systems on medication safety: a systematic review. *Archives of Internal Medicine*, 163(12), pp.1409–1416.

Kawamoto, K. et al., 2009. A national clinical decision support infrastructure to enable the widespread and consistent practice of genomic and personalized medicine. *BMC Medical Informatics and Decision Making*, 9, p.17.

Kawamoto, K. et al., 2005. Improving clinical practice using clinical decision support systems: a systematic review of trials to identify features critical to success. *BMJ (Clinical Research Ed.)*, 330(7494), p.765.

Kazim, S.F. et al., 2017. Early-Onset Network Hyperexcitability in Presymptomatic Alzheimer's Disease Transgenic Mice Is Suppressed by Passive Immunization with Anti-Human APP/Aβ Antibody and by mGluR5 Blockade. *Frontiers in aging neuroscience*, 9, p.71.

Khoury, R. et al., 2017. Recent progress in the pharmacotherapy of alzheimer's disease. *Drugs & Aging*, 34(11), pp.811–820.

Kivipelto, M. et al., 2001. Midlife vascular risk factors and Alzheimer's disease in later life: longitudinal, population based study. *BMJ (Clinical Research Ed.)*, 322(7300), pp.1447–1451.

Knopman, D.S. et al., 2001. Practice parameter: diagnosis of dementia (an evidence-based review). Report of the Quality Standards Subcommittee of the American Academy of Neurology. *Neurology*, 56(9), pp.1143–1153.

Knowles, J., 2006. Donepezil in Alzheimer's disease: an evidence-based review of its impact on clinical and economic outcomes. *Core evidence*, 1(3), pp.195–219.

Koffie, R.M. et al., 2009. Oligomeric amyloid beta associates with postsynaptic densities and correlates with excitatory synapse loss near senile plaques. *Proceedings of the National Academy of Sciences of the United States of America*, 106(10), pp.4012–4017.

Koffie, R.M., Hyman, B.T. & Spires-Jones, T.L., 2011. Alzheimer's disease: synapses gone cold. *Molecular Neurodegeneration*, 6(1), p.63.

Kuiper, J.S. et al., 2015. Social relationships and risk of dementia: A systematic review and meta-analysis of longitudinal cohort studies. *Ageing Research Reviews*, 22, pp.39–57.

Kulikowski, C.A. & Weiss, S.M., 1982. *Representation of expert knowledge for consultation: the CASNET and EXPERT projects*, Boulder: Westview Press.

Kushniruk, A.W. et al., 2013. National efforts to improve health information system safety in Canada, the United States of America and England. *International Journal of Medical Informatics*, 82(5), pp.e149–60.

Lage, J.M.M., 2006. 100 Years of Alzheimer's disease (1906-2006). *Journal of Alzheimer's Disease*, 9(3 Suppl), pp.15–26.

Lainer, M., Mann, E. & Sönnichsen, A., 2013. Information technology interventions to improve medication safety in primary care: a systematic review. *International Journal for Quality in Health Care*, 25(5), pp.590–598.

Laporta, R., Anandam, A. & El-Solh, A.A., 2012. Screening for obstructive sleep apnea in veterans with ischemic heart disease using a computer-based clinical decision-support system. *Clinical Research in Cardiology*, 101(9), pp.737–744.

Larson, E.B., 2010. Prospects for delaying the rising tide of worldwide, late-life

dementias. *International Psychogeriatrics*, 22(8), pp.1196–1202.

Lau, D.T. et al., 2010. Polypharmacy and potentially inappropriate medication use among community-dwelling elders with dementia. *Alzheimer Disease and Associated Disorders*, 24(1), pp.56–63.

Lazarou, J., Pomeranz, B.H. & Corey, P.N., 1998. Incidence of adverse drug reactions in hospitalized patients: a meta-analysis of prospective studies. *The Journal of the American Medical Association*, 279(15), pp.1200–1205.

Leape, L.L. et al., 1995. Systems analysis of adverse drug events. ADE Prevention Study Group. *The Journal of the American Medical Association*, 274(1), pp.35–43.

Leckie, R.L. et al., 2014. BDNF mediates improvements in executive function following a 1-year exercise intervention. *Frontiers in Human Neuroscience*, 8, p.985.

Lee, H.J. et al., 2010. Image-based clinical decision support for transrectal ultrasound in the diagnosis of prostate cancer: comparison of multiple logistic regression, artificial neural network, and support vector machine. *European Radiology*, 20(6), pp.1476–1484.

Leonard, B.E., 2007. Inflammation, depression and dementia: are they connected? *Neurochemical Research*, 32(10), pp.1749–1756.

Lesné, S. et al., 2006. A specific amyloid-beta protein assembly in the brain impairs memory. *Nature*, 440(7082), pp.352–357.

Lesné, S.E. et al., 2013. Brain amyloid-β oligomers in ageing and Alzheimer's disease. *Brain: A Journal of Neurology*, 136(Pt 5), pp.1383–1398.

Li, S. et al., 2018. Decoding the synaptic dysfunction of bioactive human AD brain soluble Aβ to inspire novel therapeutic avenues for Alzheimer's disease. *Acta neuropathologica communications*, 6(1), p.121.

Lista, S. et al., 2016. Application of systems theory in longitudinal studies on the origin and progression of alzheimer's disease. *Methods in Molecular Biology*, 1303, pp.49–67.

Lista, S., Dubois, B. & Hampel, H., 2015. Paths to Alzheimer's disease prevention: from modifiable risk factors to biomarker enrichment strategies. *The journal of*

nutrition, health & aging, 19(2), pp.154–163.

Liu, C.-C. et al., 2015. Neuronal LRP1 regulates glucose metabolism and insulin signaling in the brain. *The Journal of Neuroscience*, 35(14), pp.5851–5859.

Livingston, G. et al., 2017. Dementia prevention, intervention, and care. *The Lancet*, 390(10113), pp.2673–2734.

Lowe, D., Another Alzheimer's Antibody Fails. There Will Be More. *Science Translational Medicine*. Available at: https://blogs.sciencemag.org/pipeline/archives/2019/01/30/another-alzheimers-antibody-fails-there-will-be-more?r3f_986=https://www.google.com/ [Accessed March 25, 2019].

Loy, C. & Schneider, L., 2006. Galantamine for Alzheimer's disease and mild cognitive impairment. *Cochrane Database of Systematic Reviews*, (1), p.CD001747.

Loy, C.T. et al., 2014. Genetics of dementia. *The Lancet*, 383(9919), pp.828–840.

Luchsinger, J.A. et al., 2003. Antioxidant vitamin intake and risk of Alzheimer disease. *Archives of Neurology*, 60(2), pp.203–208.

Luchsinger, J.A. & Gustafson, D.R., 2009. Adiposity and Alzheimer's disease. *Current opinion in clinical nutrition and metabolic care*, 12(1), pp.15–21.

Lue, L.F. et al., 1999. Soluble amyloid beta peptide concentration as a predictor of synaptic change in Alzheimer's disease. *The American Journal of Pathology*, 155(3), pp.853–862.

Lyman, G.H. & Moses, H.L., 2016. Biomarker Tests for Molecularly Targeted Therapies--The Key to Unlocking Precision Medicine. *The New England Journal of Medicine*, 375(1), pp.4–6.

Lyman, J.A. et al., 2010. Clinical decision support: progress and opportunities. *Journal of the American Medical Informatics Association*, 17(5), pp.487–492.

Makary, M.A. & Daniel, M., 2016. Medical error-the third leading cause of death in the US. *BMJ (Clinical Research Ed.)*, 353, p.i2139.

Margallo-Lana, M.L. et al., 2007. Fifteen-year follow-up of 92 hospitalized adults with Down's syndrome: incidence of cognitive decline, its relationship to age and neuropathology. *Journal of Intellectual Disability Research*, 51(Pt. 6), pp.463–

477.

Martins, I.C. et al., 2008. Lipids revert inert Abeta amyloid fibrils to neurotoxic protofibrils that affect learning in mice. *The EMBO Journal*, 27(1), pp.224–233.

Masaki, K.H. et al., 2000. Association of vitamin E and C supplement use with cognitive function and dementia in elderly men. *Neurology*, 54(6), pp.1265–1272.

Matsunaga, S., Kishi, T. & Iwata, N., 2015. Memantine monotherapy for Alzheimer's disease: a systematic review and meta-analysis. *Plos One*, 10(4), p.e0123289.

Mayeux, R., 2003. Epidemiology of neurodegeneration. *Annual Review of Neuroscience*, 26, pp.81–104.

McCarron, M. et al., 2014. A prospective 14-year longitudinal follow-up of dementia in persons with D own syndrome. *Journal of Intellectual Disability Research*, 58(1), pp.61–70.

McCoy, S.L. et al., 2005. Hearing loss and perceptual effort: downstream effects on older adults' memory for speech. *The Quarterly journal of experimental psychology. A, Human experimental psychology*, 58(1), pp.22–33.

McGeer, P.L. et al., 1989. Immune system response in Alzheimer's disease. *The Canadian Journal of Neurological Sciences. Le Journal Canadien des Sciences Neurologiques*, 16(4 Suppl), pp.516–527.

McKhann, G.M. et al., 2011. The diagnosis of dementia due to Alzheimer's disease: recommendations from the National Institute on Aging-Alzheimer's Association workgroups on diagnostic guidelines for Alzheimer's disease. *Alzheimer's & Dementia*, 7(3), pp.263–269.

McLean, C.A. et al., 1999. Soluble pool of Abeta amyloid as a determinant of severity of neurodegeneration in Alzheimer's disease. *Annals of Neurology*, 46(6), pp.860–866.

Mega, M.S., 2000. The cholinergic deficit in Alzheimer's disease: impact on cognition, behaviour and function. *The International Journal of Neuropsychopharmacology*, 3(7), pp.3–12.

Meilandt, W.J. et al., 2019. Characterization of the selective in vitro and in vivo binding properties of crenezumab to oligomeric Aβ. *Alzheimer's research & therapy*, 11(1), p.97.

Menéndez, M., 2005. Down syndrome, Alzheimer's disease and seizures. *Brain & Development*, 27(4), pp.246–252.

Mesulam, M.-M., 2013. Cholinergic circuitry of the human nucleus basalis and its fate in Alzheimer's disease. *The Journal of Comparative Neurology*, 521(18), pp.4124–4144.

Miller, T.M. et al., 2013. An antisense oligonucleotide against SOD1 delivered intrathecally for patients with SOD1 familial amyotrophic lateral sclerosis: a phase 1, randomised, first-in-man study. *Lancet Neurology*, 12(5), pp.435–442.

Minkeviciene, R. et al., 2009. Amyloid beta-induced neuronal hyperexcitability triggers progressive epilepsy. *The Journal of Neuroscience*, 29(11), pp.3453–3462.

Mizuno, S. et al., 2012. AlzPathway: a comprehensive map of signaling pathways of Alzheimer's disease. *BMC Systems Biology*, 6, p.52.

Montine, T.J. & Montine, K.S., 2015. Precision medicine: Clarity for the clinical and biological complexity of Alzheimer's and Parkinson's diseases. *The Journal of Experimental Medicine*, 212(5), pp.601–605.

Moreth, J. et al., 2013. Globular and protofibrillar aβ aggregates impair neurotransmission by different mechanisms. *Biochemistry*, 52(8), pp.1466–1476.

Morgado, I. & Fändrich, M., 2011. Assembly of Alzheimer's Aβ peptide into nanostructured amyloid fibrils. *Current Opinion in Colloid & Interface Science*, 16(6), pp.508–514.

Morris, M.C. et al., 2002. Dietary intake of antioxidant nutrients and the risk of incident Alzheimer disease in a biracial community study. *The Journal of the American Medical Association*, 287(24), pp.3230–3237.

Mroczko, B. et al., 2018. Amyloid β oligomers (AβOs) in Alzheimer's disease. *Journal of Neural Transmission*, 125(2), pp.177–191.

Muro, N. et al., 2017. Weighting Experience-Based Decision Support on the Basis of Clinical Outcomes' Assessment. *Studies in Health Technology and Informatics*, 244, pp.33–37.

National Institute for Health and Care Excellence, 2011. Donepezil, galantamine, rivastigmine and memantine for the treatment of Alzheimer's disease. *National Institute for Health and Care Excellence*. Available at: https://www.nice.org.uk/guidance/ta217 [Accessed March 4, 2019].

National Institutes of Health, What is precision medicine? *Genetics Home Reference*. Available at: https://ghr.nlm.nih.gov/primer/precisionmedicine/definition [Accessed January 29, 2019].

Ngandu, T. et al., 2015. A 2 year multidomain intervention of diet, exercise, cognitive training, and vascular risk monitoring versus control to prevent cognitive decline in at-risk elderly people (FINGER): a randomised controlled trial. *The Lancet*, 385(9984), pp.2255–2263.

Nieuwlaat, R. et al., 2011. Computerized clinical decision support systems for therapeutic drug monitoring and dosing: a decision-maker-researcher partnership systematic review. *Implementation Science*, 6, p.90.

Norton, S. et al., 2014. Potential for primary prevention of Alzheimer's disease: an analysis of population-based data. *Lancet Neurology*, 13(8), pp.788–794.

O'Sullivan, D. et al., 2014. Decision time for clinical decision support systems. *Clinical Medicine*, 14(4), pp.338–341.

Osheroff, J. et al., 2005. *Improving Outcomes with Clinical Decision Support: An Implementer's Guide* 1st ed., Productivity Press.

Otaegui-Arrazola, A. et al., 2014. Diet, cognition, and Alzheimer's disease: food for thought. *European Journal of Nutrition*, 53(1), pp.1–23.

Palasí, A. et al., 2015. Differentiated clinical presentation of early and late-onset Alzheimer's disease: is 65 years of age providing a reliable threshold? *Journal of Neurology*, 262(5), pp.1238–1246.

Palop, J.J. et al., 2007. Aberrant excitatory neuronal activity and compensatory remodeling of inhibitory hippocampal circuits in mouse models of Alzheimer's disease. *Neuron*, 55(5), pp.697–711.

Palop, J.J. & Mucke, L., 2010. Synaptic depression and aberrant excitatory network activity in Alzheimer's disease: two faces of the same coin? *Neuromolecular Medicine*, 12(1), pp.48–55.

Pasqualetti, G. et al., 2015. Potential drug-drug interactions in Alzheimer patients with behavioral symptoms. *Clinical Interventions in Aging*, 10, pp.1457–1466.

Pearson, S.-A. et al., 2009. Do computerised clinical decision support systems for prescribing change practice? A systematic review of the literature (1990-2007). *BMC Health Services Research*, 9, p.154.

Peleg, M., 2013. Computer-interpretable clinical guidelines: a methodological review. *Journal of Biomedical Informatics*, 46(4), pp.744–763.

Perez Ortiz, J.M. & Swerdlow, R.H., 2019. Mitochondrial dysfunction in Alzheimer's disease: Role in pathogenesis and novel therapeutic opportunities. *British Journal of Pharmacology*, 176(18), pp.3489–3507.

Perrin, R.J., Fagan, A.M. & Holtzman, D.M., 2009. Multimodal techniques for diagnosis and prognosis of Alzheimer's disease. *Nature*, 461(7266), pp.916–922.

Perry, E.K. et al., 1993. Cholinergic transmitter and neurotrophic activities in Lewy body dementia: similarity to Parkinson's and distinction from Alzheimer disease. *Alzheimer Disease and Associated Disorders*, 7(2), pp.69–79.

Perry, V.H. & Gordon, S., 1988. Macrophages and microglia in the nervous system. *Trends in Neurosciences*, 11(6), pp.273–277.

Petersen, R.C. et al., 2005. Vitamin E and donepezil for the treatment of mild cognitive impairment. *The New England Journal of Medicine*, 352(23), pp.2379–2388.

Pfistermeister, B. et al., 2017. Anticholinergic burden and cognitive function in a large German cohort of hospitalized geriatric patients. *Plos One*, 12(2), p.e0171353.

Poling, A. et al., 2008. Oligomers of the amyloid-beta protein disrupt working memory: confirmation with two behavioral procedures. *Behavioural Brain Research*, 193(2), pp.230–234.

Prince, M. et al., 2014. *Dementia UK update*, Alzheimer's Society.

Qiu, C. et al., 2014. Diabetes, markers of brain pathology and cognitive function: the Age, Gene/Environment Susceptibility-Reykjavik Study. *Annals of Neurology*, 75(1), pp.138–146.

Quinn, K.J. & Shah, N.H., 2017. A dataset quantifying polypharmacy in the United States. *Scientific data*, 4, p.170167.

Rabins, P.V., 1997. Practice guideline for the treatment of patients with Alzheimer's disease and other dementias of late life. American Psychiatric Association. *The American Journal of Psychiatry*, 154(5 Suppl), pp.1–39.

Rebeck, G.W., 2017. The role of APOE on lipid homeostasis and inflammation in normal brains. *Journal of Lipid Research*, 58(8), pp.1493–1499.

Reed, M.N. et al., 2011. Cognitive effects of cell-derived and synthetically derived Aβ oligomers. *Neurobiology of Aging*, 32(10), pp.1784–1794.

Regional Drugs and Therapeutics Centre, 2018. Cost Comparison Charts. Available at: http://rdtc.nhs.uk/prescribing-analysis-reports/reports-cost-impact-and-savings/cost-comparison-charts [Accessed March 24, 2019].

Reiner, M. et al., 2013. Long-term health benefits of physical activity--a systematic review of longitudinal studies. *BMC Public Health*, 13, p.813.

Reitz, C., 2016. Toward precision medicine in Alzheimer's disease. *Annals of translational medicine*, 4(6), p.107.

Richardson, K. et al., 2018. Anticholinergic drugs and risk of dementia: case-control study. *BMJ (Clinical Research Ed.)*, 361, p.k1315.

Roberson, E.D. et al., 2011. Amyloid-β/Fyn-induced synaptic, network, and cognitive impairments depend on tau levels in multiple mouse models of Alzheimer's disease. *The Journal of Neuroscience*, 31(2), pp.700–711.

Roberson, E.D. et al., 2007. Reducing endogenous tau ameliorates amyloid beta-induced deficits in an Alzheimer's disease mouse model. *Science*, 316(5825), pp.750–754.

Roche, 2019. Roche to discontinue Phase III CREAD 1 and 2 clinical studies of crenezumab in early Alzheimer's disease (AD) - other company programmes in AD continue. Available at: https://www.roche.com/media/releases/med-cor-2019-01-30.htm [Accessed April 13, 2020].

Rodrigue, K.M. et al., 2013. Risk factors for β-amyloid deposition in healthy aging: vascular and genetic effects. *JAMA neurology*, 70(5), pp.600–606.

Rogers, D. & Pies, R., 2008. General Medical Drugs Associated with Depression. *Psychiatry (Edgmont)*, 5(12), pp.28–41.

Rosenberg, P.B., Nowrangi, M.A. & Lyketsos, C.G., 2015. Neuropsychiatric symptoms in Alzheimer's disease: What might be associated brain circuits? *Molecular aspects of medicine*, 43-44, pp.25–37.

Russ, T.C. & Morling, J.R., 2012. Cholinesterase inhibitors for mild cognitive impairment. *Cochrane Database of Systematic Reviews*, (9), p.CD009132.

Saczynski, J.S. et al., 2010. Depressive symptoms and risk of dementia: the Framingham Heart Study. *Neurology*, 75(1), pp.35–41.

Sahota, N. et al., 2011. Computerized clinical decision support systems for acute care management: a decision-maker-researcher partnership systematic review of effects on process of care and patient outcomes. *Implementation Science*, 6, p.91.

Salahudeen, M.S., Duffull, S.B. & Nishtala, P.S., 2015. Anticholinergic burden quantified by anticholinergic risk scales and adverse outcomes in older people: a systematic review. *BMC geriatrics*, 15, p.31.

Salloway, S. et al., 2014. Two phase 3 trials of bapineuzumab in mild-to-moderate Alzheimer's disease. *The New England Journal of Medicine*, 370(4), pp.322–333.

Sanchez, P.E. et al., 2012. Levetiracetam suppresses neuronal network dysfunction and reverses synaptic and cognitive deficits in an Alzheimer's disease model. *Proceedings of the National Academy of Sciences of the United States of America*, 109(42), pp.E2895–903.

Santini, Z.I. et al., 2015. The association between social relationships and depression: a systematic review. *Journal of Affective Disorders*, 175, pp.53–65.

Sassi, C. et al., 2016. ABCA7 p.G215S as potential protective factor for Alzheimer's disease. *Neurobiology of Aging*, 46, pp.235.e1–9.

Saverno, K.R. et al., 2011. Ability of pharmacy clinical decision-support software to

alert users about clinically important drug-drug interactions. *Journal of the American Medical Informatics Association*, 18(1), pp.32–37.

Scarmeas, N. et al., 2009. Mediterranean diet and mild cognitive impairment. *Archives of Neurology*, 66(2), pp.216–225.

Scarmeas, N. et al., 2011. Physical activity and Alzheimer disease course. *The American Journal of Geriatric Psychiatry*, 19(5), pp.471–481.

Schelke, M.W. et al., 2016. Nutritional interventions for Alzheimer's prevention: a clinical precision medicine approach. *Annals of the New York Academy of Sciences*, 1367(1), pp.50–56.

Schmitt, B. et al., 2004. Combination therapy in Alzheimer's disease: a review of current evidence. *CNS Drugs*, 18(13), pp.827–844.

Schneider, L.S. & Sano, M., 2009. Current Alzheimer's disease clinical trials: methods and placebo outcomes. *Alzheimer's & Dementia*, 5(5), pp.388–397.

Seifan, A. & Isaacson, R., 2015. The Alzheimer's Prevention Clinic at Weill Cornell Medical College / New York - Presbyterian Hospital: Risk Stratification and Personalized Early Intervention. *The journal of prevention of Alzheimer's disease*, 2(4), pp.254–266.

Selkoe, D.J. & Hardy, J., 2016. The amyloid hypothesis of Alzheimer's disease at 25 years. *EMBO Molecular Medicine*, 8(6), pp.595–608.

Shah, N.S. et al., 2012. Midlife blood pressure, plasma β-amyloid, and the risk for Alzheimer disease: the Honolulu Asia Aging Study. *Hypertension*, 59(4), pp.780–786.

Shankar, G.M. et al., 2008. Amyloid-beta protein dimers isolated directly from Alzheimer's brains impair synaptic plasticity and memory. *Nature Medicine*, 14(8), pp.837–842.

Shinohara, M. et al., 2017. Role of LRP1 in the pathogenesis of Alzheimer's disease: evidence from clinical and preclinical studies. *Journal of Lipid Research*, 58(7), pp.1267–1281.

Shinto, L. et al., 2014. A randomized placebo-controlled pilot trial of omega-3 fatty acids and alpha lipoic acid in Alzheimer's disease. *Journal of Alzheimer's Disease*, 38(1), pp.111–120.

Shughrue, P.J. et al., 2010. Anti-ADDL antibodies differentially block oligomer binding to hippocampal neurons. *Neurobiology of Aging*, 31(2), pp.189–202.

Singh, B. et al., 2014. Association of mediterranean diet with mild cognitive impairment and Alzheimer's disease: a systematic review and meta-analysis. *Journal of Alzheimer's Disease*, 39(2), pp.271–282.

Sitzer, D.I., Twamley, E.W. & Jeste, D.V., 2006. Cognitive training in Alzheimer's disease: a meta-analysis of the literature. *Acta Psychiatrica Scandinavica*, 114(2), pp.75–90.

Smith, A.D. & Yaffe, K., 2014. Dementia (including Alzheimer's disease) can be prevented: statement supported by international experts. *Journal of Alzheimer's Disease*, 38(4), pp.699–703.

Solfrizzi, Vincenzo et al., 2011. Diet and Alzheimer's disease risk factors or prevention: the current evidence. *Expert Review of Neurotherapeutics*, 11(5), pp.677–708.

Solfrizzi, V et al., 2011. Mediterranean diet in predementia and dementia syndromes. *Current Alzheimer research*, 8(5), pp.520–542.

Solomon, A. et al., 2007. Serum cholesterol changes after midlife and late-life cognition: twenty-one-year follow-up study. *Neurology*, 68(10), pp.751–756.

Song, J.-X. et al., 2016. A novel curcumin analog binds to and activates TFEB in vitro and in vivo independent of MTOR inhibition. *Autophagy*, 12(8), pp.1372–1389.

Song, J.-X. et al., 2020. A small molecule transcription factor EB activator ameliorates beta-amyloid precursor protein and Tau pathology in Alzheimer's disease models. *Aging Cell*, 19(2), p.e13069.

Sonnen, J.A. et al., 2011. Ecology of the aging human brain. *Archives of Neurology*, 68(8), pp.1049–1056.

Stagni, F. et al., 2015. Timing of therapies for Down syndrome: the sooner, the better. *Frontiers in Behavioral Neuroscience*, 9, p.265.

Stephenson, D. et al., 2015. Charting a path toward combination therapy for Alzheimer's disease. *Expert Review of Neurotherapeutics*, 15(1), pp.107–113.

Stern, Y., 2012. Cognitive reserve in ageing and Alzheimer's disease. *Lancet*

Neurology, 11(11), pp.1006–1012.

Sugino, H. et al., 2015. Global trends in alzheimer disease clinical development: increasing the probability of success. *Clinical Therapeutics*, 37(8), pp.1632–1642.

Suhasini, A., Palanivel, S. & Ramalingam, V., 2011. Multimodel decision support system for psychiatry problem. *Expert systems with applications*, 38(5), pp.4990–4997.

Sullivan, M.G., Alzheimer's trial design problem throws a wrench in promising BAN2401 results. *Clinical Neurology News*. Available at: https://www.mdedge.com/clinicalneurologynews/article/171238/alzheimers-cognition/alzheimers-trial-design-problem-throws [Accessed March 5, 2019].

Swan, G.E. & Lessov-Schlaggar, C.N., 2007. The effects of tobacco smoke and nicotine on cognition and the brain. *Neuropsychology Review*, 17(3), pp.259–273.

Szeto, J.Y.Y. & Lewis, S.J.G., 2016. Current treatment options for alzheimer's disease and parkinson's disease dementia. *Current neuropharmacology*, 14(4), pp.326–338.

Tachibana, M. et al., 2019. APOE4-mediated amyloid-β pathology depends on its neuronal receptor LRP1. *The Journal of Clinical Investigation*, 129(3), pp.1272–1277.

Tarasoff-Conway, J.M. et al., 2015. Clearance systems in the brain-implications for Alzheimer disease. *Nature Reviews. Neurology*, 11(8), pp.457–470.

Tariot, P.N. et al., 2018. The Alzheimer's Prevention Initiative Autosomal-Dominant Alzheimer's Disease Trial: A study of crenezumab versus placebo in preclinical PSEN1 E280A mutation carriers to evaluate efficacy and safety in the treatment of autosomal-dominant Alzheimer's disease, including a placebo-treated noncarrier cohort. *Alzheimer's & dementia : translational research & clinical interventions*, 4, pp.150–160.

Terry, R.D. et al., 1991. Physical basis of cognitive alterations in Alzheimer's disease: synapse loss is the major correlate of cognitive impairment. *Annals of Neurology*, 30(4), pp.572–580.

The White House, Precision Medicine Initiative. *The White House of President Barack Obama*. Available at: https://obamawhitehouse.archives.gov/precision-medicine [Accessed February 13, 2019].

Tilvis, R.S. et al., 2004. Predictors of cognitive decline and mortality of aged people over a 10-year period. *The Journals of Gerontology. Series A, Biological Sciences and Medical Sciences*, 59(3), pp.268–274.

Tolppanen, A.-M. et al., 2013. History of medically treated diabetes and risk of Alzheimer disease in a nationwide case-control study. *Diabetes Care*, 36(7), pp.2015–2019.

Tondelli, M. et al., 2012. Structural MRI changes detectable up to ten years before clinical Alzheimer's disease. *Neurobiology of Aging*, 33(4), pp.825.e25–36.

Treusch, S., Cyr, D.M. & Lindquist, S., 2009. Amyloid deposits: protection against toxic protein species? *Cell Cycle*, 8(11), pp.1668–1674.

US National Research Council, 2011. *Toward Precision Medicine: Building a Knowledge Network for Biomedical Research and a New Taxonomy of Disease*, Washington (DC): National Academies Press (US).

Vagelatos, N.T. & Eslick, G.D., 2013. Type 2 diabetes as a risk factor for Alzheimer's disease: the confounders, interactions, and neuropathology associated with this relationship. *Epidemiologic Reviews*, 35, pp.152–160.

Valenzuela, M.J., 2008. Brain reserve and the prevention of dementia. *Current Opinion in Psychiatry*, 21(3), pp.296–302.

Valenzuela, M.J. & Sachdev, P., 2006. Brain reserve and dementia: a systematic review. *Psychological Medicine*, 36(4), pp.441–454.

van Zundert, B. & Brown, R.H., 2017. Silencing strategies for therapy of SOD1-mediated ALS. *Neuroscience Letters*, 636, pp.32–39.

Vaughan, S. et al., 2014. The effects of multimodal exercise on cognitive and physical functioning and brain-derived neurotrophic factor in older women: a randomised controlled trial. *Age and Ageing*, 43(5), pp.623–629.

Walker, J.Q. et al., 2017. Comparing clinically based versus algorithm-generated interventions in the context of alzheimer's disease (ad) prevention. *Alzheimer's & Dementia*, 13(7), p.P871.

Walker, K.A., Ficek, B.N. & Westbrook, R., 2019. Understanding the role of systemic inflammation in alzheimer's disease. *ACS Chemical Neuroscience*, 10(8), pp.3340–3342.

Walton, R. et al., 1999. Computer support for determining drug dose: systematic review and meta-analysis. *BMJ (Clinical Research Ed.)*, 318(7189), pp.984–990.

Wavrant-DeVrièze, F. et al., 1999. Association between coding variability in the LRP gene and the risk of late-onset Alzheimer's disease. *Human Genetics*, 104(5), pp.432–434.

Westmark, C.J. et al., 2008. Seizure susceptibility and mortality in mice that over-express amyloid precursor protein. *International journal of clinical and experimental pathology*, 1(2), pp.157–168.

Williams, J.W. et al., 2010. Preventing Alzheimer's disease and cognitive decline. *Evidence report/technology assessment*, (193), pp.1–727.

Wisniewski, K.E., Wisniewski, H.M. & Wen, G.Y., 1985. Occurrence of neuropathological changes and dementia of Alzheimer's disease in Down's syndrome. *Annals of Neurology*, 17(3), pp.278–282.

Woolf, N.J. & Butcher, L.L., 2011. Cholinergic systems mediate action from movement to higher consciousness. *Behavioural Brain Research*, 221(2), pp.488–498.

Wysocki, M. et al., 2012. Hypertension is associated with cognitive decline in elderly people at high risk for dementia. *The American Journal of Geriatric Psychiatry*, 20(2), pp.179–187.

Xu, G. et al., 2012. Reduction of low-density lipoprotein receptor-related protein (LRP1) in hippocampal neurons does not proportionately reduce, or otherwise alter, amyloid deposition in APPswe/PS1dE9 transgenic mice. *Alzheimer's research & therapy*, 4(2), p.12.

Xu, W. et al., 2015. Meta-analysis of modifiable risk factors for Alzheimer's disease. *Journal of Neurology, Neurosurgery, and Psychiatry*, 86(12), pp.1299–1306.

Yaffe, K., 2007. Metabolic syndrome and cognitive disorders: is the sum greater than its parts? *Alzheimer Disease and Associated Disorders*, 21(2), pp.167–171.

Yamamoto, N. et al., 2007. A ganglioside-induced toxic soluble Abeta assembly. Its enhanced formation from Abeta bearing the Arctic mutation. *The Journal of Biological Chemistry*, 282(4), pp.2646–2655.

Yang, T. et al., 2019. Target engagement in an alzheimer trial: Crenezumab lowers amyloid β oligomers in cerebrospinal fluid. *Annals of Neurology*, 86(2), pp.215–224.

Yang, Y.C. et al., 2016. Social relationships and physiological determinants of longevity across the human life span. *Proceedings of the National Academy of Sciences of the United States of America*, 113(3), pp.578–583.

Yasojima, K. et al., 2001. Reduced neprilysin in high plaque areas of Alzheimer brain: a possible relationship to deficient degradation of beta-amyloid peptide. *Neuroscience Letters*, 297(2), pp.97–100.

Yoshiyama, Y. et al., 2007. Synapse loss and microglial activation precede tangles in a P301S tauopathy mouse model. *Neuron*, 53(3), pp.337–351.

Zhang, Y. et al., 2011. APP processing in Alzheimer's disease. *Molecular Brain*, 4, p.3.

Zhao, D., Watson, J.B. & Xie, C.-W., 2004. Amyloid beta prevents activation of calcium/calmodulin-dependent protein kinase II and AMPA receptor phosphorylation during hippocampal long-term potentiation. *Journal of Neurophysiology*, 92(5), pp.2853–2858.

Zhao, Z. et al., 2007. Insulin degrading enzyme activity selectively decreases in the hippocampal formation of cases at high risk to develop Alzheimer's disease. *Neurobiology of Aging*, 28(6), pp.824–830.

Zhuang, X.-X. et al., 2020. Pharmacological enhancement of TFEB-mediated autophagy alleviated neuronal death in oxidative stress-induced Parkinson's disease models. *Cell death & disease*, 11(2), p.128.

Zissimopoulos, J., Crimmins, E. & St Clair, P., 2014. The value of delaying alzheimer's disease onset. *Forum for health economics & policy*, 18(1), pp.25–39.

Zlokovic, B.V. & Frangione, B., 2013. Transport-Clearance Hypothesis for Alzheimer's Disease and Potential Therapeutic Implications - Madame Curie

Bioscience Database - NCBI Bookshelf.